SYNTHESIS AND CHARACTERIZATION OF MULTICOMPONENT POLYESTERS VIA STEP-GROWTH POLYMERIZATION

Qin Lin

Dissertation submitted to the Faculty of the
Virginia Polytechnic Institute and State University
in partial fulfillment of the requirements for the degree of
Doctor of Philosophy in
Chemistry

Dr. Timothy E. Long, Chairman
Dr. James E. McGrath
Dr. Judy S. Riffle
Dr. Ravi F. Saraf
Dr. Don Leo

April 10, 2003

Blacksburg, Virginia
Keywords: polyesters, ionomers, multiplets, clusters, ion hopping,
liquid crystal, hyperbranched, phosphine oxide

SYNTHESIS AND CHARACTERIZATION OF MULTICOMPONENT POLYESTERS VIA STEP-GROWTH POLYMERIZATION

Qin Lin

Abstract

Poly(ethylene terephthalate) (PET) is an important commercial polyester and widely used as fibers, packagings, containers and engineering materials. It is believed that the incorporation of a low level of ionic groups into PETs dramatically improves the mechanical performance and compatibility with other substrates. However, polymers containing ionic groups always exhibit complicated behavior due to the presence of ionic aggregates in the organic matrix, and this thesis investigates the effect of backbone architectures on the properties of PET ionomers in detail.

Three series of random and telechelic PET ionomers with equivalent molecular weights and ionic contents were synthesized using conventional melt polymerization. Solid state sodium NMR spectroscopy and melt rheological analysis demonstrated that the stability of ionic aggregates of telechelic ionomers decreased dramatically with an increase in temperature. A slightly branched structure resulted in high molecular weight ionomers bearing more than two ionic end groups. However, when the level of the branching reagent was lower than 3 mol%, the ionomers with flexible backbone (poly (ethylene terephthalate-co-ethylene isophthalate)) tended to form a high fraction of intramolecular aggregates at high temperatures. When the level of branching agent was higher than 3 mol%, the compact structures led to strong intermolecular aggregates.

PEG endcapped PET and PET random ionomers were synthesized to investigate the effect of PEG end groups on the morphology and rheology of PET and PET ionomers. A small fraction of incorporated PEG end groups increased PET crystallization rate dramatically. Moreover, the PEG endgroups tended to aggregate on the surface of PET to result in a PEG rich layer, which improved the biocompatibility and decreased protein adhesion. The PEG end groups also plasticed the ionic clusters of PET ionomers to decrease melt viscosity, and resulted in a water soluble polyester.

Hyperbranched polymers contain a well-defined plurality of peripheral functionalities. These functionalities subsequently serve as sites for further chemical modification or as templates for noncovalent intermolecular association. In most cases, hyperbranched polymers are prepared using a one-step polymerization process involving AB_n monomers. A novel AB_2 monomer, 4-(fluorophenyl)-4',4"-(bishydroxyphenyl) phosphine oxide, was synthesized. The monomer was successfully polymerized to a modest molecular weight with various catalysts, including K_2CO_3 and $Cs_2CO_3/Mg(OH)_2$. Moreover, an efficient approach to hyperbranched polyarylates via the polymerization of A_2 and B_3 monomers without gelation was also developed. A dilute bisphenol A (A_2) solution was added slowly to a dilute 1,3,5-benzenetricarbonyl trichloride (B_3) solution at 25 °C to prepare hyperbranched polyarylates in the absence of gelation.

Acknowledgements

I would like to take this opportunity to express my gratitude to my research advisor, Dr. Timothy E. Long, for his guidance, inspiration and encouragement throughout the work. Throughout my education at Virginia Tech, I have benefited not only from his profound knowledge, enormous enthusiasm, and keen insight in polymer science and technology but also his wonderful personality.

I would also like to thank the members of my advisory committee: Dr. James E. McGrath, Dr. Judy S. Riffle, Dr. Thomas C. Ward, Dr. Ravi F. Saraf and Dr. Don Leo for their time and guidance through my graduate study at Virginia Tech. I also would like to thank Dr. R. Scott Armentrout (Eastman Chemical Co.), Dr. Mark Rule (Coca Cola Company) and their companies for financial and technical support.

Special thanks go to Mr. Tom Glass for all his help with NMR, Dr. Frank Cromer for help with surface analysis, and Steven McCarthy for AFM and TEM. Thanks to Ms. Esther Brann, Ms. Laurie Good, and Ms. Millie Ryan in the office for all of their help and patience whenever I had a question or needed help with an administrative issue. In addition, Ms. Jan McGinty is acknowledged for her help with the chemistry stockroom and special orders.

Many thanks go out to all of my colleagues (both current and former) in the Long group: Dr. Zhenhe Wang, Dr. Youngtai Yoo, Dr. Anthony J. Pasquale, Dr. Vladimir A. Sinani, Dr. Ejembi Onah, Huaiying Kang, Phil Madison, Sebnem Kara, Dave Williamson, Jeremy Lizotte, Lars Kilian, Casey Hudelson, Koji Yamauchi, Serkan Unal, Ann Fornof, Matt McKee, Afia Karikari, Nicolas Gariano, Victoria K. Long and Scott Trenor .

I would like to express my thanks to my “academic uncles” in Dr. McGrath’s groups for their help and guidance, especially at the starting time: Dr. Sheng Wang, Dr. Qing Ji; Dr. Feng Wang; Dr. Charles Tchatchoua; Dr. H. K. Shobha; Dr. M. Sankarapandian, and Dr. Jimmy Yang. Moreover, I also would like to thank Dr. Liang Zhou in Dr. Gibson group, Dr. Jiangli Wang in Dr. Ward group, Mr. Zhengyu Huang in Dr. Marand group, and Mrs. Huimin Li in Dr. Anderson group for the technological help.

I would like to thank my high school chemistry teachers for initiating my interest in chemistry, and my B.E. advisor Professor Xiaoqiu Xu and M. S. advisor Professor Xuehai Yu nurturing my interest in polymer science.

Many thanks go out to all of my former colleagues in Analytical Center, Fujian Teacher University. Special thanks for all friends in elementary school of Fujian Teacher University, high school of Fujian Teacher University, Tianjin University, Nanjing University and Virginia Tech.

Finally, I would like to thank my family. My parents, Mr. Qidong Lin and Ms. Ruanxian Wang, aunt Huixian Wang and grandmother installed in me the value of perseverance and of being responsible. My wife Yuping is always my source of energy and love. Their encouragement and patience has enabled me to pursue my career through the successful completion of this thesis.

TABLE OF CONTENTS

CHAPTER 1: Introduction and Literature Review

1.1 Polyesters

Polyesters are an important family of polymeric materials, and which are widely used as fibers, engineering materials, containers, coatings and adhesives.[1] In most cases, polyesters are synthesized via methodologies described in Scheme 1.1, and termed as aromatic (amorphous or liquid crystalline), semiflexible (amorphous, semicrystalline or liquid crystalline), or aliphatic polyesters based on their structures (Figure 1.1). The most important polyesters in the market are semiflexible semicrystalline polyesters, including poly(ethylene terephthalate) (PET) and poly(butylene terephthalate) (PBT). Moreover, aromatic polyesters are also widely used as engineering materials and aliphatic polyesters exhibit potential applications as biomaterials. Because this dissertation focuses on the synthesis and characterization of poly(ethylene terephthalate) and BB-6 liquid crystalline (LC) polyester copolymers, this literature review only covers the recent progress in those two families.

---

[1]Goodman, I.; Rodriguez, M. T. *Macrol. Chem. Phys.* **1994**, 195, 1705.

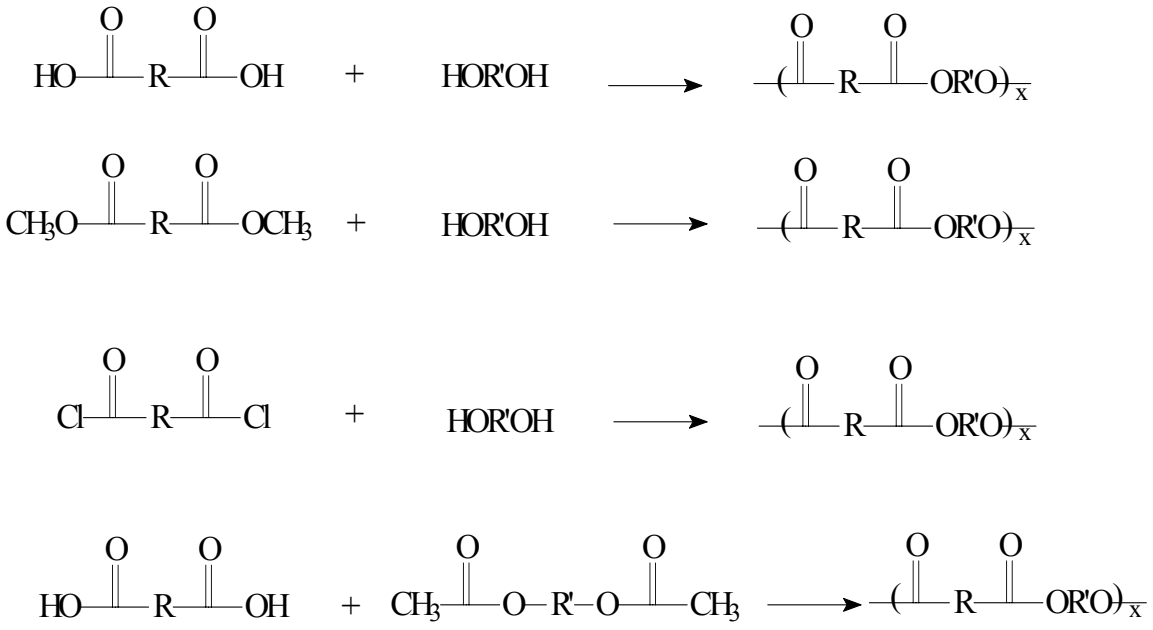

Scheme 1.1 Synthesis of polyesters[1]

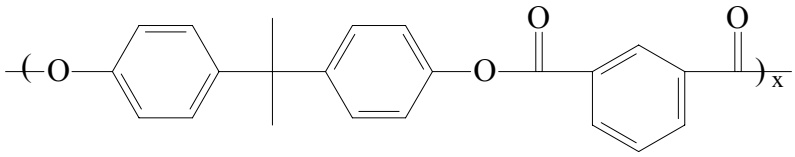

Amorphous aromatic polyester

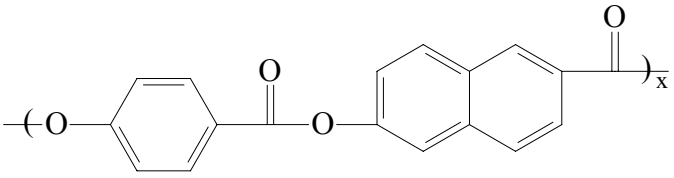

Liquid crystalline aromatic polyeter, Vectra™

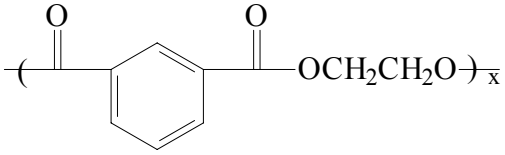

Amorphous semiflexible polyester, PEI

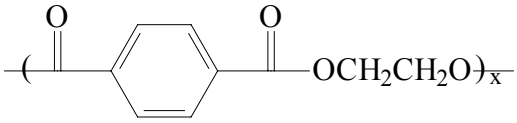

Semicrystalline polyester, PET

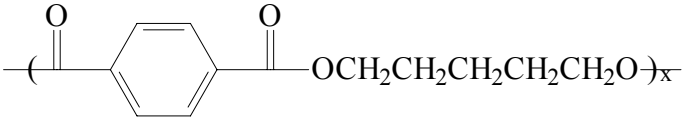

Simicrystalline polyester, PBT

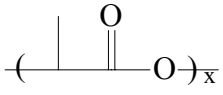

Aliphatic polyester, PLA

Figure 1.1 Polyesters[1]

1.2 Poly(ethylene terephthalate) (PET)

In most cases, PET materials are synthesized using conventional melt polymerization, which consists of two steps, i.e. transesterification and subsequent polycondensation under a reduced pressure.[2-4] Based on those two steps, two synthetic methodologies to prepare high molecular weight products are developed. The first one is a one-step reaction using dimethyl terephthalate (DMT), and a large excess amount of ethylene glycol (EG) with catalysts facilitating transesterification and polycondensation respectively (Scheme 1.2). The second one is a two-step reaction. First, the terephthalic acid reacts with an almost equal amount of EG without a catalyst under a high pressure to prepare moderate molecular weight PET oligomers (Scheme 1.2). The obtained oligomers are used for further polymerization with a catalyst facilitating polycondensation under a reduced pressure.

Moreover, MacKnight and coworkers investigated the polymerization of ethylene terephthalate cyclic oligomers (ETCs) using antimony trioxide as a catalyst.[5-6] The ETCs were prepared via a direct synthesis or cyclodepolymerization (CDP) in a dilute solution. ETCs prepared via CDP consisted of oligomeric species with a wide distribution of molecular weights, and purified ETCs (p-ETCs) were prepared using dichloromethane and tetrahydrofuran. High molecular weight PETs (M_n = 25,000 g/mol) at 293 °C within 15 minutes were obtained via polymerization of ETCs prepared via the direct synthesis method or p-ETCs with antimony trioxide. The PET with a maximum molecular weight (M_n = 32,000 g/mol) was obtained using bismuth trioxide at 293 °C for 15 minutes. PETs prepared from p-ETCs exhibited same thermal behaviors as commercial products from conventional melt polymerization.

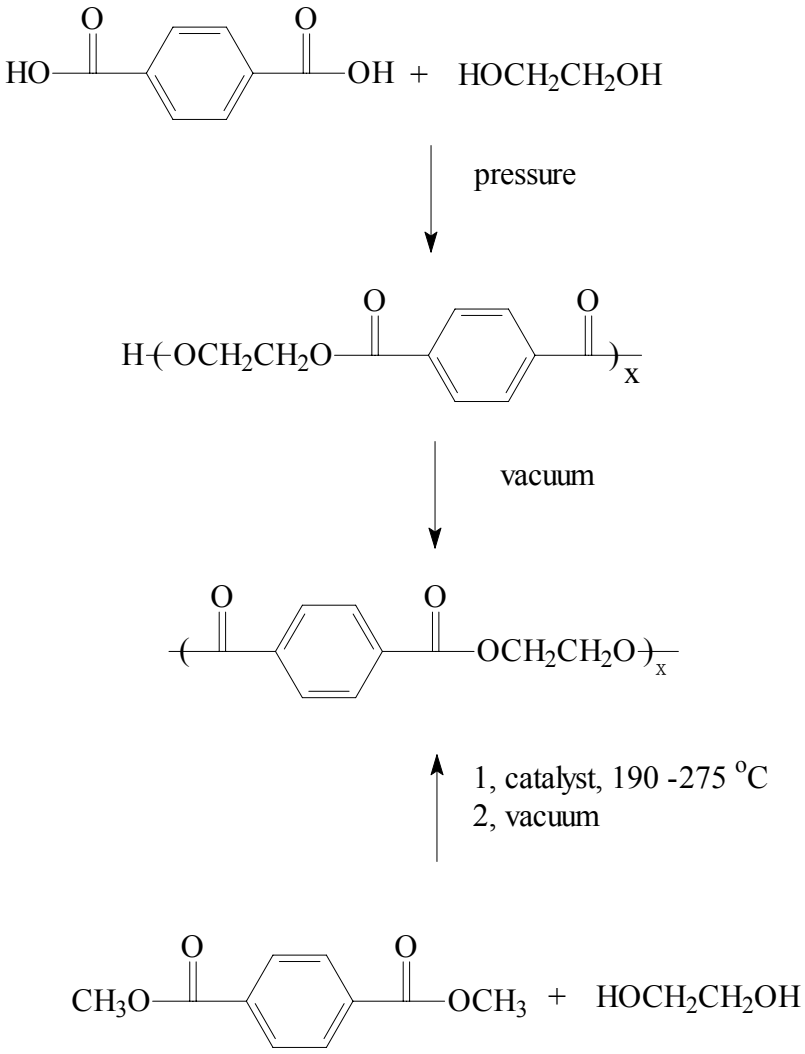

Scheme 1. 2 Synthesis of PET via melt polymerization[1]

---

[2]Goodman, I.; Sheanan, R. J. *Eur. Polym. J.* **1990,** 26, 1081.
[3]Goodman, I.; Rodriguez, M. T. *Macrol. Chem. Phys.* **1994,** 195, 1705.
[4]Lawton, E. L. *Polym. Eng. Sci.* **1985**, 25, 348.
[5]Youk, J. H.; Bolares, K. A.; Kambour, R. P.; MacKnight, W. J. *Macromolecules* **2000**, 33, 3594.
[6]Youk, J. H.; Bolares, K. A.; Kambour, R. P.; MacKnight, W. J. *Macromolecules* **2000**, 33, 3600.

1.3 PET copolymers

1.3.1 Ionomers

It is believed that the incorporation of a low level of ionic groups into PET will effectively improve the mechanic performance and compatibility with other substrates.[7-21] Random PET ionomers (Figure 1.2) are used to prepare fibers dyable with basic dyes, and fibers with antipilling and antistatic properties.[8] Even though Dupont commercialized PET ionomers in 1950's, the knowledge of the behaviors of PET ionomers is still limited.[7-21] Ostowska and coworkers investigated ionic aggregates of PET ionomers using FT-IR spectroscopy and DSC, and they found a sharp change in ionic aggregates, when the ionic level was higher than 5 mol%.[16-19] Greener and coworkers interpreted the rheological and dynamic-mechanic behaviors of PET random ionomers in term of restricted mobility model, which proposed that the clustering point was 10 mol%.[7] Small-angle X-ray scattering (SAXS) is one of the most powerful tools to investigate the ionic aggregates; however, results of SAXS analysis from various labs were not consistent.[3,20] Greener and coworkers observed the ionic peak at 8 mol%; however, Wolchowicz was not able to observe the ionic peak of the potassium salt PET ionomers.

---

[7]Greener, J.; Gillmor, J. R.; Daly, R. C. *Macromolecules* **1993**, 26, 6416. (b) Blanton, T. N.; Seyler, R. J. *Advance in X-ray Analysis*; Gilfrich, J. V., Ed.; Plenum Press: New York, **1993**; p379.
[8]Militky, J. *Modified Polyester Fibres*, Elsevier, Amsterdam, **1991**.
[9]Boykin, T. C.; Moore, R. B. *Polym. Eng. Sci.* **1998**, 38, 1658.
[10]Barber, G. D.; Carter, C. M.; Moore, R. B. *Polymeric Materials and Engineering* **2000**, 82, 241.
[11]Boykin, T. L.; Moore, R. B. *Polym. Pre.* **1998**, 39, 393.
[12]NG, C. W. A.; Macnight, W. J. *Macromolecules* **1996**, 29, 2421.
[13]NG, C. W. A.; Lindway, M. J.; Macknight, W. J. *Macromolecules* **1994**, 3027.
[15]Wlochowicz, A. J. *Macromol. Sci. Phys.* **1992**, B31, 239.

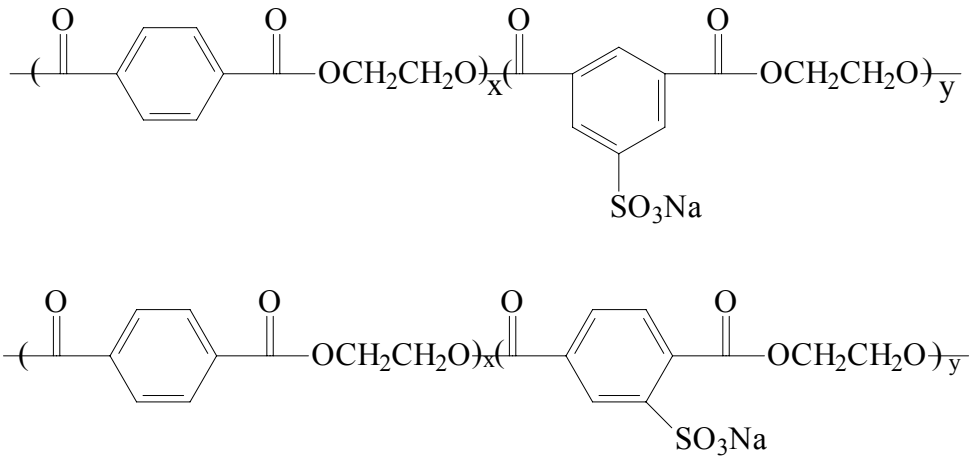

Figure 1.2 PET random ionomers[7]

Yu and coworkers prepared PETs with metal carboxylate end groups described in Scheme 1.3, and the ionic end groups formed ionic aggregates.[22] The presence of ionic aggregates performed as nuclear agents to increase the crystallization rate.

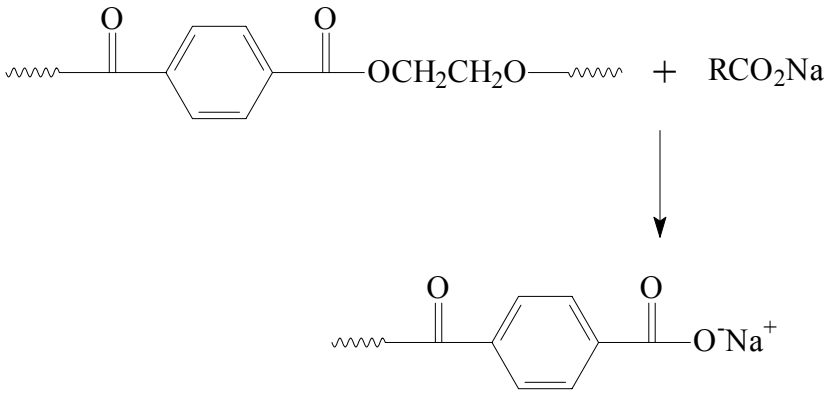

Scheme 1.3 Synthesis of PET with ionic end groups[22]

---

[16]Ostrowska-Czubenko, J.; Ostrowska-Gumkowska B. *Eur. Polym. J.* **1988**, 24, 65
[17]Ostrowska-Gumkowska, B.; Ostrowska-Czubenko, J. *Eur. Polym. J.* **1988**, 24, 803.
[18]Ostrowska-Gumkowska, B.; Ostrowska-Czubenko, J. *Eur. Polym. J.* **1991**, 27, 681.
[19]Ostrowska-Gumkowska, B.; Ostrowska-Czubenko, J. *Eur. Polym. J.* **1994**, 30, 875.
[20]Timm, D. A.; Hsieh, Y. L. *J. Appl. Polym. Sci.* **1994**, 34, 1291..
[21]Sinker, S. M. *U. S. Patent 4 554 238,* **1985**.

Long and coworkers reported the synthesis of PET ionomers containing terminal units derived from 3-sulfobenzoic acid, sodium salt (SSBA) via melt polymerization techniques.[23] DSC analysis demonstrated that the presence of ionic end groups significantly increased the crystallization half-time. A comparison of the crystallization half-time for telechelic ionomers versus non-ionomers demonstrated that ionic aggregation exerted a more profound effect in the diffusion-controlled regime (lower than 150 °C). Melt rheological analysis demonstrated that the ionic end groups increased the melt viscosity compared to non-ionomers at equivalent molecular weight, and ionic aggregation was more stable below 150 °C.

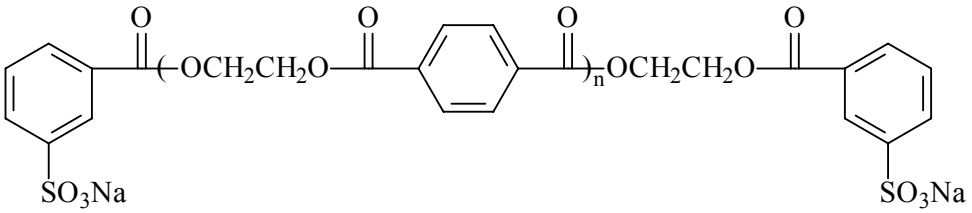

Figure 1.3 Structure of telechelic PET ionomer[23]

Endo and coworkers prepared PET ionomers with phosphonium biocides as counter ions of sulfonated moieties (Figure 1.4), and explored the surface antibacterial activity.[24] These PET films exhibited a high surface antibacterial activity against S. aureus and E. coli, particularly against S. aureus.

---

[22](a) Yu, Y.; Yu, Y.; Jin, M.; Bu, H. *Macro. Chem. Phy.* **2000**, 201, 1984. (b) Yu, Y.; Bu, H. *Macro. Chem. Phys.* **2001**, 202, 421.
[23]Kang, H.; Lin, Q.; Armentrout, R. S.; Long, T. E. *Macromolecules* **2002**, 38, 8738.
[24]Kanazawa, A.; Ikeda, T.; Endo, T. *J. Polym. Sci.: Part A, Polym. Chem.* **1993**, 31, 3003.
[25]Pohl, H. A. *J. Am. Chem. Soc.* **1951**, 73, 5660. (b) Marshall, I.; Todd, A. *Trans. Faraday. Soc.* **1953**, 49, 67.

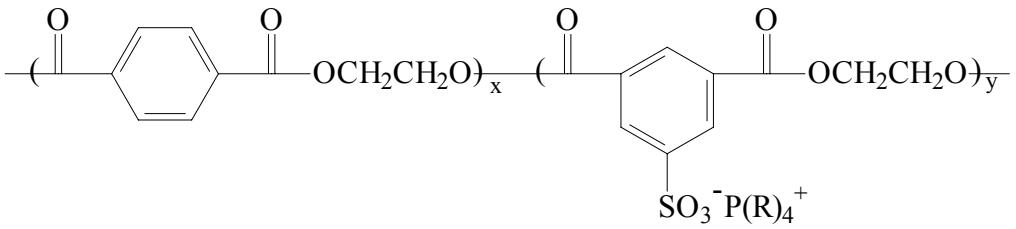

Figure 1.4 PET ionomers containing phosphonium salts[24]

1.3.2 Flame resistant PETs

Organic polymeric materials undergo thermal degradation when subjected to sufficient heat flux. In polyesters, the ester linkage is the point of primary chain scission leading to the formation of carboxylic acids and vinyl chain ends. In PET, pyrolysis starts with random chain scissions of ester bonds, which is promoted via the formation of a transition state of six member ring.[25-26] Halogenated compounds are widely used as fire retardants for polymeric materials, including PET.[27] Environmental concerns and the threat of toxic gas emissions during fires have created a considerable interest in finding environmentally friendly, nonfugitive alternatives to halogenated fire retardants. The use of reactive phosphorous-containing compounds that form a polymer-bound fire retardant appears to be an attractive solution. Phosphorous-containing compounds are generally involved in altering the pathway of thermal degradation via promoting solid-state reactions leading to carbonization.[28] Phosphoric acid formed during the degradation of phosphorous-containing polymers is also reported to reduce the permeability of the char, thus providing an enhanced barrier to air and fuel passage. Phosphorus-containing polymers and their synthesis have been well described in a review by Weil.[28] Several strategies have been utilized for producing fire-retardant polyesters with polymer bound phosphorus. Two of the most important and commercially successful approaches use

phosphorus in the form of the phosphinate group, in either the main chain or in the side chain.[2]

McGrath and coworkers first prepared phosphine oxide containing PETs as fire resistant materials. Compression molded materials showed a very low crystallinity and crystallization rate.[29] The copolymer containing 20 mol% phosphine oxide units was amorphous, and the char yield upon pyrolysis increased with an increased in the level of charged phosphine oxide content.

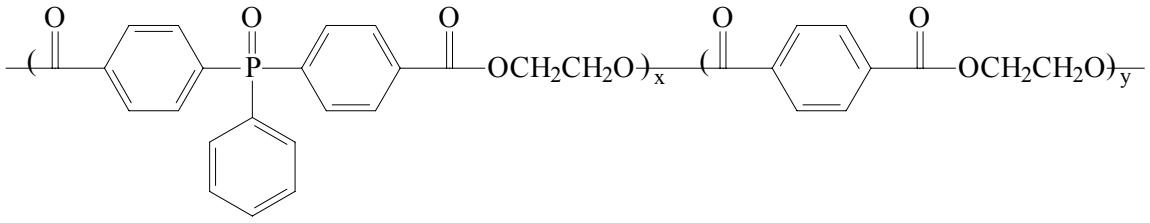

Figure 1.5 Phosphine oxide containing PET[29]

---

[26]Grassie, N.; Murray, E. *J. Poly. Deg. Stab.* **1984**, 6.
[27]Miller, D. R.; Ever, R. L.; Skinner, G. B. *Combust Flame* **1963**, 7, 137.
[28]Weil, E.D. *Handbook of Organophosphorus Chemistry*; Engel, R. E. Ed.; Marcel Dekker: New York, **1992**; Chapter 4, p. 683.
[29]Wan, I. Y.; Keifer, L. A.; McGrath, J. E.; Kashiwagi, T. *Polym. Prep.* **1995**, 36(1), 491.
[30] Chang, S.; Chang, F. *J. Appl. Polym. Sci.* **1999**, 72, 109.
[31]Asar, J.; Berger, P. A.; Hurlburt, J. *J. Polym. Sci.: Part A, Polym. Chem.* **1999**, 37, 3119.
[32]Yoshie, N.; Inoue, F.; Yoo, H. Y. Okui, N. *Polymer* **1994**, 35, 1931.
[33]Minoa, K.; Kawaabata, A.; Ozaki, Y. *J. Polym. Sci.: Part A.; Polym. Chem.* **2001**, 39, 665.
[34]Kint, D. P. R.; De Ilarduya, M.; Munoz-Guerra, S. *J. Polym. Sci.: Part A, Polym. Chem.* **2000**, 38, 1934.
[35]Somlai, L. S.; Mathias, L. J.; Schiraldi, D. A. *Polym. Prep.* **2000**, 41(1), 56-57.
[36]Saliba, K. R.; Connor, D. M.; Schiraldi, D. A.; Collard, D. M. *Polym. Prep.* **2002**, 43(1), 396.

PET-co-poly(ethylene DDP)s were synthesized based on 9,10-dihydro-9-oxa-10-phosphaphenanthrene-10-oxide (DOP), itaconic acid, terephthalic acid, and ethylene glycol (Scheme 1.4).[30] H_2PtC1_6 was a highly efficient catalyst to improve the DDP conversion.[30] The reaction of the DOP with the itaconic acid was proceeded at a significantly lower temperature (110 ^oC) in a high conversion (> 98%). The presence of the bulky pendent phosphorus side groups in the copolyesters tended to decrease the structural regularity, and retard the crystallization. The formation of a protected char layer for the phosphorus-containing copolyesters raised the decomposition temperature under an oxygen atmosphere. The limiting oxygen index values of all phosphorus-containing copolyesters were higher than 33. Higher phosphorus content resulted in decreasing crystallinity, lower melting temperature, lower decomposition temperature, as well as lower tensile strength, but increasing residual char after thermal degradation and higher limiting oxygen index value. The rheological behavior of copolyesters were similar to that of PET.

---

[37]Collard, D.; Allen, S. D. *Book of Abstract, 217 ACS National Meeting* **1999**, 327.
[38]Collarf, D.; Allen, S. D. *Polym. Prep.* **1999**, 40(1), 607.
[39] Hudson, N.; MacDonald, W. A.; Neilson, A.; Richards, R. W.; Sherrington, D. C. *Macromolecules* **2000,** 33, 9255.

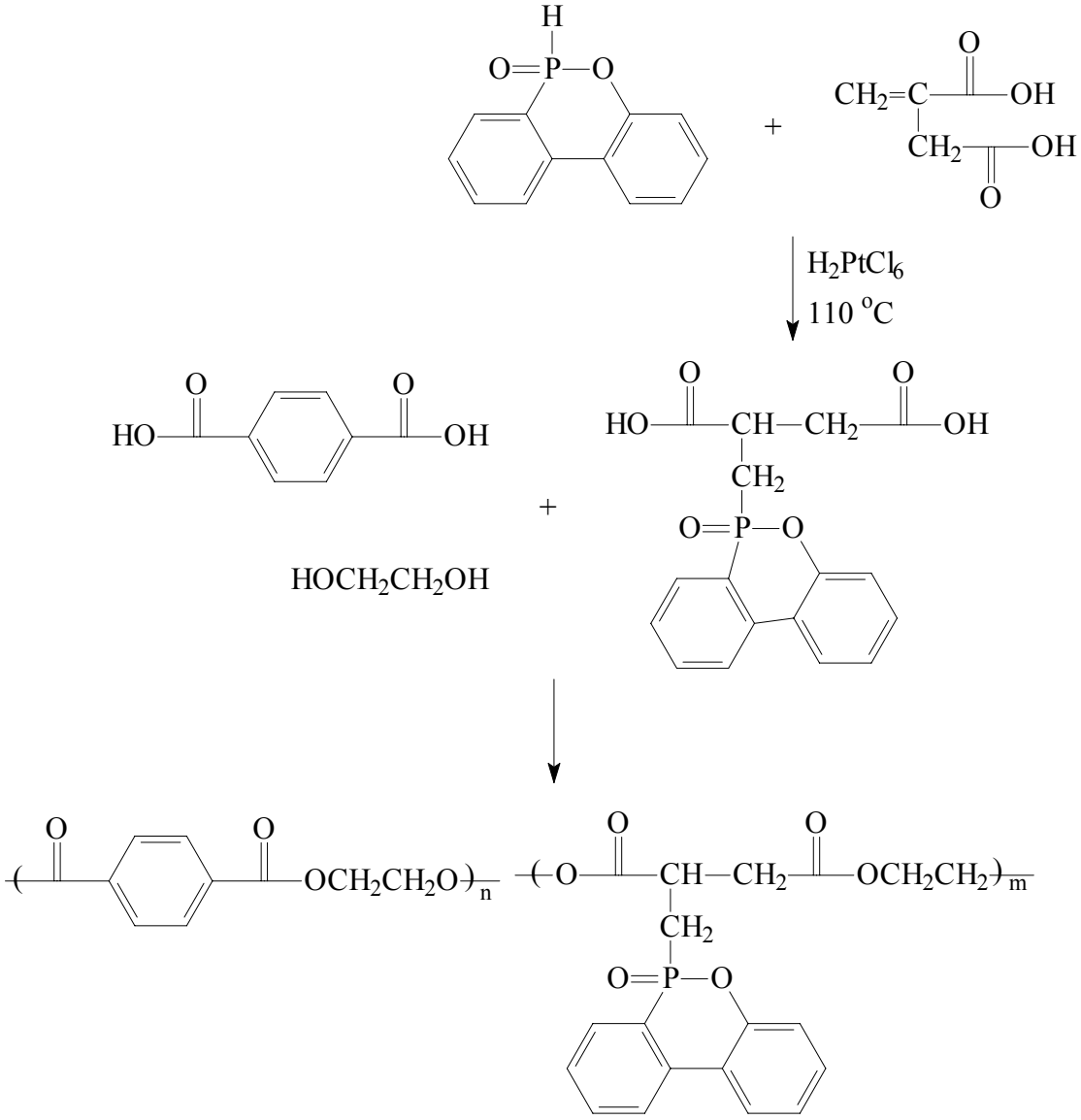

Scheme 1.4 Synthesis of phosphine oxide containing PETs[30]

CEPP, 2-carboxyethyl phenyl phosphinic acid, was used as reactive fire retardant incorporated into PETs.[31] Copolymers containing very high levels of CEPP were prepared. Although fire retardancy was achieved at relatively low levels of CEPP, copolymers with high levels of phosphorous made them very attractive as polymeric nonfugitive fire retardants for other polymers and various polymer blends. An increase in

aromaticity gained via incorporating 4,4'-biphenyldicarboxylic acid led to higher limiting oxygen index values.

1.3.3 PET copolymers with a slow crystallization rate

PET copolymers containing aliphatic six-member rings are important polyester materials in the market, which are synthesized using 1,4-cyclohexanedimethanol or 1,4-cyclohexenedimethylene terephthalate as a comonomer.[32-33] These copolymers exhibited a low crystallinity due to the presence of aliphatic ring.

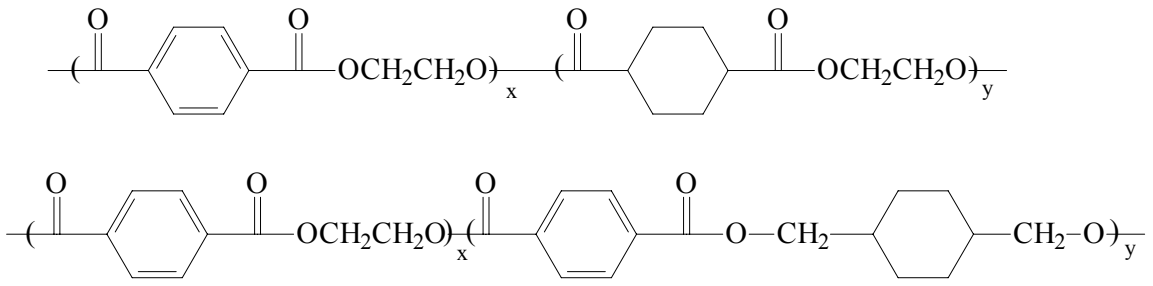

Figure 1.6 Structures of PET copolymers containing six member aliphatic rings[32-33]

Poly(ethylene terephthalate-co-5-nitroisophthalate) (PETNI) was prepared via two-step melt copolycondensation of bis(2-hydroxyethyl) terephthalate with bis(2-hydroxyethyl)-5-nitroisophthalate at monomer molar ratio 95/5 to 50/50.[34] Polymerizations were carried out at 200 - 270 ^{o}C. The copolyesters crystallized to a lower extent, and showed a steady reduction in melting temperature with an increase in nitroisophthalate content. Glass transition temperature of copolymers was higher than that of PET with a maximum value of 85 ^{o}C for the 50/50 copolymer. PETNI copolyesters were stable to 300 ^{o}C, and thermal degradation occurred in two well-differentiated steps.

Poly(ethylene terephthalate/5-adamantylisophthalic acid) copolyesters were synthesized using DMT and ethylene glycol via transesterification to produce novel pendent adamantyl containing polymers.[35] A linear increase in glass transition temperature and a decrease in melt temperature were observed with an increasing in the level of 5-adamantylisophthalic acid. However, the decomposition temperature remained unchanged.

The crystallinity of PET was reduced via the incorporation of norbornanedicarboxylate monomer units.[36] Terpolymers based on 25% cis-norbornane-endo-2,3-dicarboxylic anhydride or di-methyl trans-norbornane-2,3-dicarboxylate were prepared. These monomers were more effective than 1,4-cyclohexanedimethanol for suppressing crystallization.

1.3.4 Crosslinkable PET copolymers

PET copolymers containing 2,6-anthracenedicarboxylate units were crosslinked via irradiation at 350 nm.[37] The crosslinking was attributed to face-to-face dimerization of the anthracene units and radical reactions. Whereas model anthracene photodimers were cleaved in solid films of PET via irradiation at 254 nm, photoreactions of the polymeric anthracenes were irreversible under these conditions.

Novel PET copolymers based on DMT, ethylene glycol and 5,5-bis(hydroxymethyl)-2-phenyl-1,3-dioxane were synthesized, and then treated with diluted aqueous acid to prepare polymers with hydroxyl groups for crosslinking.[38] Crosslinking was achieved via thermal and photochemical addition reactions involving 2,6-anthracenedicarboxylate units in copolyesters.

1.3.5 Branched PETs

Rheology plays a key role in the properties of the final polymeric products, and even more sophisticated control of rheology may allow even wider technological applications.[39] The manipulation of backbone architecture is one of important ways to control the rheology of PET.[39] Manaresi and coworkers laid a scholarly foundation for the research of branched PETs.[40] Complementary work by Langla and Strazielle included the determination of absolute molecular weights from light scattering and membrane osmometry, but the distributions of molecular weights probed were rather restricted.[41]

The branched PETs produced by Rosu and coworkers were prepared not only with a branching comonomer but also in the presence of a monofunctional endcapper.[42] The objective was to use rather high levels of branching reagent but to inhibit gelation by using an endcapper. The materials prepared were deliberately of low molecular weights, and used subsequently in solid state polymerizations. Branched PETs with a rather narrow range of molecular weights were also reported recently by Hess and coworkers.[43] Those branched PETs were designed specifically for higher spinning speeds without inducing major changes in fiber properties.

---

[40] Manaresi, P.; Parrini, P.; Semeghini, G. L.; de Fonasari, E. *Polymer* **1976**, *17*, 595.
[41] Langla, B.; Strazielle, C. *Makromol. Chem.* **1986**, *187*, 591.
[42] Rosu, R. F.; Shanks, R. A.; Bhattacharya, S. N. *Polym. Int.* **1997**, *42*, 267.
[43] Audoly, L.; Cooper, D.; Weis, C. D.; Morris, K.; Johnson, C.; Hess, C.; Hirt, P.; Oppermann, W. *J. Appl. Polym. Sci.* **1999**, *74*, 728.
[44] Mougenot, P.; Marchand-Brynaert, J. *Macromolecules* **1996**, 29, 3552.
[45] Zhao, Q.; McNally, A. K.; Renier, M.; Wu, Y.; Rose-Caprara, V.; Anderson, J. M.; Hiltner, Urbranski, A. P.; Stokes, K. *J. Biomed. Mater. Res.* **1993**, 27, 379.
[46] Chen, W.; McCarthy, J. *Macromolecules* **1998**, 31, 3648.
[47] Cohn, D.; Stern, T. *Macromolecules* **2000**, 33, 137.

1.3.6 Modification of the surface of PET

One of major potential applications of PET materials is used as biomaterials, and the interface generated between implants and their physiological environment plays a crucial role in determining their biological performance.[44] This pertains to complex chemical, physical, and biological phenomena taking place on the surface of the implanted system.[45-46] In the case of blood-contacting implants, their surface thrombogenicity and long term biodurability are of special concerns.[47]

Protein adsorption and cell adhesion processes play a fundamental role in determining the hematological response elicited by prostheses implanted in the cardiovascular system.[48-49] The biomaterial's surface chemistry largely dictates the hemocompatibility of the implant's blood-facing surface.[50-51] The in vivo degradation of implanted polymers is attributed to diverse mechanisms, such as stress cracking, enzymatic attack, oxidative degradation, metal ion induced oxidation, and simple hydrolysis.[50-52] Therefore, tailoring the prosthesis surface plays a focal role in minimizing the thrombogenicity and enhancing the long-term biodurability of blood-contacting implants. One of methodologies to enhance the hemocompatibility of polymeric surfaces is via glow discharge treatments, and different approaches are developed. [53-56] Plasma treatments using polymer-forming perfluoromonomers such as tetrafluoroethylene (TFE), have been reported.[55] Glow discharge was also used to introduce various functional groups into different polymeric substrates, via using ammonia, allylamine, and allyl alcohol plasma treatments, or creating a plasma-induced free radical-containing substrate, subsequently exposed to decylamine hydrochloride or SO_2 gas. [56]

Stern and Cohn tailored the surface of PET via a multistep process using two consecutive plasma treatments, followed by derivatization reactions.[61] In the first step, tetrafluoroethylene (TFE) was plasma polymerized, generating a highly cross-linked perfluoric surface layer. The next step introduced amine groups into the plasma polymer, via exposing the surface to plasma of ammonia. The reactive amine moieties were used as anchoring sites for further derivatization. Finally, poly(ethylene glycol) (PEG) chains were grafted onto the surface via a hexamethylene diisocyanate (HDI) spacer. The ESCA spectrum of treated PET revealed a layer of CF_2 and CF moieties on the surface, as demonstrated as the large peaks appearing at 291.1 and 289.5 eV, respectively. As expected, substantial amounts of nitrogen could be seen after exposing the surface to a plasma of ammonia, as revealed as the large N_{1s} peak at 402.0 eV. ESCA also demonstrated the presence of PEG chains bound to the surface. These findings were confirmed using FTIR spectroscopy and water contact angle measurements. Special attention was given to the absorption bands of the CF groups and ether bonds belonging to the fluorinated plasma polymer and the PEG chains, respectively, as well as to the characteristic N=C=O band (2272 cm^{-1}). While the water contact angle of untreated PET was 76 ^{o}, it increased sharply after the fluorinated layer was created (93 ^{o}), decreasing drastically (to less than 20 ^{o}) once the highly hydrophilic PEG chains were grafted on the surface.

---

[48]Hastings, G. W. *Cardiovascular Biomaterials*; Springer-Verlag: London, **1992**.
[49] Bamford, C. H.; Al-Lamee, K. G. *Clin. Mater.* **1992**, 10, 243.
[50]Stokes, K. B. *Polyurethanes in Biomedical Engineering*; Plank, H., Egbers, G., Syre, I., Eds.; Elsevier: Amsterdam, **1984**; pp 243-255.
[51]Zhao, Q.; McNally, A. K.; Renier, M.; Wu, Y.; Rose-Caprara, V.; Anderson, J. M.; Hiltner, Urbanski, A. P.; Stokes, K. *J. Biomed. Mater. Res.* **1993**, 27, 379.

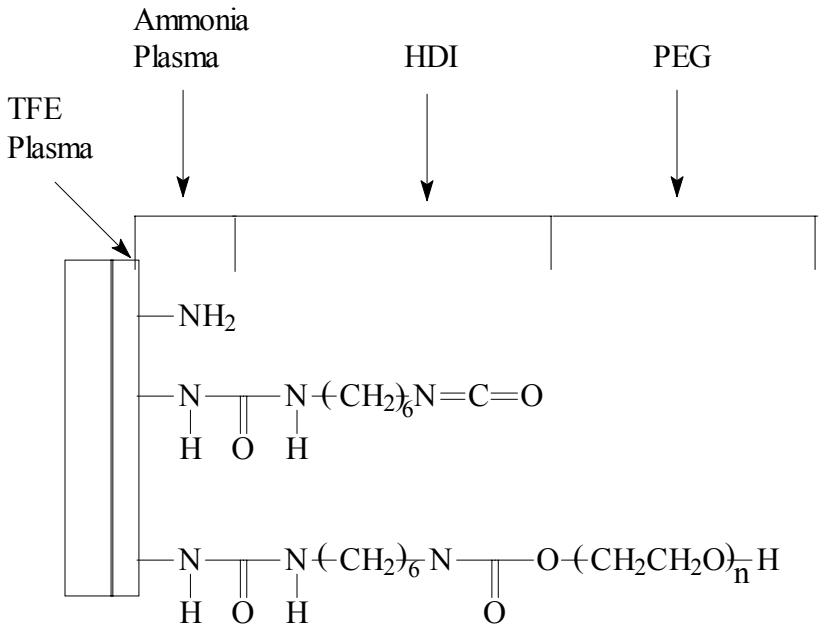

Figure 1.7 Modification of PET surface[61]

---

[52]Takahara, A.; Coury, A. J.; Hergenrother, R. W.; Cooper, S. L. *J. Biomed. Mater. Res.* **1991**, 25, 341-356.
[53]Ito, Y.; Suzuki, K.; Imanishi, Y. *ACS Symposium Series (Polymers of Biological and Biomedical Significance)* **1994**, 540, 66.
[54]Marchant, R. E.; Danilich, M. J. *Polym. Prepr* **1993**, 34 (1), 655.
[55]Hoffman, A. S *J. Appl. Polym. Sci.* **1988**, 42, 251.
[56]Hook, D. J.; Vargo, T. G.; Gardella, J. A.; Litwiler, K. S.; Bright, F. V. *Langmuir* **1991**, 7, 142.
[57]Yasuda, H.; Hsu, T. *J. Polym. Sci., Polym. Chem.* **1978**, 16, 415.
[58]Sipehia, R.; Chawla, A. S.; Chang, T. M. S. *Biomaterials* **1986**, 7, 471.
[59]Gombotz, W. R.; Hoffman, A. S. *J. Appl. Polym. Sci.: Appl. Polym. Symp.* **1988**, 42, 85.
[60]Giroux, T. A.; Cooper, S. L. *J. Appl. Polym. Sci.***1991**, 43, 145.
[61]Cohn, D.; Stern, T. *Macromolecules* **2000,** 33, 137.

1.4 Liquid crystalline BB-n polyesters

1.4.1 Introduction

The difference between crystals and liquids, two common condensed matter phases, is that the molecules in a crystal are ordered whereas in a liquid they are not. The order in a crystal is usually both positional and orientation, in that the molecules are constrained both to occupy specific sites in a lattice and to point the molecular axes in specific directions. The molecules in liquid, on the other hand, diffuse randomly throughout the sample container with the molecular axes tumbling wildly. Interestingly enough, many phases with more order than presenting in a liquid, but less order than typical of crystals also exist in nature (Figure 1.8).[62] These phases are grouped together and called liquid crystal, since they share properties normally associated with both liquid and crystal phases.

---

[62]Collings, P. J.; Hird, M. *Introduction to Liquid Crystals, Chemistry and Physics*; Taylor & Francis Ltd, **1997**.
[63]De Gennes PG, *C. R. Acad. Sci. (Paris)* **B 281**, 101 (1975).
[64]Goodman, I. *Encyclopedia of Polymer and Engineering*; John Wiley & Sons, **1988**; v12, p56.
[65]Krigbaum, W. R.; Asrar, J.; Ciferri, A.; Preston, J. *J Polym Sci: Polym Lett Edi.* **1982**, 20, 109.
[66]Watanabe, J.; Hayashi, M.; Kinoshita, S.; Nakataj, Y.; Niori, T.; Tokita, M. *Prog. Polym. Sci.* **1997**, 22, 1053.
[67]Krigbaum, W. R.; Watanabe, J.; Ishikawa, T. *Macromolecules* **1983**, 16, 1271.
[68]Maeda, Y.; Mabuchi, T.; Watanable, J. *Thermochim. Acta* **1995**, 26, 189.
[69]Krigbaum, W. R.; Wantanabe, J. *Polymer* **1983**, 24, 1299.
[70]Watanabe, J.; Hayashi, M. *Macromolecules* **1988**, 21 278.

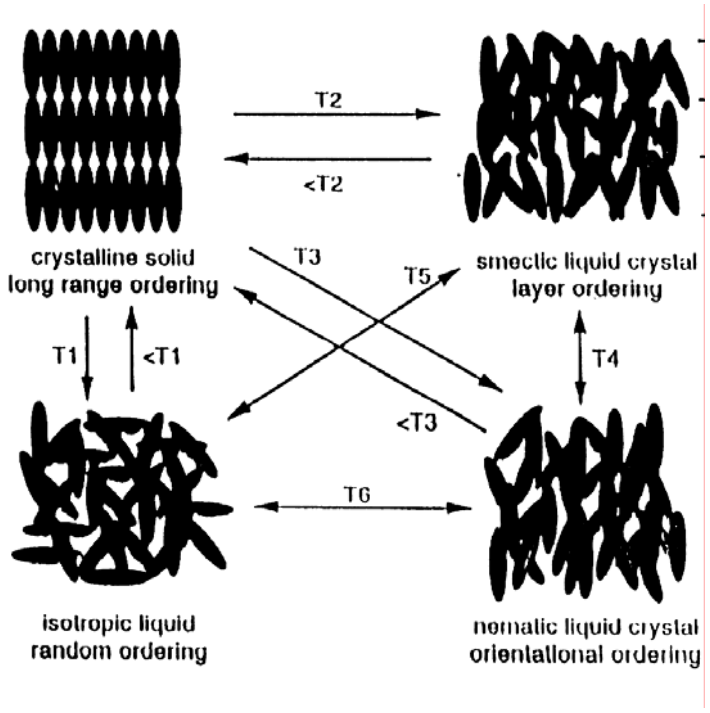

Figure 1.8 Possible melting sequences for a liquid crystalline material[62]

1.4.2 BB-n liquid crystalline polyesters

In 1975, de Gennes suggested that liquid crystalline (LC) polymers might be prepared via incorporating a rigid and a flexible segment in the repeating unit like Figure 1.9.[63] Since that time a number of scientist have reported synthesis and characterization of LC polymers using this concept.[64-66] This family of main chain LC polymers have attracted much attention owing to their scientific interest and numerous industrial applications.[64-66] The thermotropic LC polymers, whose backbones are composed of both methylene spacer and mesogenic moiety, such as 4,4'-dihydroxybipenyl, or 4,4'-biphenyldicarboxylate, were studied extensively for their very interesting liquid crystalline characteristics.[67-68] The biphenyl group is the simplest mesogen with linearity and high symmetry. Their thermal stability is also guaranteed in

the temperature range up to 300 ^{o}C. These characteristics make it easy to investigate the relationship between the structure and properties. This review will focus on describing the achievement in the research of the LC polyesters (Figure 1.10) whose backbones are composed of methylene spacer and 4, 4'-biphenyldicarboxylate. These LC polyesters are usually termed as BB-n, and n denotes the number of methylene spacer. For BB-n LC polyesters, a simple trend is seen that the mesophase temperature region decreases with increasing n, and finally the mesophase disappears when n exceeds 10.[66]

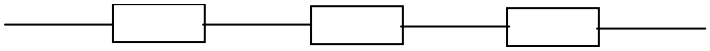

Figure 1.9 Structure of a semiflexible main chain liquid crystalline polymer[66]

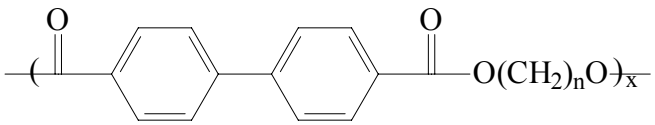

Figure 1.10 BB-n Liquid crystalline polyester, (n: Carbon number of alkylene spacer)[67]

1.4.3 Odd-even oscillation in LC properties

The LC phases of BB-n series are assigned to the smectic phase based on the X-ray observation of the sharp inner layer reflection and outer broad reflection, and also from the microscopic observation of the fan shape textures.[69-70] The odd-even oscillation in the melting temperature, isotropic temperature and smectic spacing was observed in DSC and X-ray analyses (Figure 1.11 and Figure 1.12).

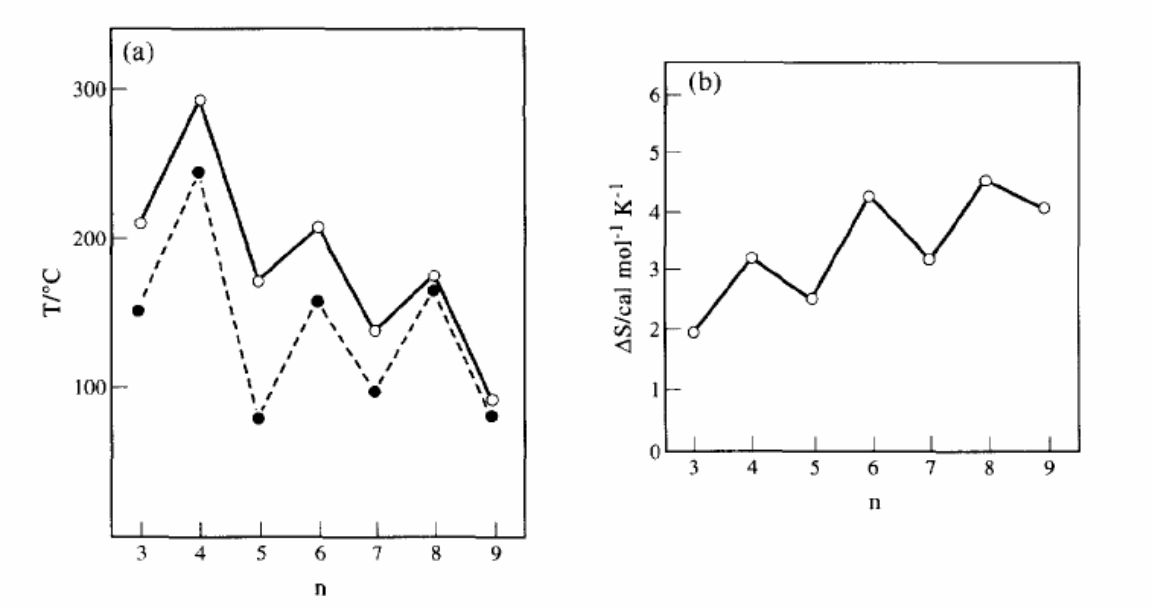

Figure 1.11 Variation with carbon number of alkylene spacer (n) of (a) transition temperatures (bottom: crystal-LC transition; top: isotropization of liquid crystal) and (b) isotropization entropy of liquid crystal.[69]

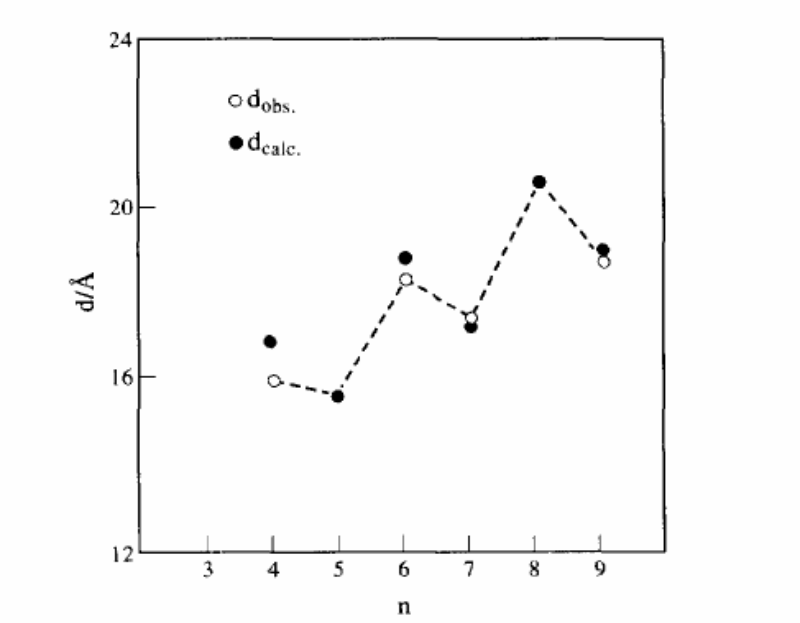

Figure 1.12 Variation of smectic layer thickness(top) with n. The calculated layer thickness (bottom) corresponds to the distance between the mesogenic groups averaged over the confined conformers with small displacement of successive mesogens.[69]

The most striking feature in this system is that the smectic LC structure also depends on the odd-even parity of n.[69-70] This was initially realized from X-ray diffraction observations of oriented fiber specimens. Figure 1.13 shows X-ray diffraction patterns of the oriented smectic phase of BB-5 and BB-6, representative of even- and odd –member polymers, respectively. In BB-6, the layer reflections were located on an equatorial line. This diffraction geometry unambiguously indicated a smectic A structure, in which the mesogenic groups forming a layer were arranged parallel to the polymer chain. BB-5 exhibited a different X-ray pattern. The broad outer reflections were split into two portions lying above and below the equator, while the layer reflections appeared on a meridional line as in BB-6. In this case, the layer packing structure was illustrated such that the polymer chains were perpendicular to the layer as in BB-6, but the mesogenic groups were tilted to the layer normal. The tilt angle was independent of temperature and estimated at ~25^{o} from the splitting angle of the broad reflection. The structure is similar to smectic C (S_c). As a conclusion, the even series of BB-n form an S_a, in which both axes of polymer chain and mesogenic group lie perpendicular to the layer, while the odd-number ones form the smectic phase S_{ca}, in which the polymer chain perpendicular to the layer but the mesogenic groups are tilted to the layer in an alternate fashion.

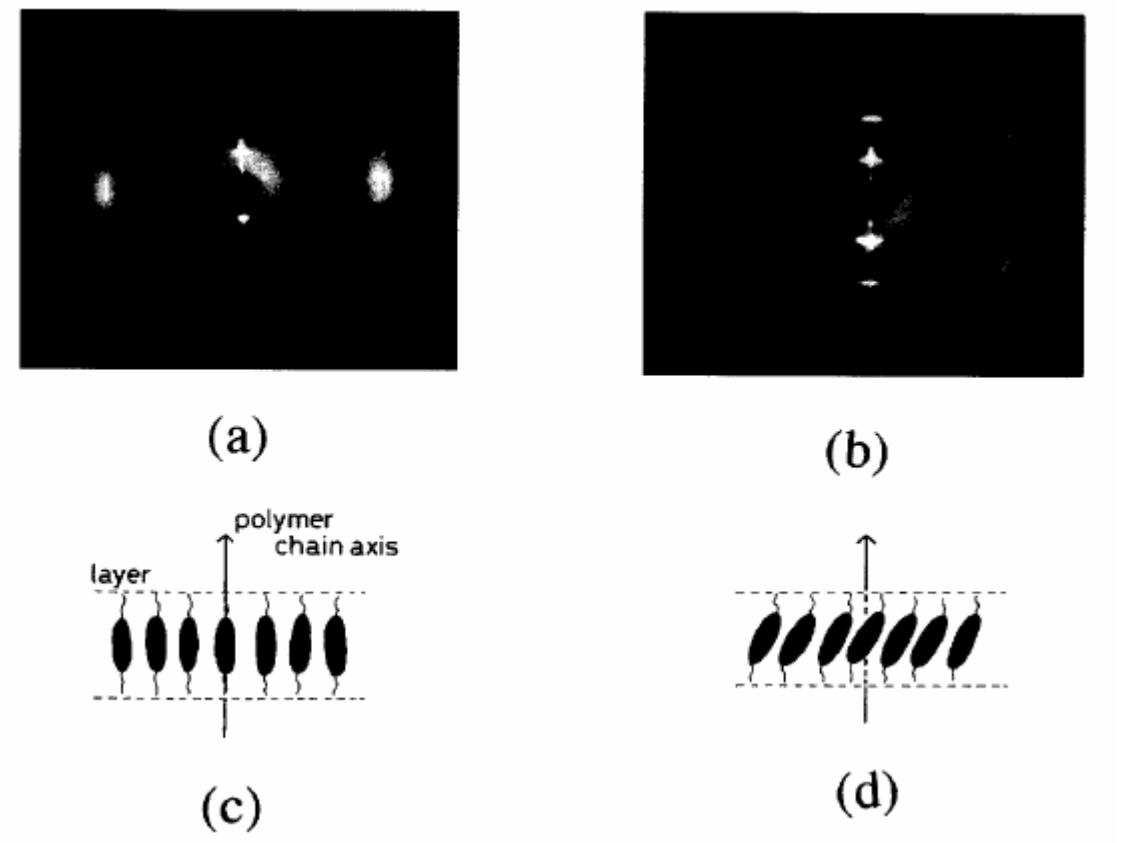

Figure 1.13 Oriented X-ray patterns of fibrous smectic phases of (a) BB-6 and (b) BB-5, (c), (d) Packing structures of mesogenic groups within a layer elucidated from the X-ray patterns.[69]

1.4.4 BB-m-n Copolymers

The most common copolymers of BB-n LC polyesters are BB-m-n copolymers, which are prepared via charging two diols in the system. The number of m and n exerted a pronounced effect on the LC structures and properties. When n and m are even, BB-4-8 and BB-4-10 formed S_a LC structures. However, in BB-4-10 system, a nematic LC phase was induced in the high level of BB-10 units.[66] The properties of copolymer BB-m-n

with odd m and odd n was also investigated using BB-5-9 as a model polymer, and the incorporation of two repeating units with different odd number did not significantly disrupt the structure of the S_{ca} phase.[66] BB-5-6 was used as a model polymer of the system composed of two diols with even and odd methylene units respectively, and the phase behavior is depicted in Figure 1.14.[66] Unlike preceding systems (even-even, odd-odd), an eutectic-like depression occurred in the isotropization temperature of the smectic phase. Irrespective of the small difference in the length of diols, the S_a phase of BB-6 and the S_{ca} of BB-5 were destabilized, when the other comonomer unit was added, showing that the two repeating units differing in even-odd nature were essentially incompatible in the smectic phase due to the conformation constraint.

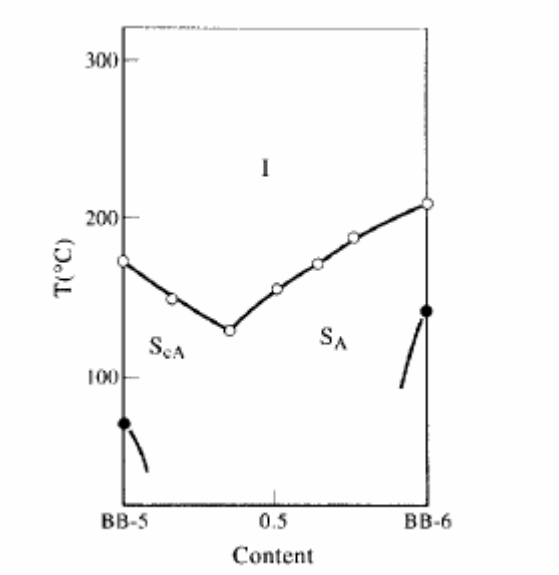

Figure 1.14 Composition dependence of phase behavior in BB-6-5 copolymers.[66]

1.4.5 Research on BB-nDMT and BB-nDMI copolymers

The structures of BB-nDMT and BB-nDMI copolymers are depicted in Figure 1.15. Krigbaum first synthesized BB-nDMT copolymers.[71-72] Ma and coworkers made a detail research on this family of copolymers, and four series of copolyesters, BB-6DMT, BB-5DMT, BB-6DMI and BB-5DMI were synthesized via melt polycondensation of dimethyl 4,4'-biphenzoate (BB) with dimethyl phthalate (DMT: dimethyl terephthalate or DMI: dimethyl isophthalate) and 1,6-hexanediol or 1,5-pentanediol.[73] The incorporation of the comonomer units significantly disrupted the regularity of the smectic structure. All BB-6DMT copolyesters were semicrystalline polymers. As x, the molar fraction of the phthalate units in the diacid units, > 0.7, the mesophase of the BB-6DMT copolymer was destroyed completely. For BB-5DMT, the mesophase disappeared as $x > 0.4$, and the copolymers became amorphous as $0.5 < x < 0.8$. The BB-6DMI copolyester lost mesophase and crystallinity as $x > 0.5$. The BB-5DMI copolyester lost the mesophase as $x > 0.3$, and become amorphous as $x > 0.4$. These results indicated that the non-liner isophthalate unit destroyed the mesophase and crystallinity of polyesters in a greater extent than the para-linked terephthalate unit.

---

[71]Krigbaum, W.R.; Taga, T. *Mol. Cryst. Liquid Cryst*. **1974**, 28, 85.
[72]Krigbaum, W. R.; Barber, P. G. *Acta Crystallogr. Sect. B* **1971**, 27,1844.
[73]Tseng, H.T.; Hsing, T.; Ma, C. M. *Macromol. Chem. Phys.* **1996**, 197, 2155.
[74]Watanabe, J.; Hayashi, M.; Atsushi, A.; Tokita, M. *Macromolecules* **1995**, 28, 8073.

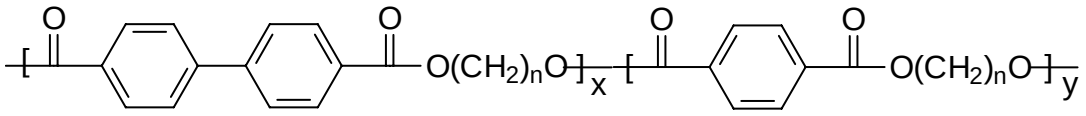

BB-nDMT

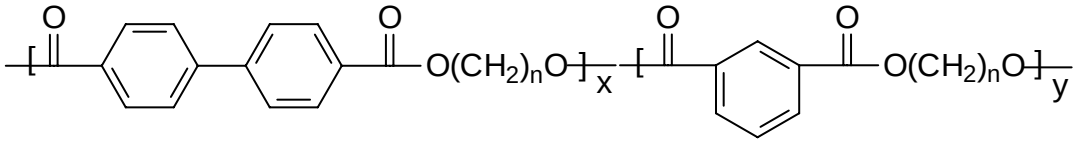

BB-nDMI

Figure 1.15 Structures of BB-nDMT and BB-nDMI[73]

1.4.6 Chiral BB-n Copolymers

A series of chiral BB-4 copolymers were also synthesized (Figure 1.16), and their thermotropic behaviors are listed in Table 1.1.[74] A pronounced effect of the presence of branched chiral methyl groups in diols on the LC properties was observed. One branched chiral methyl group in diol altered S_a phase of BB-4 to S_c phase, while two branched chiral methyl groups resulted in a nematic phase. The introduction of branched chiral methyl group into the chain of BB-n (n is even) not only changed the smectic phase from S_a to S_c, but also formed a new LC phase, chiral S_c (S_c*).

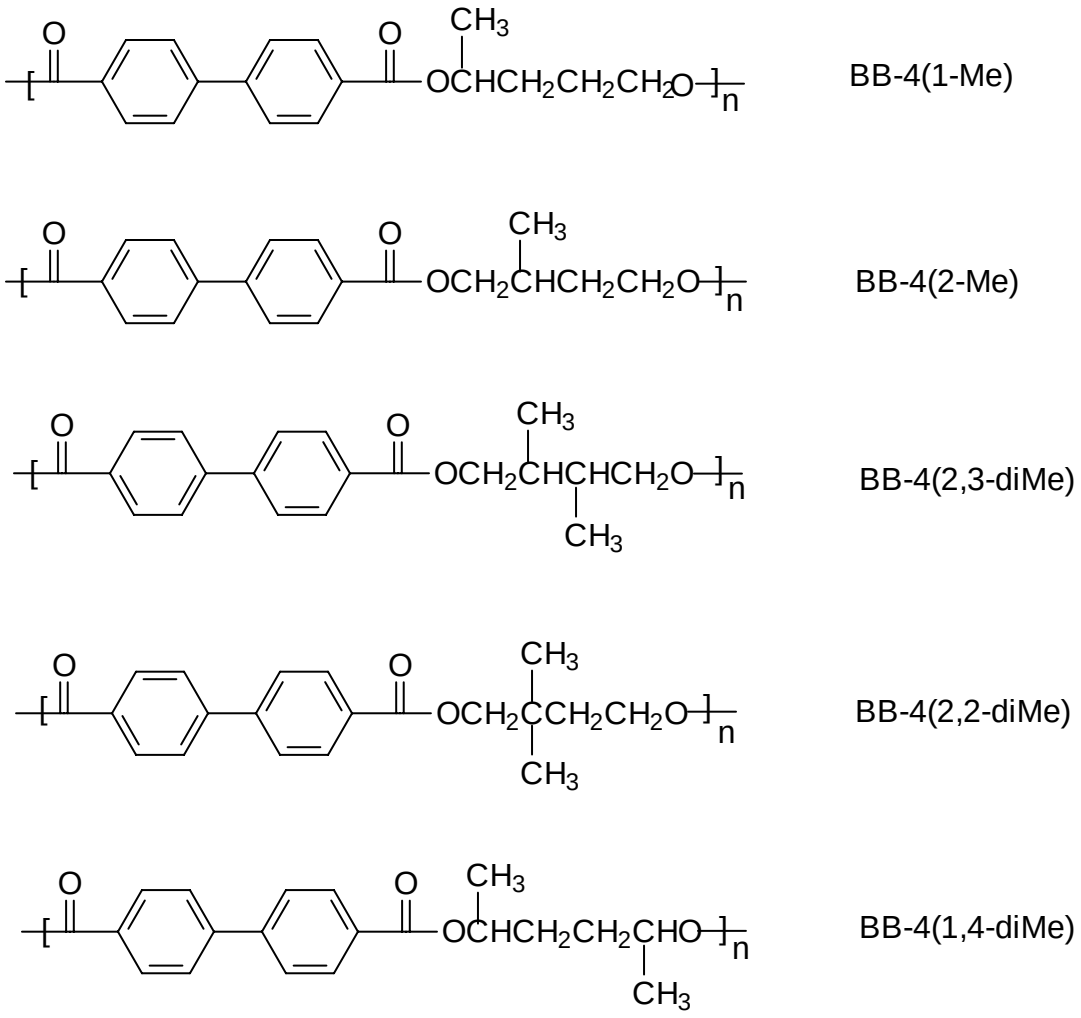

Figure 1.16 Structure of BB-4 copolymers with chiral methylene[74]

BB-4*(2-Me) formed monotropic S_c* from 185 to 140 ^oC only on cooling; however, BB-4*(2-Me) and BB-6{BB-4(2-Me)-6} formed S_c* both on heating and cooling. The x-ray observation revealed the structures of S_c phase. The dechiralization lines attributable to the helical twisting were also observed in copolymers with a low chiral content. On the other hand, in the copolymers with a higher chiral content, the selective reflection of visible light was observed, which indicated the existence of

helical structure. For all specimens, the helical pitch was less dependent on the temperature.

Table 1.1 Liquid crystalline phase behaviors of chiral BB-4 copolymers[74]

Sample	η (dl/g)	S_c	S_a	Nematic
BB-4	0.32	NO	YES	NO
BB-4(2-Me)	0.41	YES	NO	NO
BB-4(1-Me)	0.40	YES	NO	NO
BB-4(2,3-diMe)	0.45	NO	NO	YES
BB-4(2,2-diME)	0.42	NO	NO	YES
BB-4(1,4-diME)	0.35	NO	NO	NO

The most interesting property of S_c* materials is ferroelectric properties, which means the polymer chains can align with an electric field leading to potential applications as LC displays. The ferroelectric properties of S_c* phase was also observed in low molecular weight BB-4 copolymers, which originated from the transition from S_a to chiral S_c*. The value of Ps (spontaneous polarizability determined via switching current) of transition increases with decreasing temperature, and the maximum value of Ps is ~12 nC/cm.

1. 5 Ionomers

1.5.1 Introduction

Ionomers are conventionally defined as ion-containing polymers with a maximum ionic group content of approximately 15 mol %, and recognized as important engineering materials utilized in applications ranging from adhesives to fuel cell membranes.[75] Due to the electrostatic interactions and thermodynamic immiscibility between ionic groups and the polymer matrix (typically non-polar hydrocarbons), ionic groups tend to aggregate. Several models were proposed to describe the ionic aggregates, and the most

acceptable one was Eisenberg-Hird-Moore (EHM) model.[75] The basic premise of this model is that ionic units aggregate into multiplets consisting typically 2-8 ionic pairs, which is call the "core" (Figure 1.17). The chains held to the multiplets will have a lower mobility than that of free chains to form "corona". The thickness of the layers of reduced mobility is expected to be of the order of the persistence length of polymer chains. The size of the core /corona entity is too small (< 5 nm) to form a distinct phase, and its effect is limited to physical crosslink. As the ionic content increased, the number of multiplets grows, and the restricted mobility "coronas" of neighboring multiplets start to overlay and coalesce until a point is reached, where a continuous region of restricted mobility is forced, which is sufficiently large to be considered as a distinct phase with a distinct glass transition and relaxation spectrum (Figure 1.17). This aggregates of the neighbor multiplets are called clusters, and the ionic concentration of the formation of ionic clusters is termed as clustering point.

---

[75]Eisenberg, A; Kim, J. S. *Introduction to Ionomers,* John Wiley & Sons: New York, **1998**.

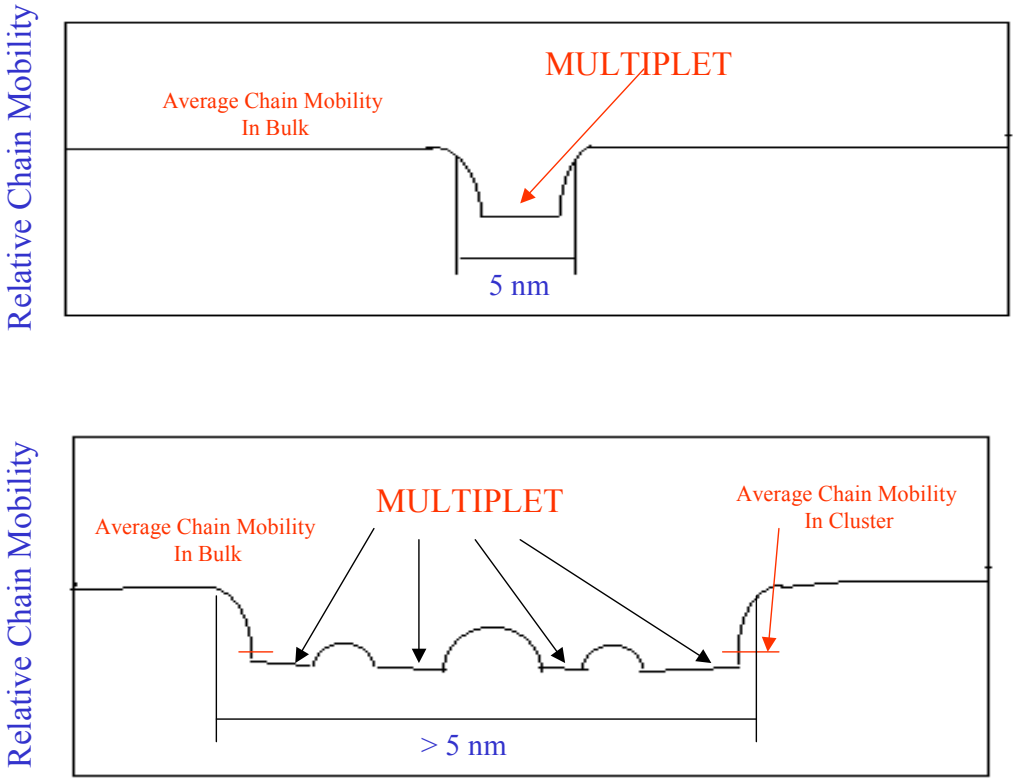

Figure 1.17 Structures of multiplet and ionic cluster[75]

Several factors exerted pronounced effects on the properties of ionomers, such as the composition of backbone, counter ions, and architectures. Previous researches demonstrated that a small change in these factors always resulted in a dramatical change in the properties. The major architectures of ionomers are depicted in Figure 1.18.[75] This review will focus on the synthesis of novel ionomers with different architectures.

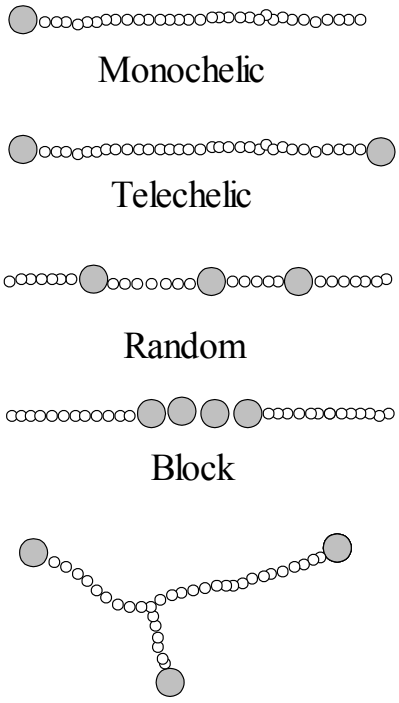

Figure 1.18 Ionomers with different architectures[75]

1.5.2 Ionomers derived from high performance polymers

Recently, the synthesis of high performance polymers containing ionic groups attracted a great interest due to their potential applications as membranes in fuel cells and gas seperation.[76] Sulfonated poly(arylene ether sulfone)s were prepared via sulfonating the commercial available bisphenol-A based poly(ether sulfone) using a 2:1 ratio of SO_3/trimethyl phosphate for water purification processes.[77] To avoid a side reaction, McGrath and coworkers prepared sulfonated poly(arylene ether sulfone)s via direct copolymerization of sulfonated monomers (Figure 1.19) and other monomers.[78] Moreover, they also prepared the sulfonated units containing polyimides via direct copolymerization of sulfonated containing monomers (Figure 1.20).[79]

---

[76]Johnson, B. C.; Yilgor, I.; Tran, C.; Iqbal, M.; Wightma, J. P.; Lloyd, D. R.; McGrath, J. M. *J. Polym. Sci.: Part A, Polym. Chem.* **1984**, 22, 721.

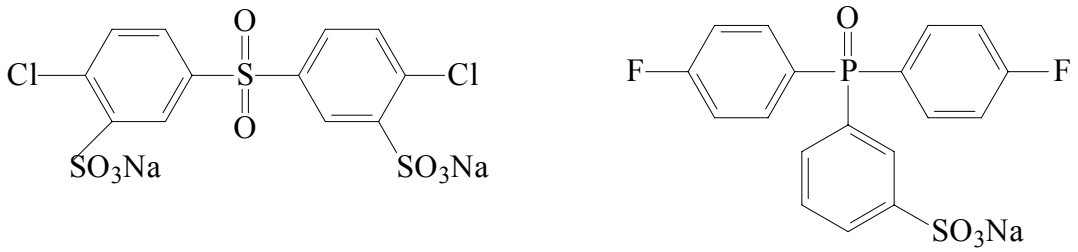

Figure 1.19 Sulfonated monomers for ionic poly(arylene ether)s[78]

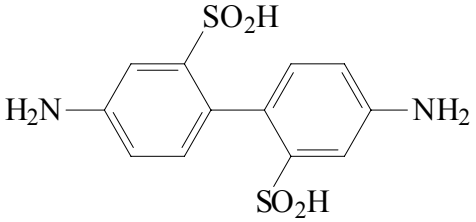

Figure 1.20 Sulfonated monomer for ionic poly(imide)s[79]

.

Kricheldorf and coworkers quantitatively methylated poly(pyridine ether)s and poly(pyridine ether sulfone)s using dimethyl sulfate in nitrobenzene.[80] Most of methylated poly(pyridinium ether)s were amorphous materials with higher glass-transition temperatures. The ionomer membranes exhibited a high selectivity for CO_2/CH_4 and He/N_2.[80]

---

[77]Wang, F.; Ji, Q.;Harrion, Mecham, J. B.; Formato, R.; Kovar, R.; Osenar, P.; Mcgrath, J. M. *Polym. Prep.* **2000**, 41, 237.
[78]Shoba, H. K.; Sankaraoandian, M.; Glass, T. E.; McGrath, J. M. *Polym. Prep.* **2000**, 42(1), 1298.
[79]Gunduz, N.; McGrath, J. E. *Polym. Prep.* **2000**, 41(1), 1565.
[80] Kricheldorf, H. R.; Jahnke, P.; Scharnagl, N. *Macromolecules* **1992**, 25, 1382.

1.5.3 Telechelic ionomers

The initial interest of the research of telechelic ionomers was to use them as model polymers of random analogues due to their well defined structures.[81-82] However, this architecture has a same importance in the academic research and industry applications as the random architecture now due to its unique properties. For example, the telechelic unsaturated polyester ionomers, which were prepared via blending the polyesters prepared from the polycondensation of propylene glycol and maleic anhydride with metal oxide, like MgO, were studied extensively.[83-90] Jerome and coworkers reported the synthesis of a series of telechelic polystyrene ionomers, including carboxylic acid or sulfonated end groups.[91-96] Hadjichristidis and coworkers reported the synthesis of ionomers via anionic polymerization using high-vacuum techniques with [3-(dimethylamino) propyl] lithium as an initiator.[97] The dimethylamino end groups of the chain were transformed to a zwitterion via reaction with cyclopropanesultone.

---

[81]Kolbet, K. A.; Schweizer, K. *Macromolecules* **2000**, 33, 1425.
[82]Nyrkova, I. A.; Khokhlov, A. R.; Doi, M. *Macromolecules* **1993**, 26, 3601.
[83]Ltvinov, V. M.; Braam, A. W. M.; van der Pleog, A. F. M. J. *Macromolecules* **2001**, 34, 489.
[84]Szilagyl, A.; Izvekov, V.; vancso-Szmercsanyi, I. *J. Polym. Sci: Polym. Chem. Ed.* **1980**, 18, 2803.
[85]Rao, K. B.; Gandhi, K. S. *J. Poly. Sci.: Polym. Chem. Ed.* **1985**, 23, 2135.
[86]Judas, D.; Fradet, A.; Marechal, E. *J. Polym. Sci; Polym. Chem. Ed.* **1984**, 22, 3309.
[87]Habassi, C.; Brigodiot, M.; Fradet, A. *Makromal. Chem.* **1990**, 191, 638.
[88]Vansco, I.; Szilagyi, A.; Izvvekov, V. *J. Poly. Sci: Polym. Chem. Ed.* **1983**, 21, 1901.
[89]Han, C. D.; Lem, K. W. *J. Appl. Polym. Sci.* **1983**, 28, 763.
[90]Laleg, M.; Blanchard, F.; Chabert, B.; Pascault, J. P. *J. Eur. Polym. Sci.* **1985**, 21, 591.
[91]Broze, G.; Jerome, R.; Teyssi, B. *Macromolecules* **1981**,14, 224.
[92]Broze, G.; Jerome, R.; Teyssi, B.; Macro, C. *Polym. Bull.* **1981**, 4, 241.
[93]Broze, G.; Jerome, R.; Teyssi, B. *Macromolecules* **1982**,15, 920.
[94]Jerome, R. *In Telechelic Polymers: Synthesis and Applications*; Goethals, E. J., Ed.; CRC Press, Inc.: Boca Raton, FL,1989; Chapter 11.
[95]Yano, S.; Tadano, K.; Jerome, R. *Macromolecules* **1991**, 24, 6439.
[96]Vanhoorne, P.; Jerome, R.; Teyssie, B. *Macromolecules* **1994**, 27, 2548.
[97]Hadjichristidis, N.; Pispas, S.; Pitsikalis, M. *Pro. Polym. Sci.* **1999**, 24, 875.

1.5.4 Block ionomers

Most block ionomers were prepared using the technology of living anionic polymerization. Long and McGrath first synthesized block ionomers derived from poly(styrene-block-tert-butyl methacrylate), and the original block nonionomers were partly hydrolyzed and neutralized to obtain block ionomers.[98] After their pioneer work, several families of block ionomers were developed based on this methodology.[99-102] Recently, Kim and coworker reported the synthesis of poly(styrene-co-itaconate) ionomers (Figure 1.21).[103] It was observed that the modulus increased as the ionic content increased, and the modulus were comparable to those of well-clustered polystyrene ionomers. Only a very weak cluster loss tangent peak was observed, which shifted to higher temperatures with an increase in the ionic content. This implies that the itaconate ionomers were weakly clustered materials. Moreover, the T_g of ionic clusters was much higher than that of the well-clustered poly(styrene-co-methacrylate) ionomers. Based on these results, it was postulated that in this ionomer system, the ion hopping played an important role in determining the mechanical properties of the ionomers. The SAXS study demonstrated that the multiplets of these ionomers were not in line with those in the EHM model. In addition, nonpolar plasticization was an effective additive to promote the formation of more clustering. However, if polar plasticization was present, interaction between ionic groups became weaker, and a more distinct cluster loss tangent peak due to ion hopping was observed at a lower temperature.

---

[98]Long, T. E.; Allen, R. D.; Mcgrath, J. M. ACS *Sym. Ser. (Chemical Reactions on Polymers)* **1988**, 364.
[99]Ku, X.; Steckle, W. P.; Weiss, R. A. *Macromolecules* **1993**, 26, 5876.
[100]Lu, X.; Steckle, W. P.; Weiss, R. A. *Macromolecules* **1993**, 26, 6525.
[101]Gauthier, S.; Eisenberg, A. *Macromolecules* **1987**, 20, 760.
[102]Yano, S.; Tadano, K.; Jerome, R. *Macromolecules* **1991**, 24, 6439.

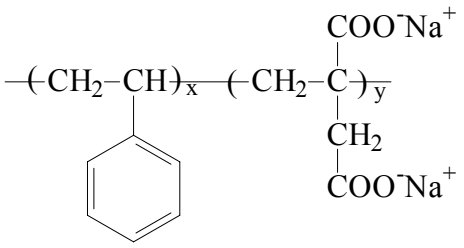

Figure 1.21 Poly(styrene-co-itaconate) ionomers[103]

1.5.5 Star telechelic ionomers

The most complicated ionomer architecture is the star telechelic structure, and these ionomers exhibits some unique properties due to its special structure.[104-108] Fetters and coworkers first reported the synthesis of star ionomers with two, three, and twelve polyisoprenes arms, and sulfozwitterion end groups.[104] Pispas and Hadjihristidis extended this work to star block copolymers of styrene and isoprene with ionic end groups.[105] The degrees of association of star telechelic ionomers are lower than those of the corresponding linear polyisoprenes.[106] Kennedy and coworkers reported the synthesis and mechanical properties of three arm star polyisobutylenes with metal sulfonated end groups.[107] Storey and coworkers prepared three arm star hydrogenated polybutadienes with oligomeric sulfonated polystyrene tails.[108] Those ionomers exhibited poor mechanical properties, which suggested that the networks were weak due to a high fraction of intramolecular aggregates, in which two or three arms of the same molecule were incorporated into the same multiplet.[108] Due to few efforts in this area, the knowledge of the behavior of telechelic branched ionomers is still limited, especially the star ionomers with greater than three arms.

---

[103]Kim, J.; Hong, M.; Nah, Y. H. *Macromolecules* **2002**, 35, 155.

1.5.6 Ionomers with a regular spacing between ionic groups

Cooper and coworkers developed model polyurethane ionomers on the basis of polyurethane chemistry (Figure 1.22), which had regularly spaced ionic groups along the polymer backbone.[109] The spacing was able to be controlled to result in ionomers soluble in different solvents. The effect of ionic content and solvent quality was studied independently.

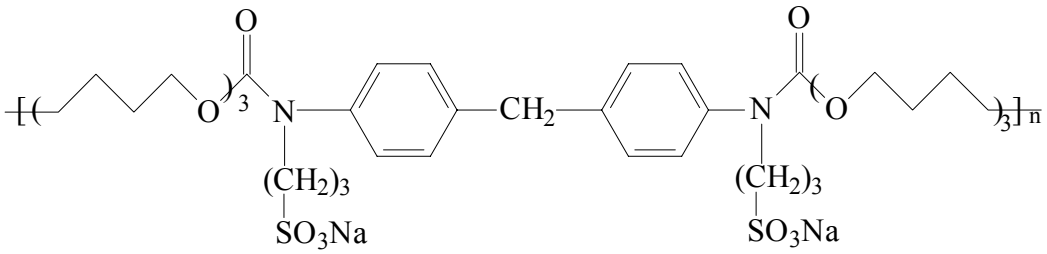

Figure 1.22 Model polyurethane ionomers with a regular spacing between ionic groups[109]

1.6 Polyester ionomers

1.6.1 Blends

MacKnight and coworkers demonstrated that the compatibilization of an immiscible polymer pair, poly(ethy1 acrylate) and poly(ethy1ene terephthalate), was accomplished via incorporating vinylpyridine groups and zinc-neutralized sulfonate groups, respectively, along the polymer chains.[110-112] The compatibility of this multiphase ionomeric blend resulted from the formation of a zinc-pyridine-sulfonate group coordination complex between polymer chains. The nature and degree of this complexation were successfully probed using FT-IR spectroscopy. Two blend

compositions with one containing a stoichiometric amount of the interacting groups were prepared. The degree of compatibility was investigated using DSC and DMTA. The level of mixing depended upon the extent of specific interactions between the polymer chains. In addition, interesting phase behavior of the blends was discovered using DMTA. Results showed that upon crystallization the PET-SO_3Zn-rich phase in both ionomeric blends exhibited an increase in the temperature of the loss peak associated with segmental motions accompanying T_g, while the EAVP-rich phase showed a decrease in the temperature of loss peak.

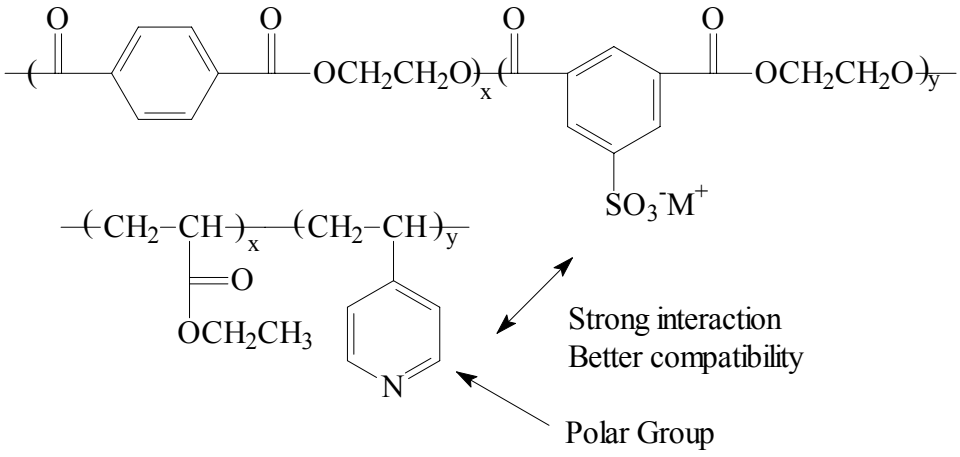

Figure 1.23 Structures of PET ionomer and poly(ethy1 acrylate – vinylpyridine)[110]

---

[104]Davidson, N. S.; Fetters, L. J.; Funk, W. J.; Graessley, W. W.; Hadjichristidis, N. *Macromolecules* **1988**, 21, 112.

[105](a) Hadjichristidis, N. *Macrol. Chem. Symp.* **1991**, 48/49, 47. (b) Pispas, S.; Hadjichristidis, N. *Macromolecules* **1994**, 27, 1891. (c) Pispas, S.; Hadjichristidis, N., Mays, J. W. *Macromolecules* **1994**, 27, 6307.

[106]Kennedy, J. P.; Ross, L. R.; Lackey, J. E.; Nuyken, O. *Polym. Bull.* **1981**, 4, 67.

[107](a) Mohair, Y.; Tyagi, T.; Wilkes, G. L.; Storey, R. F.; Kennedy, J. P. *Polym. Bull.* **1982**, 8, 47. (b)Bagrodia, S.; Mohajer, Y.; Wilkes, G. L.; Storey, R. F., Kennedy, J. P. *Poly. Bull.* **1982**, 8, 281.

[108]Storey, R. F.; George, S. E.; Nelson, M. E. *Macromolecules* **1991**, 24, 2920.

[109]Nomula, S.; Cooper, S. L. *Macromolecules* **1997**, 30, 1355.

1.6.2 PET Nanocomposites

The primary objective of the development of PET-clay nanocomposites is to improve the gas barrier property that is required for beverage and food packagings.[113] Another expectation for PET-clay nanocomposites is to be an alternative to the glass fiber reinforced PETs. Ke and coworkers first dispersed organically modified montmorillonite in PET matrix.[114] Complete delamination was not achieved, but the tensile modulus of the nanocomposites increased as much as 3 times over that of pure PET. Tsai and coworkers reported nanocomposites of PET and clay via utilizing an amphoteric surfactant and an antimony acetate catalyst.[115-116] Their nanocomposites showed higher flexural strength and modulus than pure PET with 3 wt % loading of the silicate.

It is traditionally recognized that stress transfer from the matrix to the reinforcement is essential for accomplishing high stiffness in composite materials.[117] Likewise, to accomplish high mechanical performance using nanocomposites, both sufficient exfoliation of the clay and strong adhesion of the polymer matrix to the layered silicate must be achieved. In the case of nylon-clay nanocomposites, nylon can strongly adhere to the silicates through ionic and hydrogen bonds.[118] PET is less polar and not expected to have such a strong interaction as nylon. Therefore, the PET main chain must be tethered in some sense to the silicate layer to achieve a high mechanical performance. A Japanese group developed a novel compatibilizer that connected PET through covalent bonds and the layered silicates through ionic bonds. To design the compatibilizer suitable for the PET-clay nanocomposites, they set the following conditions for comonomer: (1) possessing functional groups that can react with PET by transesterification. (2) possessing a cationic group that can interact with the negatively

charged silicate layer. (3) stable at the polymerization temperature of PET (275 ^{o}C). To satisfy condition (1), they chose the dimethyl isophthalate group, and for conditions (2) and (3), the triphenylphosphonium group was selected (Scheme 1.5 and Figure 1.24). Expandable fluorine mica (ME) was used as the layered silicate. Efforts to clarify the effect of the structure of the compatibilizer on the mechanical, thermal, and other properties of the composites as well as to develop a better process to achieve further dispersion of ME in PET are in progress.

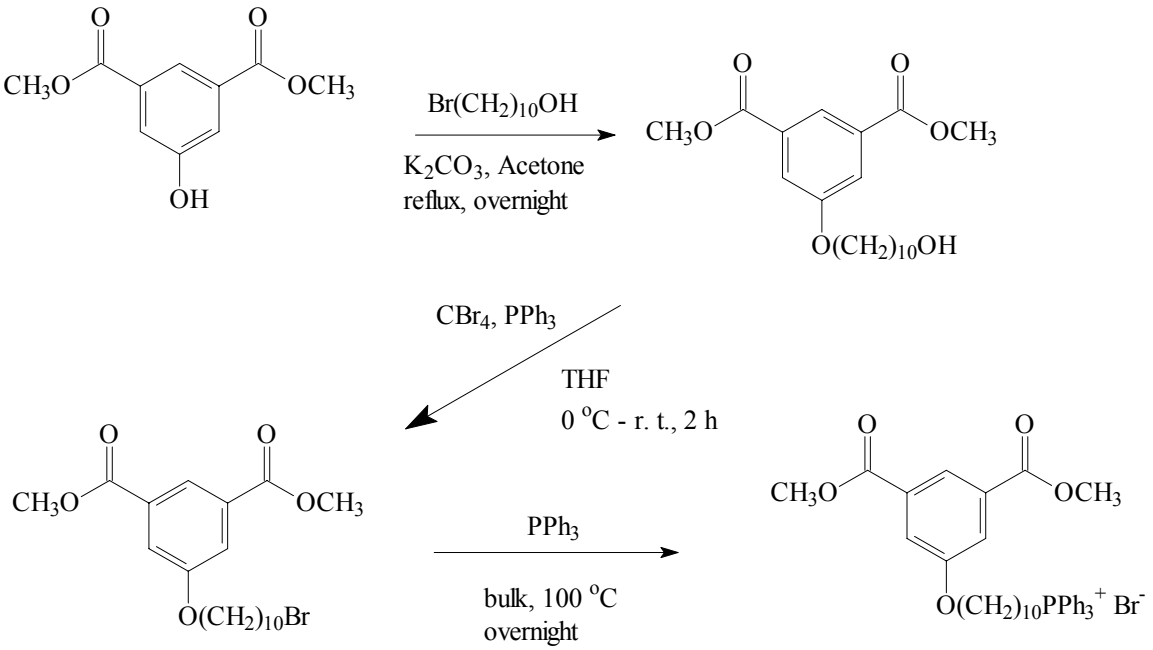

Scheme 1.5 Synthesis of phosphonium containing monomers [118]

---

[110]Alice Ng, C. W. A.; MacKnight, J. W. *Macromolecules* **1996,** 29, 2412.
[111]Ng, C. W. A.; Lindway, M. J.; MacKnight, W. J. *Macromolecules* **1994**, 27, 3027.
[112]Ng, C. W. A.; MacKnight, W. J. *Macromolecules* **1994**, 27, 3033.
[113]Matayabas, J. C., Jr.; Turner, S. R. *J. Mater. Res.* **1993**, 8, 207.
[114]Ke, Y.; Long, C.; Qi, Z. *J. Appl. Polym. Sci.* **1999**, 71, 1139.
[115]Tsai, T.-Y., *J. Mater. Res.* **1993**, 8, 173.
[116]Tsai, T.-Y.; Hwang, C.-L.; Lee, S. Y. *SPE-ANTEC Proc.* **2000**, 248, 2412.
[117] Calvert, P. *Nature* **1999**, *399*, 210.

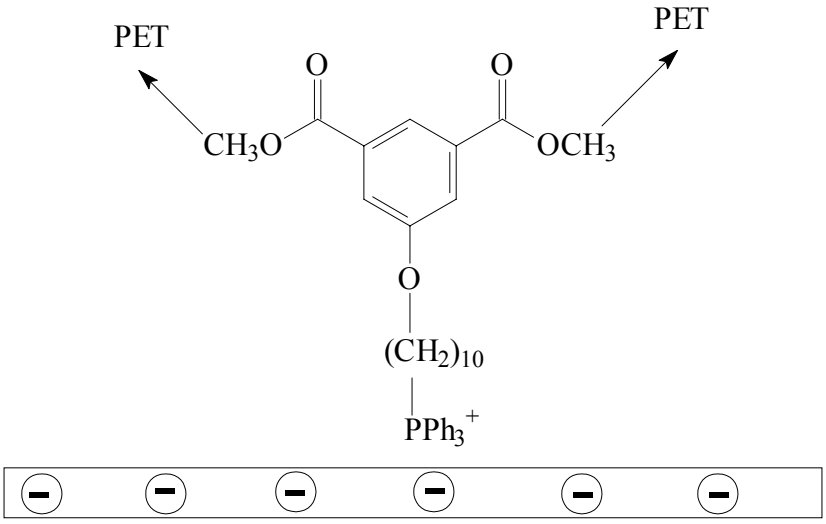

Figure 1.24 PET nanocomposites[118]

Moore and coworkers investigated the effect of the presence of poly(butylene terephthalate) (PBT) ionomers on the properties of PBT/montmorillonite composites.[119] Their results demonstrated that the organic modification of montmorillonite clay coupled with PBT ionomers, and resulted in highly exfoliated nanocomposites via a simple extrusion process. With regard to the effect of $-SO_3Na$ content, as little as 1.0 mol % ionic groups was needed to achieve considerable exfoliation of R_4N^+ montmorillonite (Figure 1.25). Although the degree of exfoliation was not observed to be strongly dependent on $-SO_3Na$ content, mechanical properties such as Young's modulus and high-temperature storage modulus at temperatures above T_g increased with an increase in ionic content. These enhancements in mechanical properties form a higher ionic content were due to an increase in the number of interactions between the clay particles and the matrix via electrostatic interactions involving the $-SO_3Na$ groups.

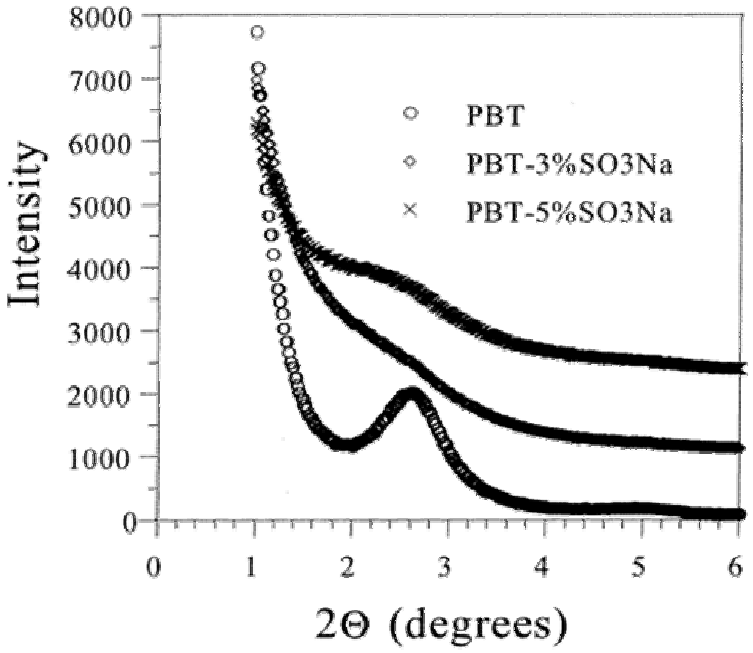

Figure 1.25 WAXD of PBT ionomer/clay nanocomposites[119]

A scheme was developed for producing poly(ethylene terephthalate (PET) ionomer)/silicate hybrid materials via in situ sol-gel reactions for tetraethylorthosilicate (TEOS) using different solvents (Scheme 1.6).[120] Scanning electron microscopy/EDAX studies revealed that silicate structures existed deep within PET ionomer films that were melt pressed from silicate-incorporated resin pellets. ^{29}Si solid state NMR spectroscopy revealed considerable Si-O-Si bond formation, but also a significant fraction of SiOH groups. ^{23}Na solid state NMR spectra suggested the presence of ionic aggregates within the unfilled PET ionomer, and that these aggregates did not suffer major structural rearrangements via silicate incorporation. For an ionomer treated with TEOS using $MeCl_2$, Na^+ ions were less associated with each other than in the unfilled control, suggesting silicate intrusion between PET-SO_3^- Na^+ ion pair associations. The ionomer

treated with TEOS and tetrachloroethane had more poorly formed ionic aggregates, which illustrates the influence of solvent type on ionic aggregation. First scan DSC thermograms for the ionomers demonstrated an increase in crystallinity after the incorporation of silicates, but solvent-induced crystallization also appeared to be operative. Second-scan DSC thermograms also suggested that the addition of silicate particles was not the only factor implicated in recrystallization, and that solvent type was important even in second-scan behavior. Silicate incorporation did not profoundly affect the second scan T_g vs. solvent type, i.e., chain mobility in the amorphous regions was not severely restricted for silicate incorporation. Recrystallization and melting in these hybrids appeared to be due to an interplay between a solvent-induced crystallization that strongly depended on solvent type and interactions between PET chains and in situ grown, sol-gel-derived silicate particles.

---

[118]Usuki, A.; Kojima, Y.; Kawasumi, M.; Okada, A.; Fukushima, Y.; Kurauchi, T.; Kamigaito, O. *J. Mater. Res.* **1993**, 8, 1179.
[119]Chisholm, B. J., Moore, R. B.; Barber, G.; Khouri, F.; Hempstead, A.; Larsen, M.; Olson, E.; Kelley, J.; Balch, G.; Caraher, J. *Macromolecules* **2002**, 35, 5508.
[120]Lambert, A. A.; Mauritz, K. A.; Schiraldi, D. A. *J. Appl. Polym. Sci.* **2002**, 84, 1749.

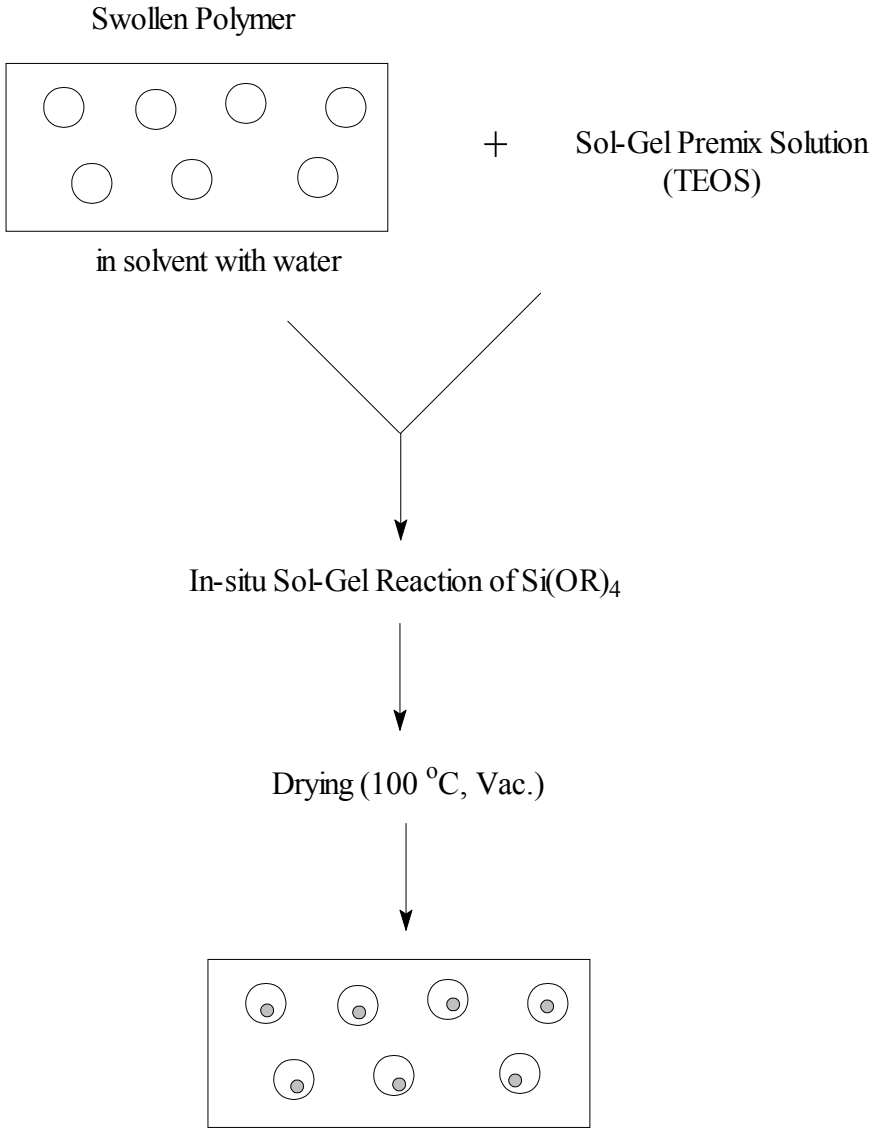

Scheme 1.6 Synthesis of PET nanocomposites via sol-gel reaction[120]

1.6.3 Ionic liquid crystalline polyesters

Although LC polymers have been widely used as high-performance polymers, two major problems prevent their extensive use. One is poor transverse and compressive properties in contrast to very high axial properties, often 1-2 orders of magnitude lower, both of which are inherent to highly unaxially oriented polymers.[121] Another problem is

poor miscibility and adhesion with other polymers, when liquid crystalline polymers and conventional polymers are mixed to produce polymer blends, which are widely used to enhance polymer properties.[122-123] Both problems basically result from weak intermolecular interactions either in the liquid crystalline polymer itself or in liquid crystalline polymer/polymer blend. Theses interactions are usually weak secondary bonds (van der Waals bonds and hydrogen bonds), in contrast to strong covalent bonds along chain directions. These problems hinder LC polymers for a wider range of applications, including conventional composites.

Various approaches were used to develop LC polymers with improved transverse and compressive properties with only marginal success. One approach to accomplish this is to enhance interchain interaction of LC polymer molecules via chemical crosslinking.[124-125] However, only a moderate improvement, if any, of fiber axial compressive strength has been achieved with a decrease, usually a substantial loss, in tensile properties. Heat treatment may increase tensile strength via raising the molecular weight, but transverse properties are essential the same.[126-127] Some groups are developing ionic LC polymers to overcome theses fundamental problems via introducing ionic groups into LC polymer molecules.[128-130] Strong ionic interaction among polymer molecules are hope to significantly enhance mechanical properties, which include compressive strength, as demonstrated for flexible ionomers, and also know to dramatically improve compatibility between different polymers in polymer blends.

It is also of interest to investigate the interaction between ionic clusters and LC phases, and overall morphology of the liquid crystalline polymers. In main chain LC polymers, the competition between the formation of the ionic cluster and liquid

crystalline phases is expected to be much stronger, because no spacer decouples the mesogenic groups from the ionic polymer chain.[128] In fact, it could be shown that the formation of ionic clustering is favored in the liquid crystalline main chain ionomers with the ionic groups separated from the polymer chain by a spacer. This was demonstrated in a series of LC polymalonates with ferrocenium ions.[128]

---

[121]Donal, A. M.; Windlew, A. H. *Liquid Crystalline Polymers*, Cambridge University Press: Cambridge, U. K., **1992**.
[122]Paul, D.R.; Newman, S. *Polymer Blends*; Academic Press: New York, **1978**.
[123]Olabisi, O., Robeson, L. M., Shaw, M. T. *Polymer-Polymer Miscibility*; Academic Press: New York, **1979**.
[124]*Liquid Crystalline Polymers;* NMAB-453, National Academy Press: Washington, DC, **1990**.
[125] Dang, T.D., Wang, C. S., Click, W. E., Chauh, H. H., Tsai, T. T.; Husband, D. M., Arnold, F. E. *Polymer* **1997**, 38, 621.
[126]Yoon, H. N. *Colloid Polym. Sci.* **1990**, 268, 230.
[127]Calundann, G. W., Jaffe, M. ProRobert A. *Welch Conf. Chem. Research* **1982**, 26, 247.
[128]Wilbert, R; Zentel, R *Macrol. Chem. Phys*. **1996,** 197, 3259.
[129]Xue, Y.; Hara, M *Macromolecules* **1997**, 30, 3803.

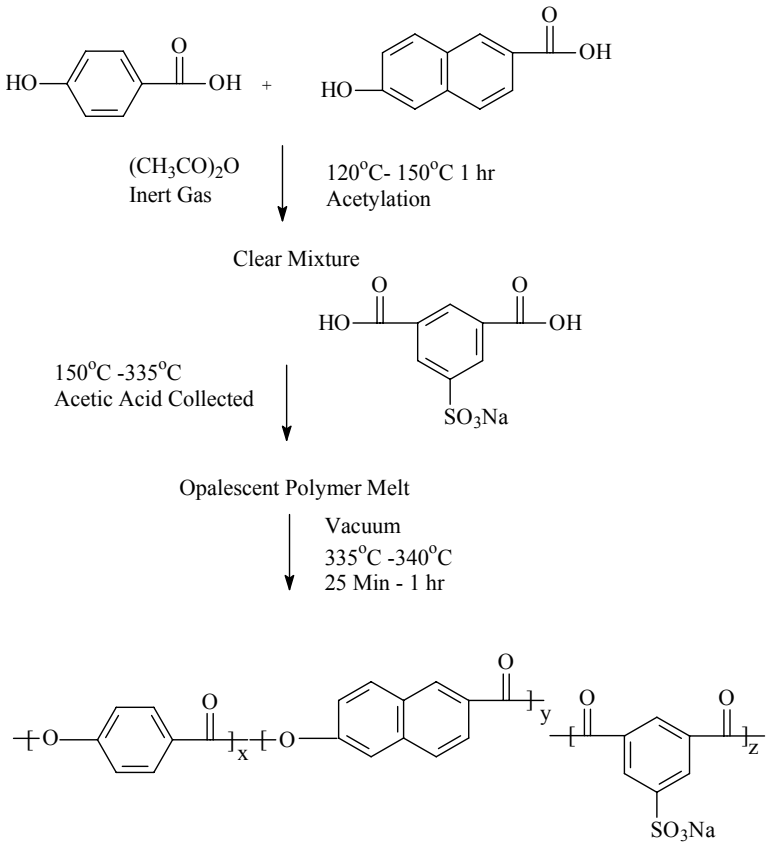

Scheme 1.7 Synthesis of ionic liquid crystalline polyesters via melt polymerization[129]

Hara and coworkers modified wholly aromatic polyesters based on random copolymer of 1,4-hydroxybenzoic acid (HBA) and 6,2-hydroxynaphthoic acid (HNA), which was first commerciallized in the mid-80s termed as Vectra^{TM}. Sodium 5-sulfoisophthalate was introduced into the Vectra^{TM} as an ionic monomer (Scheme 1.7).[129] A fiber-forming molecular weight was achieved for all the ionomers. The melt of ionomers showed extensive birefringence, and the majority of them exhibited nematic

mesophase textures over a wide temperature range, without showing a transition to an isotropic phase at least to 380 ^{o}C. The melting temperature (T_m) and crystallization temperature (T_c) of the ionomers were both decreased substantially with an increase in the ionic content due to the increase in the number of kinked units. A unique glass transition behavior was also observed: at the ionic content less than 10 mol%, the glass transition temperature is rather constant, the T_g value jumped when the ionic content reaches 15 mol%. Two distinct T_g's with about 40 ^{o}C separation were observed at 20 mol% ionic content. Fracture surfaces of the ionomer fibers indicated suppressions of spontaneous fibrillation with an increase of ionic content.

Hara and coworkers continued their research via preparing divalent salt ionic LC polyesters.[130] They synthesized Vectra^{TM} containing 1 mol% ionic groups with divalent metal counterions (Ba, Ca, Ma and Zn) via a in situ exchanging. The Ca salt ionomer had a high molecular weight, and exhibited excellent thermal and mechanical properties. Systematic comparison was made among nonionomer, ionomers (Na, Ca salt). Ionomer with monovalent Na ions demonstrated a moderate increase in tensile modulus and strength over nonionic Vectra^{TM}. However, ionomers with divalent Ca ion demonstrated a significant increase in modulus, and 147 % increase in tensile strength. Tensile fracture surface morphologies of ionic polyesters were also investigated as a function of counterion.

---

[130]Xue, Y.; Hara, M; Yoon, H. N. *Macromolecules* **1998**, 31, 1808.
[131]Zhang, B; Weiss, R. A. *J. of Polym. Sci.: Part A, Polym. Chem*. **1992**, 30, 91.

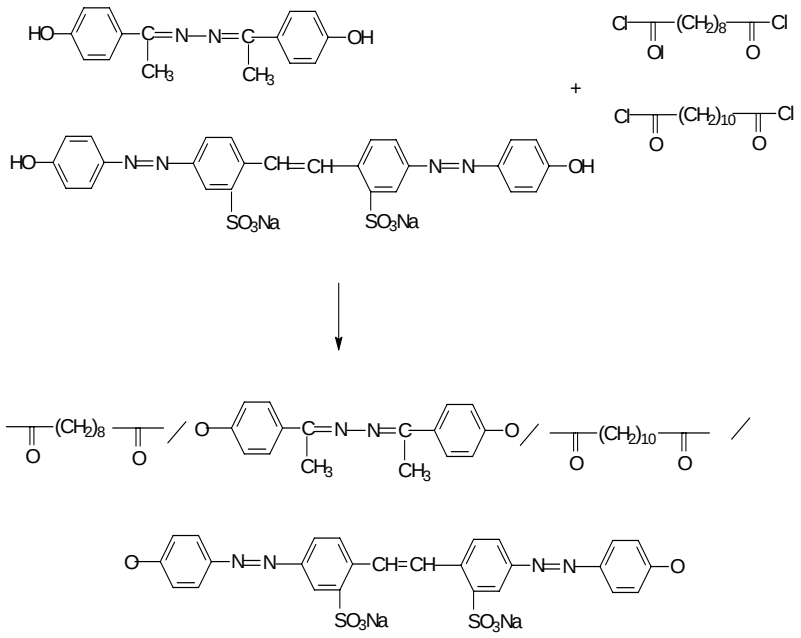

Scheme 1.8 Synthesis of ionic liquid crystalline polyesters via solution polymerization[131]

LC polyester ionomers containing sulfonate groups pendant to the polymer backbone were synthesized via an interfacial condensation reaction of brilliant yellow, a sulfonate-containing monomer, with 4,4'-dihydroxy-dimethyl benzalazine and a 50/50 mixture of sebacoyl and dodecanedioyl dichlorides (Scheme 1.8).[131] Polymers containing up to ca. 4 mol% brilliant yellow were characterized using elemental analysis and ultraviolet spectroscopy. Ionomers were thermally stable to about 300°C, and exhibited a broad nematic mesophase region of 70-100 °C. The solution viscosity behaviors in chloroform suggested that intramolecular association of sulfonate groups occurred at low polymer concentration and intermolecular association predominated at higher concentrations.

1.7 Progress in hyperbranched polymers

Flory initially described an approach for the preparation of hyperbranched polymers from AB_2 monomers in 1952.[132] However, this family of polymers were neglected for a long time until ten years ago in an effort to develop an economical replacement for perfect dendritic polymers.[133] Today, the research of hyperbranched polymers is one of the most active area in polymer science demonstrated via numerous papers published in each year. Several decent reviews have been published to describe the basic knowledge and progress in this area.[134-136] As a result, this chapter will focus the most important progresses in hyperbranched polyesters and poly(arylene ether)s.

---

[132] Flory, P.J. *J. Am. Chem. Soc.* **1952**, 74, 2178.
[133] Kim, Y. H.; Webster, O. W. *J. Am. Chem. Soc.* **1990**, 112, 4592.
[134]Kim, Y. H. *J Polym. Sci.: Part A, Polym. Chem.* **1998**, 36, 1685.
[135]Jikei, M.; Kakimoto, M. *Prog. in Polym. Sci.* **2001**, 26, 1233.
[136]Voit, B. I. *J. Polym. Sci. Part A: Polym. Chem.* **2000**, 38, 2505.
[137]Chu, F. K.; Hawker, C. J.; Pomery, P. J.; Hill, D. J. T. *J. Polym. Sci.: Part A, Polym. Chem.* **1997**, 35, 1627.
[138]Gong, C. G.; Miravet, J.; Frechet, J. M. J. *J. Polym. Sci.: Part A, Polym. Chem.* **1999**, 37, 3193.
[139] Parker, D.; Feast, W. J. *Macromolecules* **2001**, 34, 2048.
[140]Dusek, K.; Somvarsky, J.; Smrckova, M.; Wilczek, L.; Simonsick, W. J.; Hyrsl, J. *Polym. Mat. Eng.* **1999**, 80, 102.
[141]Cheng, K. C.; Wang, L. Y. *Macromolecules* **2002**, 35, 5657.
[142]Hawker, C. J.; Chu, F. K. *Macromolecules* **1996**, 29, 4370.
[143]Cheng, K. C.; Don, T. M.; Guo, W.; Chuang, T. H. *Polymer* **2002**, 43, 6315.

1.7.1 Mechanism of polymerization of AB_n monomers

Flory described the polymerization of AB_2 monomers based on the assumption that no side reaction happened, and all the functional groups exhibited same reactivity during the polymerization.[132] However, the practical polymerization of AB_n monomers is more complicated due to the presence of side reactions. The most import side reaction is the clyclization reaction during the polymerization. In initial research, the argument focused on the competition between the formation of high molecular weight hyperbranched products and the formation of low molecular weight cyclic products. The early researches demonstrated that if monomers were not highly flexible, the formation of high molecular weight hyperbranched products dominated.[137] Even for highly flexible polymers, such poly(siloxysilane), a novel methodology, slow addition of monomers, was developed to suppress the cyclization reaction to prepare high molecular weight products.[138]

However, recent research demonstrated the cyclization always happened during the polymerization, even though the high molecular weight products were obtained.[139] As a result, a maximum number average molecular weight was observed in several families of hyperbranched polymers prepared via a one-step polymerization of AB_n monomers.[139-140] Dusek reported a kinetic simulation of polymerizations of AB_2 monomers, which suggested that all the high molecular weight products were cyclized.[140]

Another problem is the reactivity of functional groups during the polymerization. If the reactivity of all functional groups keep an identical level, the branching degree will be 50%.[132] Most of products from AB_n monomers exhibited this value, which indicated that the assumption was right. To increase the branching degree (> 50 %), a method of

using B_3 core monomer was developed.[141] However, some exceptional examples were also observed. Hawker and corkers reported that when polymerization of 3,5-dihydroxy-4'-fluorobenzophenone, only 14 % branching degree was obtained, because the secondary phenate was much less reactive than the first one.[142] Chuang and coworkers used kinetic model to study the polymerization of AB_2 monomers with a substitution effect on the B groups.[143] During the polymerization, if one of the B group reacts first, the reactivity of the remaining unreacted B group will change. The weight average molecular weight and the degree of branching of the hyperbranched polymers having substitution effect differ from that with equal reactivity of the B groups. If the substitution effect causes an increase in the rate constant after one of the B groups has reacted, a broader molecular weight distribution and a higher degree of branching will be observed.

1.7.2 Synthesis and characterization of hyperbranched polymers via A_2 and B_3 monomers

In most cases, hyperbranched polymers are prepared using a one-step polymerization of AB_n monomers, and typically exhibit highly irregular structures and large molecular weight distributions. This is a direct consequence of the one-step methodology, and it was suggested that hyperbranched polymers resembled conventional networks immediately prior to the gel point.[144-146] The similarity of intermediates in a A_2 with B_3 process to intermediates in the formation of polymeric networks led chemists to consider the polymerization of A_2 with B_3 monomers as an alternative synthetic route. This complementary method is attractive since many A_2 and B_3 monomers are readily

available, and have received significant attention in the synthesis of conventionally branched polymers.

Watanebe and coworkers reported the synthesis of hyperbranched aromatic polyamides, which were derived from aromatic diamines (A_2) and trimesic acid (B_3) (Scheme 1.9).[147] Voit and coworkers investigated the structures of this family of hyperbranched polymers in detail using different NMR technologies.

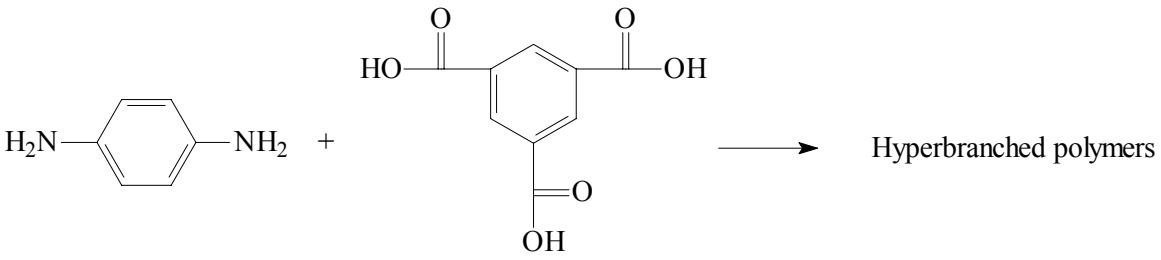

Scheme 1.9 Synthesis of hyperbranched polyamides via A_2 and B_3 monomers[147]

Frechet and coworkers reported the synthesis of hyperbranched polyether epoxies via proton transfer polymerization from 1,2,7,8-diepoxyoctane (A_2) and 1,1,1-tri(hydroxymethyl)ethane (B_3) using a 1:1 molar ratio of monomers (2 equivalents of A groups and 3 equivalents of B groups) (Scheme 1.10).[148-149] These reactions were stopped immediately prior to the gel points to form highly branched molecules.

---

[144]Burchard, W. *Macromolecules* **1972**, 5, 604.
[145]Burchard, W. *Adv. Polym. Sci.* **1983**, 48, 1.
[146]Burchard, W. *Adv. Polym. Sci.* **1999**, 143, 113.
[147]Jikei, M.; Chon, S. H.; Kakimoto, M.; Kawauchi, S.; Imase, T.; Watanabe, J. *Macromolecules* **1999**, 32, 2061.
[148]Emrick, T.; Chang, H. T.; Frechet, J. M. J. *Macromolecules* **1999**, 32, 6380.
[149]Emrick, T.; Chang, H. T.; Frechet, J. M. J. *J. Polym. Sci. Part A: Polym. Chem.* **2000**, 38, 4850.
[150]Monticelli, O.; Mariani, A.; Voit, B. I. *High Perform. Polym.* **2001**, 13, 45.

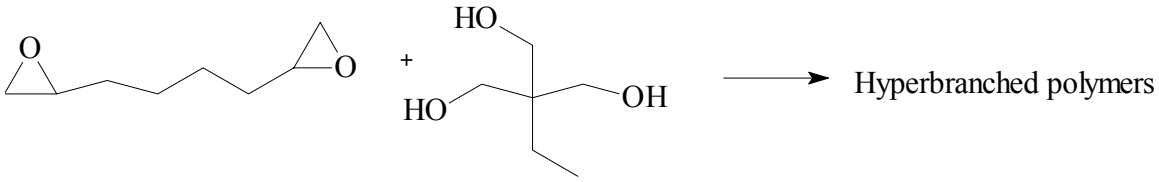

Scheme 1.10 Synthesis of hyperbranched polyether epoxies via A_2 and B_3 monomers[148]

After these two pioneering reports, a flurry of research led to the development of several new experimental procedures.[148-156] For example, Okamoto and coworkers synthesized hyperbranched polyimides via a slow addition of a dilute solution of A_2 to a dilute solution of B_3.[156]

Even though there are several reports about preparation of hyperbranched polymers using A_2 and B_3 monomers, the mechanism of the formation of high molecular weight hyperbranched polymers via A_2 and B_3 monomers is still not clear. According to classic theory of polycondensation and gelation, the final products should be gel, when the convention is higher than 80%. As a result, only low molecular weight highly branched sol fraction will be obtained, if the reaction is stopped before gel point. However, high molecular weight hyperbranched polymers were prepared using A_2 and B_3 monomers with a high conversion (> 90%). New mechanisms need to be proposed to explain the formation of high molecular weight hyperbranched products with a high conversion (> 90%). Watanebe demonstrated that if the first condensation reaction of A_2 with B_3 would be faster than subsequent propagation, an intermediate, A-ab-$(B)_2$ molecules which were similar to the traditional ABn monomers, accumulated.[147] Thus, it was proposed that the remainder of the reaction resembled the more common AB_2 polymerizations. However, this explanation is only applicable to this specific system,

and more universal mechanism need to be proposed. Recently, Kricheldof and coworkers proposed a new mechanism in their report using 1,1,1—tris(4-hydroxyphenyl) ethane and 4,4'-diflurodiphenyl sulfone to prepare hyperbranched poly(arylene ether sulfone).[150] They proposed that the formation of cyclic species during the polymerizations effectively prevented the crosslink, and resulted in soluble high molecular weight hyperbranched products bearing one or several cycles structures in a molecules. MODI-TOF was used to identify the structures of hyperbranched products, which strongly supported their theory.

1.7.3 Synthesis and characterization of branched polymers via AB and AB_2 monomers

In 1952, Flory reported the statistical calculations for not only a one-step polymerization of AB_2 type monomers, but also copolymerization of AB and AB_2 monomers.[132] However, the real research of this type of polymerization began 30 years later, and Kricheldorf reported the first synthesis of polyester copolymers from AB and AB_2 monomers in 1982 (Scheme 1.11), which was earlier than first report of one-step polycondensation of AB_2 monomers in 1990.[157] Recently, this synthetic methodology attracted a great interest because the introduction of AB monomers allows the control of the average distance between branching points. Branching density in main chains generally affect the properties of the resulting hyperbranched polymers, similar to low- and high-density polyethylenes. This methodology led to polymers with controlled branching degree, and the both advantages of linear polymers and hyperbranched polymers.

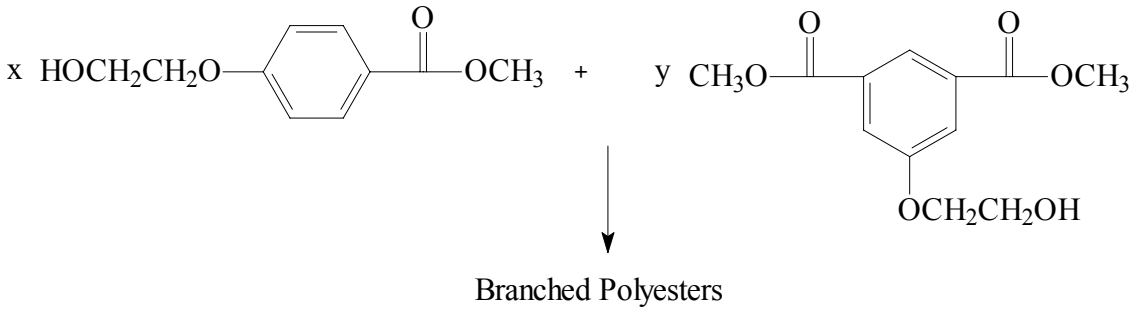

Scheme 1.11 Synthesis of branched polyesters via AB and AB_2 monomers[157]

Lee and coworkers reported the copolymerization of 3-(4-aminophenoxy)benzoic acid as an AB type monomer and 3,5-bis(4-aminophenoxy)benzoic acid as an AB_2 type monomer.[158] They found that the hyperbranched polyamides were soluble in organic solvents due to consecutive branching structures, whereas the linear analogues, such as poly(phenylene terephthalamide)s, were insoluble after the isolation from production process.

Poly(ether-ketones) (HB-PEK's) with variable degrees of branching were synthesized as Scheme 1.10.[159] The T_g of branched PEK increased to 212 ^oC, when the AB content was 50 wt%. At 75 wt% AB content, HB-PEK became a semicrystalline polymer with a melting point of 340 ^oC. Wide angle x-ray scattering (WAXS) patterns of HB-PEK's correlated well with DSC results.

---

[151]Russo, S.; Boulares, A.; Cosulich, M. E. *Macromol. Symp.* **1999**, 143, 309.
[152]Jikei, M.; Kakimoto, M. A. *High Perform. Polym.* **2001**, 13, 33.
[153]Komber, H.; Voit, B. I.; Monticelli, O.; Russo, S. *Macromolecules* **2001**, 34, 5487.
[154]Kricheldorf, H. R.; Vakhtangishvili, D.; *J. Polym. Sci. Polym. Chem.* **2002**, *40, 2967.*
[155] Fritsch, D.; Kricheldorf, H. R. *J. M. S. Pure Appl. Chem.* **2002**, 139, 1335.
[156]Fang, J.; Kita, H.; Okamoto, K. *Macromolecules* **2000**, 33, 4639.
[157]Kricheldorf, H. R.; Zhang, Q. Z.; Schwarz, G. *Polymer* **1982**, 23.
[158]Lee, A. T.; McHugh, A. J. *Macromolecules* **2001**, 34, 9080.
[159]Baek, J. B.; Tan, L. S. *Polym. Prep.* **2001**, 42(2), 469.
[160]Xu, M.; Yan, X. H.; Cheng, R. S.; Yu, X. H. *Polym. Int.* **2001**, 50, 1338.

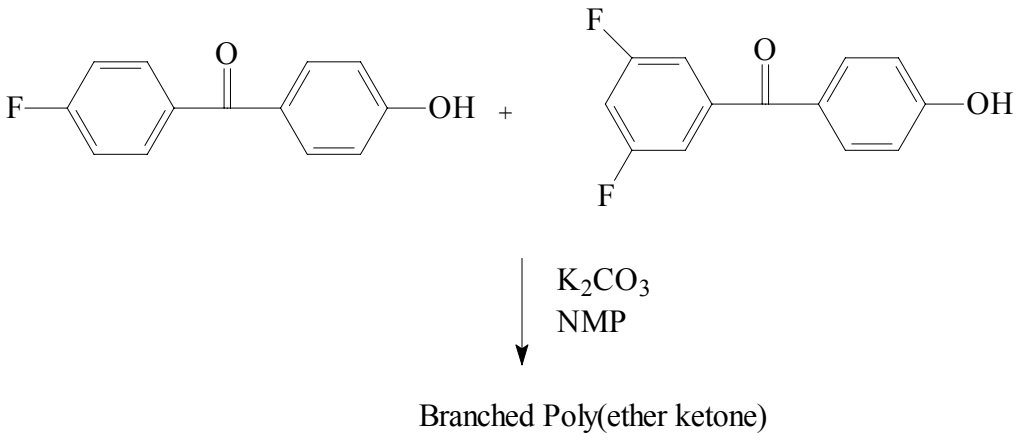

Scheme 1.12 Synthesis of branched poly(arylene ether) via AB and AB_2 monomers[159]

Hyperbranched aromatic polyamide copolymers were prepared via direct polycondensation of 3-(4-aminophenoxy)benzoic acid (AB monomer) and 3,5-bis(4-aminophenoxy)benzoic acid (AB_2 monomer) in the presence of tri-Ph phosphite and pyridine as condensation agents. ^{13}C NMR spectroscopy demonstrated that the copolymers were composed of five kinds of repeating units whose ratio was consistent with statistical distribution.[160] The feed ratio of the monomers affected the glass transition temperature, and the softening point. A minimum glass transition temperature was observed at a 50 mol% of the AB_2 monomer whereas softening point gradually decreased with an increasing in the level of AB_2 monomer, and became constant over a 60%. Young's modulus detected using tensile test decreased from 2.4 to 1.6 GPa with an increasing in the level of AB_2 monomer from 0 to 60%.

1.7. 4 Characterization on the molecular level

It is predicted that hyperbranched polymers will not have any chain entanglement due to the highly branched structures. To prove this predication, several technologies were used, including rheological analysis and solid state NMR. Rheological analysis of concentrated solution or melt of dendrimers demonstrated that Newtonian behaviors with steady shear viscosities independent of the shear rate, and roughly linearly with weight average molecular weights.[161] However, for hyperbranched polymers, it is more complicated because the structures are not perfect, and the degree of branching exerts a profound effect on the properties. Kwak and coworkers synthesized three floro-terminated hyperbranched poly(ether ketone)s with different degree of branching(0.49, 0.62and 0.67).[162] The rheological analysis indicated that the entanglement decreased with an increase in the branching degree, and when the branching degree is 0.67, it is almost Newtonian behaviors without entanglement. Moreover, they also used solid state ^{1}H wide pulsed wide-line NMR spectroscopy to reveal that those hyperbranched polymers exhibited two local movements of polymer chains, the linear one, and terminal and branched units.[163] It is more interesting that the presence of hyperbranched polymers in the blends of linear polymers and hyperbranched polymers dramatically decreased the chain entanglement among linear polymers to decrease the viscosities.

The solution properties of hydroxyl terminated hyperbranched aliphatic polyesters and their acetyl derivatives have been studied via measuring viscosity parameters.[160] The polarity of terminated groups of molecules is the most important factor affecting their properties. The intrinsic viscosity did not reflect the real monomolecular hydrodynamic volume of hydroxyl group-terminated hyperbranched

polymer due to the strong intermolecular forces which lead to the formation of stable clusters. The intermolecular association constant K_M depends not only on molecular weight, but also on the polarity of end groups. However, the dynamic contact concentration was determined accurately from reduced viscosity versus concentration plots. The reason, why the intrinsic viscosity did not change linearly with the generation of the hyperbranched aliphatic polyesters, was explained using 'free-draining' and non-draining' models. The physical state of hyperbranched polymers depended mainly on the polarity of terminal groups. The glass transition temperature will decrease with the decrease in polarity of the surface end groups. Much attention was paid to the study of the solution properties of hyperbranched polymers if the end-group was highly polar such as hydroxyl. The experimental data may lead to the wrong conclusions, such as whether the clusters exist in solution. Intrinsic viscosity of the acetyl modified aliphatic hyperbranched polymer was much lower than that of the corresponding hydroxyl end groups. The non-linear trend (or maximum) of intrinsic viscosity comes from the flow model changing from 'free-draining' to 'non-draining'. The results suggest that it is unnecessary to extrapolate to zero concentration to calculate the intrinsic viscosity, because the reduced viscosity is exactly equal to the intrinsic viscosity in the dilute regime. The hyperbranched polymer with the fewer polar end-groups gives a suitable model system for examining the viscosity theory. The dynamic contacting concentration can be easily defined in the plot of the reduced viscosity versus concentration. The large difference in the dependence of C_s on molecular weight for hyperbranched polymer can be attributed to its chemical architecture. Intermolecular interactions should be taken into consideration when the solution properties are explored. The dynamic contacting

concentration C_s and the association equilibrium constant K_M depend on not only the generation number (or molecular weight) but also the intermolecular interaction force.

CHAPTER 2

Synthesis and Characterization of Telechelic and Random Poly(ethylene terephthalate) (PET) Ionomers with Equivalent Molecular Weights and Ionic Contents

(Published as: Lin, Q.; Gariano, N.; Madison, P. H.; Wang, Z.; Long, V. K. *Polymer Preprints* **2002**, 43(1), 197.)

2.1 Abstract

Backbone architectures exert pronounced effects on the physical properties of PET ionomers, and this chapter focuses on the effects of the location of ionic groups on the stability of ionic aggregates at various temperatures. Three series of random and telechelic PET ionomers with equivalent molecular weights and ionic contents were synthesized using conventional melt polymerization. Quantitative incorporation of ionic groups into polymers was revealed using ^{1}H NMR spectroscopy, and subsequent measurement of inherent viscosity confirmed that the different architecture PET ionomers had equivalent molecular weights. The telechelic ionomers exhibited lower melt viscosities than the random analogues (240 – 290 ^{o}C), suggesting that the thermal energy more easily disrupted the ionic aggregates in the melt of telechelic ionomers at high temperatures. Solid state sodium NMR spectroscopy revealed that the ionic interaction in telechelic ionomers was slightly stronger at ambient temperature due to less steric effect. However, at high temperatures the activation energy of ion hopping dominated the stability of ionic aggregates, and the ease of ion hopping for end groups resulted in less stable ionic aggregates.

2.2 Introduction

Poly(ethylene terephthalate) (PET) is an important polyester composition for a myriad of applications, including textile filaments, packaging materials, and films and bottle products.[1-2] It is believed that incorporating a low level of ionic groups into PET will dramatically improve mechanical performance and compatibility with other substrates.[3-20] Random PET ionomers prepared *via* incorporation of dimethyl-5-sodiosulfoisophthalate sodium salt (SIP) are widely used to make fibers dyable with basic dyes, as well as fibers with antipilling and antistatic properties.[20] Recently, it has been suggested that the high elongational melt viscosity and strong melt strength of PET ionomers will facilitate the blow molding production of PET bottles.[21] However, random PET ionomers exhibit extremely high melt viscosity due to the presence of highly stable ionic aggregates within the range of temperatures required for melt polymerization and thermal processing (240-300^{o}C). Thus, efforts to facilitate additional potential applications of PET ionomers would be significantly enhanced through the development of PET ionomers bearing ionic aggregates wherein stability decreases dramatically with an increase in temperature. Previous research has demonstrated that a small change in ionomer structure can result in obvious differences in physical properties. Therefore, developing PET ionomers with diverse architectures may reduce current problems of viscosity.[22-24]

---

[1]Goodman, I.; Sheanan, R. J. *Eur. Polym. J.* **1990**, 26, 1081.
[2]Goodman, I.; Rodriguez, M. T. *Macrol. Chem. Phys.* **1994**, 195, 1705.
[3] (a) Greener, J.; Gillmor, J. R.; Daly, R. C. *Macromolecules* **1993**, 26, 6416. (b) Blanton, T. N.; Seyler, R. J. In Advance in X-ray Analysis; Gilfrich, J. V., Ed.; Plenum Press: New York, 1993; p379.
[4]Hara, M.; Xue, Y. *Macromolecules* **1997**, 30**,** 3803.
[5](a) Zhang, B.; Weiss, R. A. *J Polym Sci Polym Chem* **1992**, 30**,** 91. (b) Zhang, B.; Weiss, R. A. *J Polym Sci Polym Chem* **1992**, 30:989.

There are a variety of major architectures associated with ionomers, including random, monochelic, telechelic, telechelic branching, and block ionomers.[25] Telechelic ionomers were first produced as model polymers of the random analogues due to their well defined structures.[26-27] However, these random architecture polymers are similarly important for academic research and industry applications due to their unique properties. For example, telechelic unsaturated polyester ionomers, which are prepared *via* blending the polyesters prepared from the polycondensation of propylene glycol and maleic anhydride with metal oxide, like MgO, were studied extensively.[28-35] In addition, it has been shown that a low level of ionic end groups may act as nuclear agents to increase the crystallization rate of PET.[36-37] Recently, a new family of telechelic PET ionomers were developed by incorporating 3-sulfobenzoic acid, sodium salt, and a high level of ionic end groups (3 and 5 mol%) were shown to effectively increase melt viscosity and retard crystallization.[9] This document, therefore, details additional findings and particularly focuses on investigating the effect of the location of the ionic groups on the rheology and morphology. As it is well known that molecular weight exerts a pronounced effect on the properties of ionomers, while investigating the effect of ionic location it was necessary to prepare samples with equivalent molecular weights.[38] As previously report, 1-dodecanol was successfully used to control the molecular weight of PET random ionomers.[9] Three series of different architecture PET ionomers with equivalent molecular weight and ionic content were prepared via melt polymerization.

---

[6]Xue, Y.; Hara, M.; Yoon, H. N. *Macromolecules* **1998**, 31, 1808.
[7]Xue, Y.; Hara, M.; Yoon, H. *Macromolecules* **2001**, 34, 2001.
[8] Lin, Q.; Pasatta, J.; Wang, Z. H.; Ratta, V.; Wilkes, G.; Long, T. E. *Polym. Int.* **2002**, 51, 540.
[9]Kang, H.; Lin, Q.; Long, T. E., Armentrout, R. S. *Macromolecules* **2002**, 35, 8738.

Several models have been proposed to describe ionic aggregates, and discussions reported herein will be based on the Eisenberg-Hird-Moore model (EHM) derived from random poly(styrene-methalate sodium salt)s.[25] The basic premise of this model is that a low level of ionic units aggregate into multiplets consisting typically 2-8 ionic pairs, which are referred to call the "core". The chains held to the multiplets will have lower mobility than that of free chains and form a "corona". The thickness of the layers of reduced mobility is expected to be of the order of persistence length of the polymer chain. Typically, the size of the core/corona entity is too small (< 5 nm) to form a distinct phase, and its effect is limited to physical crosslink. As the ionic content increases, the number of multiplets grows, and the restricted mobility "coronas" of neighboring multiplets start to overlay and coalesce until a point is reached where a continuous region of restricted mobility occurs, whose size is sufficiently large to be considered a distinct phase having a distinct glass-transition and relaxation spectrum. This aggregation of the neighbor multiplets is called a cluster, and the ionic concentration of the formation of ionic clusters is referred to as the clustering point. Moreover, the ionic aggregates of some ionomers can be disrupted at a high temperature, allowng ionic groups to migrate among the multiplets, which is termed ion hopping.[39-40] As a result, these ionomers are able to flow and be processed at higher temperatures. The stability of ionic aggregates strongly depends on the speed of ion hopping or the relaxation time of ionic aggregates. For example, a higher rate of ion hopping will lead to loose ionic aggregates and low melt viscosity. Ion hopping speed depends on several factors, such as temperature, ionic concentration, polarity of polymer backbone and location of ionic groups. Thus, this

report investigates the effect of the location of ionic groups on the stability of ionic aggregates of PET ionomers at various temperatures.

2.3 Experimental

2.3.1 Materials

Dimethyl terephthalate (DMT), trimethyl 1,3,5-benzenetricarboxylate, 3-sulfobenzoic acid, sodium salt (SSAP) and 1-dodecanol were purchased from Aldrich, and used as received. Ethylene glycol and dimethyl-5-sodiosulfoisophthalate were kindly donated from Eastman Chemical Co., and used as received. Titanium tetraisopropoxide, antimony oxide and phosphoric acid were purchased from Aldrich, and detailed procedures for preparing catalysts solutions were previously described.[9]

2.3.2 Synthesis

A typical synthetic scheme for preparing dodecanol endcapped PET random ionomers is described as follows, and other PET copolymers were prepared via a similar procedure. The dodecanol endcapped PET random ionomers were prepared via the melt condensation of dimethyl-5-sodiosulfoisophthalate sodium salt, 1-dodecanol, DMT and EG. Both titanium tetraisopropoxide (20 ppm) and antimony oxide (180 ppm) were added to facilitate ester exchange and subsequent polycondensation. The reactor consisted of a 500 mL round-bottomed flask equipped with an overhead mechanical stirrer, nitrogen inlet, and condenser. The reactor containing the monomers and catalysts was degassed using vacuum and nitrogen three times, and subsequently heated to 190 °C. The reactor was maintained at 190 °C for 2 h, and the temperature was increased to

275°C over 2 h. The reaction was allowed to proceed for 30 min at 275°C, and then phosphoric acid was added to deactive the titanium catalyst. Vacuum was gradually applied up to higher than 0.5 mm Hg and polycondensation continued for 2 h at 275°C.

2.3.3 Characterization

The inherent viscosities of the copolymers were measured at 25 ^{o}C in a capillary viscometer using 0.5 g/dL solution in a 60/40 w/w mixture of phenol and tetrachloroethane. ^{1}H NMR spectra were recorded on a Varian 400 MHz spectrometer using trifluoroactetic acid-d as a solvent, and the ethylene unit at 4.80 ppm as an internal standard. Solid state ^{23}Na NMR was performed using MSL-300 on 79.2 MHz. NaCl was used as secondary reference with a chemical shift of 7.1 ppm. Samples were run in zirconia rotors using magnetic angle spinning and high power proton decoupling. To achieve uniform excitation, a pulse of 1.2 μs was used, although it was necessary to use a pulse delay of 10 s to obtain fully relaxed spectra. The measurement of residual metal catalysts was performed at Eastman Chemical Co.. Thermal transitions were determined on a Perkin-Elmer DSC Pyris 1 at a heating rate of 10 °C/min under N_2 purge, and the reported data are obtained from the second heating cycle. Rheological characterization was performed using a TA instruments AR 1000 melt rheometer.

---

[10]Boykin, T. C.; Moore, R. B. *Polym. Eng. Sci.* **1998**, 38, 1658.
[11]Barber, G. D.; Carter, C. M.; Moore, R. B. *Polymeric Materials and Engineering* **2000**, 82, 241.
[12]Boykin, T. L.; Moore, R. B. *Polym. Pre.* **1998**, 39, 393.
[13]NG, C. W. A.; Macnight, W. J. *Macromolecules* **1996**, 29, 2421.
[14]NG, C. W. A.; Lindway, M. J.; Macknight, W. J. *Macromolecules* **1994**, 3027.
[15]Wlochowicz, A. J. Macromol. Sci. Phys. 1992, B31, 239.
[16]Ostrowska-Czubenko, J.; Ostrowska-Gumkowska B. *Eur. Polym. J.* **1988**, 24, 65
[17]Ostrowska-Gumkowska, B.; Ostrowska-Czubenko, J. *Eur. Polym. J.* **1988**, 24, 803.
[18]Ostrowska-Gumkowska, B.; Ostrowska-Czubenko, J. *Eur. Polym. J.* **1991**, 27, 681.

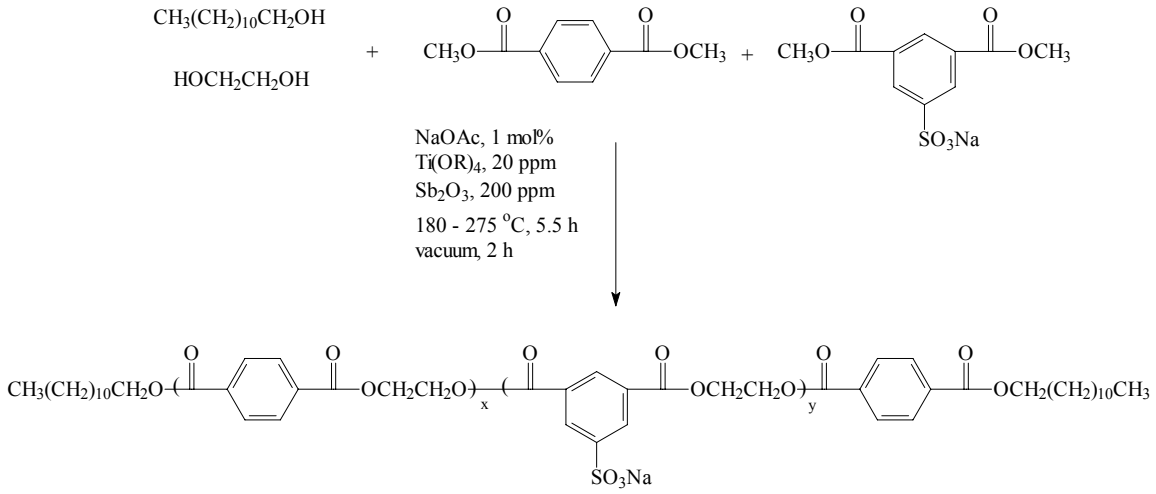

Scheme 2.1. Synthesis of dodecanol endcapped PET random ionomers, PET- DR_x

---

[19]Ostrowska-Gumkowska, B.; Ostrowska-Czubenko, J. Eur. Polym. J. **1994**, 30, 875.
[20]Militky, J. *Modified Polyester Fibres*, Elsevier, Amsterdam, 1991.
[21]Sinker, S. M. *U. S. Patent 4 554 238,* **1985**.
[22]Judas, D.; Fradet, A.; Marechal. E. *Polym. Bull.* **1986**, 16, 13.
[24]Eisenberg, A.; King, K. *Ion –Containing Polymers*; Academic Press: New York, 1977; 15.
[25]Fitzgeralld, J. J.; Weiss, R. A. *J. Macromol. Sci., Rev. Macromol. Chem. Phys.* **1988**, C28, 99.
[26]Eisenberg, A; Kim, J. S. *Introduction to Ionomers,* John Wiley & Sons: New York, 1998.
[27]Kolbet, K. A.; Schweizer, K. *Macromolecules* **2000**, 33,1425.
[28]Nyrkova, I. A.; Khokhlov, A. R.; Doi, M. *Macromolecules* **1993**, 26, 3601.
[29]Ltvinov, V. M.; Braam, A. W. M.; van der Pleog, A. F. M. J. *Macromolecules* **2001**, 34, 489.
[30]Szilagyl, A.; Izvekov, V.; vancso-Szmercsanyi, I. *J. Polym. Sci: Polym. Chem. Ed.* **1980**, 18, 2803.
[31]Rao, K. B.; Gandhi, K. S. *J. Poly. Sci.: Polym. Chem. Ed* **1985**, 23, 2135.
[32]Judas, D.; Fradet, A.; Marechal, E. *J. Polym. Sci; Polym. Chem. Ed.* **1984**, 22, 3309.
[33]Habassi, C.; Brigodiot, M.; Fradet, A. *Makromal. Chem.* **1990**, 191, 638.
[34]Vansco, I.; Szilagyi, A.; Izvvekov, V. *J. Poly. Sci: polym. Chem. Ed.* **1983**, 21, 1901.
[35]Han, C. D.; Lem, K. W. *J. Appl. Polym. Sci.* **1983**, 28, 763.
[36]Laleg, M.; Blanchard, F.; Chabert, B.; Pascault, J. P. *J. Eur. Polym. Sci.* **1985**, 21, 591.
[37]Yu, Y.; Yu, Y.; Jin, M.; Bu, H. *Macrol. Chem. Phy.* **2000**, 201, 1894.
[38]Yu, Y.; Bu, H.; *Macrol. Chem. Phy.* **2001**, 202, 421.
[39]Kim, J. S.; Yoshikawa, K.; Eisenberg, A. *Macromolecules* **1994**, 6437.
[40]Cooper, S. L. *J. Polym. Sci.* **1958**, 28, 195.

2.4 Results and Discussion

2.4.1 Compositions and molecular weights

PET ionomers of various architectures but with equivalent molecular weights and ionic contents, and nonionomers with equivalent molecular weights were synthesized *via* conventional melt polymerization. Scheme 2.1 depicts the synthesis of a dodecanol endcapped random PET ionomer, and PET ionomers and nonionomers with various architectures are described in Figure 2.1. These ionomers are termed as PET-Y_x, where Y denotes the location of the ionic groups. For example, T refers to the telechelic architecture, and x denotes the molar fraction of ionic units. The use of a trifunctional branching agent to prepare branched PETs offsets the negative effect of the telechelic architecture with a high level of endcapper that results in low molecular weight products. A high molecular weight telechelic ionomer with high ionic content (10.0 mol%) was prepared via incorporating a low level of a trifunctional branching agent (3.0 mol%), trimethyl 1,3,5-benzenetricarboxylate. Meanwhile, in order to compare the effect of the presence of dodecanol end groups, dodecanol endcapped PETs and PETs with equivalent molecular weight were also prepared.

---

[41]Tierney, N. K.; Register, R. A. *Macromolecules* **2002**, 35, 2385.
[42]Lin, Q.; Unal, S.; Fornof, A. R.; Wei, Y., Li, H., Armentrout, R. S., Long, T. E. *Macrom. Symp.* **2002**, in press.
[43]Nelson, C. J. *J. Polym. Chem. Ed.* **1974**, 44, 2905.
[44]Youk, J. H.; Kambour, R. P.; MacKnight, W. J. *Macromolecules* **2000**, 33, 3594.
[45]Lin, Q.; Long, T. E. *Macromolecules*, in preparation.
[46]O'Connell, E. M.; Root, T. W.; Cooper, S. L. *Macromolecules* **1994**, 27, 5803.
[47]O'Connell, E. M.; Root, T. W.; Cooper, S. L. *Macromolecules* **1995**, 28, 3995.
[48]O'Connell, E. M.; Root. T. W.; Cooper, S. L. *Macromolecules* **1995**, 28, 4000.
[49] Eisenberg, A.; Hird, B.; Moore, R. B. *Macromolecules* **1990**, 23, 4098.
[50]Rane, S. S,; Gujrati, P. D. *Polym. Mater. Sci. and Eng.* **2002**, 87, 157.
[51]Kim, J. S.; Hong, M.; Nah, Y. H. *Macromolecules* **2002**, 35, 155.
[52]Nykova, I. A.; Kholhlov, A. R.; Doi, M. *Macromolecules* **1993**, 26, 3601.

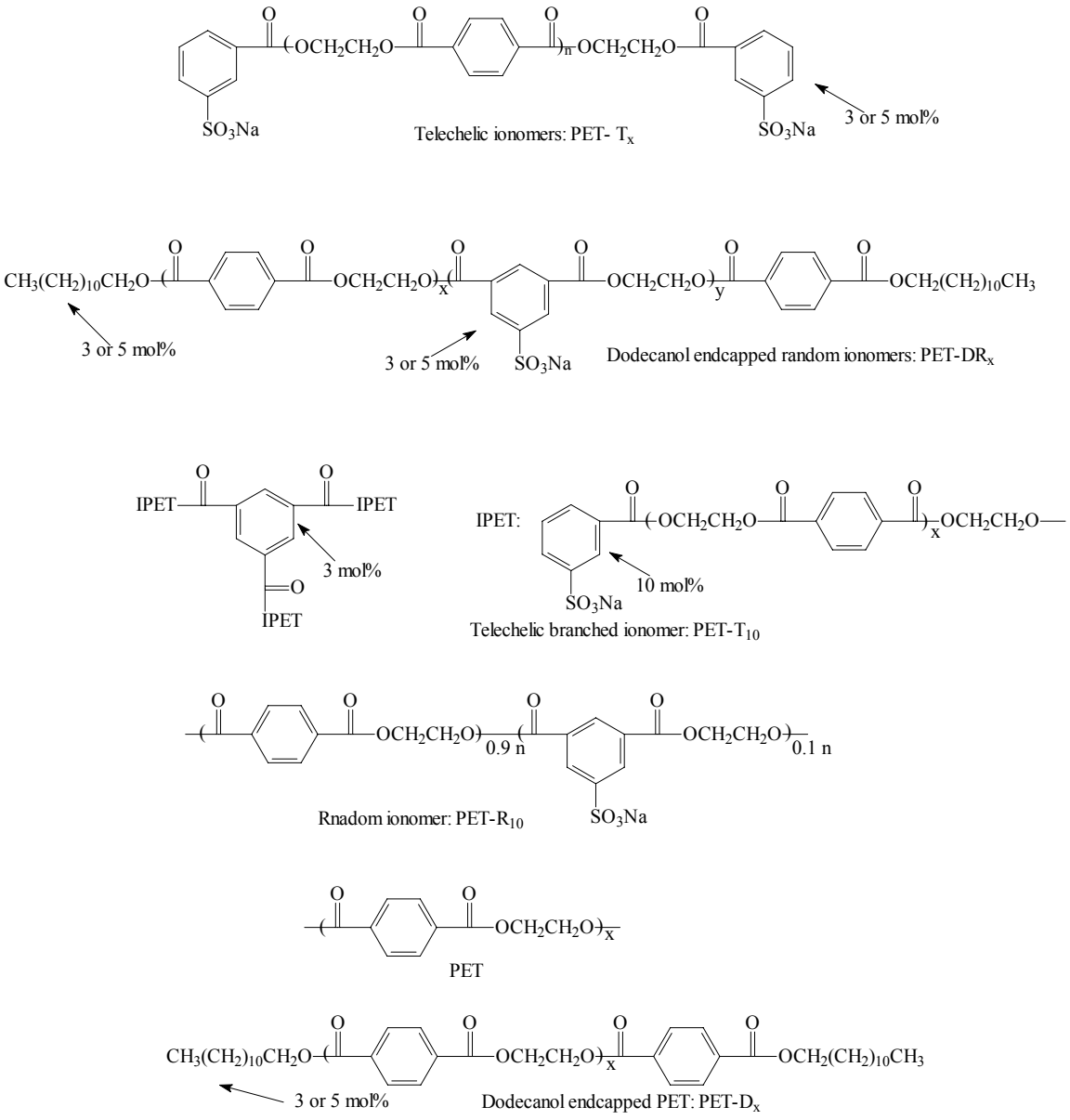

Figure 2.1 PET copolymers with different architectures

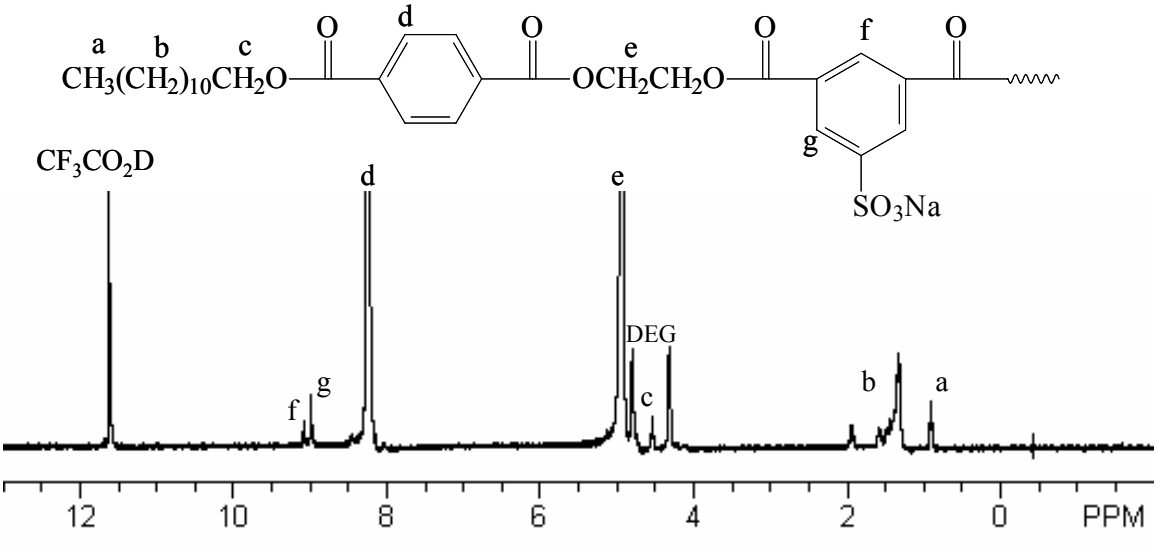

Figure 2.2 ^{1}H NMR spectrum of dodecanol endcapped PET ionomer, PET-DR_3, F_3CO_2D, 400 MHz

Table 2.1 Molecular weight of PET polymers and concentration of residual catalysts[a]

Sample	η (dl/g)[b]	Theoretical M_n[c] (g/mol)	Estimated M_n[b] (g/mol)	P (ppm)	Sb (ppm)	Ti (ppm)
PET-T_3	0.34	12,800	11,500	59	182	22
PET-DR_3	0.32	12,800	11,000	53	185	21
PET-D_3	0.36	12,800	12,500	58	189	22
PET-T_5	0.28	8,100	8,200	64	175	32
PET-DR_5	0.27	8,100	8,100	46	178	22
PET-D_5	0.26	8,100	8,000	49	190	22
PET-R_{10}	0.36	--------	12,500	62	180	20
PET-T_{10}	0.36	--------	12,500	57	187	21

a: measured by Eastman Chemical Co.; b: 25 ^{o}C in a capillary viscometer using 0.5 g/dL solution in a 60/40 w/w mixture of phenol and tetrachloroethane; c: estimated using Equation 1; d: estimated using Mark-Houwink formula equation.

Table 2.2 Thermal transition of PET copolymers

Sample	T_g[a] (ºC)	C_p (J / g* °C)	T_c (ºC)	ΔH (J/g)	T_m (ºC)	ΔH (J/g)
PET-T_3	78	0.36	149	30.4	250	49.7
PET-DR_3	68	0.29	138	27.0	245	45.3
PET-D_5	------	-------	-----	------	254	46.2
PET-T_5	76	0.34	147	32.6	242	43.3
PET-DR_5	63	0.28	143	26.0	235	35.2
PET-D_5	-------	-------	------	-------	254	47.0
PET-R_{10}	71	0.16	------	-------	-------	-------
PET-T_{10}	80	0.22	189	5.9	227	6.8

a: Data obtained from second heat cycle.

^{1}H NMR spectroscopy was used to verify the compositions of the PET ionomers. The ^{1}H NMR spectra of telechelic ionomers and dodecanol endcapped nonionomers were previously reported.[9] ^{1}H NMR spectrum of a typical dodecanol endcapped PET random ionomer, PET-DR_5, is depicted in Figure 2.2 and shows that the ionic groups were incorporated into the polymers in quantity. In addition, our previous research has demonstrated that the presence of residual catalysts exerts a pronounced influence on the morphology and rheology of PET ionomers.[9] Elemental analysis (Table 2.1) indicates that the residual catalysts agree well with charged values, and the effect of residual catalysts on resulting properties is considered to be identical in all ionomers.

Since excess ethylene glycol was used in the polymerization, and subsequently was removed via distillation during polycondensation, the conventional equation, X = (1+r)/(1-r), is not appropriate for estimating the molecular weight of telechelic ionomers.[9] Based on the assumption that the end capping reaction was quantitative and restricted to the polymer chain end, a modified equation (Equation 1) was utilized to estimate the

theoretical number average molecular weights. Table 2.1 includes the theoretical number average molecular weights for the PET-T_x ionomers.

<Mn> = (total mass of product molecules) / (moles of product molecules)

$= [\Sigma (m_e + x * m_{ru})] / (N(A)/2)$ (Equation 1)

where

m_e = the molar mass of the combined end groups

m_{ru} = the molar mass of an internal repeat unit

N(A) = moles of monofunctional end capping reagent

x = the number of internal repeat units

The inherent solution viscosity was measured at 25 ^{o}C, and the Mark-Houwink equation was used to estimate the approximate molecular weights of the products (Table 2.1).[5,42-43] The predicted values of ionomers with 5 mol % end-capper agreed well with the values estimated using this equation. However, the estimated values of ionomers with 3 mol% endcapper were slightly lower than the predicted value (Table 2.1), which is ascribed to the formation of intramolecular ionic aggregation in a diluted solution using a mixture of nonpolar solvents.[3]

2.4.2 Thermal transitions and rheological analysis

The presence of ionic aggregates in a polymer matrix exert a pronounced influence on the morphology and rheology of PET ionomers. According to the EHM model, the level of incorporated ionic groups significantly affects the properties of ionomers, and the clustering point of PET ionomers may range between 5 and 10 mol% based on the data from different technologies.[3,44] For this study, three series of ionomers

with different ionic contents (3, 5 and 10 mol%) were prepared as typical representatives of ionomers containing a low, medium, or high level of ionic groups, respectively.[3,44] Based on previous research, the ionomers with 3 mol% ionic groups are considered as ionomers without ionic clusters, since the ionic aggregates only result in physical crosslinking.[25] Ionomers with 5 mol% ionic groups contain a medium concentration of ionic groups around the clustering point, and 10 mol% ionomers are believed to exhibit behaviors typical of clustering ionomers.

Ionomers with 3 and 5 mol% ionic groups were semicrystalline polymers, and their thermal transitions behaved like high molecular polymers because the presence of the ionic aggregates increased their apparent molecular weights. DSC analysis (Table 2.2) indicates that dodecanol endcapped low molecular weight nonionomers (PET-D_5 and PET-D_3) did not exhibit an obvious glass transition and crystallization transition in the second heat cycle because rapid crystallization was completed during quenching (180 ºC/min) from 290 ºC to room temperature using nitrogen gas. However, the presence of ionic aggregates retarded crystallization, and an obvious glass transition and crystallization transition appeared in DSC analysis of the 3 and 5 mol% ionomers with an identical thermal history and inherent viscosities. Moreover, the telechelic ionomers and random ionomers exhibited slightly different thermal transition behaviors due to the difference in chain regularity. The ionic groups of telechelic ionomers act only as end groups, and have no obvious effect on the regularity and packing of the polymer backbone. As a result, the glass transition temperature, crystallization transition temperature and the heat of fusion (related with the degree of crystallinity) are similar to a common high molecular weight PET (Table 2.2). However, the bulky and *meta* ionic

units of random ionomers locate randomly in the polymer chain, which disrupts the regularity of the polymer chain. The presence of ionic aggregates in random ionomers restricts the polymer chains, which increase with an increase in molecular weight, and may partially balance the negative effect of incorporating kinked groups.[8,38] However, the dodecanol endcapped PET random ionomers only exhibited moderate molecular weights, and the ionic interaction was not strong enough to offset the disruptive effect of *meta* linked groups. As a result, the random ionomers exhibited behaviors similar to high molecular weigh poly(ethylene terephthalate – ethylene isophthalate) copolymers with a lower crystallization, glass transition temperature, and smaller heat of fusion (lower crystallinity).

For PET ionomers with 10 mol% ionic groups, the ionic aggregates exerted a more pronounced effect on the thermal transitions due to the presence of stronger ionic interaction. PET-R_{10} was a transparent product because the extremely high melt viscosity prevented crystallization. However, PET-T_{10} was a semicrystalline polymer with a higher crystallization temperature (189 ^{o}C) than regular PETs (140 ^{o}C), mostly due to the fact that high viscosity levels retarded the movement of the polymer chains at low temperatures (Table 2.2). These results indicate that the local mobility of telechelic ionomer chains was higher than that in random analogues, and this was confirmed by rheological analysis.

The rheological analysis of the ionomers with 5 mol% ionic groups and corresponding nonionomers is depicted in Figure 2.4. The melt viscosities of the dodecanol endcapped PET were smaller than those of the pure PET with an equivalent molecular weight, which indicates that the effect of the flexible endcapper, dodecanol, on

the melt viscosity of low molecular weight PETs can not be neglected. The PET-T_5 and PET-DR_5 ionomers had obviously higher melt viscosities than nonionomers, which was ascribed to the presence of ionic aggregates in the melt. Moreover, PET-R_5 exhibited higher melt viscosity than PET-T_5, which indicates that the ionic aggregates of random ionomers were more stable, and that ion hopping in the melt of PET-R_5 proceeded at a slower rate. The melt viscosity of ionomers with 3 mol% ionic groups exhibited similar behaviors as ionomers with 5 mol% ionic groups, except for one slight difference – the melt viscosities of the telechelic ionomers were very close to nonionomers, especially when the temperature was higher than 290 °C (Figure 2.3). This result suggests that the ionic aggregates in the melt of PET-T_3 were very loose, and ions were able to hop among multiplets without any extra activation energy at high temperature (> 290 ^{o}C). To conclude, when the ionic level was lower than 3 mol%, the presence of ionic groups as end groups did not exert any pronounced effect on melt viscosity at high temperature due to the ease of ion hopping, and thus will facilitate the synthesis and thermal processing of PET ionomers.

The temperature ramp of ionomers with 10 mol% ionic groups with an inherent viscosity of 0.36 dl/g is depicted in Figure 2.5. Between 240 and 290 ^{o}C, PET-R_{10} ionomers exhibited extremely high melt viscosity levels due to highly stable ionic aggregates with a low rate of ion hopping. However, PET-T_{10} exhibited much lower melt viscosities than PET-R_{10}, due to less stable ionic aggregates. Frequency sweeps of 10 mol% ionomers at different temperatures were also performed to generate a time-temperature superposition relationship. The relaxation time of the PET-R_{10} ionic clusters appeared in an extremely low frequency because the relaxation of highly restricted ionic

clusters generally requires a very long time. The large discrepancy in the relaxation time between the organic matrix and ionic clusters allows the time-temperature superposition to work well (Figure 2.6). However, Figures 2.7 indicates that the G' curves of PTE-T_{10} at different temperatures cross over at one point, and thus the time-temperature superposition fails. This result indicates that the relaxation time of ionic clusters of PET-T_{10} was close to the relaxation time of the organic matrix, and the two relaxations interacted in such a way that the time-temperature supposition failed. Thus, the telechelic ionomers exhibited lower melt viscosities at high temperature than the random analogues based on rheological analysis, which suggests that the telechelic architecture results in less stable ionic aggregates.

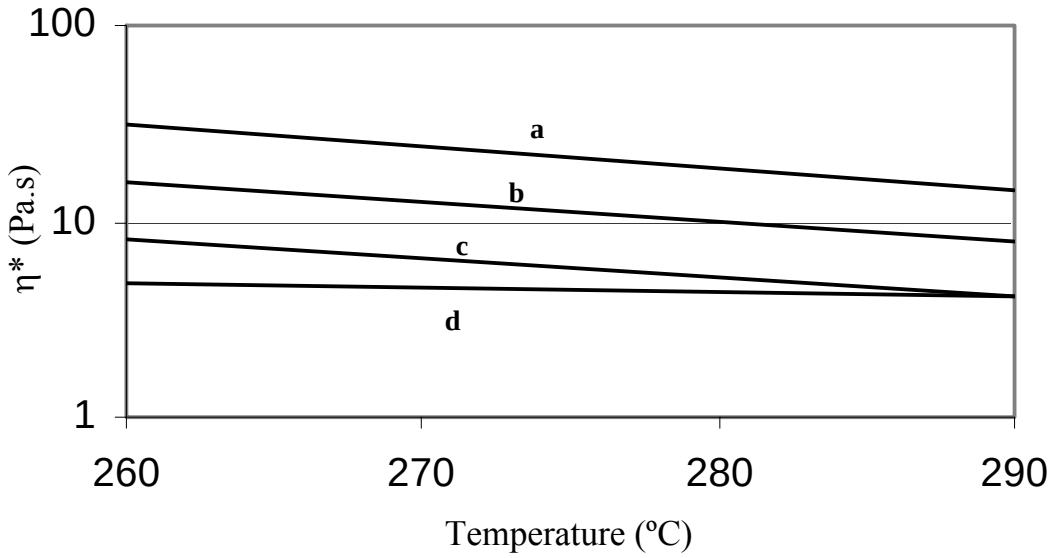

Figure 2.3 Temperature ramp of PET ionomers with 5 mol% ionic groups and nonionomers with equivalent inherent viscosity (0.28 dL/g), a: dodecanol endcapped random ionomer, PET-DR_5; b: telechelic ionomer, PET-T_5; c: PET; d: dodecanol endcapped PET, PET-D_5.

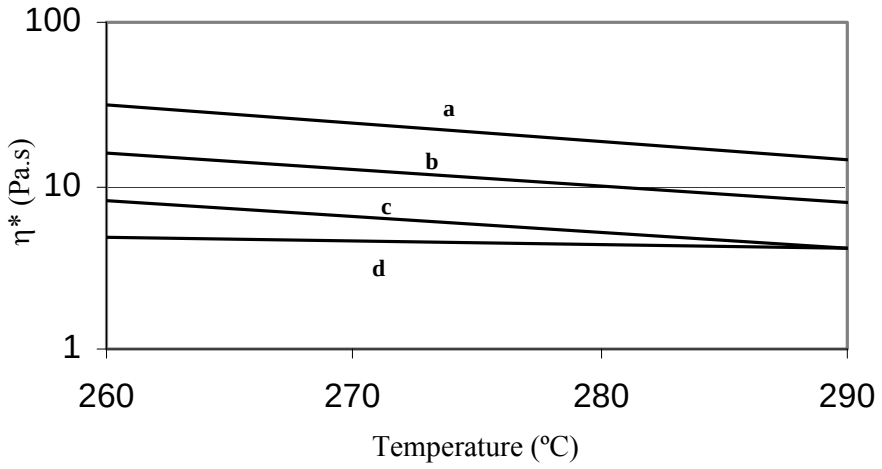

Figure 2.4 Temperature ramp of PET ionomers with 3 mol% ionic groups and nonionomers with equivalent inherent viscosity (0.34 dL/g), a: dodecanol endcapped random ionomer, PET-DR_3; b: telechelic ionomer, PET-T_3; c: dodecanol endcapped PET, PET-D_3; d: PET.

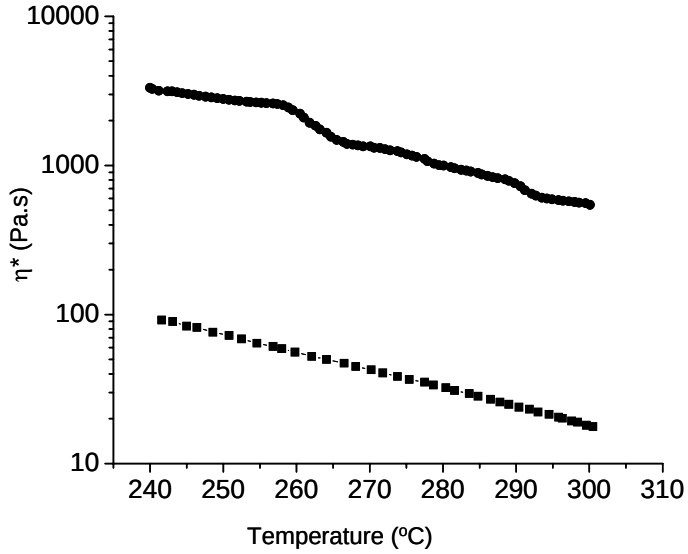

Figure 2.5 Temperature ramp of PET ionomers with 10 mol% ionic groups (0.81 dL/g), PET-R_{10} (top) and PET-T_{10} (bottom)

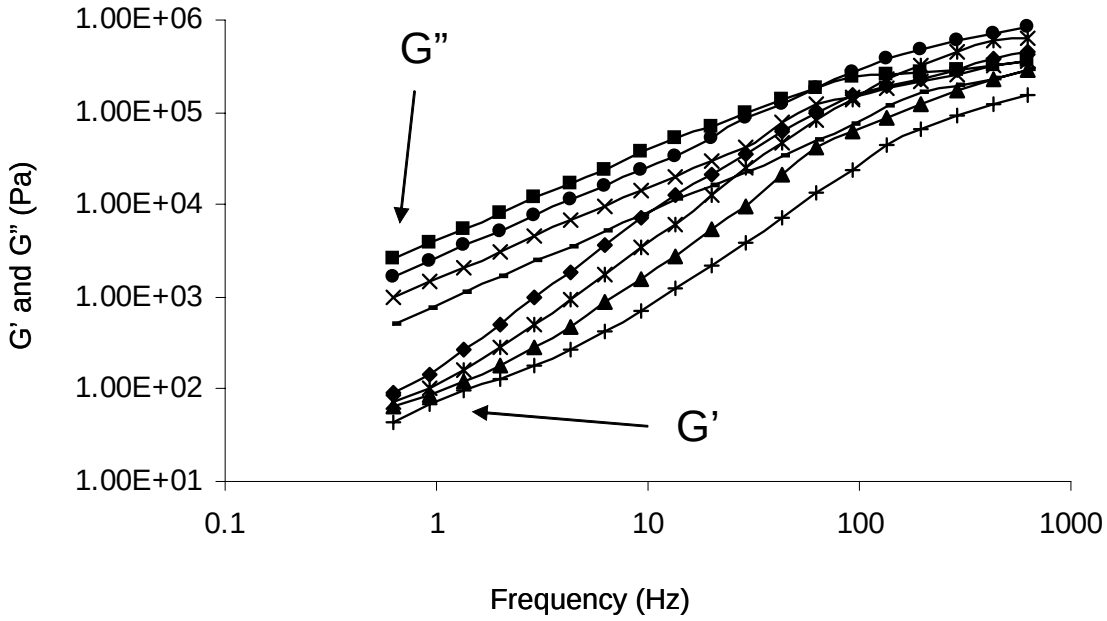

Figure 2.6 Frequency sweep of PET-R_{10} at different temperatures, form top: 260, 270, 280 and 290 ^{o}C

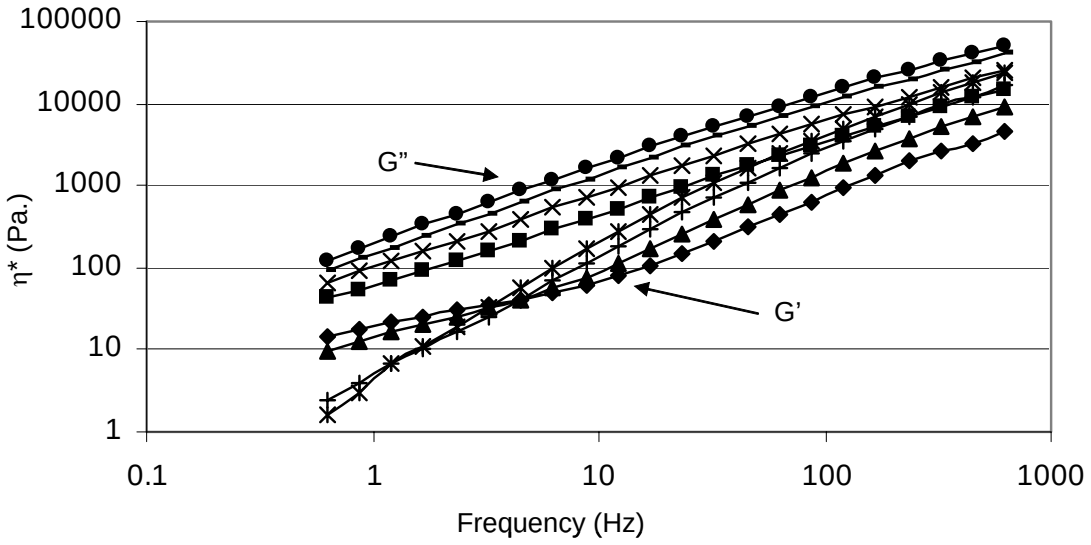

Figure 2.7 Frequency sweep of PET-T_{10} at different temperatures, form top: 260, 270, 280 and 290 ^{o}C

2.4.3 Solid State ^{23}Na NMR Spectroscopy

Cooper and coworkers demonstrated that specific ionic environments yield different electrical field gradients surrounding the nuclei due to the quadrupolar coupling interaction of the ^{23}Na nuclei, and this results in distinctly different quadrupolar coupling constants (QCC).[45-47] As a result, QCC can be used to measure the strength of interactions between the quadrupolar sodium nuclei and the electric field gradients in their surrounding environment. In most cases, up-field shifts or increases in QCC was observed when the ionic aggregates became more stable. This may be attributed to stronger interactions beween the ionic groups resulting from a apparent combination of a greater number of ions held in aggregates, closer packing between ions, and/or a less symmetrical packing of the ionic groups.

Solid state ^{23}Na NMR spectra of PET-T_{10} and PET-R_{10} are depicted in Figure 2.8. Contrary to results of rheological analysis at high temperatures, PET-T_{10} exhibited slightly increased negative chemical shifts, which indicates that the telechelic ionomers had slightly stronger ionic interactions at ambient temperature due to closer packing or the larger size of multiplets. Thus, it can be concluded that the stability of ionic aggregates of telechelic ionomers changes dramatically with an increase in temperature, and the resultng increase in thermal energy can more easily disrupt these aggregates.

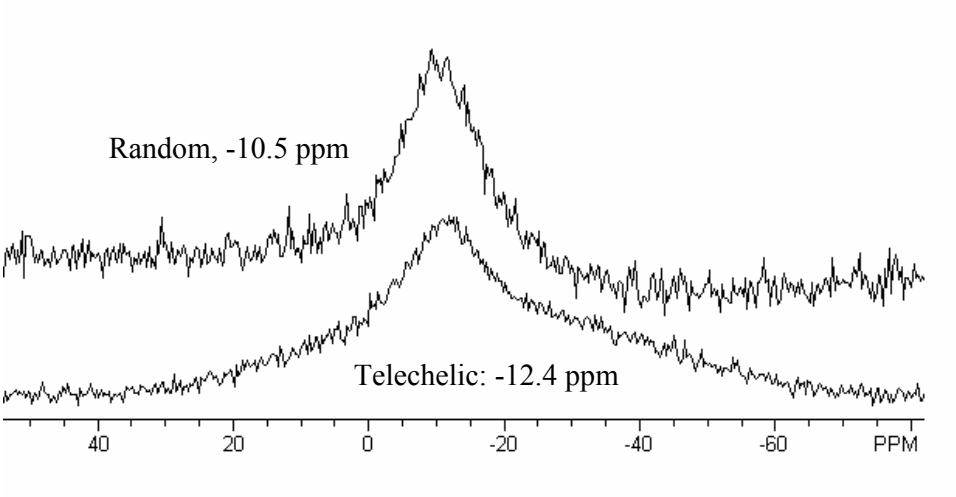

Figure 2.8 Solid state sodium NMR spectra of ionomers with 10 mol% ionic groups (sodium salt)

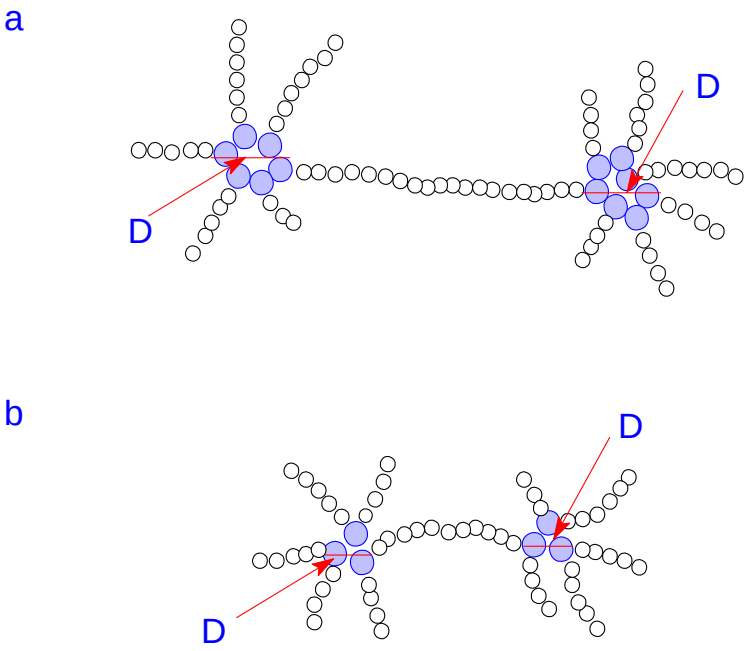

Figure 2.9 Structures of multiplets of telechelic and random ionomers, a: telechelic ionomers; b: random ionomers.

2.4.4 Discussion

To illustrate the difference in the stability of telechelic and random ionomers, a molecular model (Figure 2.9) was generated based on the concept of the EHM model, wherein the basic units of ionic aggregates were multiplets.[25] Several factors determine the stability of multiplets, such as temperature, counter ions, flexibility of polymer backbone, and the dielectric properties of the polymer backbone. If these factors are identical, steric effect alone will determine the stability of the ionic aggregates.[25] Less bulky ionic units result in larger multiplet sizes, because more ionic groups come into a fixed volume, or the ionic groups pack closer, which promotes ionic interaction to result in more stable multiplets.[25] Based on the above analysis, telechelic ionomers will thus form more stable ionic aggregates due to a reduction in steric effect. At low temperature without ion hopping, results obtained from solid state sodium NMR agreed well with results derived from the EMH model. Melt rheological analysis, however, revealed a reduction in the stability of ionic aggregates at high temperatures. Because the EMH model generated was based on ionic aggregates of random ionomers, the individualized properties of end groups must be considered when investigating the stability of ionic aggregates in the melt of telechelic ionomers at high temperature.

It is well known that the higher mobility of end groups exert a pronounced effect on the physical properties of polymers.[48] Recently, Kim and coworkers demonstrated that the stability of ionic aggregates changed from thermodynamic control to kinetic control at high temperatures. They suggested that the activation energy of ion hopping plays a determining role in the stability of ionic aggregates at high temperatures rather than the interaction among ions.[50] It is obvious that end groups, which are connected to

only one polymer chain, need a lower activation energy to hop among multiplets, and this ease of ion hopping significantly impacts the less stable ionic aggregates in the melt of telechelic ionomers at high temperatures. However, at low temperatures ion hopping does not occur, and the strength of ion interaction dominates the stability of ionic aggregates. Thus, telechelic ionomers demonstrate stronger ionic interaction due to less steric effect when ion hopping does not occur, which is consistent with the results from solid state sodium NMR at ambient temperature.

It should also be noted that the sequence in ionomers with a high level of ionic groups becomes an important factor in determining the stability of ionic aggregates.[51] As the level of charged ionic groups increases, the possibility of dimer, dy II (Figure 2.10), increases dramatically in random ionomers. Dy II dramatically improves the stability of ionic aggregates at high temperature, because it is very difficult for two repeat units to hop simultaneously, which results in highly stable ionic aggregates. However, telechelic ionomers do not have this accelerating effect because the ionic groups are always found at the ends of the polymer. Moreover, an increase in the ionic level decreases the distance between ionic groups, which reduces the driving force for phase separation, and negatively impacts the stability of ionic aggregates. As a result, it can be predicted that the stability differential of ionic aggregates between telechelic and random ionomers at high temperatures will increase with an increase in the level of ionic groups. And in fact, the ionomers with 10 mol% ionic groups (0.36 dL/g) exhibit much larger differences in melt viscosity than the 3 mol% ionic groups (0.34 dL/g) (Figure 2.3 and Figure 2.5).

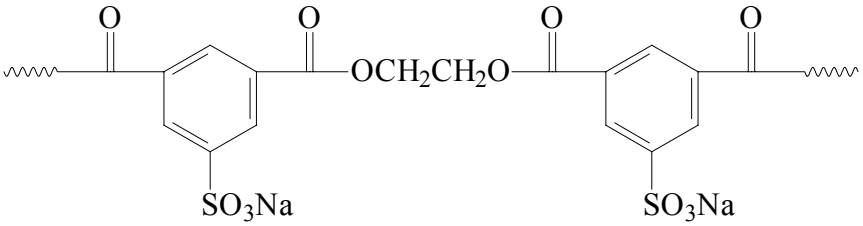

Figure 2.10 Structure of dimer of ionic unit – ionic unit, dy II

2.5 Conclusions

Three series of random and telechelic PET ionomers with equivalent molecular weights and ionic contents were synthesized using conventional melt polymerization. The telechelic ionomers exhibited lower melt viscosities than the random analogues (240 – 290 ^{o}C), which suggests that the ionic aggregates of telechelic ionomers more easily disrupted ionic hopping by thermal energy at high temperatures. Solid state ^{23}Na NMR demonstrated that the ionic interaction in telechelic ionomers was slightly stronger at ambient temperatures due to less steric effect. However, at high temperature, the activation energy of ion hopping dominated the stability of the ionic aggregates, and the ease of ion hopping in end groups resulted in less stable ionic aggregates.

CHAPTER 3

Synthesis and Characterization of Branched Telechelic Polyester Ionomers

(Published as: Lin, Q.; Long, T. E. *Macromolecules*, in progress.)

3.1 Abstract

Branched polyesters [poly(ethylene terephthalate) (PET) and poly(ethylene terephthalate-ethylene isophthalate) (PETI)] with ionic end groups were synthesized via conventional melt polymerization using trimethyl 1,3,5-benzenetricarboxylate as a branching agent and 3-sulfobenzoic acid, sodium salt as an end capping reagent. To investigate the effect of endcapper and branching reagent on the molecular weights of polyesters via GPC, 1-dodecanol endcapped branched PETIs were also synthesized. GPC investigation demonstrated that a low level of branching reagent increased weight average molecular weights and molecular weight distributions; however, the number average molecular weights remained constant. The temperature ramp curves of telechelic branched PETI ionomers in rheological analysis were characterized as three distinct regions. At low temperatures, the whole multiplets moved along the flow without ion hopping. When ions were able to hop among multiplets, melt viscosity dropped dramatically. Moreover, above a certain point, an increase in temperature did not increase the ion hopping rate, and the melt viscosity remained constant. Evidence of shear thickening in PETI ionomers at high frequency and high temperature suggests that a high fraction of intramolecular ionic aggregates are present.

Keywords: branched, telechelic, intramolecular, intermolecular, viscosity

3.2 Introduction

Ionomers are conventionally defined as ion-containing polymers with a maximum ionic content of approximately 15 mol %.[1] Due to electrostatic interactions and the thermodynamic immiscibility between ionic groups and the polymer matrix (typically nonpolar hydrocarbons), ionic groups tend to aggregate.[1] The presence of ionic aggregates in the organic matrix exerts profound effects on the mechanical properties and melt viscosities of polymeric materials.[2-5] Although several models have been proposed to describe the ionic aggregates,[1,6-8] this discussion will be based on the Eisenberg-Hird-Moore (EHM) model.[1] The basic premise of this model is that a low level of ionic units aggregate into multiplets consisting typically of 2-8 ionic pairs, which are too small(< 5 nm) to form a distinct phase, and can only be considered as physical crosslinks. As the ionic content increases, the number of multiplets grows, and the neighboring multiplets start to overlay and coalesce until a point is reached wherein a continuous region is sufficiently large to be considered a distinct phase with a distinct glass transition and relaxation spectrum. These aggregates of the neighbor multiplets are termed as clusters, and the ionic concentration of the formation of ionic clusters is called the clustering point.

---

[1]Eisenberg, A; Kim, J. S. *Introduction to Ionomers,* John Wiley & Sons: New York, 1998.
[2]Holliday, L. Ed. *Ionic Polymers*, John Wiley & Sons: New York, 1975.
[3]Li, C.; Registers, R. A.; Cooper, S. L. *Polymer* **1989**, 30, 1227.
[4]Eisenberg, A.; Hird, B.; Moore, R. B. *Macromolecules* **1990**, 23, 4098.
[5]Kim, J. S., Eisenberg, A. *Macromolecules* **1994**, 27, 2789.
[6]Judas, D.; Fradet, A.; Marechal. E. *Polym. Bull.* **1986**, 16, 13.
[7]Judas, D.; Fradet, A.; Marechal, E. *Polym. Bull.* **1986**, 16, 13.

Although ionomers have been extensively studied for approximately 30 years, their complicated behaviors have challenged many researchers. For example, a small change in structure, such as the location of ionic groups or the spacing between the ionic groups, typically results in significant changes in their properties.[9] The ionomers with a most complicated architectures are the branched telechelic ionomers, which exhibit some unique properties as a result of their unique structures.[10-14] Fetters and coworkers first reported the synthesis of star two, three, and twelve arms polyisoprenes with sulfozwitterion end groups.[10] Pispas and Hadjihristidis extended these studies to star block copolymers of styrene and isoprene with ionic end groups.[11] Other researchers have reported that the degree of association of star telechelic ionomers is lower than those of corresponding linear polyisoprenes.[12] Kennedy and coworkers reported the synthesis and mechanical properties of three-arm star polyisobutylenes with metal sulfonated end groups.[13] Storey and coworkers prepared three-arm star hydrogenated polybutadienes with oligomeric sulfonated polystyrene tails.[14] Those ionomers exhibited poor mechanical properties, which suggests that the networks were weak due to a high fraction of intramolecular aggregates, in which two or three arms of the same molecule were incorporated into the same multiplet.[14] Even with this growing body of knowledge, the behaviors of telechelic branched are still not well understood.

---

[8]Fitzgeralld, J. J.; Weiss, R. A. *J. Macromol. Sci., Rev. Macromol. Chem. Phys.* **1988**, C28, 99.

[9](a) Delf, B. W.; MacKnight, W. J. *Macromolecules* **1969**, 2, 309. (b) Yarusso, D. J.; Cooper, S. L. *Macromolecules* **1983**, 16, 1871.

[10]Kang, H.; Lin, Q.; Armentrout, R. S.; Long, T. E. *Macromolecules* **2002**, 35, 8738.

[11](a) Davidson, N. S.; Fetters, L. J.; Funk, W. J.; Graessley, W. W.; Hadjichristidis, N. *Macromolecules* **1988**, 21, 112. (b) Fetters, L. J.; Braessley, W. W.; hadjichristidis, N.; Kiss, A. D; Pearson, A. D.; Younghouse, L. B. *Macromolecules* **1988**, 21, 1644. (c) Shen, Y.; Safinya, C. R.; Fetters, L. J.; Adam, M.; Witten, T.; Hadjichristidis, N. *Phys.Rev.* **1991**, 43, 1886.

Polyesters are important materials with various applications, such as plastic bottles, fibers and film products.[15] Since morphology and rheology play key roles in the properties of the resulting products, more sophisticated control of these factors may facilitate even wider technological applications.[15-18] One of methodologies used to control the morphology and rheology of polyesters is to incorporate branched structures via small amount of trifunctional monomer.[18] However, the use of trifunctional branching reagents always results in a crosslinked network. Recently, it was demonstrated that using an endcapped reagent prevented crosslinking, and thus facilitated the preparation of polyesters with a higher level of branching.[18] Like other polymeric materials, end groups play an important role in the applications of polyesters, especially in adhesives and coatings, since the hydrophilic end groups tend to aggregate on the surface to improve the interaction with polar substrates.[19] It has been reported that functionalizing the end groups of PET provide a method to improve performance, and a series of telechelic polyester ionomers was prepared using 3-sulfobenzoic acid sodium salt as an endcapper.[9] Moreover, these telechelic polyester ionomers have been shown to form unique ionic aggregates whose stability dramatically decreases with an increase in temperature, resulting in improved mechanical properties and ease of melt polymerization and processing.[20] Conversely, an increase in the level of endcapper results in low molecular weight products with poor mechanical properties. To balance this negative effect, a branching agent can be used to prepare high molecular weight products with a high level of functional end groups. It is also interesting to investigate the effect of the number of arms in one molecule on the stability of ionic aggregates.

In this section, the synthesis and characterization of branched telechelic polyester ionomers is reported. These ionomers are typical representatives of ionomers with a branched backbone, ionic end groups and broad molecular weight distributions. This investigation will provide some additional information to better understand the behaviors of ionomers with complex structures.

3.3 Experimental

3.3.1 Materials

Dimethyl terephthalate (DMT, 99%), dimethyl isophthalate (DMI), 3-sulfobenzoic acid, sodium salt (SSAP) and trimethyl 1,3,5-benzenetricarboxylate (98%) were purchased from Aldrich and used as received. Ethylene glycol (EG) was purchased from J. T. Baker and used as received. Titanium tetraisopropoxide (99%) and antimony oxide (99%) were purchased from Aldrich, and the preparation of the catalyst solutions has been previously described[9]

---

[12](a) Hadjichristidis, N. *Macrol. Chem. Symp.* **1991**, 48/49, 47. (b) Pispas, S.; Hadjichristidis, N. *Macromolecules* **1994**, 27, 1891. (c) Pispas, S.; Hadjichristidis, N., Mays, J. W. *Macromolecules* **1994**, 27, 6307.

[13]Kennedy, J. P.; Ross, L. R.; Lackey, J. E.; Nuyken, O. *Polym. Bull.* **1981**, 4, 67.

[14](a) Mohair, Y.; Tyagi, T.; Wilkes, G. L.; Storey, R. F.; Kennedy, J. P. *Polym. Bull.* **1982**, 8, 47. (b)Bagrodia, S.; Mohajer, Y.; Wilkes, G. L.; Storey, R. F., Kennedy, J. P. *Poly. Bull.* **1982**, 8, 281.

[15]Storey, R. F.; George, S. E.; Nelson, M. E. *Macromolecules* **1991**, 24, 2920.

[16](a) Goodman, I.; Sheanan, R. J. *Eur. Polym. J.* **1990**, 26, 1081. (b) Goodman, I.; Rodriguez, M. T. *Macrol. Chem. Phys.* **1994**, 195, 1705. (c) Lawton, E. L. *Polym. Eng. Sci.* **1985**, 25, 348.

[17](a) Manaresi, P.; Parrini, P.; Semeghini, G. L.; De Fonasari, E. *Polymer* **1976**, 17, 595. (b) Langla, B.; Strazielle, C. *Macromol. Chem.* **1986**, 187, 591.

[18](a) Rosu, R. F.; Shanks, R. A.; Bhattacharya, S. N. *Polym. Int.* **1997**, 42, 267. (b) Jaykannan, M.; Ramakrishan, S. *J. Polym. Sci.: Part A, Polym. Chem.* **1998**, 36, 309. (c) Hess, C.; Hirt, P.; Oppermann, W. *J. Appl. Polym. Sci.* **1999**, 74, 728.

3.3.2 Synthesis

Ionomers were prepared via the melt condensation of DMT, DMI, EG, and SSAP with or without a branching agent. Both titanium tetraisopropoxide (20 ppm) and antimony oxide (200 ppm) were added to facilitate ester exchange and subsequent polycondensation. The reactor consisted of a 250 mL round-bottomed flask equipped with an overhead mechanical stirrer, nitrogen inlet, and condenser. The reaction was maintained at 190 °C for 2 h, and then the temperature was increased to 275 °C over 2 h. The reaction was allowed to proceed for 30 min at 275 °C. Vacuum was gradually applied to higher than 0.5 mmHg and polycondensation continued for 2 h at 275 °C. The ionomers were termed as PETI-B_xT_y, where B denotes the branching agent, x denotes the molar fraction of branching agent, T denotes the ionic end groups, and y denotes the molar fraction of ionic groups. Dodecanol end capped branched PETI nonionomers were also synthesized using an identical procedure.

---

[19]Hudson, N.; MacDonald, Neilson, A.; Richard, R. W.; Sherrington, D. C. *Macromolecules* **2000**, 33, 9255.
[20]Boiko, Y. M.; Guerin, G.; Marikhin, V. A.; Prud'homme, R. E. *Polymer* **2001**, 8659.
[21](a) Lin, Q.; Long, T. E. , in preparation for *Macomolecules.* (b) Lin, Q.; Gariano, N.; Madison, P. H.; Wang, Z.; Long, V. K.; Long, T. E. *Polym. Prep.* **2002**, 43(1), 254.
[22]Semenov, A. N.; Joanny, J. F.; Khokhlov, A. R. *Macromolecules* **1995**, 28, 1066.
[23]Greener, J.; Gillmor, J. R.; Daly, R. C. *Macromolecules* **1993**, 26, 6416.
[24]Hird, B.; Eisenberg, A. *Macromolecules* **1992**, 25, 6466.
[25](a) Chassenieux, C.; Tassin, J. F.; Gohy, J. F.; Jerome, R. *Macromolecules* **2000**, 1796. (b) Ilarduya, A. M.; Kint, D. P. R.; Munoz-Guerra, S. M. *Macromolecules* **2000**, 33, 4596.
[26]Witten, T. A.; Cohen, M. H. *Macromolecules* **1985**, 18, 1915.

3.3.3 Characterization

The inherent viscosity of the copolymers was measured at 25 ^{o}C using a capillary viscometer in a 0.5 g/dL solution of 60/40 w/w mixture of phenol and tetrachloroethane. ^{1}H NMR spectra were recorded on a Varian 400 MHz spectrometer, and trifluoroactetic acid–d was used as a NMR solvent. GPC measurements were performed on a Waters SEC (515 pump, 717 autosampler) with an external 410 refractive index detector. Multiangle laser light scattering (MALLS) was also performed using an in-line Wyatt Minidawn. A Polymer Laboratories PLgel, 5 micron MIXED-C column with a length of 300 mm and inner diameter of 7.5 mm was used. The flow rate was 1.00 mL/min and the temperature was 40 °C. Thermal transitions were determined on a Perkin-Elmer DSC Pyris 1 under N_2 purge. The rheological analyses were performed using a TA instrument AR 1000 melt rheolometer.

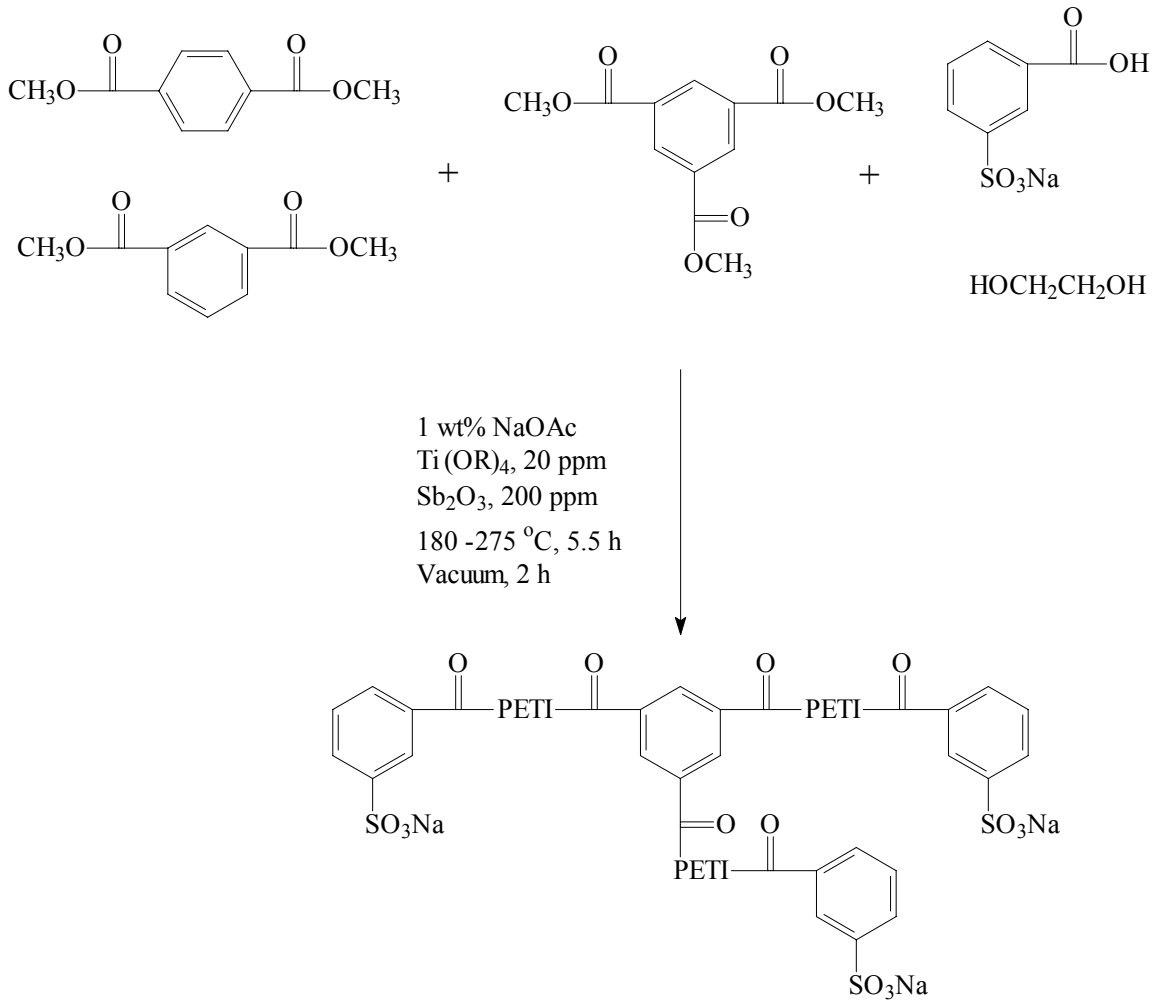

Scheme 3.1 Synthesis of telechelic branched poly(ethylene terephthalate-isophthalate) (PETI) ionomers

3.4 Results and discussion

3.4.1 Synthesis

As expected, the presence of an endcapper effectively prevented gelation, without which gelation products could only be obtained when the level of the branching agent was higher than 1 mol%.[18] However, when a high level of endcapper (5 mol%) was present, the level of branching reagent improved to 3 mol%. As a result of these studies, it appears that a critical point (3.0 mol%) is needed for the branching agent to have an impact on the melt viscosities of PETI during the polymerizations. Below 3 mol%, the increase in melt viscosity is not obvious. However, as indicated, melt viscosity increases dramatically when the concentration of the branching agent is 3 mol%. Moreover, this critical level (3 mol%) was also observed in later experiments (solution viscosity and melt rheological analysis), which was presumed to be related to the presence of a high fraction of intramolecular ionic aggregates in ionomers with lower levels of branching reagent.

In order to investigate the effect of backbone on the properties of the branched telechelic polyester ionomers, branched telechelic PET ionomers were also synthesized. PET ionomers exhibited higher melt viscosity due to their rigid backbone, and the ionomers (5 mol% ionic end groups) with branching agent levels higher than 1.0 mol% were not attainable due to extremely high melt viscosity. Previous research has demonstrated that GPC has not been effective in measuring the molecular weight of ionomers due to the presence of ionic groups.[9] In order to investigate the effect of the presence of an endcapper and a branching agent on molecular weights using GPC, dodecanol endcapped branched PETI were also prepared.

Figure 3.1 depicts the NMR spectrum of PET-T_5, and the charged level of SSBA agrees well with the SSBA concentration in the polyester as determined using ^{1}H NMR spectroscopy. ^{1}H NMR spectroscopy was also utilized to ascertain DEG levels (Figure 3. 1), and the presence of sodium acetate ensured that DEG levels were reproducibly lower than 3 mol%. For the PETI ionomers, ^{1}H NMR spectrum did not reveal ionic units due to the overlay of the resonances of the isophthalate units and ionic units. However, based on later characterization studies of PET ionomers, it was presumed that the ionic groups were incorporated into the ionomers quantitatively.

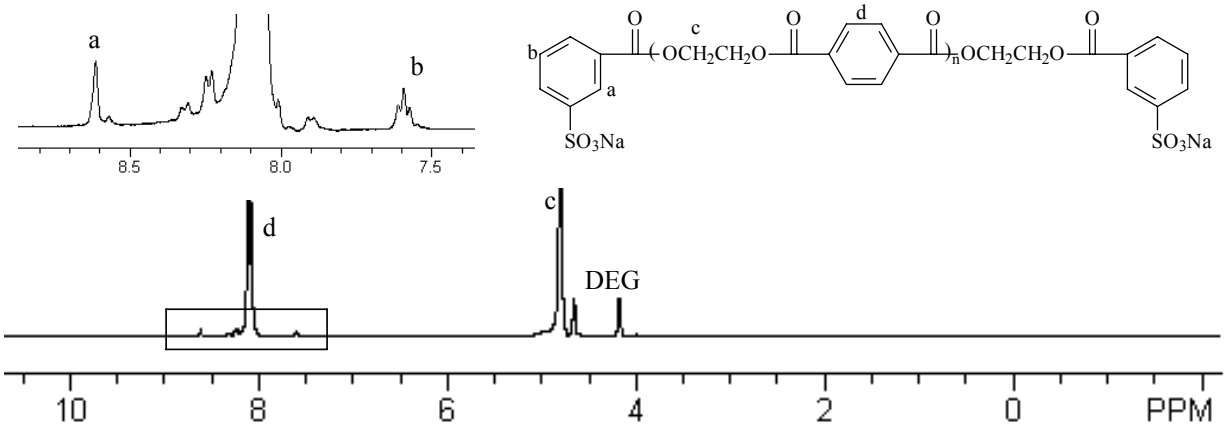

Figure 3.1 ^{1}H NMR Spectrum of telechelic branched PET ionomer, PET-T_5, CF_3CO_2D, 400 MHz

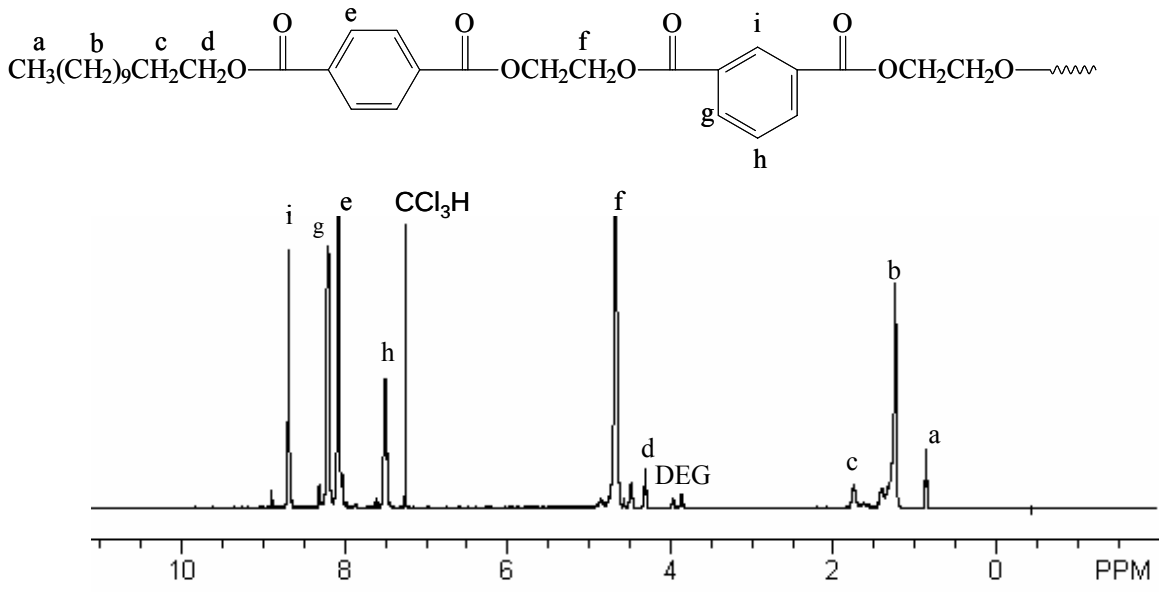

Figure 3.2 ^{1}H NMR spectrum of dodecanol endcapped branched PETI, PETI-B_3D_5, $CDCl_3$, 400 MHz

Table 3.1 Compositions and molecular weight of polyester ionomers

Sample	Ionic (mol%)	Branching Reagent (mol%)	$\eta_{inherent}$ [a] (dL/g)	M_n [b] (g/mol)
PET-T_5	5.0	0	0.28	8400
PET-$B_{0.5}T_5$	5.0	0.5	0.31	------
PETI-T_3	3.0	0	0.20	12800
PETI-T_5	5.0	0	0.18	8400
PETI-B_2T_5	5.0	2.0	0.17	-------
PETI-B_3T_5	5.0	3.0	0.44	-------

[a:] measured at 25 ^{o}C using a capillary viscometer in a 0.5 g/dL solution of 60/40 w/w mixture of phenol and tetrachloroethane; b: estimated based on Equation 1 and NMR spectroscopy.

Table 3.2 Compositions and molecular weights of dodecanol endcapped branched PETI model polyesters

Sample	Charged Dodecanol (mol%)	Residual Dodecanol (mol%)	M_n[a] (g/mol) NMR	M_n[b] (g/mol) GPC	M_w (g/mol) GPC	$\eta_{inherent}$[c] (dL/g)
PETI-D_5	15.0	5.4	7100	7400	17000	0.22
PETI-B_2D_5	15.0	5.2	------	8100	25000	0.27
PETI-B_3D_5	15.0	5.4	------	8000	36000	0.33

[a:] estimated using Equation 1 and NMR spectroscopy; [b:] MALLS detector, 40 °C, chloroform; [d:] measured at 25 °C using a capillary viscometer in a 0.5 g/dL solution of 60/40 w/w mixture of phenol and tetrachloroethane.

3.4.2 Model polymers and molecular weights

Branched PETIs with nonionic end groups were prepared as model polymers to provide information about the molecular weight of telechelic branched ionomers. Our previous research has demonstrated that 1-dodecanol is an effective endcapper to control the molecular weight of polyesters via melt polymerization.[9] For this research, howver, dodecanol was used as a nonionic endcapper to synthesize the model polymers. ^{1}H NMR spectroscopy was used to confirm the polymer composition and end groups for PET-B_xD_y polyesters (Figure 3.2 and Table 3.2). ^{1}H NMR spectra confirmed that the level of incorporated dodecanol was significantly lower than the dodecanol feed due to its relatively low boiling temperature (260 ~ 262 °C), as compared to the final polymerization temperature (275 ºC). Table 2.2 summarizes the level of dodecanol incorporation versus the mol % charged.

The number average molecular weight (NMR) of linear telechelic ionomers and nonionomers without branching agent was estimated using Equation 1. Since excess

ethylene glycol was used in the polymerization, and subsequently was removed via distillation during polycondensation, the conventional equation, X = (1+r)/(1-r), was not appropriate for estimating molecular weight.[9] Based on the assumption that the end capping reaction was quantitative and restricted to the polymer chain end, a modified equation (Equation 1) was utilized to estimate the NMR number average molecular weights. Table 3.1 includes the theoretical number average molecular weights for the PET-T_x ionomers.

$$\langle Mn \rangle = (\text{total mass of product molecules}) / (\text{moles of product molecules})$$

$$= [\Sigma (m_e + x * m_{ru})] / (N(A)/2) \qquad \text{(Equation 1)}$$

where

m_e = the molar mass of the combined end groups

m_{ru} = the molar mass of an internal repeat unit

N(A) = moles of monofunctional end capping reagent

x = the number of internal repeat units

Results of GPC investigations involving dodecanol endcapped PETIs are listed in Table 3.2. The estimated number average molecular weights of dodecanol end capped linear PETI using Equation 1 agrees well with results from the GPC investigation, which verifies that the endcapped reaction was fully complete. Moreover, GPC investigations of branched dodecanol endcapped PETI ionomers demonstrate that the presence of a branching agent did not significantly influence number average molecular weight; however, the weight average molecular weight and molecular weight distribution increased with an increase in the level of the branching agent.

Ionomers always exhibit complicated solution behaviors due to the presence of ionic aggregates in solution. It is interesting that the presence of a low level (< 3 mol%) of branching reagent in PETI ionomers (5 mol% ionic end groups) results in a slightly lower inherent viscosity. Moreover, linear telechelic PETI ionomers also display lower inherent viscosities than the corresponding dodecanol endcapped PETIs with equivalent molecular weights, which indicates the domination of intramolecular ionic aggregates.[21] Greener and coworker reported that PET ionomers display lower inherent viscosities than nonionomers with equivalent molecular weights due to the formation of intramolecular ionic aggregates in dilute solution.[22] As reported, the intramolecular aggregates exclude the solvent molecules, which provides a force to shrink the molecular coils, and results in lower solution viscosity. Linear telechelic PETI ionomers exhibit lower inherent solution viscosity than the corresponding dodecanol endcapped analogues with equivalent molecular weights, which is also indicative of the presence of a high fraction of intramolecular ionic aggregates. The presence of a branching agent exerts two distinct effects on solution viscosity: (1) increased molecular weight increases solution viscosity, and (2) branching structure decreases solution viscosity. Meanwhile, previous research on telechelic star ionomers with three arms has shown that these materials tend to form intramolecular aggregates.[14] Branched telechelic ionomers prepared using a low level of branching agent displayed structures similar to the three arm star telechelic ionomer. Moreover, intramolecular aggregates tended to dominate solution properties and as a result, inherent viscosity was slightly decreased. However, when the branching agent was increased to 3 mol%, the compacted structures prevented the formation of intramolecular aggregates, and intermolecular ionic aggregates dominated. As a result,

inherent solution viscosity increased dramatically, and was higher than that of dodecanol endcapped PETIs. However, the effect of the formation of intramolecular ionic aggregates on resulting properties was also dependent on the structure of the backbone. Since PET ionomers display more rigid polymer chains, the molecular coils do not shrink so easily. Thus, the effect of the presence of intramolecular ionic aggregates was not very obvious, although inherent viscosity slightly increased when the level of branching reagent was increased from 0 mol% to 0.5 mol% (Table 3.1).

3.4.3 Rheological analysis

As expected, the presence of a low level of branching reagent and ionic groups did not exert a pronounced influence on the thermal transitions of polyesters. PET-T_5 is a typical semicrystalline ionomer,[9] and PETI ionomers are amorphous polymers with a similar glass transition temperature (60 ^{o}C).

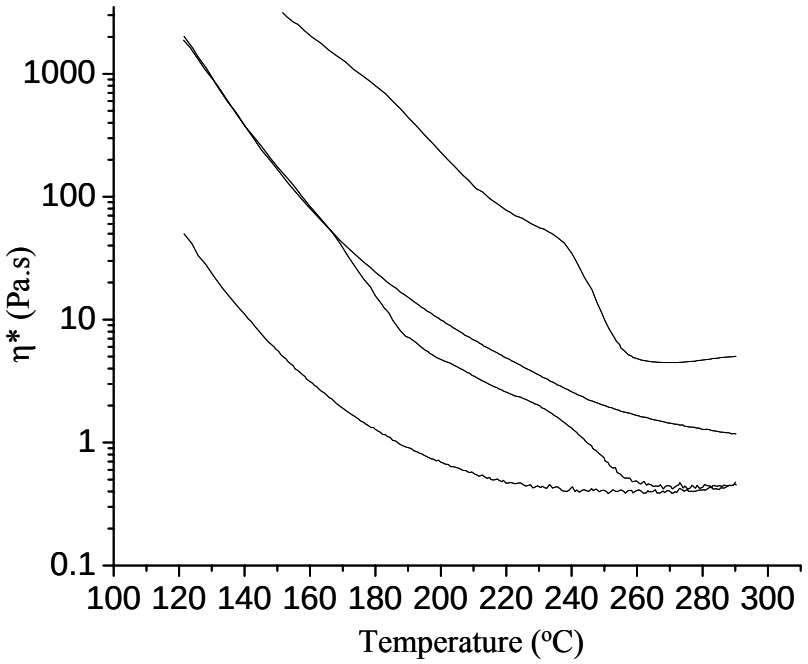

Figure 3.3 Melt viscosities vs temperatures: (form top to bottom): PETI-B_3T_5; PETI-T_3; PETI-B_2T_5; PETI-T_5.

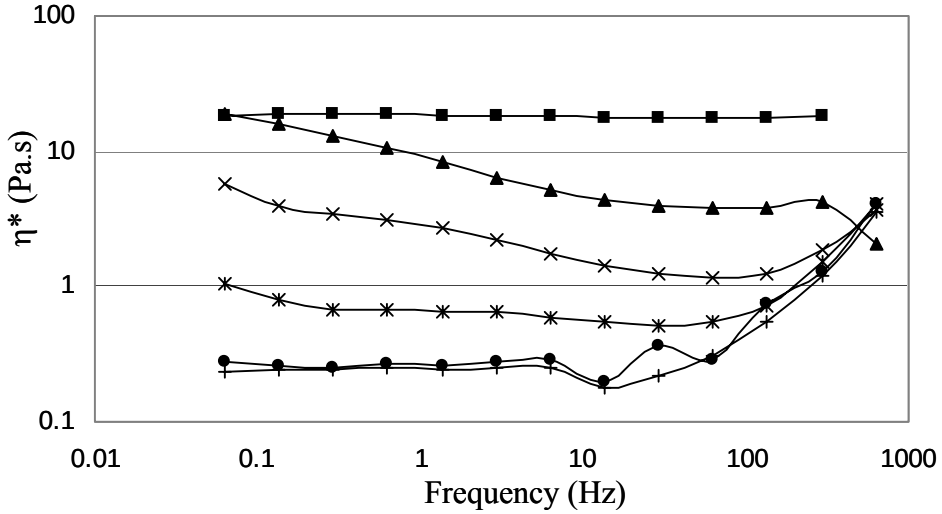

Figure 3.4 Curves of frequency sweep of PETI-B_2T_5: (from top to bottom): 140, 160, 180, 200, 220, 240 and 260 ^oC.

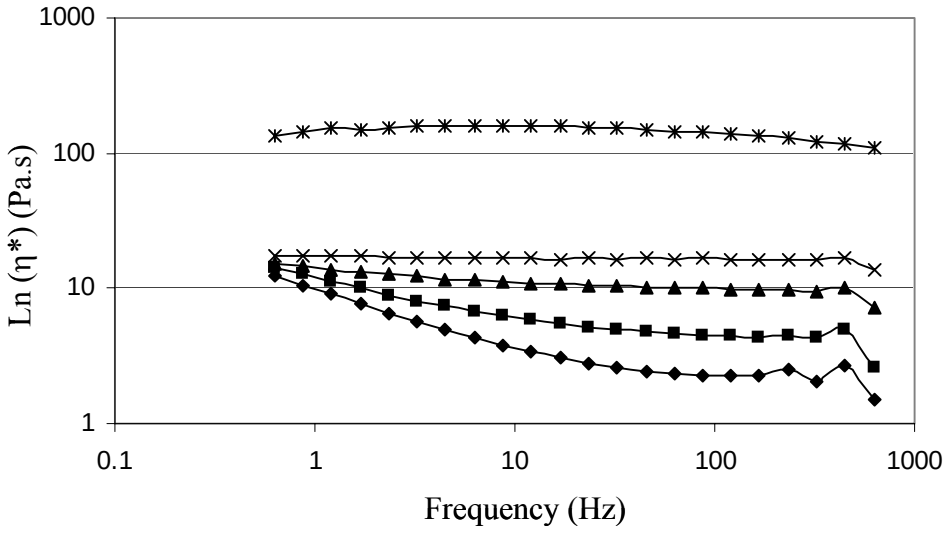

Figure 3.5 Curves of frequency sweep of PET-$B_{0.5}T_5$: (from top to bottom): 240, 250, 260, 270 and 280 ^oC.

Melt rheological analysis of amorphous PETI ionomers was performed between 120 and 300 ^{o}C (Figure 3.3). The PETI-T_3 exhibited higher melt viscosity than PETI-T_5, which indicates that the effect of ionic aggregates on melt viscosity was less significant than the effect of an increase in molecular weight. PETI-B_2T_5 and PETI-B_3T_5 exhibited some interesting behaviors, which were not observed in other polyester ionomers.[9] For example, PETI-B_2T_5 exhibited higher melt viscosity than PETI-T_5 before 240 ^{o}C, and melt viscosity dropped dramatically around 170 ^{o}C and 240 ^{o}C. After 240 ^{o}C, PETI-B_2T_5 exhibited a similar melt viscosity as the PETI-T_5. This unique behavior is attributed to the stability and state of ionic aggregates at various temperatures. Previous research has demonstrated that the response of ionomers to an increase in thermal energy is significantly different before and after the onset of ion hopping. Hird and Eisenberg observed a dramatic drop in storage modulus and large increase in flow activation energy (200 KJ/mol) in sulfonated polystyrenes at the onset of ion hopping.[23] Our previous research has shown that no drop in melt viscosity of PET and PEI telechelic ionomers occurs as a result of the presence of weak ion aggregates; however, some indirect evidence indicates that ion hopping did occur at 150 ^{o}C.[9] Eisenberg and Hird demonstrated that an increase in molecular weight results in stronger ionic aggregates, which significantly effects morphology and rheology.[23] The presence of a branching reagent increased not only the weight average molecular weight, but also the crosslinking points of one molecule. As a result, the onset of ion hopping exerts a more pronounced influence on melt rheology, and this was verified in the temperature ramp of PETI branched telechelic ionomers. For PET-B_2T_5, the multiplets were highly stable between 120 and 160 ^{o}C, and ion hopping almost did not occur. In this case, the ionomers were

most likely slightly crosslinked polymers, and the whole multiplets moved with the flow along the shear force. Due to the presence of a low level (2 mol%) of branching agent, the PETI-B_2T_5 had more than two ionic end groups, which increased the number of crosslinking points in one molecule. As a result, the PETI-B_2T_5 formed stronger networks and exhibited higher melt viscosities than the PETI-T_5. However, between 160 and 180 ^oC, the network became unstable due to the onset of ion hopping, and melt viscosity dropped dramatically. After 180 ^oC ion hopping occurred at a rapid rate, although subsequent increases in temperature did not further affect this rate. As a result, melt viscosity decreased slightly with an increase in temperature, and the PETI-B_2T_5 still exhibited higher melt viscosity than the PET-T_5 due to an increase in crosslinking. At approximately 200 ^oC, another dramatic drop in melt viscosity appeared, which may be related to the formation of a high fraction of intramolecular ionic aggregates. After 240 ^oC, the PETI-B_2T_5 exhibited similar melt viscosity as the PETI-T_5 since the two ionomers had molecular coil sizes when the intramolecular aggregates dominated. These results were consistent with inherent viscosity measurements.

PETI-B_2T_5 exhibited higher melt viscosity due to higher weight average molecular weight and the presence of more ionic end groups. Their compact structures (due to the presence of a higher levels of branching agent) repressed the intramolecular ionic aggregates and decreased the ease of ion hopping. As a result, the PETI-B_3T_5 exhibited higher melt viscosity, and the onset of ion hopping was observed at a higher temperature, namely 240 ^oC, with a large flow activation energy (250 KJ/mol).

It is interesting to note that although shear thickening at medium frequency and high temperature (after ion hopping occurred) was observed in the PETI-T_3, PETI-T_5 and

PETI-B_2T_5, it was the PET-B_2T_5 that exhibited the most pronounced shear thickening. Moreover, this phenomenon was not observed in the PETI-B_3T_5 or the PET ionomers. Shear thickening was observed in several semidilute ionomer solutions using nonpolar solvent; however, it was not observed in melt rheological analysis.[24] One explanation for shear thickening is that the transition of intramolecular ionic aggregates into structures with extended chains under shear force results in an increase in melt viscosity.[25] If this hypothesis is accurate, the occurrence of shear thickening would corroborate the existence of a high fraction of intramolecular ionic aggregates in the melt of PETI-T_3, PETI-T_5 and PETI-B_2T_5.

The unique behavior of branched PETI ionomers is due to the presence of a high fraction of intramolecular ionic aggregates at high temperature (> 220 ^oC). In most cases, this increased presence of intramolecular ionic aggregates occurred in semidilute ionomer solution, when the polymer chains were highly solvated and flexible. However, previous investigations of telechelic star ionomers (three arms) with flexible polybutadiene backbones suggest that if the backbone is extremely flexible and the number of arms is small, a high fraction of intramolecular ionic aggregates exist -- even at ambient temperatures. In our investigations, PETI has a more rigid backbone relative to polybutadiene, but it is only when the backbone was sufficiently flexible that a higher fraction of intramolecular aggregates appeared at high temperatures. Along those same lines, the rigid backbone of PET prevented the presence of a high fraction of intramolecular aggregates, with no obvious shear thickening appearing until 280 ^oC (Figure 3.5). Moreover, a slightly branched structure promoted the formation of intramolecular aggregates due to the increase in the number of ionic end groups.

However, the compact structure resulting from more branched structure stretched the PETI chains and decreased the number of conformations. As a result, PETI-B_3T_5 tended to form intermolecular ionic aggregates. Based on these results, it is believed that in star telechelic ionomers with a high number of arms, the intermolecular interaction will dominate.

3.5 Conclusions

Telechelic branched polyester (poly(ethylene terephthalate) (PET) and poly(ethylene terephthalate-isophthalate) (PETI)) ionomers using 3-sulfobenzoic acid sodium salt as ionic end capper and trimethyl 1,3,5-benzenetricarboxylate as branching reagent were synthesized using conventional melt polymerization. To investigate the effect of presence of endcapper and branching agent on the molecular weights using GPC, 1-dodecanol endcapped branched poly(ethylene terephthalate-isophthalate)s were also synthesized as model polymers. GPC results demonstrated that a low level of branching agent increased weight average molecular weight, but did not exert a pronounced effect on number average molecular weight. Temperature ramp curves of telechelic branched PETI ionomers in rheological analysis was characterized in several regions. At low temperatures, whole multiplets moved along the flow without ion hopping. However, when ion hopping occurred, melt viscosity dropped dramatically. In addition, shear thickening at mediate frequency was observed in telechelic PETI ionomers due to the presence of a high fraction of intramolecular aggregation.

CHAPTER 4

Synthesis and Characterization of Poly(ethylene terephthalate) (PET) Random Ionomers

(Published as: Lin, Q.; Long, T. E. *Macromolecules*, in progress.)

4.1 Abstract

Poly(ethylene terephthalate) (PET) random ionomers based on dimethyl terephthalate (DMT), ethylene glycol (EG) and dimethyl-5-sodiosulfoisophthalate sodium salt (SIP) were synthesized via conventional melt polymerization. The quantitative incorporation of ionic groups was confirmed using ^{1}H NMR spectroscopy. Solid state polymerization, DSC analysis and melt rheological analysis all revealed that the local mobility of polymer chains strongly depends on the level of incorporated ionic groups. At a low ionic levels (< 5 mol%), the effect of weak ionic aggregates was limited to physical crosslinking. A novel phase appeared when the ionic concentration was approximately 5 mol%, which could be considered as ionic clustering as defined in the Eisenberg-Hird-Moore (EHM) model. When the ionic concentration was lower than 10 mol%, ionomers were able to flow via ionic hopping between 240 and 290 ^{o}C. When the ionic concentration was higher than 10 mol%, ionic hopping occurred after a relaxation of ionic aggregates at 262 ^{o}C. Around 20 mol%, ionic clustering became a dominant continuous phase, and the organic matrix phase developed into dispersed domains.

4.2 Introduction

Poly(ethylene terephthalate) (PET) is an important commercial polymer that widely used as fibers, packaging, containers and engineering materials.[1-2] Although the weak interaction among the polymer chains of this rigid polymer facilitates melt polymerization and processing, it has also been shown to have several drawbacks, including poor compatibility with other polymers or substrates, a low crystallization rate, and low impact properties.[3-21] It is believed that incorporating a low level of ionic groups, which will promote intermolecular interaction, will partially address these shortcomings.[3-21] PET ionomers prepared by randomly incorporating a low level of dimethyl-5-sodiosulfoisophthalate sodium salt (SIP) are widely used to prepare fibers dyable with basic dyes, and fibers with antipilling and antistatic properties.[20] Recently, it has been suggested that the high elongational melt viscosity and strong melt strength of PET ionomers will facilitate blow molding to produce PET bottles.[21] Modifying PET ionomers to increase their compatibility with other polymers, fillers or substrates has also been widely investigated.[13-14]

Ionic groups tend to aggregate in the organic matrix to form ionic aggregates, which exerts a pronounced effect on the morphology and rheology of ionomers. Several models have been proposed to describe ionic aggregates,[22-25] and the following results are based on Eisenberg-Hird-Moore (EHM) model.[25] The basic premise of this model is that a low level of ionic units aggregate into multiplets consisting typically of 2-8 ionic pairs, which is too small (< 5 nm) to form a distinct phase. As ionic content increases, the number of multiplets grows and the neighboring multiplets start to overlay and coalesce until they are sufficiently large to be considered as a distinct phase, with a distinct glass

transition and relaxation spectrum. This aggregation of neighboring multiplets is termed a "cluster," and the ionic concentration of the formation of ionic clusters is called the "clustering point." Eisenberg and Hird pointed out that ionic clusters can be divided into three types based on their stability and relaxation time.[25] The first type of ionomer is characterized by extremely stable multiplets, with glass transition occurring at a temperature at which the mobility of polymer chains in the cluster phase becomes high enough to allow them to go through a glass transition, while the multiplets remain completely unaffected and rigid. Ionomers of the second variety experience a glass transition, at which point the multiplets remain stable, but loss their rigidity. Within this model, ions become free to move inside the multiplets when the temperature is higher than the glass transition. The third ionomer type is characterized by actual ion hopping among the multiplets as a result of sufficient thermal energy. With this variety, glass transition occurs only when the ions can move outside the multiplets at a sufficiently high rate.

---

[1]Goodman, I.; Sheanan, R. J. *Eur. Polym. J.* **1990**, 26, 1081.
[2]Goodman, I.; Rodriguez, M. T. *Macrol. Chem. Phys.* **1994**, 195, 1705.
[3](a) Greener, J.; Gillmor, J. R.; Daly, R. C. *Macromolecules* **1993**, 26, 6416. (b) Blanton, T. N.; Seyler, R. J. *Advance in X-ray Analysis*; Gilfrich, J. V., Ed.; Plenum Press: New York, 1993; p379.
[4]Hara, M.; Xue, Y. *Macromolecules* **1997**, 30**,** 3803.
[5](a) Zhang, B.; Weiss, R. A. *J Polym Sci Polym Chem* **1992**, 30**,** 91. (b) Zhang, B.; Weiss, R. A. *J Polym Sci Polym Chem* **1992**, 30:989.
[6]Xue, Y.; Hara, M.; Yoon, H. N. *Macromolecules* **1998**, 31, 1808.
[7]Xue, Y.; Hara, M.; Yoon, H. *Macromolecules* **2001**, 34, 2001.
[8]Lin, Q.; Pasatta, J.; Wang, Z. H.; Ratta, V.; Wilkes, G.; Long, T. E. *Polym. Int.* **2002**, 51, 540.
[9]Kang, H.; Lin, Q.; Long, T. E., Armentrout, R. S. *Macromolecules* **2002**, 35, 8738.

Even though DuPont de Nemours, Inc. commercialized PET ionomers based on SIP in the 1950's, knowledge concerning the behaviors of PET ionomers is still limited.[3,9,15-19] Ostowska and coworkers investigated ionic aggregates of PET ionomers using FT-IR spectroscopy and DSC, and they reported a sharp change in ionc aggregates when ionic level were higher than 5 mol%.[16-19] Greener and coworkers interpreted the rheological and dynamic-mechanic behaviors of PET random ionomers in term of restricted mobility model and consequently proposed that the clustering point was 10 mol%.[3]

Small-angle X-ray scattering (SAXS) is one of the most powerful tools to investigate ionic aggregates; however, results of SAXS analyses from various researchers have not been consistent.[3,15] Greener and coworkers observed the ionic peak at 8 mol%, while Wolchowicz was not able to determine the ionic peak of potassium salt PET ionomers. In order to fully understand the behaviors of PET ionomers, much more work need to be performed. This section will focus on the synthesis and melt rheological analysis of random PET ionomers with various ionic contents.

---

[10]*Boykin, T. C.; Moore, R. B. Polym. Eng. Sci.* ***1998****, 38, 1658.*
[11]Barber, G. D.; Carter, C. M.; Moore, R. B. *Polymeric Materials and Engineering* **2000**, 82, 241.
[12]Boykin, T. L.; Moore, R. B. *Polym. Pre.* **1998**, 39, 393.
[13]NG, C. W. A.; Macnight, W. J. *Macromolecules* **1996**, 29, 2421.
[14]NG, C. W. A.; Lindway, M. J.; Macknight, W. J. *Macromolecules* **1994**, 3027.
[15]Wlochowicz, A. J. *Macromol. Sci. Phys.* **1992**, B31, 239.
[16]Ostrowska-Czubenko, J.; Ostrowska-Gumkowska B. *Eur. Polym. J.* **1988**, 24, 65
[17]Ostrowska-Gumkowska, B.; Ostrowska-Czubenko, J. *Eur. Polym. J.* **1988**, 24, 803.
[18]Ostrowska-Gumkowska, B.; Ostrowska-Czubenko, J. *Eur. Polym. J.* **1991**, 27, 681.
[19]Ostrowska-Gumkowska, B.; Ostrowska-Czubenko, J. *Eur. Polym. J.* **1994**, 30, 875.
[20]Militky, J. *Modified Polyester Fibres*, Elsevier, Amsterdam, 1991.
[21]Sinker, S. M. *U. S. Patent 4 554 238,* **1985**.
[22]Judas, D.; Fradet, A.; Marechal. E. *Polym. Bull.* **1986**, 16, 13.
[23]Eisenberg, A.; King, K. *Ion –Containing Polymers*; Academic Press: New York, **1977**; 15.

4.3 Experimental:

4.3.1 Materials

Dimethyl terephthalate (99%) (DMT) was purchased from Aldrich and used as received. Ethylene glycol (EG) and dimethyl-5-sodiosulfoisophthalate sodium salt (SIP) were kindly donated from Eastman Chemical Co., and used as received. Titanium tetraisopropoxide, antimony oxide and phosphoric acid were purchased from Aldrich, solution catalysis was performed according to established procedures.[9]

4.3.2 Synthesis

PET ionomers were prepared via melt condensation of dimethyl terephthalate (DMT), ethylene glycol (EG), various levels of dimethyl-5-sodiosulfoisophthalate sodium salt (SIP) and sodium acetate (1.0 mol% of SIP). Both titanium tetraisopropoxide (20 ppm) and antimony oxide (180 ppm) were added to facilitate ester exchange and subsequent polycondensation. The reactor consisted of a 500 mL round-bottomed flask equipped with an overhead mechanical stirrer, nitrogen inlet, and condenser. The flask containing the diester (0.52 mol) and EG (1.04 mol) and catalysts was degassed using vacuum and nitrogen three times, and subsequently heated to 190 °C. The reactor was maintained at 190 °C for 2 h, and the temperature was increased to 275 °C over 2 h. The reaction was allowed to proceed for 30 min at 275 °C, and then phosphoric acid was added to deactive the titanium catalyst. Vacuum was gradually applied up to 0.5 mmHg and polycondensation continued for 2 h at 275 °C. The ionomers were termed as PET-$R_{x,}$ x denoted the molar fraction of ionic units.

4.3.3 Solid state polymerization

Products prepared via melt polymerization were ground into particles with a diameter of approximately 1.0 mm for further solid state polymerization. The particles were heated at 225 °C under high vacuum (< 0.1 mmHg) for 14 h.

4.3.4 Characterization

The inherent viscosities of the samples were measured at 25 ^{o}C in a capillary viscometer using 0.5 g/dL solution in a 60/40 w/w mixture of phenol and tetrachloroethane. ^{1}H NMR spectra were recorded on a Varian 400 MHz spectrometer using trifluoroactetic acid-d as a solvent. Thermal transitions were determined on a Perkin-Elmer DSC Pyris 1 at a heating rate of 10 °C/min under nitrogen purge. Melt rheological analysis was performed using a TA instruments AR 1000 melt rheometer.

---

[24]Fitzgeralld, J. J.; Weiss, R. A. *J. Macromol. Sci., Rev. Macromol. Chem. Phys.* **1988**, C28, 99.
[25]Eisenberg, A; Kim, J. S. *Introduction to Ionomers,* John Wiley & Sons: New York, **1998**.
[26]Wang, X. Q.; Deng, D. C. *J. Appl. Polym. Sci.* **2002**, 83, 3133.
[27]James, N. R.; Ramesh, C.; Sivaram, S. *Macrom. Chem. Phys.* **2001**, 202, 1200.
[28]Register, R. A.; Cooper, S. L. *Macromolecules* **1990**, 23, 318.
[29]Pang, Y. X.; Jia, D. M.; Hu, H. J.; Hourston, D. J.; Song, M. *J. Appl. Polym. Sci.* **1999**, 74, 2868.
[30]Lin, J.; Shenogin, S.; Nazarenko, S. *Polymer* 2002, 43, 4733.
[31](a) Sakamoto, K.; Macnight, W. J.; Porter, R. S. *J. Polym. Sci. Polym. Phys. Ed.* **1970**, 8, 277. (b) Shohamy, E.; Eisenbere, A. J. *J. Polym. Sci. Polym. Phys. Ed.* **1976**, 14, 1211.

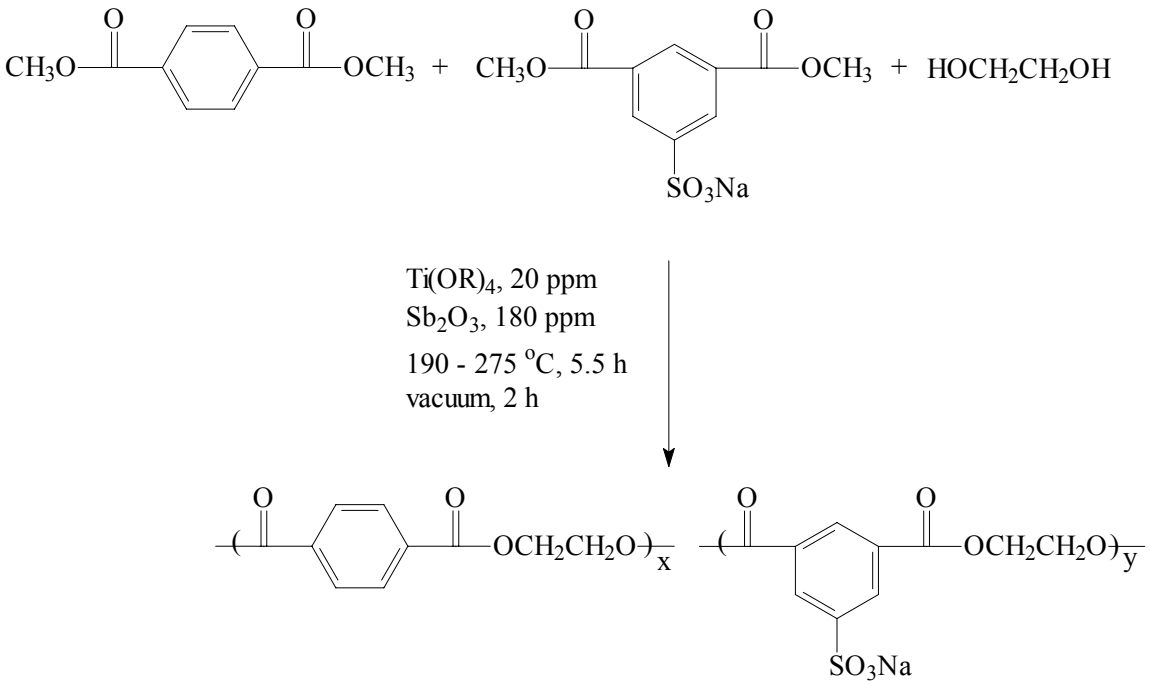

Scheme 4.1 Synthesis of PET random ionomers based on SIP

4.4 Results and discussion

4.4.1 Synthesis

As expected, a small amount of ionic commoner dramatically increased melt viscosity as observed in the reaction vessel, and stirring failed in about 30 minutes after the vacuum was applied to the system. The resulting PET-R_8 was a hazy product because increaed viscosity repressed crystallization. In addition, when the level of SIP was higher than 8 mol%, melt viscosity increased dramatically and final products were transparent foam materials, because the extremely high viscous melt trapped gas during the polymerization.

^{1}H NMR spectroscopy was used to verify the composition of the copolymers. The assignment of peaks is depicted in Figure 4.1, and the ionic content determined using ^{1}H NMR spectroscopy agrees well with the charged concentration at various levels (Table 4.1). The content of di(ethylene glycol) (DEG), a byproduct of side reaction at 275 ^{o}C, was also revealed using ^{1}H NMR spectroscopy. When the ionic concentration was lower than 5 mol%, the presence of sodium acetate (1 mol% of SIP) ensured that the levels of DEG were lower than 3 mol%. However, the level of DEG increased with an increase in the level of ionic commoner when the ionic level was higher than 5 mol% (Table 4.1).

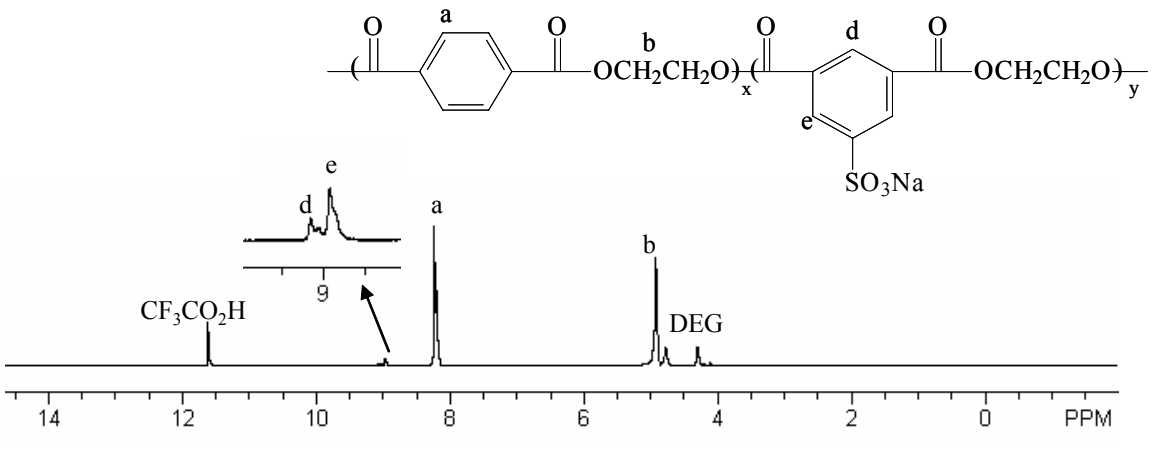

Figure 4.1 ^{1}H NMR spectrum of a PET random ionomer, PET-R_5, CF_3CO_2D, 400 MHz

Table 4.1 Composition of PET random ionomers and inherent viscosity[a]

Sample	Residual Ionic Level (mol%)	DEG (mol%)	I. V. (dL/g)	I. V.[b] (dL/g)	E_a (KJ)
PET-R_0	0	2.60	0.47	0.62	------
PET-R_1	0.95	2.75	0.46	0.62	53.56
PET-R_3	2.97	2.56	0.43	0.57	75.09
PET-R_5	4.86	3.01	0.41	0.48	74.64
PET-R_8	7.78	4.52	0.31	0.40	72.31
PET-R_{10}	9.92	6.81	0.36	0.41	83.96
PET-R_{13}	12.65	7.76	0.25	-----	70.50
PET-R_{20}	19.78	10.21	0.16	-----	------

[a]: 25 ^{o}C in a capillary viscometry using 0.5 g/dL solution in a 60/40 w/w mixture of phenol and tetrachloroethane. [b]: after solid state polymerization.

When polymerization temperature was higher than 225 ^{o}C, the side reactions occurring as a result of thermal degradation increased dramatically.[26] In order to prepare high molecular weight ionomers without exposing them to 275 ^{o}C for longer than 2.5 h, solid state polymerization (SSP) at approxmiately 220 ^{o}C under an inert gas flow or high vacuum is widely used.[26-27] SSP always results in a highly crystalline product (up to 60 %), because the polymer is simultaneously annealed at a temperature higher than needed for glass transition. The end groups are considered as defects to be excluded from the crystalline phase. As a result, the actual end group level in the amorphous phase is higher than the concentration, based on the weight of whole material. The end groups are able to move at a temperature higher than the glass transition temperature, and to react with the other groups, thereby increasing molecular weight. The byproduct, ethylene glycol, is removed using a vacuum or inert gas flow.

Previous research has also demonstrated that ionic aggregates are considered as defects to be removed from the crystalline phase.[28] If ionic aggregates are present in amorphous phase, the mobility of end groups decrease depending on the number of ionic aggregates. The results of SSP of PET random ionomers are listed in Table 3.1, which demonstrate that the effect of SSP on molecular weight strongly depends on the level of incorporated ionic units. When ionic concentration is lower than 5 mol%, inherent viscosity improves to more than 0.10 dL/g, which suggests that the presence of ionic groups does not exert a pronounced effect on the mobility of the amorphous phase. However, when ionic concentration is higher than 3 mol%, inherent viscosity dramatically decreases. These results indicate that the mobility of polymer chains in the amorphous phase dramatically decreases at about 5 mol%.

4.4.2 Thermal transitions

Standard DSC procedures were as follows: samples were heated to 290 ^{o}C, and held to eliminate the thermal history for 10 minutes. The heated samples were quenched using nitrogen gas to room temperature to prepare samples with an identical thermal history. The quenched samples were heated at a rate of 10 ^{o}C /min to 290 ^{o}C, and all reported data were obtained from the second heat cycle. Previous investigations of ionomers prepared from neutralized products of addition polymerization demonstrated that the presence of ionic aggregates effectively increased the glass transition temperature, which could be characterized using the parameter: dT_g/dc, where c denotes the concentration of ionic groups.[25] For PET ionomers, these procedures were more complicated, since the presence of a crystalline phase and flexible DEG units significantly influenced glass transition temperature.[16-19,26] Greener and coworkers reported a small value of dT_g/dc for the PET ionomers, which indicates that the ionic aggregates had only a minor impact on the glass transition temperature of the organic matrix phase. However, other researchers have observed that the glass transition of ionomers would decrease before 10 mol% ionic units, mostly due to the fact that an increasing DEG content and kinked ionic groups decreased the glass transition temperature.[16-19,26] Our data agreed well with later reports, which suggested that the negative effect on glass transition dominated before 10 mol%, which results in an irregular distribution of glass transition temperature.

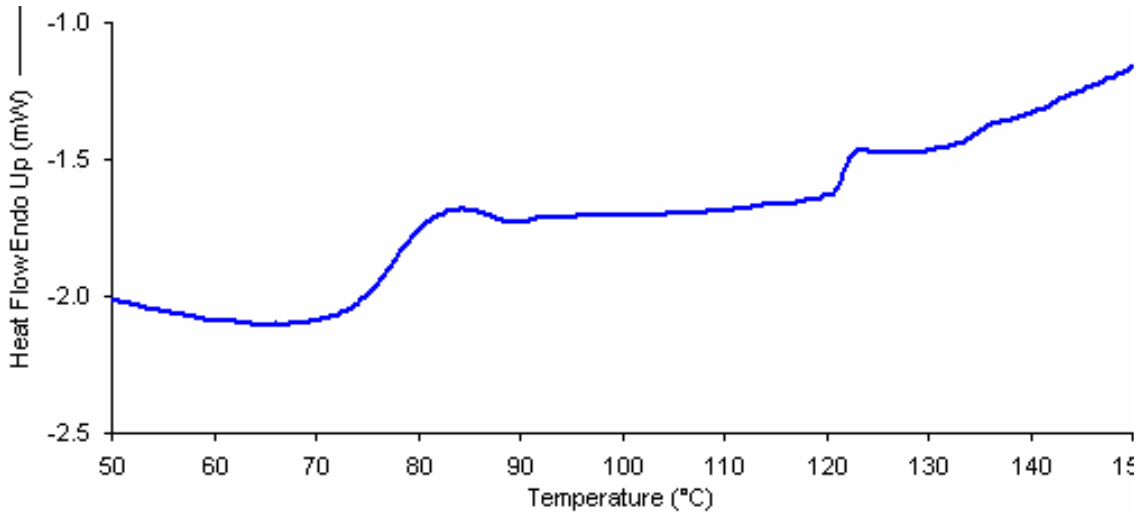

Figure 4.2 DSC analysis of PET-R_8, 20 ^{o}C/minute, thermal history as described in text.

Table 4.2 Thermal transitions of PET ionomers

Sample	T_g[c] (^{o}C)	ΔC_p (j/g* ^{o}C)	ΔC_p[a] (j/g* ^{o}C)	T_{hc} (^{o}C)	ΔH (J/g)	T_m (^{o}C)	ΔH (J/g)
PET-R_0	78	0.262	0.349	139	15.9	255	45.2
PET-R_0	70	0.339	0.349	139	31.3	252	45.6
PET-R_1	80	0.320	0.346	140	24.4	252	40.9
PET-R_3	78	0.364	0.334	154	30.3	246	37.0
PET-R_5	81	0.270	0.331	178	26.91	241	24.3
PET-R_8	78	0.254	0.321	189	9.61	227	9.2
PET-R_{10}	71	0.235	0.314	--------	--------	--------	--------
PET-R_{13}	83	0.186	0.304	--------	--------	--------	--------
PET-R_{20}	81	0.165	0.223	--------	--------	--------	--------

[a]: theoretical ΔC_p after calibrated by weight fraction

It is generally agreed that the heat capacity of a given material is constant at a given temperature and pressure.[29] Moreover, the increment of heat capacity (ΔC_p) at glass transition of a pure material is also a specific constant under fixed conditions of determination, whether it is in the bulk state or dispersed in another medium.[29-30] Thus, the value of ΔC_p at glass transition is directly proportional to the weight fraction of materials in pure amorphous phase, which can be used as a parameter to characterize the phase behaviors of heterogeneous polymer systems.[29-30] The measured values of ΔC_p are listed in Table 4.2. In fact, ΔC_p increased form homo-PET to PET-R_3 due to the decrease in the level of crystallinity in the quenched samples, and PET-R_3 had a maximum ΔC_p. In order to quench samples more efficiently, ice water rather than nitrogen gas was used to prepare completely amorphous PET films. Measured ΔC_p of the ice water quenched film (Table 4.2) agreed well with the values of amorphous PET reported in previous literatures.[29] The quenched ionomers (using nitrogen gas) with an ionic level higher than 3 mol% were completely amorphous, because the high melt viscosities repressed the crystallization during the quenching. The maximum value of ΔC_p in PET-R_3 suggested that phase separation did not happen before 3 mol%, and ionic aggregates only performed as physical crosslinking. However, when the ionic level reached 5 mol%, the value of ΔC_p began to decrease, which indicated the formation of a novel phase, ionic clusters, and the PET chains in ionic clusters were still restricted after the glass transition of organic matrix. It was interesting that around 20 mol%, ΔC_p of organic matrix was smaller than half value of ΔC_p of pure PET, which indicated that the ionic clusters became continuous dominant phase, and organic matrix turned into dispersed domains.

The EHM model proposes that clustering ionomers have multiphase structures, and each phase has its own glass transition temperature. However, only the glass transition of weakly clustering ionomers with sufficient ion hopping after the glass transition of ionic clusters can be detected using DSC.[25, 31-33] Greener and coworkers reported that DMTA analysis of PET ionomers indicated a secondary transition starting from 120 ºC, which was related to the relaxation of ionic clusters.[3] However, they did not observe the peak of this transition, and the value of tanδ reached 300 ^{o}C. Moreover, their rheological data suggests that the ionic clusters of PET ionomers were highly movable between a range of 240 and 290 ºC.[3] Based on the above observations, Greener predicted that the relaxation temperature of ionic clusters should be between 120 ºC and 230 ºC, and ascribed the disappearance of the glass transition peak to low molecular weight. Moreover, there are few reports related to the behavior of ionic aggregates of polyester ionomers. For example, Hara and coworkers report that the random aromatic liquid crystalline polyesters (Vectra^{TM}) ionomer with 20 mol% ionic groups exhibited a secondary glass transition at about 150 ºC, and the difference between two glass transitions was about 40 ºC.[4] According to Greener and Hara's studies of polyester ionomers, the onset of glass transition of ionic clusters for PET random ionomers may be around 130 ºC, which is much lower than sulfonated polystyrenes.[25] However, compared to polystyrene, polyesters are more polar and flexible due to the presence of ester linkage in the backbones, and it is believed that the ionic aggregates of PET ionomers relax at a lower temperatures. Moreover, as previously discussed, base line DSC analysis between glass transition and crystallization changed dramatically below and above 5 mol%.[26] Prior to 5 mol%, the base line remained flat between two

transitions. Around 5 mol%, however, the base line was not flat after the glass transition of an organic matrix, which indicates that the authors might have overlooked a small transition between two large transitions without careful analysis. To investigate the DSC curves between two transitions, a higher heating rate (20 ºC/min) was used to postpone the crystallization transition to broaden the window of observation, and a small transition at around 120 ºC was observed in DSC traces of PET-R_5 and PET-R_8 (Figure 4.2). The possibility of the relaxation of amorphous regions between the crystalline lamellar structures at high temperature was excluded, because PET-R_5 and PET-R_8 were completely amorphous (from the fusion heat of the peaks of crystallization and melt). According to previous reports,[3-4,26] this secondary glass transition can be ascribed to the relaxation of the ionic clusters. In fact, this secondary glass transition could only be observed in the 5 mol% random ionomers and low molecular weight 8 mol% ionomers, which indicates that this transition occurred as a result of the relaxation of weakly clustering ionic aggregates with sufficient ion hopping after glass transition of ionic clusters. However, these unstable ionic clusters only exist at the medium ionic levels. Ionic clusters of PET random ionomers became highly stable with a longer relaxation time while undergoing DSC measurement when the ionic concentration was higher than 8 mol%. As a result, DSC was able to detect the relaxation of ionic clusters of PET-R_{10}. These results were later confirmed by melt rheological analysis.

4.4.3 Rheological Analysis

Temperature ramp curves of rheological analysis are depicted in Figure 4.3 and Figure 4.4. Flow activation energy of ionomers can be estimated using following equation:

$$\mathrm{Ln}(\eta^*) = A + (E_a/R)*(1/T) \quad \text{(Equation 1)}$$

The ionomers with ionic contents below and above 10 mol% exhibited different rheological behaviors. The temperature ramp curves of ionomers with low ionic content appear as straight lines with similar flow activation energies (Figure 4.3 and Table 4.1). Even though the inherent solution viscosities of ionomers decreased with an increase in the level of incorporated ionic groups, melt viscosity increased due to an increase in the number of multiplets in the ionomer melts. PET-R_{10} and PET-R_{13} exhibited different behaviors from ionomers with lower ionic contents, which were characterized by three regions. Before 260 ^{o}C, melt viscosity remained constant, which indicates that the thermal energy was not able to disrupt the ionic aggregates. In this case, the whole multiplets flowed along the shear force as fillers with few ion hopping, and the materials exhibited storage modulus close to rubber state. A dramatic drop in melt viscosity appeared at around 260 ^{o}C, and then the melt flowed with a similar flow activation energy as the ionomers with lower ionic contents. This transition of 262 ^{o}C should be considered as the starting point of ion hopping and the glass transition of the ionic clusters.[25] After this relaxation, the ionomers flowed via ion hopping, and exhibited similar rheological behaviors as ionomers with lower ionic content. The ionic aggregates of PET-R_{20} were so strong that the ionomer was not able to flow under 300 ^{o}C.

Previous research has demonstrated that the breakdown of time-temperature superposition due to the presence of several relaxation mechanisms related with various phases was an effective marker for the onset of clustering, and is applicable to several families of ionomers.[3,31] Below the clustering point, the multiplets acted as simple physical crosslinkers, which modified the topology of the polymeric matrix without affecting its fundamental relaxation behaviors. Above the clustering point, two relaxation mechanisms appeared, one associated with the hydrocarbon phase and the other with ionic clustering. Greener demonstrated that time temperature superposition of G' failed at 10 mol% due to the presence of ionic clusters.[3] The ionomers synthesized for this study altered the ideal polymer behavior at about 5 mol%, and the G' curves of different temperatures crossed at one point around 10.0 Hz (Figure 4.5). Just as Greener maintained, superposition only failed in curves of G', indicating that the ionic clusters were highly movable. Rheological analysis agreed well with DSC data showing the clustering point about 5.0 mol%, and the ionic clusters of PET-R_5 were unstable at high temperature with sufficient ion hopping. For PET-R_8, the crossing point was reduced to a lower frequency (around 1.0 Hz), which indicates that the stability of ionic aggregates increased with an increase in ionic content. But for 10 mol% random ionomers, the crossing point moved to a frequency lower than 0.1 Hz, and the time-temperature superposition had recovered during melt rheological analysis (Figure 4.6).

The effect of molecular weight on the crossing point was also investigated. Rheological analyses of PET-R_5 (η = 0.41 dL/g) and PET-$R_{5'}$ (η = 0.48 dL/g) demonstrated that the crossing point moved to a lower frequency with an increase in

molecular weight, which indicates that the stability of ionic clusters increased with an increase in molecular weight.

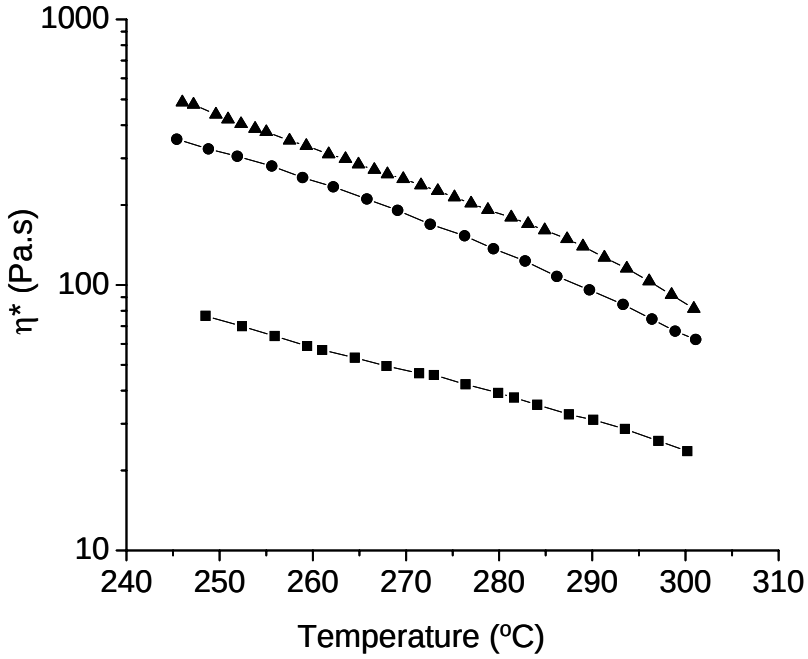

Figure 4.3 Temperature ramp of PET random ionomers with low levels of ionic groups, from top to bottom, 5 mol%, 3 mol% and 1 mol%.

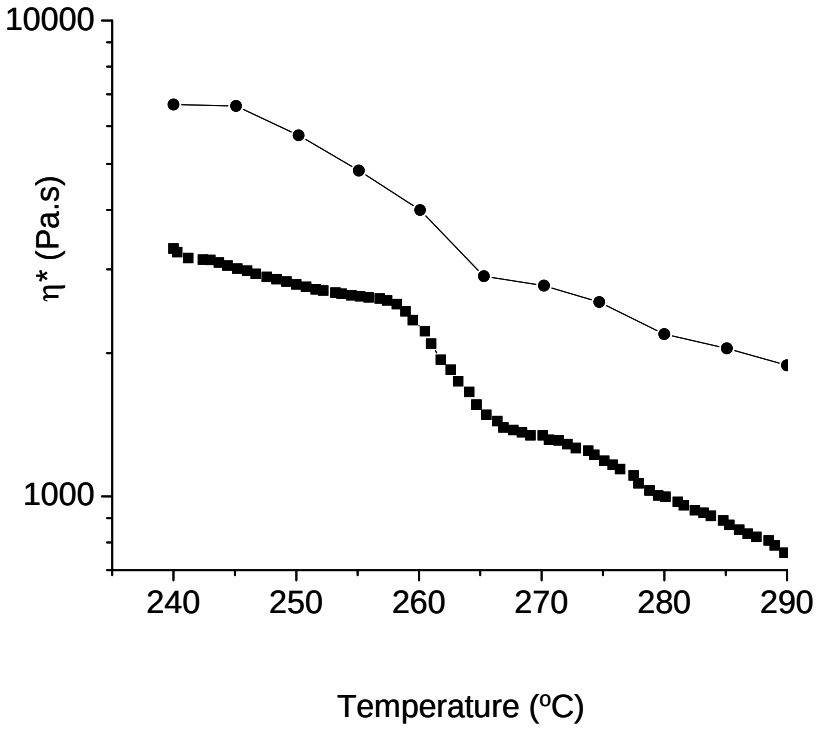

Figure 4.4 Temperature ramp of PET random ionomers with high levels of ionic groups, top: 13 mol%; bottom: 10 mol%.

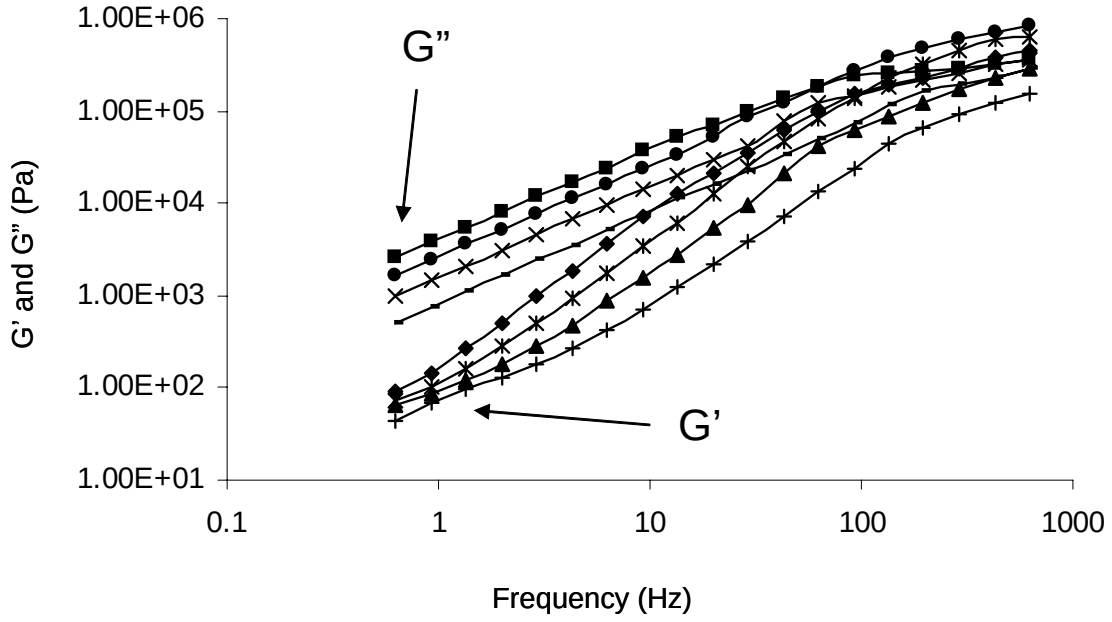

Figure 4.4 Temperature ramp of PET random ionomers with high ionic levels, top: 13 mol%; bottom: 10 mol%.

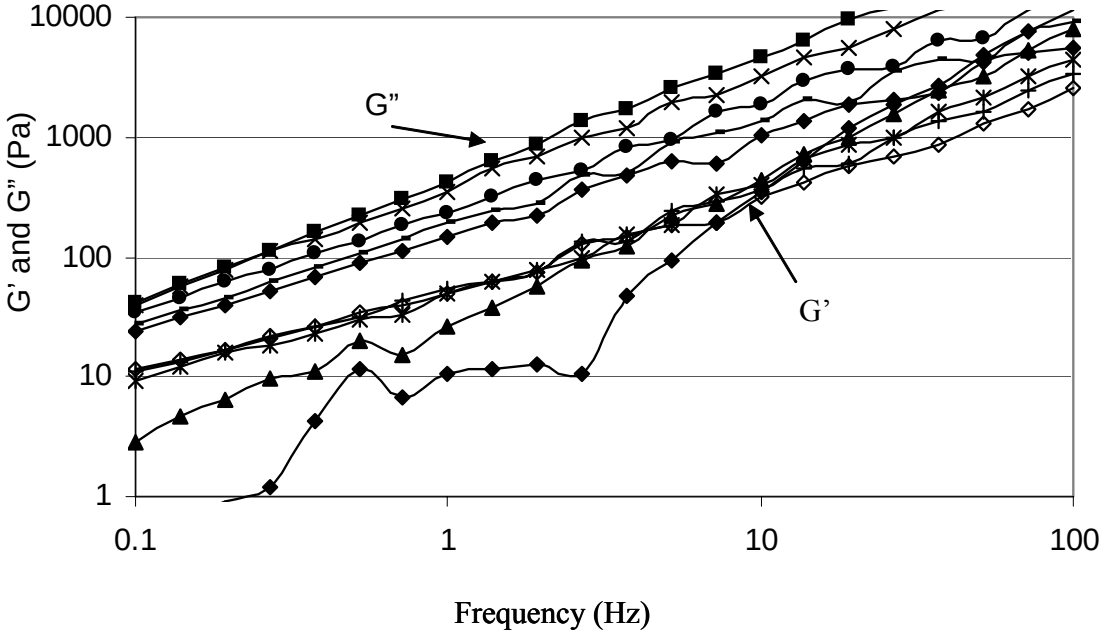

Figure 4.5 Frequency sweep of PET-R_5 at various temperatures, form top to bottom: 250, 260, 270, 280 and 290 ^{o}C.

4.4.4 Discussion

Our DSC and rheological analysis indicates that the clustering point of PET ionomers based on SIP was around 5 mol%; however, Greener and coworkers demonstrated that the clustering point was 8 mol% (SAXS) or 10 mol% (melt rheology). Despite the apparent large discrepancy between 5 and 10 mol%, the results of these two reports actually do agree well with each other. Greener pointed out that the ionic concentration in units of mol% for PET ionomers was somewhat misleading. Since it does not adequately represent the interionic spacing along the chain, mol% has a different meaning for PET ionomers from ionomers obtained from addition polymerization.[3] The repeat units of PET are large (11 Å) compared to vinyl polymers (2.5 Å). Moreover, the actual level of ionic groups in PET ionomers is much lower than those of polyvinyl ionomers. As a result, the standard deviation of 2-3 mol% concentration for PET ionomers was small, and can be considered acceptable. Moreover, ionomers synthesized in different labs are certain to exhibit small disparities in molecular weight, sequence and residual catalysis, which can also account for these relatively minor property deviations.

4.5 Conclusions

Random poly(ethylene terephthalate) ionomers based on dimethyl terephthalate (DMT), ethylene glycol (EG) and dimethyl-5-sodiosulfoisophthalate sodium salt (SIP) were synthesized via conventional melt polymerization. ^{1}H NMR spectroscopy confirmed the quantitative incorporation of ionic groups. Results of solid state polymerization, DSC and melt rheological analysis indicate that the mobility of chains is strongly dependent on the level of incorporated ionic groups. At low ionic levels (< 5 mol%), the poor stability of the ionic aggregates results in physical crosslinking. A novel

phase was formed when the ionic concentration was approximately 5 mol%, which could be considered as clustering, as defined by the Eisenberg-Hird-Moore (EHM) model. When ionic concentration was lower than 10 mol%, the polymer melt was able to flow via ionic hopping. However, when the ionic concentrations were higher than 10 mol%, ion hopping occurred after 262 ^{o}C. Around 20 mol%, ionic clustering became the dominant phase, and the organic matrix became dispersed domains in the continuous and highly restricted ionic cluster phase.

CHAPTER 5

Synthesis and Characterization of Poly(ethylene glycol) Methyl Ether Endcapped Poly(ethylene terephthalate)s

(Published as: Lin, Q.; Sercan, U.; Fornof, A. R.; Wei, Y. *Polymer Prepints* **2003**, 44(1), 191)

5.1 Abstract

Linear and branched poly(ethylene terephthalate) (PET) copolymers with poly(ethylene glycol) (PEG) methyl ether (700 g/mol or 2000 g/mol) as end groups were synthesized using conventional melt polymerization. DSC analysis demonstrated that a small fraction of incorporated PEG effectively accelerated the crystallization, which further increased with increasing levels of PEG. Incorporating the PEG end groups also decreased the crystallization temperature of PET, and copolymers with a high level of PEG (>17.6 wt%) were able to crystallize at room temperature. Rheological analysis confirmed that the mobility of the polymer chains was effectively improved due to the presence of PEG end groups. XPS and ATR-FTIR revealed that the PEG block tended to aggregate on the surface, and the resulting film had a 34 wt% content of PEG, but was covered with a rich layer (85 wt% PEG). To investigate biocompatibility, PEG endcapped PET (34 wt% PEG) and PET films were immersed in a protein solution (0.7 mg/mL BSA) for 72 h. XPS analysis demonstrated that the concentration of nitrogen (1.05%) on the surface of the immersed PEG endcapped PET film, which was proportional to the concentration of adsorbed protein, was much lower than that of the PET (7.67%). SEM photographs were consistent with XPS results.

5.2 Introduction

Poly(ethylene terephthalate) (PET) is one of the most important polyester materials and is used as textile filament, packaging materials, films and bottle products.[1] Regrettably, this polymer has limited applications as engineering materials or as adhesives due to the low speed of crystallization and poor compatibility with other substrates, fillers and polymers.[2-3] To improve the performance of PET, several modification were developed.[2-8] For example, inorganic nucleating agents such as talc are used to accelerate the speed of crystallization.[2] However, those heterogeneous particles may act as stress concentrationors to decrease impact strength, and as a result, glass fibers are needed to reinforce the nucleated PET.[2] Thus, the development of novel methodologies to accelerate the speed of crystallization will greatly enhance the potential applications of PET as engineering materials.

---

[1]Goodman, I.; Sheanan, R. J. *Eur. Polym. J.* **1990**, 26, 1081.
[2](a) Goodman, I.; Rodriguez, M. T. *Macrol. Chem. Phys.* **1994**, 195, 1705. (b) Lawton, E. L. *Polym. Eng. Sci.* **1985**, 25, 348.
[3]Kang, H. Y,; Lin, Q.; Long, T. E., Armentrout, R. S. *Macromolecules* **2002**, 38, 8738.
[4]Flanigan, J. E.; Mortimer, G. A. *J. Polym. Sci.: Polym. Chem. Edn.* **1978**, 16, 1221.
[5](a) Greener, J.; Gillmor, J. R.; Daly, R. C. *Macromolecules* **1993**, 26, 6416. (b) Lin, Q., Pasta, J.; Wang, Z. H.; Varian. R.; Wilkes, G. H.; Long, T. E. *Polymer International* **2002**, 51, 540.
[6]Gordon III, B., Mera, A.E. *Polym. Bull.* **1989**, 22, 273.
[7]Nagata, N.; Kiyotsukuri, T.; Minami, S.; Tsutsumi, N.; Sakai, W. *Polym. Int.* **1996**, 39, 83.
[8]Kint, D. P. P.; Martinez de Llarduya, A.; Munoz-Guuerra, S. *J. Polym. Sci,: Part A, Polym. Chem.* **2000**, 38, 3761.

Recently, Xue and coworkers have studied the crystallization behaviors of PET/PEG (poly(ethylene glycol)) solutions.[9-11] PET was dissolved in PEG at elevated temperatures to form a concentrated solution (30 wt %), which formed a gel rapidly on cooling. Their results demonstrated that only a short time was needed to form the highly crystalline PET phase in the PET/oligomer system. The crystallinity of PET recovered from polymer/oligomer gel was near 72% using wide-angle X-ray diffraction, which was about 20% higher than PET samples from solution crystallization using small molecule solvents, high temperature annealing, and stretching techniques. Results of fluorescence and Raman spectroscopy indicated that this reduction in chain entanglement in the PET/PEG solution/gel resulted in rapid crystallization. For practical applications, it is more advantageous to incorporate PEG into the PET backbone to avoid PEG loss during processing. In fact, PET segmented block copolymers prepared using di-functional aliphatic polyethers, such as PEG and PTMO, have been extensively studied.[12] However, others have shown that randomly incorporating aliphatic polyether segments decreased chain regularity and resulted in soft multiphase elastomers with a low level of crystallinity.[12-15] Earlier research has demonstrated that the incorporation of functional groups as end groups did not significantly impact the properties of the polymer backbone.[3] In order to exclude the disruptive effect of the random incorporation of PEG, mono-functional PEG was used to synthesize PET copolymers with PEG end groups that exhibited a high speed of crystallization and a high level of crystallinity.

PET has also been widely used as a biomaterials such as non-resorbable structures, tendon, ligament and facial implants.[16] The interface generated between implants and their physiological environment plays a crucial role in determining their biological

performance.[17-18] Complex chemical, physical, and biological phenomena take place at the surface of the implanted system. The surface of polymers are often purposely modified via physical or chemical treatments to improve their performance for biomedical and biotechnological applications.[16-19] PEG has proved to be an effective surface modifier to prepare materials with a low level of protein adsorption and cell adhesion.[16-19] The incorporation of PEG has been accomplished via several methodologies such as covalent grafting, segmental copolymerization and spin coating.[16-19] Incorporating PEG as an end group provides a novel method for modifying the surface of PET materials. Furthermore, adding a PEG layer to the surface of PET copolymers not only improves biocompatibility but also adhesion performance due to the fact that the hydrophilic surface promotes interaction with other polar substrates.[20]

---

[9]Xue, G.; Ji, G. D.; Yan, H.; Guo, M. M. *Macromolecules* **1998**, 31, 7706.
[10]Xue, G.; Ji, G. D.; Li, Y. Q. *J. Polym. Sci.: Part B, Polym. Phys.* **1998**, 36, 1219.
[11]Ji, G. D.; Xue, G.; Zhang, X. N., Liu, B.; Zhou, D. S.; Gu, X, H. *Macromol. Chem. Physic.* **1996**, 197, 2149.
[12]Miller, J. A.; McKenna, J. M.; Pruckmayr, G.; Epperson, J. E.; Cooper, S. L.; *Macromolecules* **1985**, 18, 1727.
[13]Veenstra, H.; Hoovgvliet, R. M.; Norder, B.; Posthuma, de Boer, A. *J. Polym. Sci. Part B* **1998**, 36, 1795.
[14]Zhu, L. L.; Wenger, G,; Bandara, U. *Macromol. Chem.* **1981**, 182, 3639.
[15]Gabriellse, W.; Soliman, M.; Dijlstra, K. *Macromolecules* **2001**, 34, 1685.
[16]Mougenot, P.; Marchand-Brynaert, J. *Macromolecules* **1996**, 29, 3552.
[17]Zhao, Q.; McNally, A. K.; Renier, M.; Wu, Y.; Rose-Caprara, V.; Anderson, J. M.; Hiltner, Urbranski, A. P.; Stokes, K. *J. Biomed. Mater. Res.* **1993**, 27, 379.
[18]Chen, W.; McCarthy, J. *Macromolecules* **1998**, 31, 3648.
[19]Cohn, D.; Stern, T. *Macromolecules* **2000**, 33, 137.
[20]Petit, S.; Laurens, P.; Amouroux, J.; Arefi-khonscui, F. *Appl. Sur. Sci.* **2000**, 168, 300.

In this section, the synthesis of PEG endcapped linear and branched PET copolymers is reported. Generally, a small fraction of incorporated PEG effectively accelerated the rate of crystallization. However, a higher level of incorporated PEG results in a rich PEG layer on the surface of materials. This hydrophilic surface improves biocompatibility and decreases protein absorbance.

5.3 Experimental

5.3.1 Materials

PET oligomer and PETs with different molecular weights were kindly donated from Eastman Chemical Co., and used as received. Dimethyl terephthalate (DMT, 99%), and trimethyl 1,3,5-benzenetricarboxylate (98%) were purchased from Aldrich and used as received. Ethylene glycol (EG) was purchased from J. T. Baker and used as received. Titanium tetra(isopropoxide) (99%) and antimony oxide (99%) were purchased from Aldrich, and the preparation of the catalyst solutions was previously described.[3] Poly(ethylene glycol) methyl ether (2000 g/mol) was kindly donated from Dow Chemical Company and used as received. Poly(ethylene glycol) methyl ether (700 g/mol and 5000 g/mol) were purchased from Aldrich, and used as received. Fibrinogen from human plasma (product number: 46331) was purchased from Aldrich, and used as received.

---

[21](a) Chen, L. W.; Chen, J. W. J. Appl. Polym. Sci. 2000, 75, 1221. (b) Chen, L. W.; Chen, J. W. *J. Appl. Polym. Sci.* **2000**, 75, 1229. (c) Chen, J. W.; Chen, L. W. *J. Polym. Sci.: Part A, Polym. Chem.* **1998**, 36, 3037.
[22]Besnoin, J. M.; Choi, K. Y. *J Macro. Sci. Rew. Macro Chem. Phys.* **1989**, C29, 55.
[23]Youk, J. H.; Kambour, R. P.; Macknight, W. J. *Macromolecules* **2000**, 33, 3594.
[24]Hergenrother, W. L.; Nelson, C. J. *J. Polym. Sci., Polym. Chem. Ed.* **1974**, 12, 2905.
[25]Zhang, B. Y.; Weiss, R. A. J. *Polym. Sci. Part A: Polym. Chem.* **1992**, 30, 91.

5.3.2 Synthesis

Synthesis of linear PEG endcapped PETs. Linear PEG endcapped PET copolymers were prepared via the melt polymerization of PET oligomer and various levels of PEG end cappers. Antimony oxide (150 ppm) was added to facilitate polycondensation. The reactor consisted of a 250 mL round-bottomed flask equipped with an overhead mechanical stirrer, nitrogen inlet, and condenser. The reactor containing the monomers and catalysts was degassed using vacuum and nitrogen three times, and subsequently heated to 275 °C. The reaction was maintained at 275 °C for one hour, and vacuum was gradually applied to more than 0.5 mmHg and polycondensation continued for 2 h at 275 °C. The resulting copolymers were identified as PET-x-y (for example PET-700-1.5), wherein x denotes the molecular weight of PEG end capper, and y denotes the mole percentage of end capper of the total PET repeat units.

Synthesis of a PEG end-capped branching PET. PEG endcapped branched PET was prepared via the melt polymerization of DMT, EG and 3 mol% branching agent. Both titanium tetra(isopropoxide) (20 ppm) and antimony oxide (150 ppm) were added to facilitate ester exchange and subsequent polycondensation. The reactor consisted of a 250 mL round-bottomed flask equipped with an overhead mechanical stirrer, nitrogen inlet, and condenser. The reaction was maintained at 190 °C for 2 h, and the temperature was increased to 275 °C over 2 h. The reaction was allowed to proceed for 30 min at 275 °C. Vacuum was gradually applied up to 0.5 mmHg and polycondensation continued for 2 h at 275 °C. The product was named as BPET-2000-5.

5.3.3 Protein adhesion

Fibrinogen (50.0 mg) was dissolved in 100 mL PBS solution (PH = 0.74), and filtered using a syringe filter. The relative concentration of protein was measured using a "Lowry protein assay" procedure. BSA standard tubes containing 0, 10, 20, 40, 70, 100 μg BSA (Sigma) in a total volume of 100 μL were prepared. A standard reagent was prepared as follows: 0.20 mL of 4.00% K Na Tartrate and 0.20 ml of 1.28% $CuSO_4$ were mixed together, and then 10.0 mL of 3.00% Na_2CO_3 dissolved in 0.10 N NaOH was added. A standard reagent (0.10 mL) and 0.10 mL phenol agent (Sigma) were added into each BSA tube. The absorbance of solutions at 750 nm was measured to build up a standard curve. The concentration of fibrinogen was measured using identical procedures, which was approximately 0.72 mg/mL BSA.

PET and BPET-2000-5 films were immersed into a PBS solution for 2 h at 37 ^{o}C, and then into a fibrinogen solution for different periods (24, 48 and 72 h). The films were rinsed using PBS solution for 20 seconds to remove weakly absorbed fibrinogen, and dried at room temperature for 72 h for further analysis.

---

[26]Zhang, B. Y.; Weiss, R. A. *J. Polym. Sci. Part A: Polym. Chem.* **1992**, 30, 989.
[27]Lin, Q.; Gariano, N.; Madison, P. H.; Wang, Z. H.; Long, V. K.; Armentrout, R. S.; Long, T. E. *Polymer Preprints* **2002**, 43(1).
[28]Kint, D. P. R.; Martiez de llarduya, A.; Munoz-Guerra, S. *J. Polym. Sci.: Part A, Polym. Chem.* **2001**, 39, 1994.
[29]Kint, D. P. R.; Martiez de llarduya, A.; Munoz-Guerra, S. *J. Polym. Sci.: Part B, Polym. Phys.* **2001**, 39, 1553.
[30]Avrami, M. J. *J. Chem. Phys.* **1939**, 7, 1103.
[31]De Gennes, P. *J. Chem. Phys.* **1971**, 55, 572.
[32]Klein, J. *Macromolecules* **1986**, 19, 105.
[33]Doi, M.; Graessley, W. W.; Helfand, E.; Pearson, D. S. *Macromolecules* **1987**, 20, 1990.

5.3.4 Characterization

The inherent viscosity of the copolymers was measured at 25 ^{o}C using a capillary viscometer in a 0.5 g/dL solution of 60/40 w/w mixture of phenol and tetrachloroethane. Analysis of residual catalysts was performed at Eastman Chemical Company. ^{1}H NMR spectra were recorded on a Varian 400 MHz spectrometer, and trifluoroacetic acid–d was used as the NMR solvent. Thermal transitions were determined on a Perkin-Elmer DSC Pyris 1 under N_2 purge. Thermogravimetric analysis (TGA) was performed on a Perkin-Elmer TGA 7 under a nitrogen atmosphere at a heating rate of 10 ^{o}C/min. Contact angle measurements were conducted using the static drop method with a Rame-Hart NRL contact angle goniometer. Drops of pure water were used as the probe liquid, and values reported were the average of a minimum of 3 drops per sample. Angular dependent X-ray photoelectron spectroscopy (XPS) was performed on a Perkin–Elmer physical Electronic Model 5400 with a hemisphere analyzer and a position sensitive detector. The spectrometer was equipped with a Mg/K_α (1253.6 eV) achromatic X-ray source operated at a power of 400 W and three take off angles (15, 45, 75°) were used. The spot size used was 1 mm×3 mm. Survey scans were taken in the range of 0–1100 eV. Any significant peaks in the survey scan were then subjected to narrow scans in the appropriate ranges for atomic concentration analysis. Photopeaks were curve fitted using Apollo Version 4.0 ESCA software to obtain information on the bonding state of the elements. The ATR-FTIR spectra of the surface of PET copolymer films were obtained using a MIDAC spectrophotometer equipped with a ZnSe reflection element. Rheological analysis was performed using a TA instrument AR 1000 melt rheolometer. SEM was performed on a (JEOL-JSM 5800), and samples were coated with Au prior to the analysis.

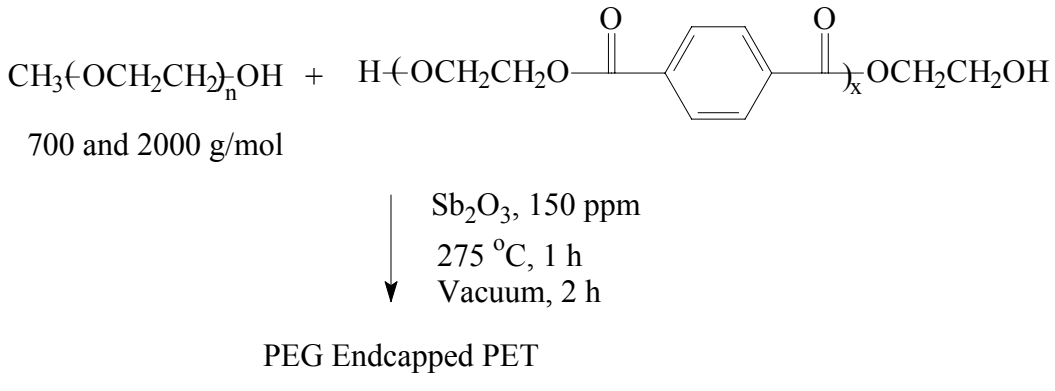

Scheme 5.1 Synthesis of poly(ethylene glycol) methyl ether endcapped poly(ethylene terephthalate)s

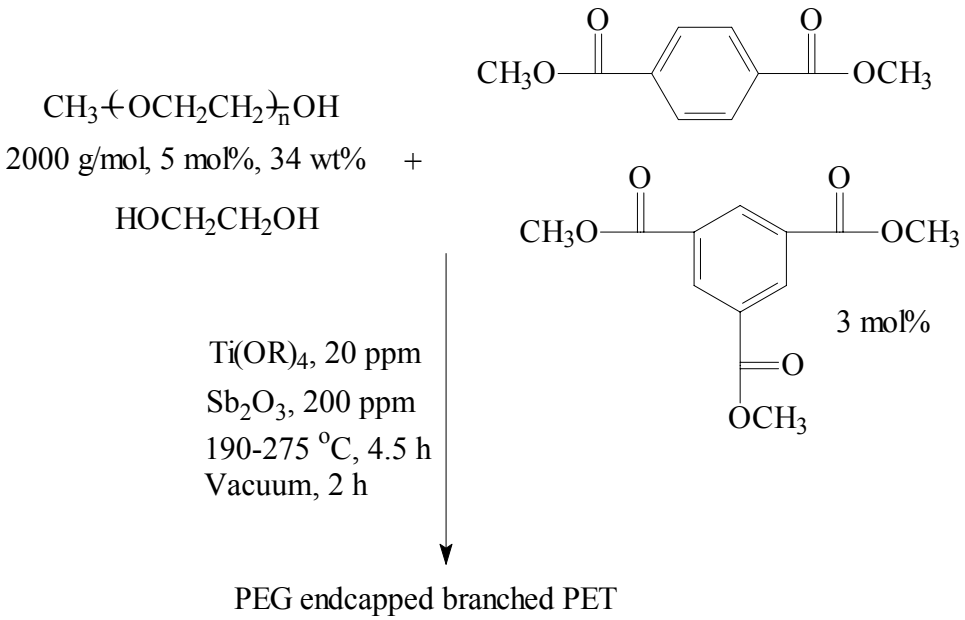

Scheme 5.2 Synthesis of poly(ethylene glycol) methyl ether endcapped branched poly(ethylene terephthalate)

5.4 Results and discussion

5.4.1 Synthesis

Synthesizing polyesters via conventional melt polymerization consists of two steps: transesterification and subsequent polycondensation under reduced pressure. Based on this two-step process, two synthetic methodologies were developed to prepare high molecular polyesters.[2] The first is a one-step reaction using DMT and a large excess amount of EG with a variety of catalysts to facilitate transesterification and polycondensation. The second is a two-step reaction. First, terephthalic acid is reacted with almost equal amount of EG without catalysts under high pressure to prepare low molecular weight PET oligomers. The obtained oligomers are further polymerized with

catalysts to facilitate polycondensation under reduced pressure. To reduce the amount of residual catalysts, linear PEG endcapped PETs were synthesized via the copolymerization of a PEG endcapper with a PET oligomer prepared without any catalyst. A low level of antimony oxide (150 ppm) was used to facilitate the polycondensation. The level of residual catalyst identified during elemental analysis was close to the charged value. The effect of residual catalyst on the properties of linear PEG endcapped PET copolymers was considered to be identical for all the polymers tested.

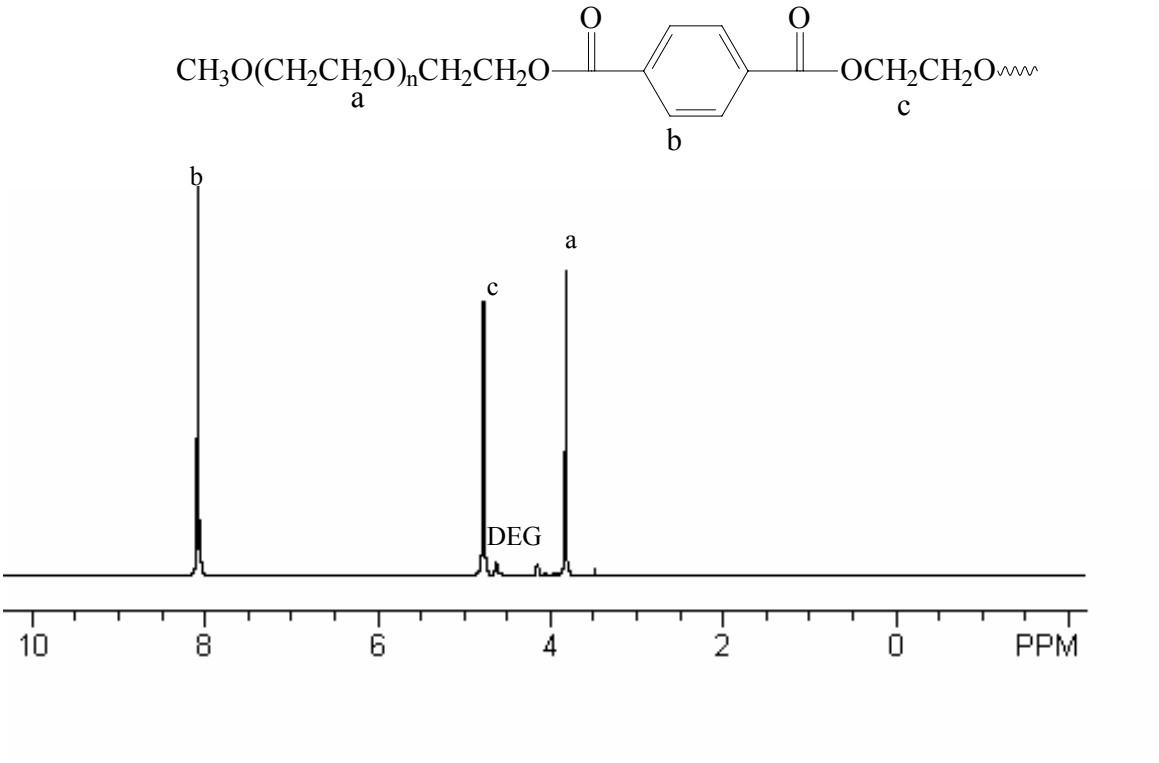

Figure 5.1 ^{1}H NMR spectroscopy of poly(ethylene glycol) methyl ether endcapped poly(ethylene terephthalate) (17.6 wt% PEG, trifluoroactetic acid-d, 400 MHz)

A significant disadvantage of using an endcapper is that the molecular weight of the resulting polymers will decrease with an increase in the level of incorporated endcapper. To overcome this disadvantage and synthesize high molecular weight PET copolymers with increased PEG end groups, trimethyl 1,3,5-benzenetricarboxylate was used as a branching agent to synthesize branched PEG endcapped PET. This copolymer was synthesized via a one step polymerization using DMT, excess amount of EG, PEG

endcapper (5 mol%) and a branching reagent (3 mol%) (Scheme 2). Titanium tetra (isopropoxide) (20 ppm) and magnesium acetate (60 ppm) were used as transesterification catalysts.

During polymerization, copolymers with endcappers (700 and 2000 g/mol) exhibited transparent melt. However, when a 5000 g/mol endcapper was used, the melt became opaque due to the fact that the high molecular PEG was not soluble in the PET. The resulting product was water bathed to remove unreacted PEG. ^{1}H NMR spectra of the washed products demonstrated that this endcapper (5000 g/mol) could not be incorporated into PET efficiently due to macrophase separation.

The composition of PEG endcapped copolymers (700 g/mol and 2000 g/mol) was verified using ^{1}H NMR spectroscopy. To remove unreacted PEG, the copolymer films were immersed into water for 2 h. A typical spectrum of PEG end-capped linear PET is depicted in Figure 5.1. The results of integration (Table 5.1) indicate that the PEG endcapper had been efficiently incorporated into the copolymers. The di-(ethylene glycol) (DEG) content of final products was lower than 3 mol%, which is analogous to the value of DEG in commercial products.[21-22]

Linear copolymers had similar solution viscosities ranging from 0.47 to 0.42 dL/g, which minimized the effect of molecular weight on resulting properties. The Mark–Housin equation was used to estimate number average molecular weight of the PEG endcapped PET copolymers (Table 5.1)[23-26] If the perfect tri-block copolymers, PEG-PET-PEG, were formed, their molecular weights could be estimated using the formula derived from the structures[2,27]:

$<M_n>$ = (total mass of product molecules) / (moles of product molecules)

$= [\Sigma (m_e + x * m_{ru})] / (N(A)/2)$ (Equation 1)

where

m_e = the molar mass of the combined end groups

m_{ru} = the molar mass of an internal repeat unit

N(A) = moles of monofunctional end capping reagent

x = the number of internal repeat units

Table 5.1 Composition and molecular weights of PEG endcapped PET copolymers

Sample	Charged PEG (mol%)	Charged PEG (wt%)	Residual PEG (wt%)	$\eta_{inherent}$ (dl/g)[a]	Estimated M_n (g/mol)[b]	Theoretical M_n (g/mol)[c]
PET	0	0	0	0.47	17,700	----------
P-700-1.5	1.5	5.2	5.0	0.42	15,200	26,800
P-2000-1	1.0	9.4	8.9	0.47	17.700	32,400
P-2000-1.5	1.5	13.5	12.7	0.46	17,200	29,500
P-2000-2	2.0	17.6	16.5	0.44	16,200	23,200
P-2000-5	5.0	34.0	31.2	0.81	37,370	----------

[a]: Determined at 25 ^oC using a capillary viscometer in a 0.5 g/dL solution of 60/40 w/w mixture of phenol and tetrachloroethane; [b]: Estimated using Mark –Housin formula; [c]: Estimated using Equation 1.

Table 5.2 DSC analysis and water contact angle of quenched copolymer films

Sample	T_c(C)	ΔH_c(J/g)	T_m	ΔH_m (j/g)	ΔH_m' (j/g)*	Contact Angle (^{o})
PET	138.5	16.2	237.6	45.2	45.2	82
PET-700-1.5	111.1	28.11	240.0	44.1	46.2	73
PET-2000-1	106.4	27.1	240.1	43.0	47.5	46
PET-2000-1.5	100.5	25.7	239.7	42.2	48.8	35
PET-2000-2	90.6	18.4	236.5	38.3	46.4	23
BPET-2000-5	-----	-----	239.4	28.1	42.6	----

* Melt fusion heat calibrated via the weight fraction of PET

Table 5.3 Results of isothermal crystallization of quenched copolymer films at 85 ^{o}C

Sample	t_{onset} (minute)	$t_{1/2}$ (minute)	ΔH (j/g)	ΔH' (j/g)	n
P-700-1.5	1.61	6.78	25.1	26.5	2.50
P-2000-1	0.68	3.21	21.9	24.2	2.33
P-2000-1.5	0.38	1.10	19.4	22.4	2.22
P-2000-2	0.21	0.42	19.0	23.1	2.29

' *Melt fusion heat calibrated via the weight fraction of PET

Estimated molecular weights of the perfect triblock polymers are listed in Table 5.1. However, these estimated values are much higher than the real values of the obtained products. This indicates that the obtained products are a mixture of copolymers with one or two PEG end groups since the reaction time was not sufficiently long to achieve perfect triblock copolymers. Instead, perfect triblock copolymers can be prepared via solid state polymerization or by increasing the concentration of the endcapper. However, high levels of PEG endcapper resulted in brittle products due to low molecular weight. Thus, this section focuses on the crystallization behaviors of copolymers with low a level of end-capper and their potential as engineering materials.

5.4.2 Thermal transitions and rheological analysis

Thermogravimetric analysis (TGA) demonstrated that the presence of PEG end groups did not exert a significant impact on the thermal stability of the resulting copolymers, which exhibited a similar loss profile versus temperature as the homo-PET copolymers and the onset of degradation was around 360 ºC. DSC was used to study the crystallization behaviors of PEG endcapped PETs. Samples were heated to 290 ºC and held at this temperature for 10 minutes to eliminate thermal history, then quenched to

room temperature using nitrogen gas to achieve an identical thermal history, and heated again to 290 ºC at a rate of 10 ºC/min. An amorphous homo PET was obtained after quenching and an obvious glass transition, crystallization transition and melt transition were all observed in the DCS trace during the second heat. However, all the PEG endcapped PET copolymers crystallized so easily that crystallization was completed during quenching, with only a melt transition observed at approximately 240 ºC in the second heat. Earlier reports have shown that PET copolymers tend to exclude the units of incorporated comonomers from the PET crystalline cells and subsequently form a pure PET crystalline phase, which display melt transition behaviors similar to those of the homo-PET.[28-29] Using these earlier results, the melt transition observed at 240 ºC was ascribed to the melt transition of the pure crystalline phase of the PET block.

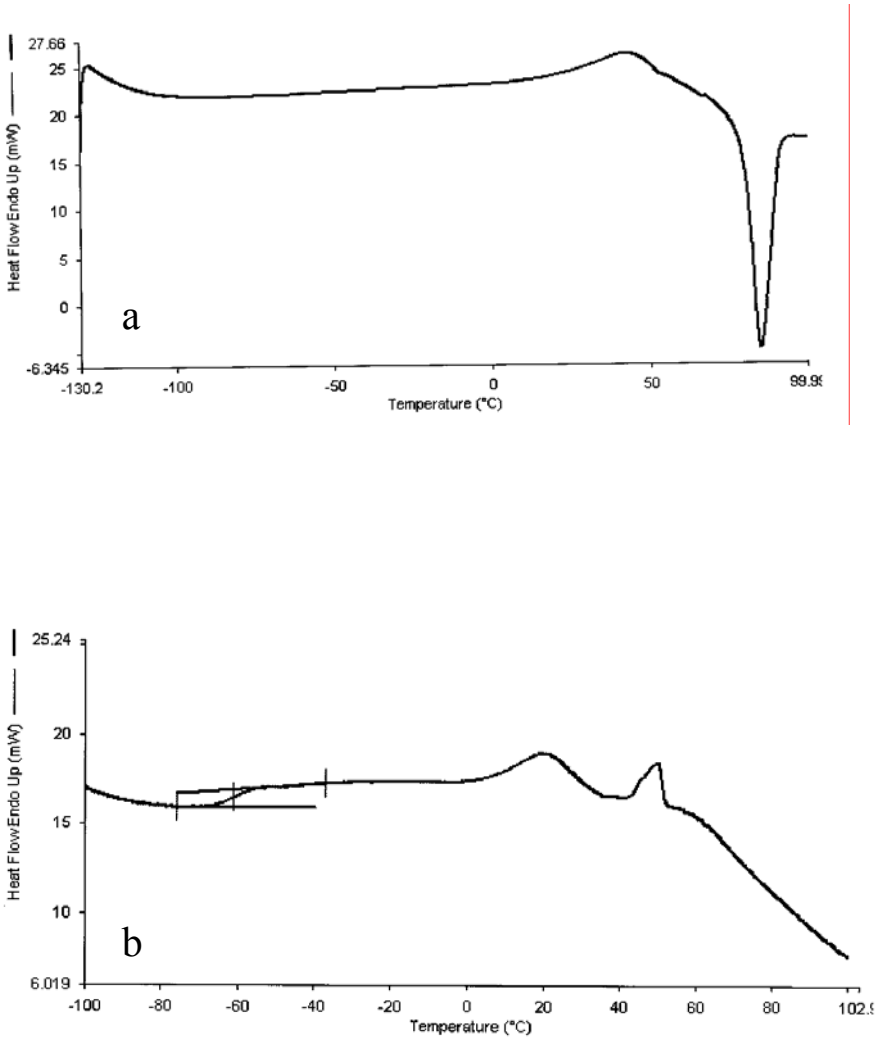

Figure 5.2 Cryogenic DSC analysis of poly(ethylene glycol) methyl ether end-capped branched poly(ethylene terephthalate) at a heating rate of 10 ^{o}C /min: (a): PET-2000-2; (b) : BPET-2000-5.

In order to study the crystallization behaviors of PEG endcapped PET copolymers, amorphous copolymer compressed films were prepared. The polymer melt was quenched using ice water, and transparent films were subsequently obtained. The BPET-2000-5 film, however, became hazy in several minutes after quenching, while the PET-2000-2 formed a soft film. However, this film gradually became opaque and stiff over the course of two weeks, primarily because crystallization happened slowly at ambient temperatures. DSC analysis of the opaque PET films revealed a melt transition at 240 °C, which indicated that these two copolymers crystallized at room temperature, and that crystallization increased with an increase in the level of PEG.

The thermal transitions of the transparent films were studied using a DSC at a heating rate of 10 ºC/minute (Table 5.2), which revealed that PEG endcapped PETs began to crystallize earlier than PET, and that the onsets and maximum positions of the crystallization peaks decreased with an increase in the PEG content. The heat values of the melt transition were used to characterize the level of crystallinity (Table 5.2), which was approximately 42 j/g (~35% crystallinity degree).[1] An increase in the level of crystallinity as previously reported, however, was not observed.[9-10] Isothermal crystallization of the transparent films was also performed at 85 °C. PET was not able to crystallize at this temperature due to the fact that it is slightly higher than its glass transition temperature. However, the PEG endcapped PET copolymers were able to crystallize since the presence of PEG end groups improved the mobility of the polymer chains. The characteristic indexes for crystallization rate, time of onset and half time of crystallization all decreased with an increase in the level of PEG. Isothermal crystallization was also analyzed using the following Avrami equation[30],

$$\ln[-\ln(1-X_t)] = \ln K + n\ln t \qquad \text{(Equation 2)}$$

where X_t is the weight fraction of materials crystallized at time t, K is the kinetics growth constant , and n is the Avrami exponent. The n was determined to be in the range 2.0 - 2.5 (the linear regression correlation coefficients were at least $r^2 = 0.98$), which indicates that the crystal grew in two dimensions.

To study the thermal transitions of quenched films at low temperatures, a cryogenic DSC (from -150 ºC) was used. For linear PEG end-capped linear PET, an obvious glass transition during the PEG amorphous phase at low temperature was not observed (Figure 5.2). However, a novel broad transition at around 30 ºC was noted (Figure 5.2), immediately after which PET crystallization occurred. These results confirm that the PEG and PET blocks form a homogeneous solution at high temperature, and that this homogenous solution can be frozen with ice water. However, when the temperature was higher than 30 ºC, the released thermal energy was sufficient to break the frozen state and form a phase separation, after which the PET block precipitated from the frozen solution to form a crystalline phase. It should also be noted that the quenched branched PEG endcapped PET film exhibited complicated thermal behaviors (Figure 5.2). For example, the glass transition of the amorphous PEG phase was observed at approximately -60 ^{o}C, followed by a broad transition after the melt transition of the PEG crystalline phase and the crystallization transition of the PET block. These results indicate that two micro-phases exist in the PEG-PET solution at the processing temperature (275 ^{o}C) due to the high content of PEG -- one rich with PET and the other almost purely PEG.

DSC results based on a variety of procedures indicate that the incorporation of PEG end groups effectively increases the rate of crystallization. Xue and coworkers proposed that the chain movement of PET within PEG molecules can be described using the reptation model proposed by De Gennes.[9-10, 31-33] In a PEG solution, PET interchain entanglement were partially replaced by PET/PEG interpenetration, which imposed only a weak constraint and let the long chain move in a rapidly renewed tube. When temperature was decreased, the more mobile polymer chains resulted in a high crystallization rate. Meanwhile, low temperature phase separation provided an additional thermal dynamitic driving force for PET chains to move out of the PEG environment with a low level of entanglement.

To study the mobility of copolymer chains directly, melt rheological analysis was performed between 240 and 280 ºC. A temperature sweep demonstrated that copolymers exhibited lower melt viscosities than homo PET with an identical solution viscosity, and that the difference in melt viscosity increased with an increase in PEG content (Figure 5.3). These results verified that when the interchain entanglement of PET molecules was replaced by the PET/PEG interpenetration, the mobility of polymer chain increased due to the weak constraint. Frequency sweeps at different temperatures were also performed to create a time-temperature superposition (TTS) relationship. The Cox-Merz rule works well for linear copolymers with a PEG content lower than 17.6 wt%, which indicates a homogenous PET-PEG solution without micro-phase separation between 250 -290 ºC. However, TTS of BPET-2000-5 is invalid due to the existence of two phases, a pure PEG phase and a solution phase containing PEG and PET. These results are consistent with the results of cryogenic DSC.

5.4.3 Surface analysis and biocompatibility

Table 5.2 lists the water contact angles of PEG endcapped PET copolymer films, all of which exhibit a gradual change from hydrophobic surface to hydrophilic surface with an increase in PEG concentration. Carbon, oxygen and trace amount of silicon atom on the surface of the films were identified in the X-ray photoelectron (XPS) spectra (Figure 5.5). The characteristic carbon 1s peaks at 285.0, 286.4, 288.9 eV were assigned to aromatic, ether and ester carbons. In fact, the surface of the processed films was the breaking interface between the polyimide film and the bulk of the copolymers. A dirty surface on the linear copolymer films was revealed using XPS, likely as a result of some hydrocarbon components of the polyamide films adhering to the surface. For example, if the surface of PET film was clean, the ratio of the three C1 peaks should be 1:1:3. The experimental results derived this ratio in a large amount (Table 5.4) due to the appearance of contaminants on the surface. However, the results of XPS spectroscopy revealed a clean, PEG rich (85 wt%) layer on the surface of the BPET-2000-5 (34 wt%). The highly hydrophilic surface of this copolymer resulted in a good adhesion between the copolymer and the polyimide films. On the other hand, adhesion failure occurred in the bulk of copolymer close to the interface, where the resulting surface did not contact the polyimide films. The PEG tended to strongly aggregate on the surface, thus reducing the free energy of the system. The appearance of a strong peak from the vibration of the C-H bond in the ATR-FTIR spectrum of BPET-2000-5 also verified the presence of a PEG rich layer on the surface (Figure 5.6).

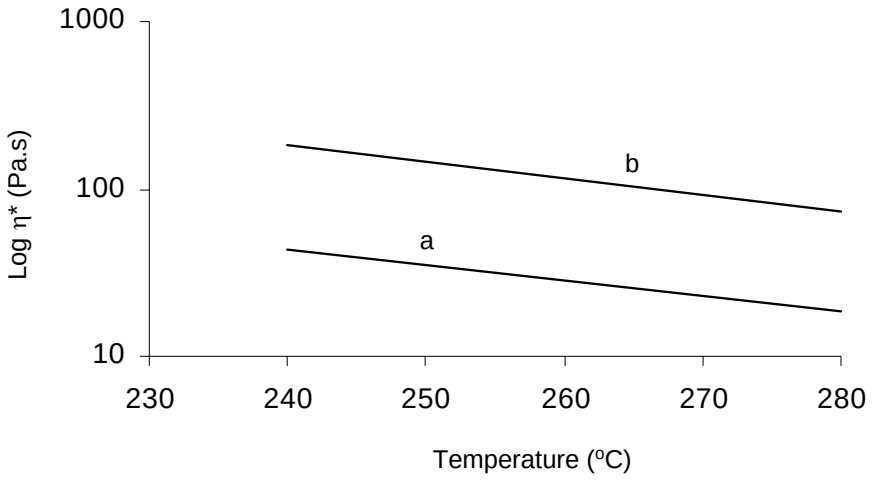

Figure 5.3 Rheological analysis (temperature sweep) of poly(ethylene glycol) methyl ether endcapped poly(ethylene terephthalate)s vs. poly(ethylene terephthalate)s with identical molecular weights. (a) PET-2000-2; (b) PET.

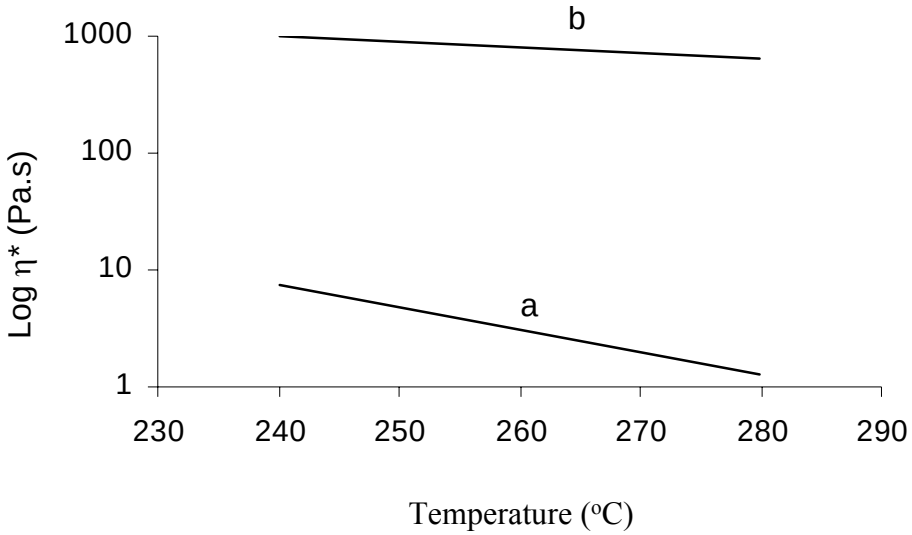

Figure 5.4 Rheological analysis (temperature sweep) of poly(ethylene glycol) methyl ether endcapped poly(ethylene terephthalate)s vs poly(ethylene terephthalate)s with identical molecular weights. (a) BPET-2000-5; (b) PET

Table 5.4 Results of isothermal crystallization of quenched copolymer films at 85 °C

Take off angle	C-C	C-O	C=O
15	66.06 %	19.15 %	14.79 %
45	67.15 %	19.51 %	13.42 %
75	67.22 %	19.82 %	12.95 %

Table 5.5 XPS results (C_{1s} peak) of quenched PET film

Sample	0 h	24 h	48 h	72 h
PET	0	5.48 %	6.89 %	7.37 %
P-2000-5	0	0.56 %	1.05 %	1.31 %

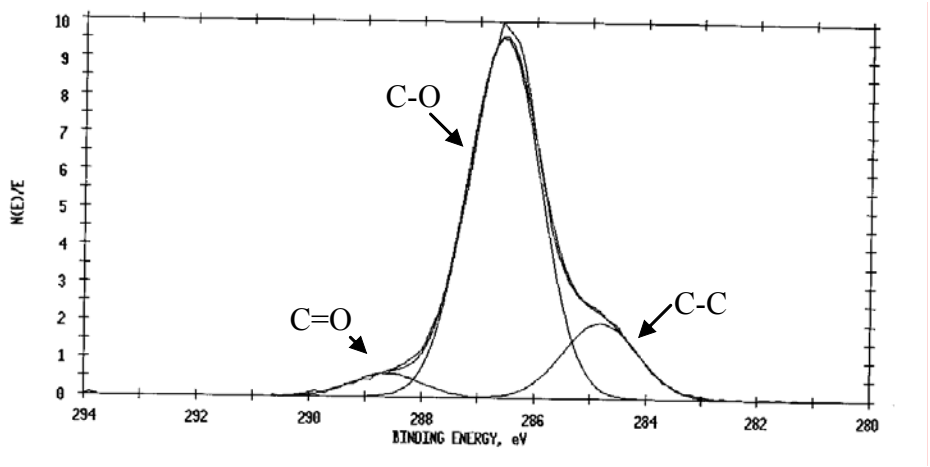

Figure 5.5 Surface analysis of BPET-2000-5 film using XPS

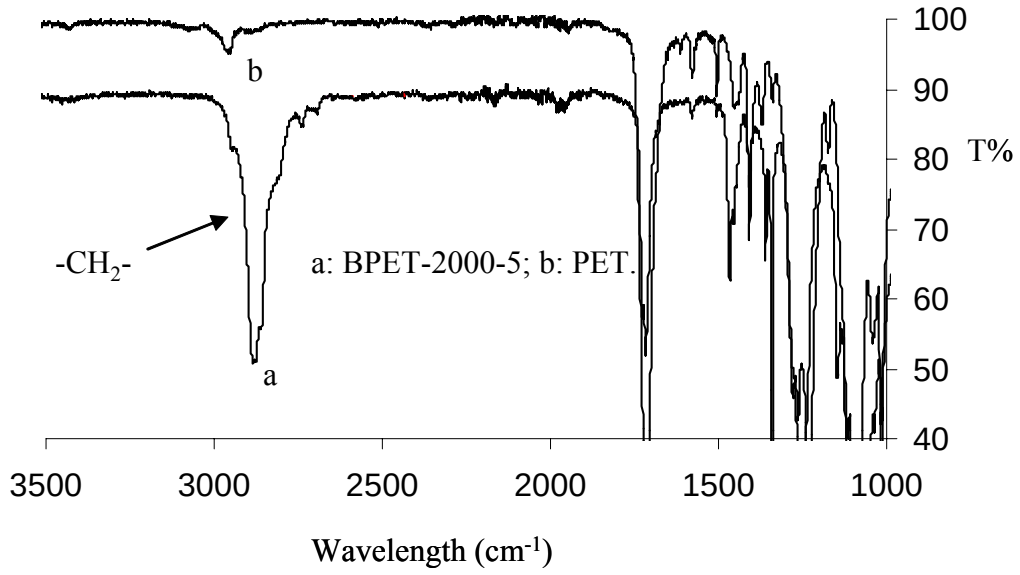

Figure 5.6 Surface analysis of BPET-2000-5 film using ATR-FTIR

To investigate biocompatibility, PET and BPET-2000-5 films were immersed into a fibrinogen solution. The XPS spectra of dried immersed films are shown in Figure 5.5 and the concentration of nitrogen atom are listed in Table 5.5. The control PET film and the BPET-2000-5 film did not exhibit any signal related to the nitrogen atom. However, a nitrogen peak appeared in the XPS spectra of the immersed films due to the presence of adsorbed protein on the surface, which increased over time. Furthermore, the concentration of nitrogen atoms on the surface of the BPET-2000-5 film was much lower than on the PET films, even when both were immersed for the same duration (Table 5.5). SEM photographs reveal large aggregates of adsorbed protein on the surface of the PET film immersed into fibrinogen solution for 72 hours. However, similar aggregates were not observed on the surface of the BPET-2000-5 film, which exhibited a similar surface morphology as that of the control PET film. These results confirm that the existence of a PEG rich layer on the PET surface was able to improve biocompatibility and decrease the absorbance of protein. Thus, this polymer has excellent potential for applications in the area of biomaterials.

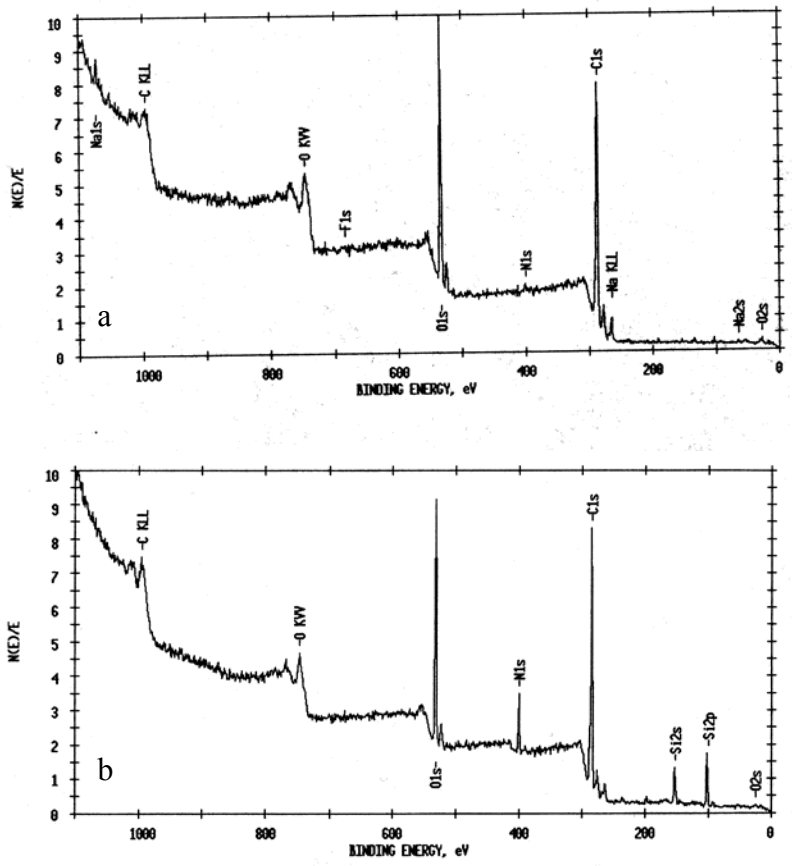

Figure 5.7 XPS analysis of films immersed into fibrinogen solution. (a) BPET-2000-5, 72 h; (b) PET, 48 h.

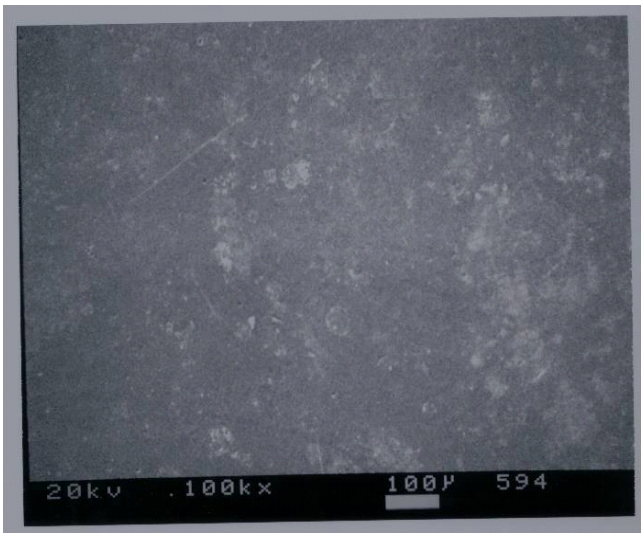

a

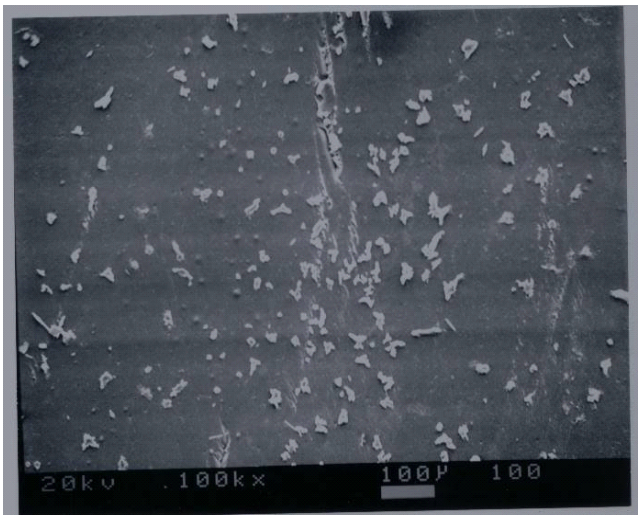

b

Figure 5.8 SEM photographs of the surface of films immersed into fibrinogen solution. (a): BPET-2000-5, 72 h; (b) PET, 72 h.

5.5 Conclusions

PEG end-capped linear PETs with a low content of residual antimony were synthesized using PEG (700 and 2000 g/mol) methyl ether and PET oligomer. High molecular weight PEG end-capped PETs with a high level of PEG could be obtained using a branching agent. DSC analysis demonstrated that a small fraction of incorporated PEG was able to both accelerate the crystallization of PET and decrease the crystallization temperature dramatically. A PEG rich layer (85 wt%) on the surface of PEG end-capped branched PET (34 wt%) was revealed using XPS and ATR-FTIR. This highly hydrophilic surface is likely to improve biocompatibility while decreasing protein absorbance.

CHAPTER 6

Synthesis and Characterization of Self-plasticizing Poly(ethylene glycol) Endcapped Poly(ethylene terephthalate)s Random Ionomers

(Published as: Lin, Q.; Long, T. E. *Macromolecules*, in progresss.)

6.1 Abstract

Poly(ethylene glycol) (PEG) methyl ether endcapped poly(ethylene terephthalate) (PET) ionomers based on dimethyl terephthalate (DMT), ethylene glycol (EG), dimethyl-5-sodiosulfoisophthalate sodium salt (SIP) and poly(ethylene glycol) (PEG) methyl ether were synthesized using conventional melt polymerization. The presence and quantification of both ionic units and PEG were surveyed using ^{1}H NMR spectroscopy. Melt rheological analysis demonstrated that PEG end groups effectively destabilized the ionic aggregates to decrease melt viscosity and the relaxation time of ionic clusters at high temperatures (240 – 290 ^{o}C). Moreover, DSC analysis and ^{23}Na solid state NMR at 25 ^{o}C demonstrated that PEG end groups were excluded from the ionic clusters at low temperatures. A high level of PEG endcapper (2 mol%, 16 wt%) and SIP (20 mol%) resulted in a polymer ($R_{20}PEG_2$) soluble in a wide range of solvents, including water and chloroform. The solution behaviors of $R_{20}PEG_2$ strongly depend on the concentration and the polarity of the solvents. The appearance of the polyelectrolyte effect in neutral $R_{20}PEG_2$ aqueous solution indicates that this polymer was fully solvated at the molecular level.

6.2 Introduction

Ionomers are conventionally defined as ion-containing polymers with a maximum ionic group content of approximately 15 mol %, and have been recognized as important engineering materials utilized in applications ranging from adhesives to fuel cell membranes.[1-9] Due to electrostatic interactions and thermodynamic immiscibility between the ionic groups and the polymer matrix (typically non-polar hydrocarbons), ionic groups tend to aggregate.[1-8] The presence of these ionic aggregates not only dramatically improves the mechanical properties of the polymeric materials, but also results in higher melt viscosities since the ionic aggregates perform as physical crosslinkers.[1-8] Previous research has demonstrated that the flow of ionomers is associated with "ion hopping", where bound ionic groups hop between aggregates in a thermal active process over a given period of time (τ).[10-11] Meanwhile, polymer chains in an organic matrix also have a terminal relaxation time (t_d). The difference between τ and t_d may vary in different ionomers depending on the stability of the multiplets. Eisenberg and coworkers proposed three models of ionic clustering based on stability.[12] If the τ is much shorter than t_d, the ionic groups are able to hop between the multiples when the temperature is higher than the glass transition temperature of the ionic clusters. As a result, the polymer melt is able to flow via ion hopping. Some ionomers, such as the salts of ethylene-methacrylic acid (E/MAA) copolymers, exhibit similar flow behaviors, and are able to be melt processed utilizing conventional equiments.[13] If the multiplets exhibit higher stability, ion hopping does not occur due to the long relaxation time. In several instances, however, some ionomer melts are still able to flow if the multiplets lose their rigidity and move with flow, for example, diblock ionomers and polystyrene-b-

poly(sodium methacrylate) sodium salts.[14] In this case, the whole multiples move in a similar fashion as fillers in the melt. If the multiples are highly stable, the ionomers behave like cross-linked networks, which are not able to flow. In order to process ionomers with highly stable multiplets, plasticizers are often used to reduce τ to obtain suitable melt viscosities.[2,15-32] Moreover, the presence of plasticizers not only modifies melt viscosity, but also provides a wide scope for modifying physical properties. For example, the presence of ionic aggregates in slightly sulfonated syndiotactic polystyrenes results in an amorphous polymer.[32] However, Moor and coworkers found that a low level of surfactant plasticizes ionic aggregates and improves the mobility of the crystallizable chain segments. With enhanced chain mobility, a higher degree of crystallinity and an elevated rate of crystallization is observed.

---

[1]Holliday, L. Ed. *Ionic Polymers*, John Wiley & Sons: New York, **1975**.
[2]Eisenberg, A; Kim, J. S. *Introduction to Ionomers,* John Wiley & Sons: New York, **1998**.
[3]Li, C.; Registers, R. A.; Cooper, S. L. *Polymer* **1989**, 30, 1227.
[4]Eisenberg, A. *Macromolecules* **1970**, 3, 147.
[5]Eisenberg, A.; Hird, B.; Moore, R. B. *Macromolecules* **1990**, 23, 4098.
[6]Lantman, C. W.; MacKnight, W. J.; Lundberg, R. D. *Annu. Rev. Mater. Sci.* **1989**, 19, 295.
[7]Kim, J. S., Eisenberg, A. *Macromolecules* **1994**, 27, 2789.
[8]Yarusso, D. J.; Cooper, S. L. *Macromolecules* **1983**, 16, 1871.
[9]Wang, F.; Hichner, M.; Kim, Y. S., Zawodzinski, T. A., Mcgrath, J. E. *J. Membrane Sci.* **2002**, 197, 231.
[10]Cooper, S. L. *J. Polym. Sci.* **1958**, 28, 195.
[11]Tierney, N. K.; Register, R. A. *Macromolecules* **2002**, 35, 2385.
[12]Hird, B.; Eisenburg, A. *Macromolecules* **1992**, 22, 6466.
[13]Longworth, R.; Nagel. H. In *Ionomers: Synthesis, Structure, Properties and Applications*: Tant, M. R., Mauritz, K. A.; Wilkes, G. L., Eds.; Chapman & Hall: New York, 1997; p 365.
[14]Yoshikawa, K.; Desjardins, A.; Dealy, J. M.; Eisenberg, A. *Macromolecules* **1996**, 29, 1235.
[15]Weiss, R. A.; Fitzgerald, J. J.; Kim, D. *Macromolecules* **1991**, 24, 1064.

PET is one of the most important commercially available polyester materials, and it is believed that incorporating a low level of ionic groups will greatly promote its performance.[33-43] According to previous reports, the clustering point of PET is around 8-10 mol% based on results from DSC, rheological analysis and SAXS. In order to suppress the high melt viscosity of PET ionomers, Greener and coworkers also studied the effect of an internal plasticizer, poly(ethylene glycol) (PEG), on the melt rheology and phase behavior of PET ionomers.[33] The ionomer of choice was a poly(ethylene terephthalate) (PET) modified by copolycondensation with dimethyl-5-sodiosulfoisophthalate sodium salt and PEG. PEG strongly suppresses melt viscosity, glass transition temperature and the glassy and rubbery moduli of the ionomer without altering the breadth of its transition range. Based on dynamic mechanical data in the terminal zone, it has also been shown that the ionic level at which the time-temperature superposition rule breaks down was substantially increased by adding PEG to the polyester chain. These results suggest that PEG is an effective "cluster-breaker". However, randomly incorporated PEG segments into the polymer chain changed the structures of the polymers dramatically, especially by significantly increasing the spacing among the ionic groups, which played a dramatic role on the properties of ionomers. In order to investigate the presence of PEG on the ionic aggregates without changing the basic structure, PEG endcapped PET ionomers were synthesized using two clustering ionomers (10 and 20 mol% ionic groups) with multiphase structures.

The presence of ionic groups in the polymer backbone exerts a profound influence not only on morphology and melt rheology, but also on solution behavior.[43-53] It has been well established that ionomer solutions exhibit two types of behaviors depending on the

polarity of the solvent used, namely (1) aggregation due to dipolar attractions between chain segments in nonpolar or low polarity solvents, and (2) polyelectrolyte behavior due to Coulombic interactions in highly polar solvents. Moreover, other unique solution behaviors were observed, such as hydrophobic aggregations of nonpolar backbones in polar solvents and shear-thickening of semidiluted solutions at high frequency.[54-62] This research examines a special polymer soluble in a wide range of solvents. Solution rheological analysis was performed using water and chloroform as solvents in order to investigate its special solution behaviors.

---

[16]Orler, E. B.; Gummaraju, B. H.; Calhoun, B. H.; Moore, R. B. *Macromolecules* **1999**, 32, 1180.
[17]Hara, M.; Sauer, J. A. J. *Macromol. Sci.: Rev. Macromol. Chem. Phys.* **1994**, C34 (3), 325.
[18]Kim, J. S.; Roberts, S. B.; Eisenberg, A.; Moore, R. B. *Macromolecules* **1993**, 26, 5256.
[19]Bazuin C. G.; Eisenberg, A. *J. Polym. Sci., Polym. Phys. Ed.* **1986**, 24, 1137.
[20]Weiss, R. A.; Fitzgerald, J. J.; Kim, D. *Macromolecules* **1991**, 24, 1604.
[21]Gauthier, M.; Eisenberg, A. *Macromolecules* **1989**, 22, 3751.
[22]Navratil. M.; Eisenberg, A. *Macromolecules* **1974**, 7, 84.
[23]Plante, M.; Bauzin, C. G.; Jerome, R. *Macromolecules* **1995**, 28, 1567.
[24]Ma, X.; Sauer, J. A.; Hara, M. *Polymer* **1997**, 38, 4425.
[25]Wollmann, D.; Williams, C. E. Eisenberg, A. *Macromolecules* **1992**, 25, 6775.
[26]Fitzerald, J. J.; Weiss, R. A. *J. Polym. Sci., Polym. Phys. Ed.* **1990**, 28, 1719.
[27]Plannte, M.; Bazuin, C. G. *Macromolecules* **1997**, 30, 2613.
[28]Plannte, M.; Bazuin, C. G. *Macromolecules* **1997,** 30, 2618.
[29]Kurian, T,; Khastigir, D.; De, P. P.; Tripathy, D. K.; De, S. K. *Polymer* **1991**, 32, 2811.
[30]Villeneuve, S.; Bazuin, C. G. Polymer 1991, 32, 2811.
[31]Tong, X.; Bauzin, C. G. *J. Polym. Sci., Polym. Phys. Ed.* **1992**, 30, 389.
[32]Goodman, I.; Sheanan, R. J. *Eur. Polym. J.* **1990**, 26, 1081.
[33]Goodman, I.; Rodriguez, M. T. *Macrol. Chem. Phys.* **1994**, 195, 1705.
[34]Lawton, E. L. *Polym. Eng. Sci.* **1985**, 25, 348.
[35]Kang, H.; Lin, Q.; Long, T. E., Armentrout, R. S. *Macromolecules* **2002**, 35, 8738.
[36](a) Greener, J.; Gillmor, J. R.; Daly, R. C. *Macromolecules* **1993**, 26, 6420. (b) Greener, J.; Gillor, J. R.; Daly, R. C. *Annual Technical Conference-Society of Plastic Engineering* **199**, 53(2), 1964.

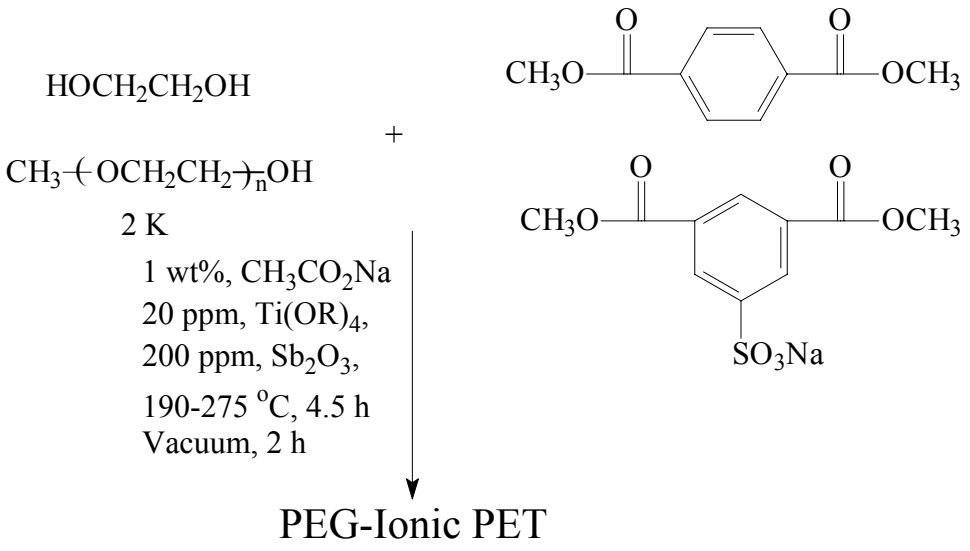

Scheme 6.1 Synthesis of PEG endcapped PET ionomers

6.3 Experimental

6.3.1 Materials

Dimethyl-5-sodiosulfoisophthalate sodium salt (SDMI) was kindly donated from Eastman Chemical Company, and used as received. Dimethyl terephthalate (DMT, 99%) was purchased from Aldrich, and used as received. Ethylene glycol (EG) was purchased from J. T. Baker, and used as received. Titanium tetraisopropoxide (99%) and antimony oxide (99%) were purchased from Aldrich, and the preparation of the catalyst solutions was previously described.[23] Poly(ethylene glycol) methyl ether (2000 g/mol) was kindly donated from Dow Chemical Company, and used as received.

---

[37]Lin, Q.; Pasatta, J.; Wang, Z. H.; Ratta, V.; Wilkes, G.; Long, T. E. *Polym. Int.* **2002**, 51, 540.
[38]Boykin, T. C.; Moore, R. B. *Polym. Eng. Sci.* **1998**, 38, 1658.
[39]Barber, G. D.; Carter, C. M.; Moore, R. B. *Polymeric Materials and Engineering* **2000**, 82, 241.

6.3.2 Synthesis

PET ionomers were prepared via the melt condensation of DMT, EG, and SDMI with or without poly(ethylene glycol) (PEG) methyl ether (2000 g/mol) (Scheme 6.1). Both titanium tetraisopropoxide (20 ppm) and antimony oxide (150 ppm) were added to facilitate ester exchange and subsequent polycondensation. The reactor consisted of a 250 mL round-bottomed flask equipped with an overhead mechanical stirrer, nitrogen inlet, and condenser. The reaction was maintained at 190 °C for two hour, and the temperature was increased to 275 °C over 2 h. The reaction was allowed to proceed for 30 min at 275 °C. Vacuum was gradually applied up to 0.5 mmHg and the polycondensation continued for 2 h at 275 °C. The products were identified as R_xPEG_y, where x denotes the molar fraction of the ionic groups, and y denotes the molar fraction of PEG. For example $R_{10}PEG_1$ represents a copolymer with 10 mol% ionic groups and 1.0 mol% PEG-2000 endcapper.

---

[40]Boykin, T. L.; Moore, R. B. *Polym. Pre.* **1998**, 39, 393.
[41]NG, C. W. A.; Macnight, W. J. *Macromolecules* **1996**, 29, 2421.
[42]NG, C. W. A.; Lindway, M. J.; Macknight, W. J. *Macromolecules* **1994**, 3027.
[43]Lundberg, R. D.; Makowski, H. S. *J. Polym. Polym. Phys. Ed.* **1980**, 18, 1821.
[44]Siadat, B.; Lundberg, R. D.; Lenz, R. W. *Macromolecules* **1981**, 14, 773.
[45]Lungberg, R. D.; Philips, R. P. *J. Polym. Sci. Polym. Phys. Ed.* **1982**, 20, 1143.
[46]Nomula, S.; Cooper, S. L. *Macromolecules* **1997**, 30, 1355.
[47]Karayianni, E.; Jerome, R.; Cooper, S. L. *Macromolecules* **1997**, 30, 7444.
[48]Nomula, S.; Cooper, S. L. *Macromolecules* **2001**, 2653.
[49]Nomula , S.; Cooper, S. L. *Macromolecules* **2001**, 34, 925.
[50]Bhargava, S.; Cooper, S. L. *Macromolecules* **1998**, 31, 508.
[51]Peiffer, D. G.; Lundberg, R. D.; Duvdevani, I. *Polymer* **1986**, 27, 1457.
[52]Lundberg, R. D.; Duvdevani, I. *Polym. Mater. Sci. Eng.* **1989**, 61, 259.
[53]Broze, G.; Jerome, R.; Teyssie, P.; Marco, C. *Macromolecules* **1983**, 16, 996.
[54]Xue, G.; Ji, G. D.; Yan, H.; Guo, M. M. *Macromolecules* **1998**, 31, 7706.
[55]Xue, G.; Ji, G. D.; Li, Y. Q. *J. Polym. Sci.: Part B, Polym. Phys.* **1998**, 36, 1219.
[56]Ji, G. D.; Xue, G.; Zhang, X. N., Liu, B.; Zhou, D. S.; Gu, X, H. *Macromol. Chem. Physic.* **1996**, 197, 2149.
[57]Lin, Q.; Unal, S.; Fornof, A. R.; Wei, Y., Li, H., Armentrout, R. S., Long, T. E. *Macrom. Symp.* **2002**, in press.

6.3.3 Characterization

The inherent viscosity of the copolymers was measured at 25 ^{o}C using a capillary viscometer in a 0.5 g/dL solution of 60/40 w/w mixture of phenol and tetrachloroethane. The reduced solution viscosity of the $R_{20}PEG_2$ aqueous solutions was measured at 25 ^{o}C using a capillary viscometer. ^{1}H NMR spectra were recorded on a Varian 400 MHz spectrometer, and trifluoroactetic acid–d was used as an NMR solvent. Solid state ^{23}Na NMR was performed on MSL-300 on 79.2 MHz. NaCl was used as secondary reference with a chemical shift 7.1 ppm. Samples were run in zirconia rotors using magnetic angle spinning and high power proton decoupling. To achieve uniform excitation, a pulse with a 1.2 μs was used. It was necessary to use a pulse delay of 10 s to obtain fully relaxed spectra. Thermal transitions were determined on a Perkin-Elmer DSC Pyris 1 under N_2 purge. Melt rheological analysis was performed using a TA instrument AR 1000 melt rheolometer. Solution rheological analysis was performed on a Bohlin Vor rheometer, 30 mm parallel plate configuration at 25 ^{o}C.

---

[58]O'Connell, E. M.; Root, T. W.; Cooper, S. L. *Macromolecules* **1994**, 27, 5803.
[59]O'Connell, E. M.; Root, T. W.; Cooper, S. L. *Macromolecules* **1995**, 28, 3995.
[60]O'Connell, E. M.; Root. T. W.; Cooper, S. L. *Macromolecules* **1995,** 28, 4000.
[61]Chassenieux, C.; Tassin, J. F.; Gohy, J. F.; Jerome, R. *Macromolecules* **2000**, 1796.
[62]Ilarduya, A. M.; Kint, D. P. R.; Munoz-Guerra, S. M. *Macromolecules* **2000**, 33, 4596.
[63]Lin, Q.; Long, T. E. *Macromolecules*, in preparation.
[64](a) Miller, R. A.; George, S. E. *J. Adhesive and Sealant Council* **1995**, 26(1), 209. (b) Raynolds, P. W. *Surf. Phenom. Fin. Part. Water-based Coat Print. Technol. (Proc. Fine Part. Soc. Symp.)* **1991**, Plenum, New Work, 275.
[65](a) Peiffer, D. G.; Lundberg, R. D.; Duvdvani, I. *Polymer* **1986**, 27, 1457. (b) Ballard, M. J.; Buscall, R.; Waite, F. A. *Polymer* **1988**, 29, 1287. (c) Wang, S. Q. *Macromolecules* **1992**, 25, 7003.

6.4 Results and discussion

6.4.1 Synthesis

As expected, the presence of a high level of ionic comonomer, SDMI, dramatically increased melt viscosity due to the presence of ionic aggregates in the melt. The resulting products were transparent and colorless, except for the $R_{10}PEG_1$ ionomers, which were opaque and semicrystalline. ^{1}H NMR spectra confirmed that the PEG and ionic units were incorporated into the polymer chains quantitatively (Figure 6.1).

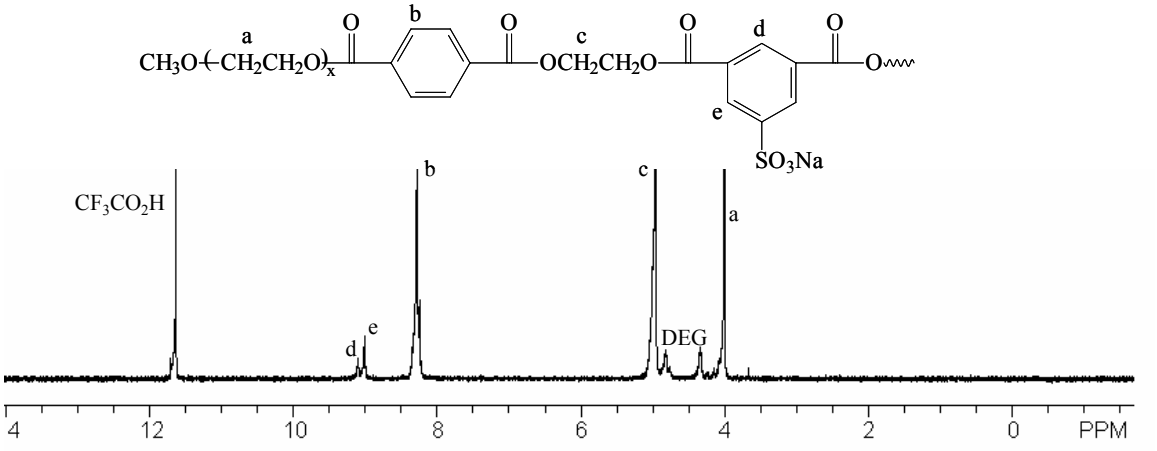

Figure 6.1 ^{1}H NMR spectrum of $R_{20}PEG_2$, CF_3CO_2D, 400 MHz

The extremely high melt viscosity of these ionomers resulted in moderate molecular weight products. Much higher molecular weight was required to prepare the perfect triblock copolymers, although this was quite difficult due to the exceptionally high melt viscosity of the ionomers. Consequently, the precise structure of resulting products could not be readily defined because the products were a mixture of polymers

with one or two PEG end groups. However, the literature reveals that polyesters prepared from melt polymerization tend to have structures close to the statistical value, while ionomers tend to display a random dispersion of ionic groups in the PET block and a PEG end group.[62] When the ionic level was 10 mol%, the presence of PEG did not exert a pronounced impact on molecular weight, and ionomers with or without PEG end groups displayed similar inherent solution viscosities. However, the presence of PEG end groups improved the molecular weights of 0.13 dL/g (R_{20}) to approximately 0.24 dl/g ($R_{20}PEG_1$).

Table 6.1 Composition of ionomers and inherent viscosity

Sample	Ionic (mol%)	Ionic (wt%)	PEG (mol%)	PEG (wt%)	η^a (dL/g)
R_{10}	10	15	0	0	0.36
$R_{10}PEG_1$	10	14	1	9	0.36
R_{20}	20	28	0	0	0.13
$R_{20}PEG_1$	20	26	1	9	0.24
$R_{20}PEG_2$	20	24	2	16	0.23

[a]: Determined at 25 ^oC using a capillary viscometer in a 0.5 g/dL solution of 60/40 w/w mixture of phenol and tetrachloroethane

Table 6.2 Thermal transitions of ionomers and activation energy of flow

Sample	T_g (°C)	ΔC_p (J/g*°C)	T_{hc} (°C)	ΔH_{hc} (j/g)	T_m (°C)	ΔH_m (j/g)	E_a (kj/mol)
R_{10}	71.2	0.21	-------	-------	-------	-------	80.42
$R_{10}PEG_1$	61.3	0.31	165.3	26.91	256.5	22.70	70.87
R_{20}	81.3	0.16	-------	-------	-------	-------	------
$R_{20}PEG_1$	53.5	0.64	-------	-------	-------	-------	88.68
$R_{20}PEG_2$	31.0	1.08	-------	-------	-------	-------	54.90

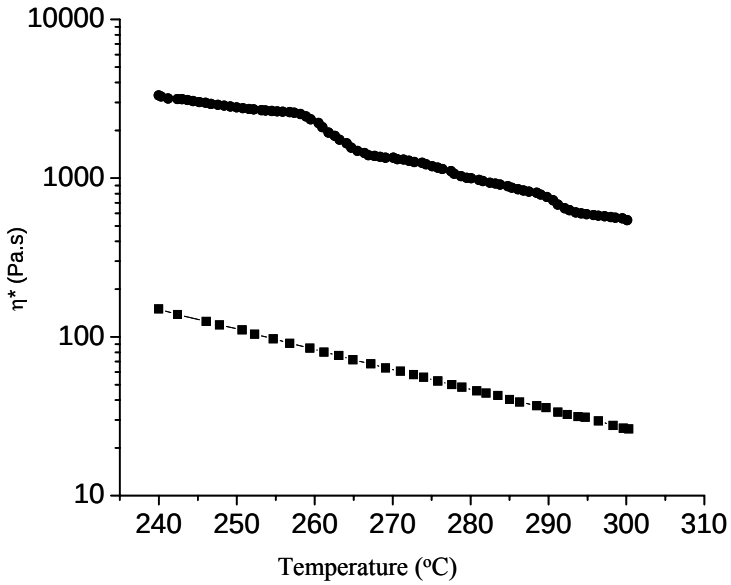

Figure 6.2 Temperature ramp of R_{10} (top) and $R_{10}PEG_1$ (bottom)

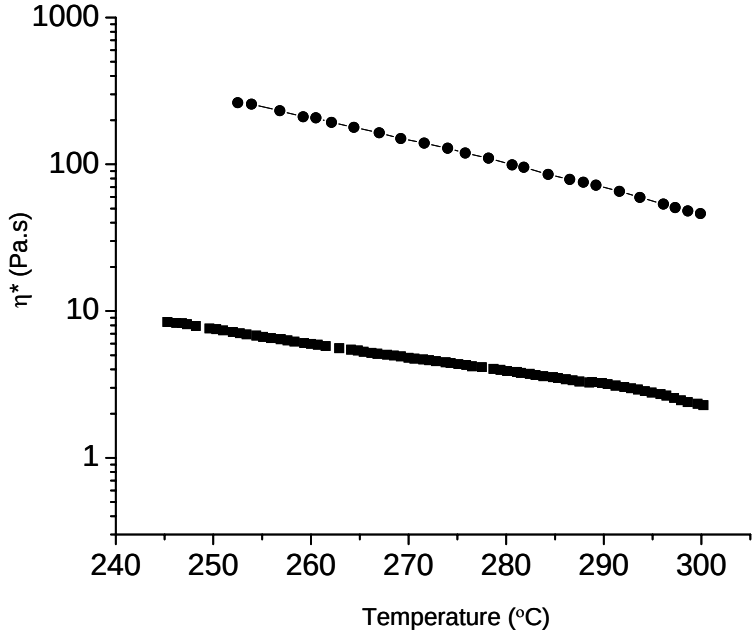

Figure 6.3 Temperature ramp of $R_{20}PEG_1$ (top) and $R_{20}PEG_2$ (bottom)

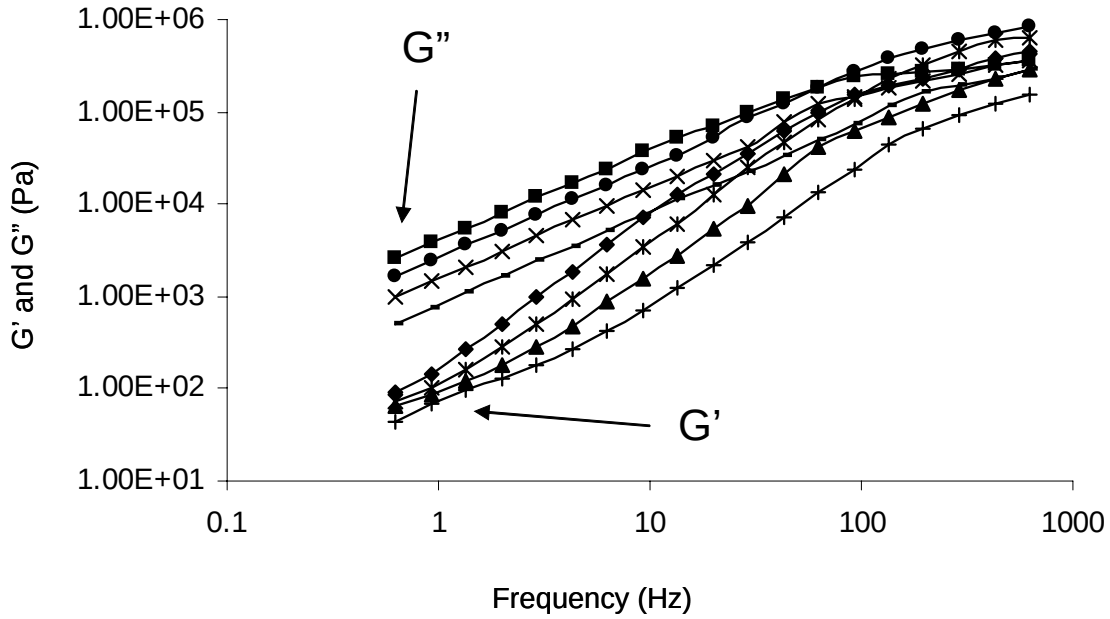

Figure 6.4 Frequency sweep of R_{10} at different temperatures (from top, 260, 270, 280 and 290 ^{o}C)

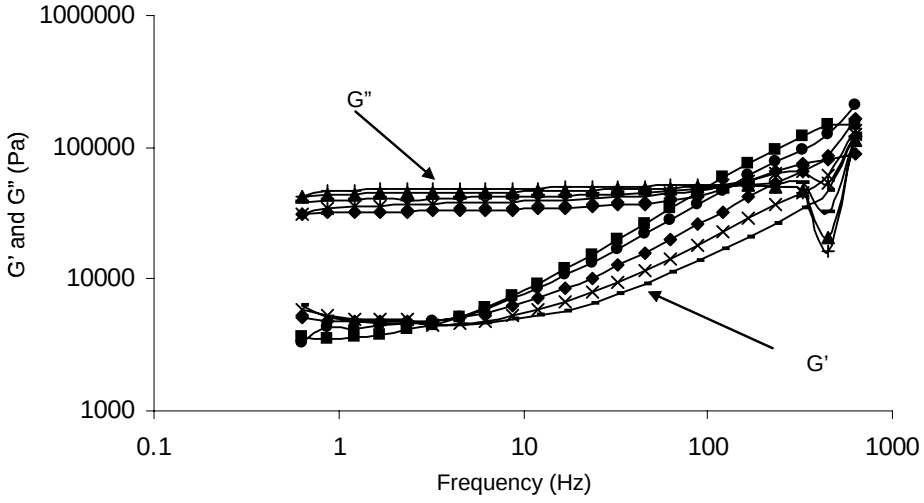

Figure 6.5 Frequency sweep of $R_{10}PEG_1$ at different temperatures (from top, 250, 260, 270, 280 and 290 ^{o}C)

6.4.2 Thermal transitions and rheological analysis

DSC analysis demonstrated that all the ionomers except $R_{10}PEG_1$ were completely amorphous (Table 6.2). Based on previous research involving PET random ionomers in which the clustering point was between 5-8 mol%, all the ionomers studied with higher ionic group content display a multiphase structure: (1) an organic phase with a lower glass transition temperature, and (2) ionic clustering with higher glass transition temperature.[36] The literature has shown that PEG is able to plasticize the organic matrix phase and improve polymer chain mobility.[54-57] Thus, the glass transition temperature of the organic matrix phase decreases with an increase in the level of PEG.[57] Meanwhile, an incremental increase in heat capacity (ΔC_p) at glass transition was also observed when the quenched homogenous PET/PEG solution at low temperature passed through a glass transition. These values increased with an increase in the level of PEG.[57] For PEG endcapped PET ionomers, the plasticization effect from PEG end groups partially offset the constraint effect from the ionic aggregates and improved the mobility of crystallizable chains, resulting in the semicrystalline ionomer, $R_{10}PEG_1$. However, even though the organic matrix of $R_{20}PEG_1$ had a lower glass transition temperature, the size of the organic phase was too small to form a detectable crystalline phase.[63] The $R_{20}PEG_1$ exhibited a lower glass temperature and a larger increment in heat capacity at glass transition than the $R_{10}PEG_1$, even though they had similar weight fractions of PEG based on total weight (Table 6.1). These results indicate that at low temperature the PEG was excluded from the ionic clusters, and that the organic matrix phase was a homogenous solution of PET/PEG. Because the weight fraction organic matrix in R_{20} was smaller than that of R_{10},[63] the relative concentration of PEG in $R_{20}PEG_1$'s organic matrix was

higher than that in $R_{10}PEG_1$, which led to a lower glass transition and larger increment in heat capacity. DSC could not detect the secondary glass transition related to the relaxation of ionic clustering because the highly restricted polymer chains in these ionic clusters require a long relaxation time.

Melt rheological analysis is one of the most effective tools to investigate the plasticization effect of PEG end groups.[36] The temperature ramp curves of these ionomers are depicted in Figure 6.2 and Figure 6.3. R_{20} formed ionic aggregates that were too stable to flow under 300 ^{o}C, and thus performed as a crosslinked network. However, increasing levels of incorporated PEG end groups dramatically decreased melt viscosity (Figure 6.3). Activation energy values for these ionomers are listed in Table 6.2. These data also demonstrate that the presence of PEG groups plasticized the ionic clusters and thus decreased activation energy.

Multi-temperature frequency sweeps of ionomers with and without PEG end groups were also performed in order to generate a time-temperature superposition relationship (Figure 6.4 and 6.5). Previous temperature ramp results already demonstrated that the R_{10} exhibited more stable ionic aggregates with a longer relaxation time than the $R_{10}PEG_1$. As a result, this time-temperature superposition correlates well for the R_{10} because the relaxation time of ionic clusters appears in extremely low frequencies. However, the presence of PEG end groups decreased the relaxation time of ionic clusters to that of an organic matrix phase, and invalidated the time temperature superposition. Figures 4 shows that the G' frequency sweep curves of $R_{10}PEG_1$ at different temperatures cross at one point. For an ionomer with 20 mol% ionic groups, the time-temperature superposition worked well for $R_{20}PEG_1$, but failed for $R_{20}PEG_2$, which

suggests that the effect of plasticization increased with an increase in the level of PEG. Based on melt rheological analysis, it was concluded that PEG end groups are able to diffuse into ionic clusters at high temperature, thus dissolving the ionic groups and in turn decreasing ionic interaction and destabilizing physical crosslinking. With decreased interaction and enhanced mobility, the ionic groups were able to hop among multiplets with escalating rapidity as temperature was increased.

6.4. 3 Sodium Solid State NMR Spectroscopy

Results of melt rheological analysis demonstrated that PEG end groups were able to break the ionic aggregates effectively at high temperature. However, DSC analysis indicates that PEG end groups were extruded from the ionic clusters at low temperature, and solid state ^{23}Na NMR was performed to confirm these results. Cooper and coworkers reported that the specific ionic environment yields different electric field gradients surrounding the nuclei due to the quadrupolar coupling interaction of the ^{23}Na nuclei, which results in distinctly different quadrupolar coupling constants (QCC).[58-60] As a result, QCC can be used to identify the strength of interaction between the quadrupolar sodium nuclei and the electric field gradients in their surrounding environment. In most cases, an up-field shift or increase in QCC was observed when the ionic aggregates became more stable. This may be attributed to stronger interactions among the ionic groups from a possible combination of (1) a greater number of ions held in aggregates, (2) closer packing between ions, and/or (3) less symmetrical packing of the ionic groups. Moreover, they demonstrated that the presence of a polar solvent in an ionic cluster resulted in a decrease in QCC.[58-60] Moore and coworkers reported that QCC is also

effective for investigating the effect of plasticization of surfactant on slightly sulfonated syndiotactic polystyrenes.[32] Sodium solid state NMR spectra of PET ionomers with or without PEG end groups are depicted in Figure 6. The ionomers with PEG end groups exhibited an increase in QCC, which suggests stronger ionic group interaction. The improved mobility of polymer chains at high temperature (due to low viscosity) results in closer packing of the ionic groups or larger ionic aggregates, which results in stronger ionic interaction or more stable ionic aggregates at low temperature. Meanwhile, these results also confirm that PEG end groups are extruded from the ionic aggregates at low temperatures. Had that not been the case, a decrease QCC would be observed.

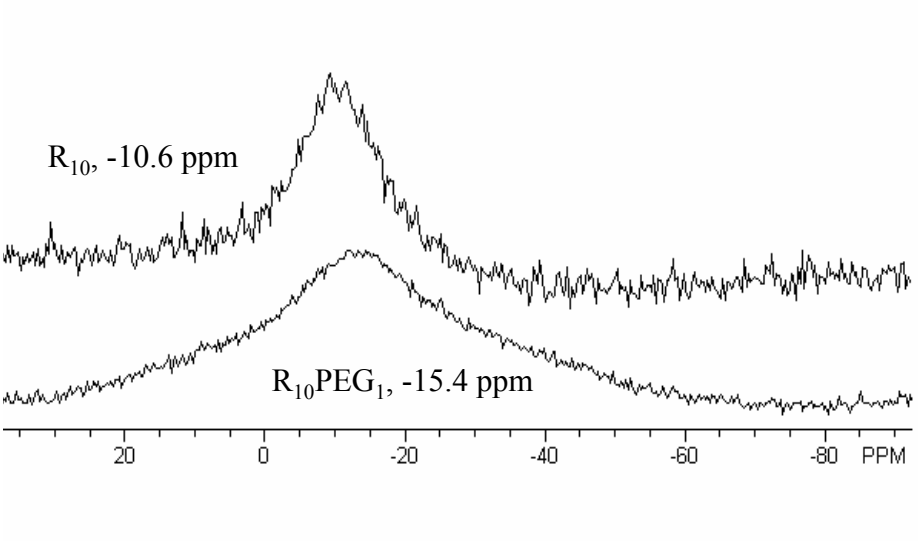

Figure 6.6 Solid state ^{23}Na NMR spectra of R_{10} and $R_{10}PEG_1$, 25 ^{o}C

6.4.4 Solution behaviors

A unique property of $R_{20}PEG_2$ is its solubility in a wide range of solvents of differing polarities, such as water and chloroform. Other ionomers are not soluble in these two solvents, which indicate that the presence of PEG has a significant impact on solubility. DSC and solid state ^{23}Na NMR have already demonstrated that PEG end groups were excluded out from the ionic clusters, and that the organic matrix phase was a PET/PEG solution. With higher concentrations of PEG, the solvent was able to disrupt the weak entanglement between the PEG and PET chains and thus dissolve the ionomers. However, when PEG was present in low concentrations, water or chloroform were not able to the PET chain entanglements.

The presence of a solvent also exerted a pronounced effect on the morphology of the ionomers, and the transparent films cast from water and chloroform were no longer soluble in these solvents. Moreover, high concentrations of solutions prepared via vaporizing solvents from diluted solutions behaved as gels, which could not be dissolved into freshly added solvents. Previous research has demonstrated that the backbone can also form aggregates in concentrated solutions, and ionomer films cast from solution exhibited closer packing since the presence of a solvent decreased viscosity and improved the mobility of the polymer chains.[58-60] Moreover, a small fraction of crystallinity may exist in the dried film due to closer packing, even though it is too small to be detected by DSC. The closer packing of the polymer chain or crystallinity resulted in crosslinking, thus preventing the highly concentrated solution cast films to be redissolved into solvents.

Dilute solutions (1.0 g/dL) and semidilute solutions (10.0 g/dL) of $R_{20}PEG_2$ in water (polar) and chloroform (less polar) were prepared. The solution viscosity curves vs. shear rate are depicted in Figure 6.7. When the concentration of solution was 1.0 g/dL, the aqueous solution exhibited a higher solution viscosity than the chloroform solution. When a less polar chloroform was used as a solvent, the ionic groups tended to aggregate in solution. However, the intermolecular aggregates in a dilute solution were very easily broken via mechanical force or thermal energy.[36,58-60] As a result of solution viscosity measurements, intramolecular aggregates may exist due to the presence of shear force.[36] The intramolecular aggregates are extruded from the solvent molecules, which provides a force to shrink the molecular coils, resulting in lower solution viscosity. However, when the solvent of choice was water, the incorporated ionic groups tended to aggregate on the surface of the coils to interact with the water, which provided an additional force to extend the polymer chain, and resulted in a higher solution viscosity than the less polar solutions. However, in a semi-dilute, less polar solution, the ionic groups formed strong intermolecular aggregates that performed as physical crosslinkers. As a result, semidilute chloroform solution exhibits extremely high solution viscosity, and performs like a gel. In aqueous solutions, the presence of water destroys or destabilizes the ionic aggregates via solvated ionic groups. As a result, the semidilute aqueous solution exhibits lower solution viscosity than the semidilute chloroform solution.

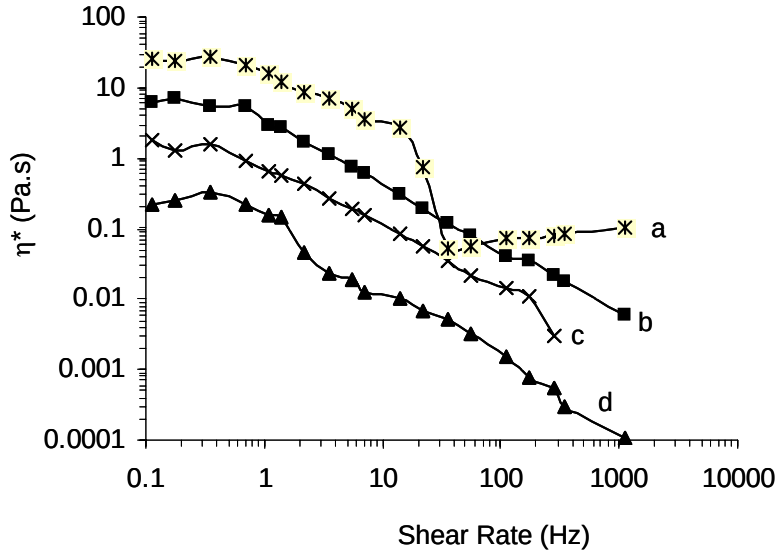

Figure 6.7 Solution viscosity *vs.* shear rate of $R_{20}PEG_2$, 25 ^{o}C, a: chloroform solution, 10 g/dL; b: neutral aqueous solution, 1 g/dL; c: neutral aqueous solution, 10 g/dL; d: chloroform solution, 1 g/dL

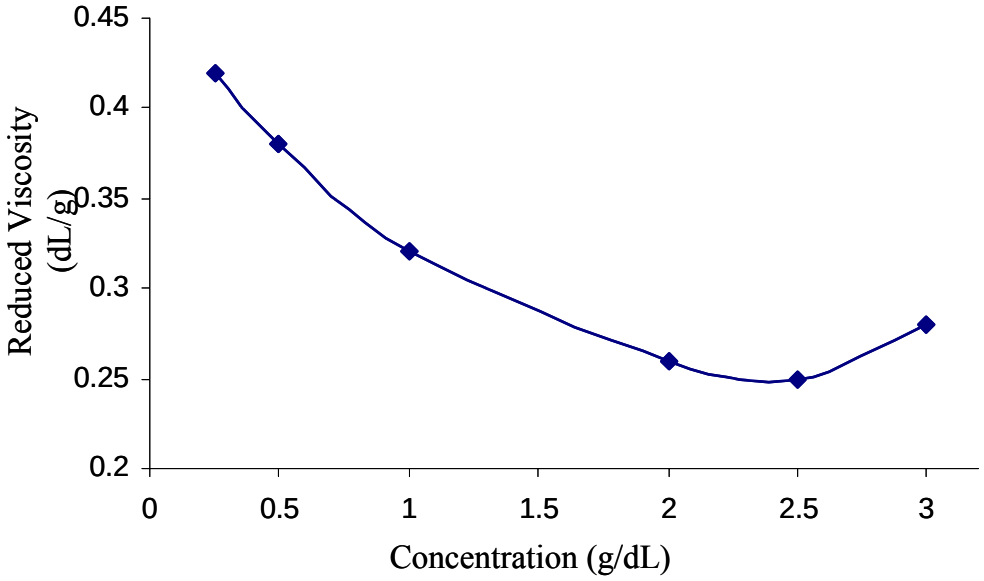

Figure 6.8 Reduced solution viscosity of $R_{20}PEG_2$ in neutral aqueous solutions, 25 ^{o}C

In a high polarity solution, ionomers may exhibit more complicated behaviors depending on their structures. For example, ionomers used with solvents that are able to dissolve the polymer backbone demonstrate characteristic polyelectrolyte behaviors. On the other hand, ionomer solutions in polar solvents, in which the analogous neutral polymer is not soluble, are characterized by polymer-solvent phase separation, which leads to colloidal dispersion. Recently, Cooper and coworkers demonstrated that the level of ionic groups exerts a pronounced influence on solution behavior. Specifically, they determined that a high level of incorporated ionic units could eliminate backbone aggregation in polar solvents.[48-50] In aqueous solutions, water cannot dissolve the polyester backbone. Earlier reports have demonstrated that polyesters with a low level of incorporated ionic groups (Eastman AQ^{TM} sulfonated polyesters) are able to form a colloidal dispersion in aqueous solution.[63] It is interesting to note the dispersion characteristics of ionomers with higher levels of ionic groups and PEG. The semidilute (10 g/dL) neutral aqueous solution exhibited lower solution viscosity than the dilute solution (1 g/dL), which suggests the occurrence of a polyelectrolyte effect. In order to confirm this theory, a capillary viscometer was used to measure the reduced solution viscosity of a neutral aqueous solution at different concentrations (Figure 6.8), which verified the occurrence of the polyelectrolyte effect. Moreover, these results demonstrate that this polymer was fully solvated, and support Cooper's proposal that a high level of ionic content could eliminate hydrophobic aggregation of backbones in polar solvents.

Another unique behavior of a semidilute chloroform solution of $R_{20}PEG_2$ was the presence of shear thickening at a mediate frequency, which has been previously observed in several semidilute ionomer solutions.[61,65] The semidilute chloroform solution (10

g/dL) can be characterized by three distinct regions (Figure 6.7). At a low shear rate, a Newtonian plateau was observed, followed by conventional shear thinning. At an intermediate shear rate, shear thickening was observed (although the mechanism by which this occurred is still unclear).[61] However, in aqueous solution this behavior was not observed since water destroyed or destabilized the ionic aggregates – and this is consistent with previous reports.[50,61,65]

6.5 Conclusions

Poly(ethylene glycol) (PEG) methyl ether endcapped poly(ethylene glycol) (PET) random ionomers based on dimethyl terephthalate (DMT), ethylene glycol (EG), dimethyl-5-sodiosulfoisophthalate sodium salt (SDMI) and poly(ethylene glycol) methyl ether were synthesized using conventional melt polymerization. PEG end groups effectively plasticized the ionic clusters to decrease melt viscosity and relaxation time at high temperature. DSC analysis and sodium solid state NMR demonstrated that PEG end groups were extruded from ionic clusters. A higher content of PEG end-capper (2 mol%) and SDMI (20 mol%) resulted in a polymer that was soluble in a wide range of solvents with different polarities, such as water and chloroform. Investigations of solution viscosity revealed that the polymers could be dissolved in aqueous solution, and that the solution behaviors of ionomers strongly depends on the polarity and concentration of the solvents used.

CHAPTER 7

Synthesis and Characterization of Telechelic Phosphine Oxide Polyester Macroligands and Cobalt(II) Chloride Polymer Complexes

(Published as: Lin, Q.; Unal, S.; Long, T. E. *Macromolecules*, in progress.)

7.1 Abstract

A phosphine oxide containing endcapper, 4-carboxyphenyl biphenyl phosphine oxide, was synthesized to prepare polyester macroligands. The purity of the endcapper was verified using NMR spectroscopy, mass spectroscopy and elemental analysis. Fully endcapped products were prepared via copolymerization of moderate molecular weight polyester oligomers and endcappers. The quantitative incorporation of phosphine oxide functionality was confirmed using ^{1}H NMR spectroscopy and elemental analysis. The complexes of macroligands and cobalt (II) chloride were prepared via charging the salt at the beginning of melt polymerization. The results of NMR spectroscopy, FT-IR spectroscopy and UV-Vis spectroscopy indicate that the cobalt (II) ions preferentially coordinated with the phosphine oxide end groups. The complexes exhibited higher melt viscosity than their salt-free analogues due to the formation of coordinated linear polymers. The presence of the phosphine oxide end groups helped to disperse the cobalt salt evenly in the PET matrix.

7.2 Introduction

Metal containing polymers have been used for a wide variety of applications, such as conductive adhesives, supported catalysts, sensors, luminescent films and devices.[1-8] However, the presence of metal salts in the polymer matrix exerts a pronounced influence on the morphology and rheology of polymeric materials. For example, when inorganic materials such as salts, metal oxides or clay are dispersed in nanosize quantities into the polymer matrixes, special properties can be obtained.[1-8] In order to reduce the incidence of large aggregates, several kinds of functional groups, such as a Schiff-base, pyridine and phosphine oxide, have been incorporated into the polymeric backbone to stabilize the metal salts via coordination.[1-8] Phosphine oxide is one of most interesting functionalities to be incorporated into polymers as a macroligand due to its excellent thermal stability, resulting in macroligands and complexes that are processable at high temperatures.[8] McGrath and coworkers developed several families of phosphine oxide containing high performance polymers,[8-9] in addition to studying poly(arylene ether phosphine oxide) and metal salt complexes in detail.[8] Their results demonstrate that phosphine oxide containing poly(arylene ether)s and polyimides can evenly disperse metal salts into polymer matrixes via the coordination of metal salts and phosphine oxide groups.

---

[1]Manners, I. *Science* **2001**, 294, 1664.

[2](a) Smith, A. P.; Fraser, C. L. *Macromolecules* **2002**, 35, 594. (b) Bender, J. L.; Corbin, P. S.; Fraser, C. L.; Metcalf, D. H.; Richardson, F. S.; Thomas, E. L.; Urbras, A. M. *J. Am. Chem. Soc.* **2002**, 223, 408. (c) McAlvin, J. E.; Scott, S. B.; Fraser, C. L. *Macromolecules* **2000**, 33, 6953. (d) Fraser, C. L.; Smith, A. P.; Wu, X. F. *J. Am. Chem. Soc.* **2000**, 122, 9026. (e) Wu, X. F.; Fraser, C. L. *Macromolecules* **2000**, 33, 4053. (f) Wu, X. F.; Collings, J. E.; McAlvin, J. E. Fraser, C. L. *Macromolecules* **2001**, 34, 223.

[3]Vitalini, D.; Mineo, P.; DiBella, S.; Fragala, I.; Maravigna, P.; Scamporrino, E. *Macromolecules* **1996**, 29, 448.

Poly(ethylene terephthalate) (PET) is an important polyester for textile filaments, packaging materials, films and bottle products.[10] In fact, PET prepared via melt polymerization contains a trace amount of residual metal salt catalysts.[10] Titanium and cobalt salts were used as catalysts for a transesterfication reaction, and antimony oxide was used as a catalyst to facilitate polycondensation. However, the residual metal salts resulted in obvious degradation during melt processing. As a result, phosphoric acid was added at the polycondensation stage to deactivate the catalysts.[10] Even though the presence of metal salts normally results in degradation, efforts to develop PET matrixes with metal salts has continued due to the excellent mechanical properties and low cost of these polymers.[11-12] Most of these efforts have focused on incorporating strong ligands into the PET backbone to form macroligands, as it was believed that metal salts preferentially coordinated with the strong ligand groups without interacting with carbonyl groups. As noted above, phosphine oxide is a strong ligand, and McGrath and coworkers demonstrated that when phosphine oxide containing polyimides were used as polymer matrixes, the metal salt coordinated with the phosphine oxide groups, even though an excess amount of carbonyl groups were also present.[8] Fraser and coworkers demonstrated that in complexes of polyesters and metal salts, the melt salts preferred to coordinate with the strong ligands without interacting with the carbonyl groups.[2] This selective coordination facilitates the preparation of complexes of polyesters and metal salts without degradation. In addition, McGrath and coworkers randomly incorporated phosphine oxide units into the PET backbone via the comomoner, 4,4'-biscarboxyphenyl phenyl phosphine oxide.[9(a)] However, the asymmetrical structure of the phosphine oxide units disrupted chain regularity, resulting in amorphous products.[13] Our previous

research demonstrated that incorporating functional groups as end groups does not significantly influence backbone properties.[9,14] Moreover, incorporating ligand groups at the chain ends results in well defined structures. Recently, Fraser and coworkers synthesized linear and star polymers via the coordination of metal salts and bipyridine end groups of oligomers. However, if the ligands were randomly incorporated into the backbone, intermolecular coordination resulted in crosslinking.[8] In this section, the synthesis of phosphine oxide endcappers, macroligands and complexes with cobalt (II) chloride will be reported.

---

[4]Yang, J. M.; Hsiue, G. H. *Macromolecules* **1991**, 24, 4010.

[5](a) Chen, L.; Xu, H.; Yu, X. H., Yang, C. Z. *J. Polym. Sci.: Part A, Polym. Chem.* **1996**, 34, 721. (b) Lin, Q.; Cheng, D.; Yu, X. *Chinese Journal of Inorganic Chemistry* **1998**, 14, 287.

[6]Peters, M. A.; Belu, A. M.; Linton, R. W.; Dupray, L.; Meyer, T. J.; Desimone, J. M. *J. Am. Chem. Soc.* **1995**, 117, 3380.

[7](a) Hechet, S.; Ihre, H.; Frechet, J. M. J. *J. Am. Chem. Soc.* **1999**, 121, 9239. (b) Giannelis, E. P. *Adv. Mater.* **1996**, 8, 29.

[8](a) Bonaplata, E.; Smith, C. D.; McGrath, J. E. *ACS Sym. Ser.* **1995**, 603, 227. (b) Wang, S.; Zhuang, H.; Sankarapandian, M.; Shoba, H. K.; Ji, Q.; Shultz, A. R.; McGrath, J. E. *Polymer Preprints* **2000**, 41(2), 1350. (c) Spinu, M.; McGrath, J. E. *J. Org. Inorganomet. Chem. Polym.* **1992**, 2, 103. (d) Wang, S. *Ph.D. dissertation, Virginia Polytechnic Institute and State University*, **2000**.

[9](a) Wan, I.; Keifer, L. A.; McGrath, J. E.; Kashiwagi, T. Polym. Prepr. 1995, 36(1), 491. (b) Wang, S., Zhuang, H.; Shobba, H. K.; Glass, T. E.; Sankarapandian, M.; Ji, Q.; Shultz, A. R.; McGrath, J. E. Macromolecules 2001, 34, 8051. (c) Ji, Q.; Muggli, M.; Wang, F.; Ward, T. C.; Burns, G.; Sorathia, U.; McGrath, J. E. *Polym. Prepr.* **1997**, 273 (2), 120. (d) Smith, C. D.; Grubbs, H. J.; Webster, H, F.; Gungor, A.; Whightman, J. P.; McGrath, J. E. *High Perform. Polym.* **1991**, 4, 211. (e) Riley, D. J.; Gungor, S. A.; Srinivasan, S.; Sankarapandian, M.; Tchatchoua, C. N., Muggli, M. W.; Ward, T. C.; Magrath, J. E. *Polym. Eng. Sci.* **1997**, 37, 150.

[10](a) Goodman, I.; Sheanan, R. J. *Eur. Polym. J.* **1990,** 26, 1081. (b) Goodman, I.; Rodriguez, M. T. *Macrol. Chem. Phys.* **1994,** 195, 1705. (c) Lawton, E. L. *Polym. Eng. Sci.* **1985**, 25, 348.

[11]Simionescu, C.; Vasiliu-Opre,C. *Polym. Prep.* **1972**, 13(1), 584.

[12]Simionescu, C. *Makromol. Chem.* **1973**, 163, 75.

7.3 Experimental

7.3.1 Materials

Magnesium powder (99%), biphenyl phosphinic chlorine (99%), 1-bromo-4-toluene (99%), triphenyl phosphine oxide (99%), iodine (99%), potassium permanganate (97%), cobalt chloride (99%) and pyridine were purchased from Aldrich, and used as received. PET oligomer was kindly donated from Eastman Chemical Co., and used as received. Dimethyl terephthalate (DMT, 99%), and dimethyl isophthalate (DMI, 98%) were purchased from Aldrich, and used as received. Ethylene glycol (EG) was purchased from J. T. Baker, and used as received. Titanium tetra(isopropoxide) (99%) and antimony oxide (99%) were purchased from Aldrich, and the preparation of the catalyst solutions was described in a previous report.[14]

7.3.2 Synthesis

Synthesis of endcapper: 4-Toluenemagnesium bromide, (1). In a three-necked flask equipped with a magnetic stir bar, reflux condenser, and addition funnel, magnesium powder (6.0 g, 0.25 mole) was added, and subsequently flushed with ultrapure argon. Approximately 200 mL THF and iodine (10.0 mg) were added.[16] The heterogeneous mixture was stirred at 25 ºC until the iodine color faded to colorless, and immediately after which a solution of 1-bromo-4-toluene (35 g, 0.2 mole) in THF (50 mL) was added drop-wise over a one hour period. The temperature was then raised to 65 ºC, and maintained at reflux for 6 hours. The product was used without isolation or characterization.

4-methylphenyl biphenyl phosphine oxide, (2). A solution of biphenyl phosphinic chlorine (0.20 mol) in 50 mL THF was added to the compound **1** solution via an addition funnel at room temperature over 30 minutes. The temperature was raised to 65 ºC and maintained at reflux for 6 hours. THF was removed using distillation under nitrogen purge, and vacuum was finally applied to ensure complete removal. Isolation of the resulting product was accomplished by adding 300 mL toluene and 300 mL 10% H_2SO_4 solution, and allowed to stir at 60 ºC for 30 minutes. The organic layer was separated, and washed repeatedly with 200 mL 1N NaOH solution, and finally with 300 mL deionized water. The toluene was removed in a distillation apparatus to yield a white crystal that was subsequently dried in vacuo at 80 °C for 24 hours. Typical isolated yields ranged from 80% to 85%. ^{1}H-NMR (DMSO-d_6, ppm): δ 2.10 (s, 3H,-CH_3); 7.25-7.38 (m, 2H); 7.45-7.62 (m, 12H). ^{13}C NMR (DMSO-d_6): δ 76.9; 127.8-128.8; 128.6-128.6; 128.9; 131.6-131.0; 132.6; 140.8. ^{31}P NMR (DMSO-d_6): δ 25.6. Mass spectra (FAB): $(M+H)^+$= 293 Da.

---

[13]Lin, Q.; Wang, Z. H.; Ratta, V.; Wilkes, G. L.; Long, T. E. *Polym. Int.* **2002**, 51, 540.
[14]Kang, H.; Lin, Q.; Armentrout, R. S.; Long, T. E. *Macromolecules* **2002**, 35, 8738.
[15]Lin, Q., Unal, S.; Fornof, A.; Wei, Y.; Li, H.; Armentrout, R. S. *Macro. Symp.* **2003**, in press.
[16]Lin, Q.; Long, T. E. *J. Polym. Sci.: Part A., Polym. Chem.* **2001**, 38, 3736.
[17](a) Nelson, C. J. *J. Polym. Sci. Chem. Ed.* **1974**, 44, 2905. (b) Youk, J. H.; Kambour, R. P.; Macknight, W. J. *Macromolecules* **2000**, 33, 3594. (c) Zhang, B.; Weiss, R. A. *J. Polym. Sci. Polym. Chem.* **1992**, 30, 91. (d) Zhang, B.; Weiss, R. A. *J. Polym. Chem.* **1992**, 30, 989.
[18]Blyer, L. L.; Hass, T. W. *J. Appl. Polym. Sci.* **1969**, 13, 2721.
[19]Cotton, E. A.; Soderberg, R. H. *J. Am. Chem.* **1960**, 82, 5771.

4-carboxyphenyl biphenyl phosphine oxide (3). In a 1000 mL three-necked flask equipped with a magnetic stir and condenser, compound **2** (56.96 g, 0.16 mole), 300 mL pyridine and 200 mL water were added, and the temperature was raised to 70 ºC. The $KMnO_4$ was added in 6-8 aliquots at 30 minutes intervals. After the last addition, the temperature was raised to 80-90 ºC for 12 hours. At the end of the reaction, the mixture was allowed to cool to room temperature and excess $KMnO_4$ was filtered off. The red solution was then acidified with concentrated HCl, and white powder was collected using a filter funnel. ^{1}H NMR revealed a small amount of residual methyl group due to the incomplete oxidation. The second oxidation was performed in a stoichiometric amount of aqueous sodium hydroxide solution to obtain pure product. A slight stoichiometric excess (from ^{1}H NMR spectrum) of $KMnO_4$ was added into solution, and the reaction was allowed to proceed at 80 ^{o}C for 6-8 h. The solution was filtered, acidified and the white powder was collected using a filter funnel. Typical isolated yields after two oxidation were 90-95%. ^{1}H NMR (DMSO-d_6): δ 7.55-7.61 (m, 4H); 7.61-7.69 (m, 4H); 7.31-7.45 (m, 6H, ArH_4); 7.74-7.81 (m, 2H); 8.08 – 8.13 (m, 2H). ^{13}C NMR (DMSO-d_6): δ 120.8; 129.4; 131.6; 132.4, 132.8, 134.0; 136.8; 138.0; 166.8. ^{31}P NMR (DMSO-d_6): δ 26.1. Mass spectra (FAB): $(M+H)^+$: 323 Da. Elemental analysis of $C_{19}H_{15}O_3P$: calculated (found): C, 70.80%, (70.45%); H, 4.60%, (4.49%); P, 9.61%, (9.50 %).

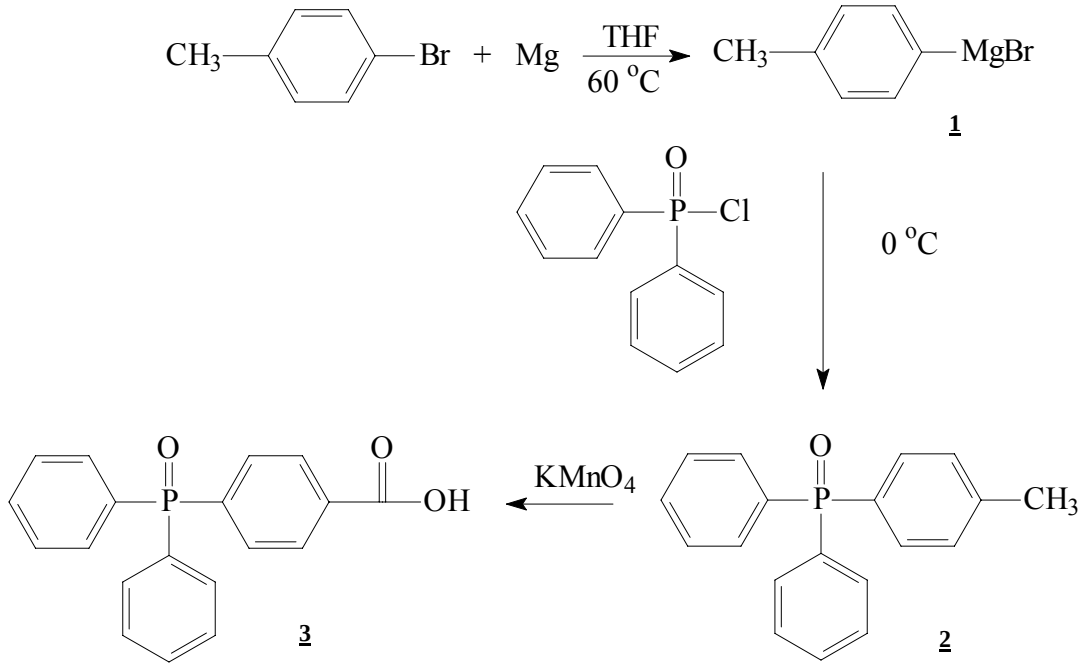

Scheme 7.1 Synthesis of 4-carboxyphenyl biphenyl phosphine oxide

Synthesis of Polymers: PET-1-5. PET-1-5 was prepared via melt condensation of DMT, EG and phosphine oxide endcapper. Both titanium tetraisopropoxide (20 ppm) and antimony oxide (200 ppm) were added to facilitate ester exchange and subsequent polycondensation. The reactor consisted of a 100 mL round-bottomed flask equipped with an overhead mechanical stirrer, nitrogen inlet, and condenser. The flask containing the monomers and catalysts was degassed using vacuum and nitrogen three times, and subsequently heated to 180 °C. The reactor was maintained at 190 °C for one hour, and the temperature was increased to 275 °C over 2 h. The reaction was allowed to proceed for 30 min at 275 °C. Vacuum was gradually applied up to 0.5 mmHg and polycondensation continued for 2 h at 275 °C.

PET-2-x and PET-3-x: Polymers were prepared via the melt condensation of PET oligomer, phosphine oxide end cappers with (PET-3-x) or without (PET-2-x) cobalt(II) chloride (50 mol% of phosphine oxide endcapper), where x denotes the molar ratio of the phosphine oxide endcapper. Antimony oxide (200 ppm) was added to facilitate polycondensation. The reaction was allowed to proceed for 30 minutes at 275 °C. Vacuum was gradually applied up to higher than 0.5 mmHg and polycondensation continued for 2 h at 275 °C.

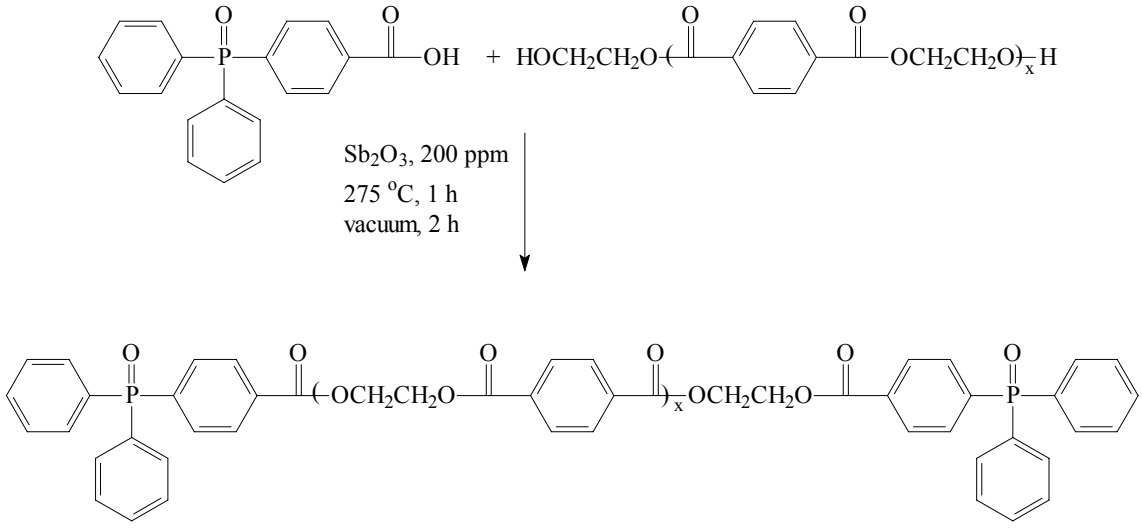

Scheme 7.2 Synthesis of phosphine oxide endcapped PET macroligands

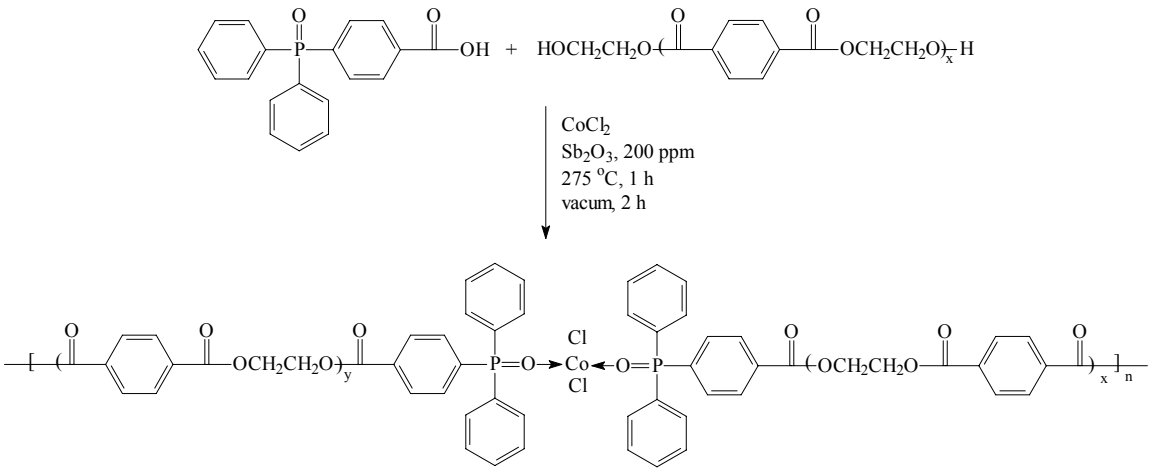

Scheme 7.3 Synthesis of complexes of phosphine oxide endcapped PET and cobalt(II) chlorine

PETI oligomer: PETI oligomer was prepared via the melt condensation of dimethyl terephthalate (50 mol% of repeat units), dimethyl isophthalate (50 ml% of repeat units) and ethylene glycol (200 mol% of repeat units). Both titanium tetraisopropoxide (20 ppm) and antimony oxide (200 ppm) were added to facilitate ester exchange and subsequent polycondensation. The reactor consisted of a 100 mL round-bottomed flask equipped with an overhead mechanical stirrer, nitrogen inlet, and condenser. The reactor containing the monomers and catalysts was degassed using vacuum and nitrogen three times, and subsequently heated to 190 °C. The reactor was maintained at 190 °C for one hour, and the temperature was increased to 275 °C over 2 h. The reaction was allowed to proceed for 30 min at 275 °C. Vacuum was gradually applied up to higher than 0.5 mmHg and polycondensation continued for 10 min at 275 °C.

PETI-1-5: PETI-1-5 was prepared using an identical procedure as used for PET-2-x.

PETI-2-5: PETI-2-5 was prepared using an identical procedure as used for PET-3-x.

Preparation of Model Compounds: M-1: PET (7.0 g) and 3.0 g triphenyl phosphine oxide were mixed together in a 25 ml flask under nitrogen atmosphere at 275 ^{o}C for 5 minutes.

M-2: PET (7.0 g), 3.0 g triphenyl phosphine oxide (10.8 mmol) and 0.70 g (5.4 mmol) cobalt chloride salt were blended in a 25 mL flask under nitrogen atmosphere at 275 ^{o}C for 5 minutes.

7.3.3 Characterization

The inherent viscosities of the samples were measured at 25 ^{o}C in a capillary viscometer using 0.5 g/dL solution in a 60/40 w/w mixture of phenol and tetrachloroethane. Solution ^{1}H, ^{13}C and ^{31}P NMR spectra were recorded on a Varian 400 MHz spectrometer, and solid state NMR was performed on MSL-300. Thermal transitions were determined on a Perkin-Elmer DSC Pyris 1 at a heating rate of 10 °C/min under N_2 purge, and the reported data were obtained from the second heating cycle. Melt rheological analysis was performed using a TA instruments AR 1000 melt rheometer. Reflective UV-Vis spectra were obtained on a Perkin-Elmer-300 spectrometer. Elemental analysis was performed at Eastman Chemical Co. GPC measurements were performed on a Waters SEC (515 pump, 717 autosampler) with an external 410 refractive index detector. Multiangle laser light scattering (MALLS) was

also performed using an in-line Wyatt Minidawn. A Polymer Laboratories PLgel, 5 micron MIXED-C column with a length of 300 mm and inner diameter of 7.5 mm was used. The flow rate was 1.00 mL/min and the temperature was 40 °C. FTIR spectra of samples were obtained using a MIDAC spectrophotometer equipped with a ZnSe reflection element.

7. 4 Results and discussion

7.4.1 Synthesis

The synthetic scheme for preparing monofunctional phosphine oxide endcappers is shown in Scheme 7.1. A double oxidation of 4-methylphenyl biphenyl phosphine oxide was used to ensure a highly purified resulting product. ^{1}H spectrum is depicted in Figure 7.1. Only the resonances in the aromatic region verified that the oxidation reaction was fully complete. The phosphorus atom also has ½ spin, which couples with the hydrogen atoms to result in multi-split peaks (Figure 7.1); the assignment of the peaks is based on a previous report.[8a] One sharp peak in the ^{31}P NMR spectrum also suggests that no other impurities containing phosphorus were present. Moreover, mass spectroscopy and elemental analysis also proved that the product had the desired structure.

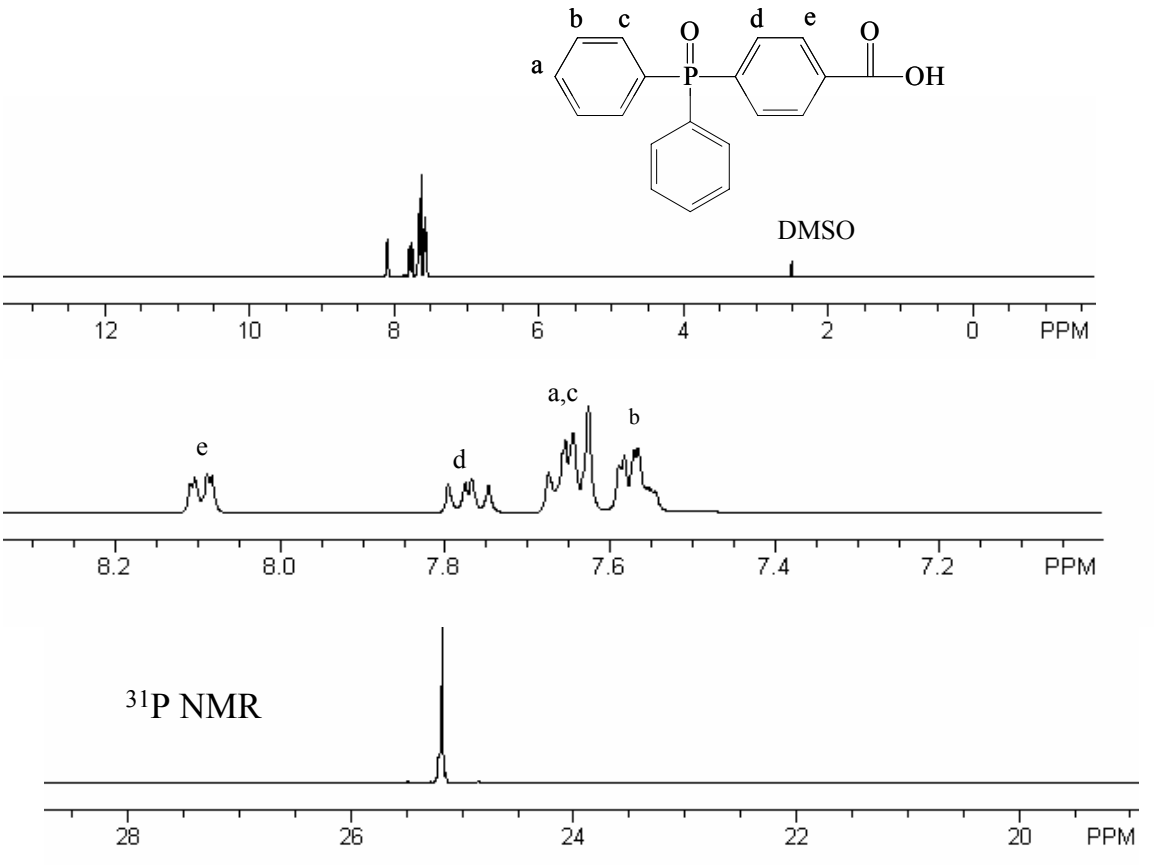

Figure 7.1 ^{1}H and ^{31}P NMR specra of 4-carboxyphenyl biphenyl

Table 7.1 Molecular weights of macroligands and complexes

Sample	P (mol%)	$\eta_{inherent}$ [a] (dL/g)	M_n [b] (g/mol)	M_n [c] (g/mol)
PET-2-3	3.3	0.33	11700	11000
PET-3-3	3.3	0.32	11700	10500
PET-2-5	5.2	0.25	7400	6600
PET-3-5	5.2	0.25	7400	6600
PETI-1-5	5.2	0.21	-------	-------
PETI-2-5	5.2	0.20	-------	-------

[a:] measured at 25 ^{o}C in a capillary viscometer using 0.5 g/dL solution in a 60/40 w/w mixture of phenol and tetrachloroethane; [b:] estimated based on Equation 1 and ^{1}H NMR spectrum; [c:] estimated using Mark-Houwink equation.

Table 7.2 Results of elemental analysis

Sample	P (mol%)	P[a] (wt%)	Co[a] (wt%)	P[b] (wt%)	Co[b] (wt%)
PET-2-3	3.3	0.48	0	0.47	0
PET-3-3	3.3	0.48	0.46	0.48	0.39
PET-2-5	5.2	0.81	0	0.80	0
PET-3-5	5.2	0.81	0.77	0.82	0.76
PETI-1-5	5.2	0.81	0	0.81	0
PETI-2-5	5.2	0.81	0.77	0.80	0.76

[a:] theoretical values; [b:] measured value.

The synthesis of PET via conventional melt polymerization consists of two steps, i.e. transesterification and subsequent polycondensation under reduced pressure.[10] Based on these steps, two synthetic methodologies used to prepare high molecular weight PETs were developed.[2] The first one is a one-step reaction using DMT and a large excess amount of EG with various kinds of catalysts to facilitate transesterification and polycondensation. The second is a two-step reaction. First, terephthalic acid is reacted with almost equal amounts of EG without catalysts under a high pressure to prepare moderate molecular weight PET oligomers. Then, the obtained oligomer is further polymerized with a catalyst to facilitate polycondensation under reduced pressure.

Efforts to synthesize macroligands via the one step reaction using DMT, EG, phosphine oxide endcapper, and catalysts for transesterification failed, since the phosphine oxide groups deactivated the catalysts. When the temperature was higher than 220 ^{o}C, a significant amount of the low boiling point starting material, DMT, vaporized out and condensed on the condenser due to the low efficiency of the ester exchange without active catalysts. ^{1}H NMR spectra revealed a high level of alcohol end groups, and inherent viscosity measurements (0.08 dL/g) also confirmed that only a low molecular weight product was obtained.

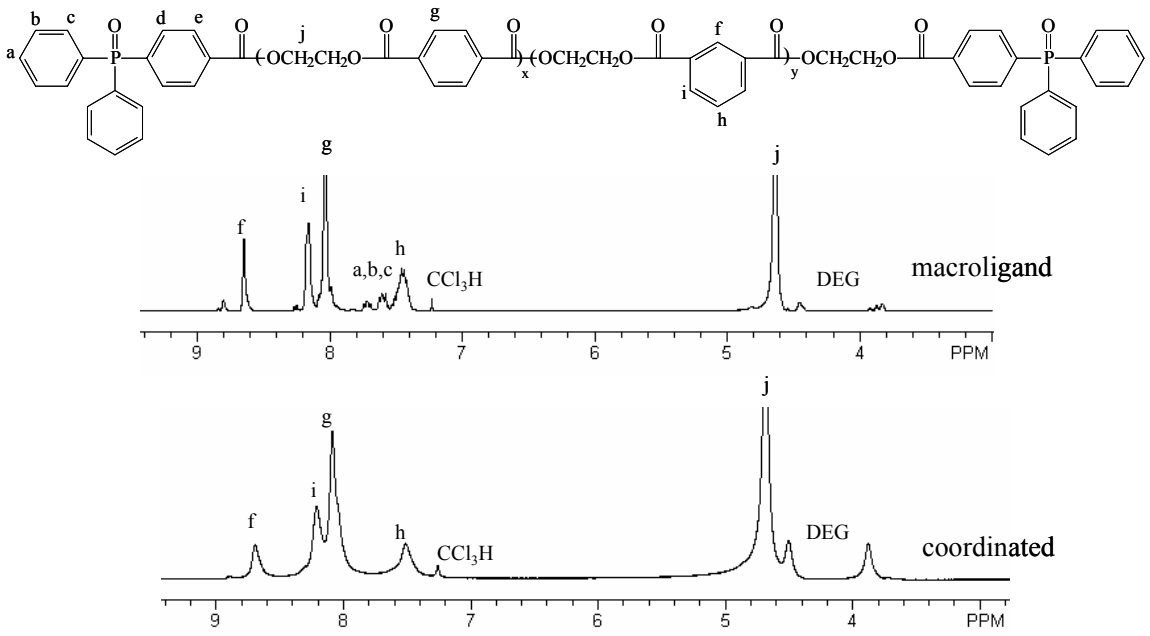

Figure 7.2 ^{1}H spectra (chloroform, 400 MHz): PETI macroligand, PETI-1-5 (top); complex of phosphine oxide endcapped PETI with cobalt(II) chlorine, PETI-2-5 (bottom).

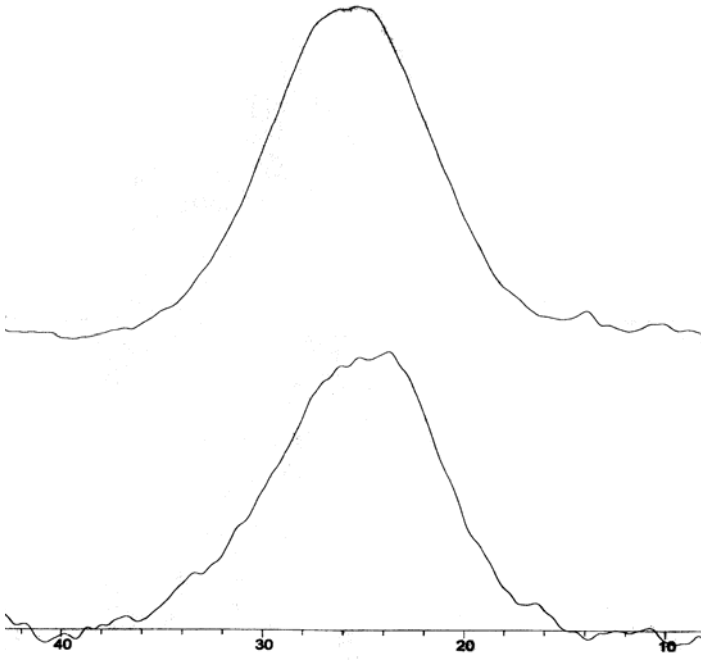

Figure 7.3 Solid state ^{31}P NMR spectroscopy: complex of phosphine oxide endcapped PET and cobalt(II) chlorine, PET-3-5, (top); macroligand, PET-2-5, (bottom).

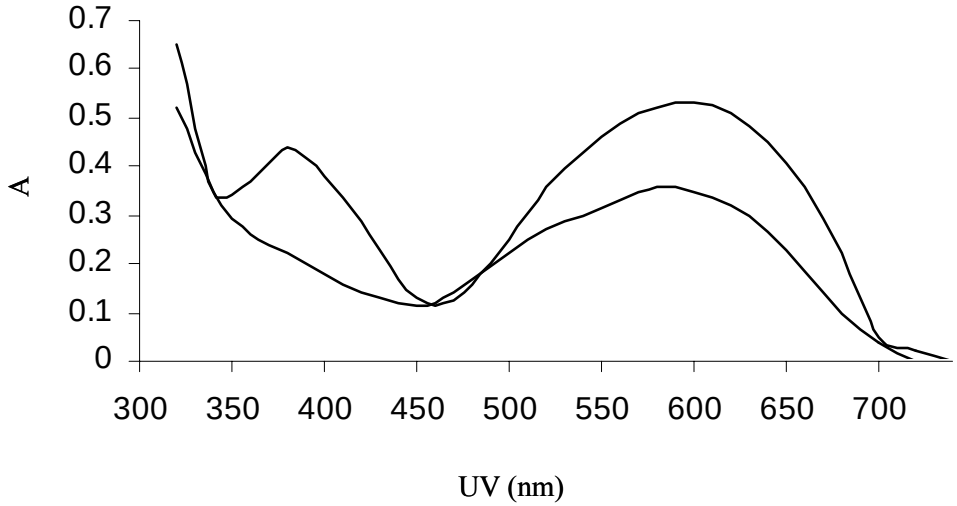

Figure 7.4 Reflective UV- Vis spectra of films of blends of PET and cobalt chloride: 5 mol% phosphine oxide endcapped PET macroligand, PET-2-5 (top); PET (bottom).

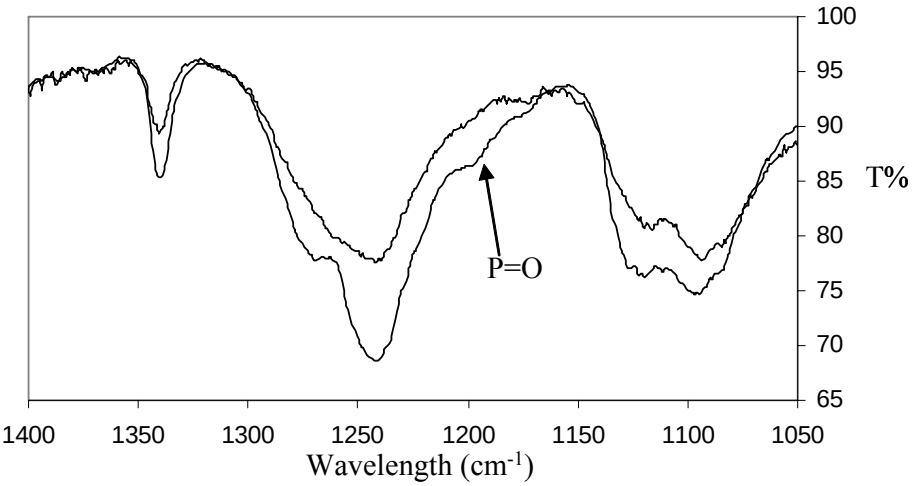

Figure 7.5 ATR FT-IR spectra of macroligand, PET-2-5, (top); complex of phosphine oxide endcapped PET and cobalt chloride, PET-3-5, (bottom).

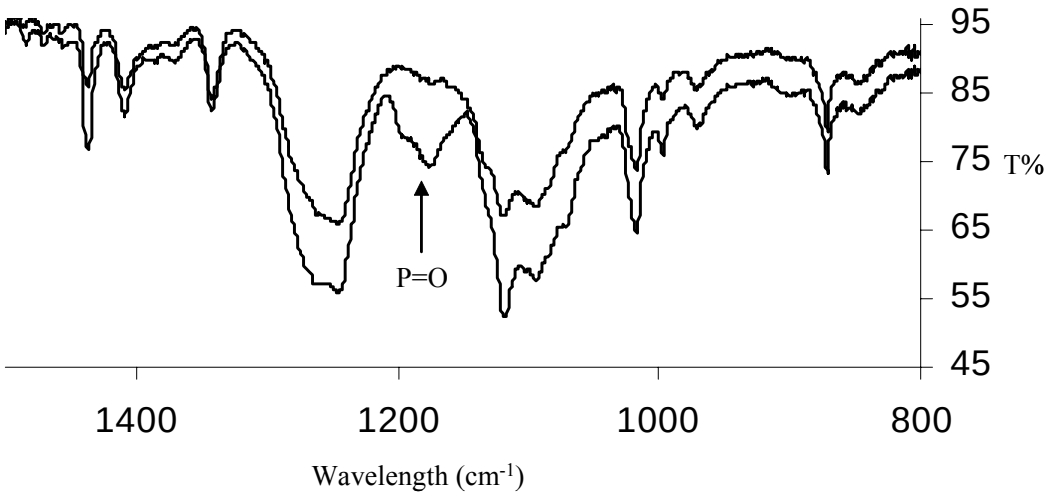

Figure 7.6 ATR FT-IR spectra of model polymers: M-1, blend of PET and triphenyl phosphine oxide (top); M-2, blend of PET, triphenyl phosphine oxide and cobalt(II) chloride, (bottom).

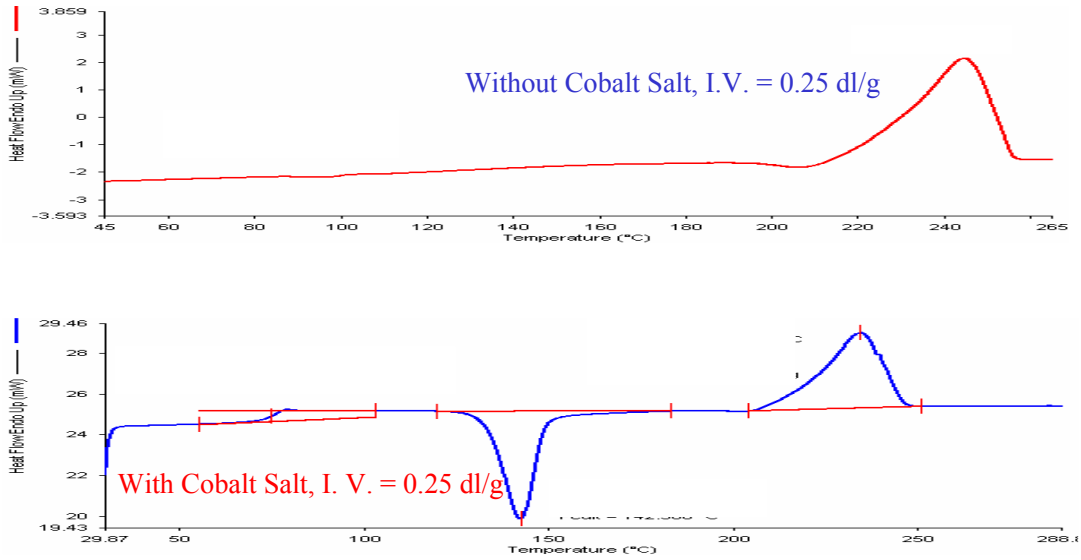

Figure 7.7 DSC analysis: macroligand, PET-2-5, $\eta_{inherent}$ = 0.25 dL/g, (top); complex of phosphine oxide endcapped PET and cobalt chloride, PET-3-5, $\eta_{inherent}$ = 0.25 dL/g, (bottom).

As an alternative methodology, macroligands were successfully prepared via the copolymerization of a PET oligomer and a phosphine oxide endcapper. ^{1}H NMR and elemental analysis demonstrated that the phosphine oxide endcapper was quantitatively incorporated into the polymer (Figure 7.2 and Table 7.2). PET is a semicrystalline polymer that is not soluble in regular organic solvents. In order to characterize the macroligands using GPC and NMR spectroscopy in organic solvent, phosphine oxide endcapped PETIs [poly(ethylene terephthalate–ethylene isophthalate)] were also synthesized as model polymers.

Since excess ethylene glycol was used during the polymerization and subsequently removed via distillation during polycondensation, the conventional equation, X = (1+r)/(1-r), was not applicable to estimate molecular weight.[14] Based on the assumption that the end capping reaction was quantitative and restricted to the polymer chain end, a modified equation (Equation 1) was utilized to estimate theoretical number average molecular weight. Table 1 lists the theoretical number average molecular weights for the phosphine oxide endcapped polyester macroligands.

$$\langle M_n \rangle = (\text{total mass of product molecules}) / (\text{moles of product molecules})$$

$$= [\Sigma (m_e + x * m_{ru})] / (N(A)/2) \qquad \text{(Equation 1)}$$

where

m_e = the molar mass of the combined end groups

m_{ru} = the molar mass of an internal repeat unit

N(A) = moles of monofunctional end capping reagent

x = the number of internal repeat units

Inherent solution viscosity was measured at 25 ^{o}C, and the Mark-Houwink equation was used to estimate the approximate molecular weights of the PET macroligands (Table 7.1).[17] The molecular weight of 5.2 mol% phosphine oxide endcapped PETI copolymer

measured using GPC (M_n = 6300 g/mol, M_w = 14200 g/mol) was consistent with the predicted value (M_n = 7400 g/mol) using NMR spectrum and Equation 1. Moreover, the predicted values of the PET macroligands using Equation 1 agreed well with the values estimated via the Mark-Houwink equation (Table 7.1). All these results suggest that the endcapping reaction was fully complete, and that the macroligands had well defined structures.

Complexes of macroligands and cobalt(II) chloride were prepared via charging cobalt(II) chloride, phosphine oxide endcapper and polyester oligomers into the flask simultaneously at the beginning of polymerization. The polymer melts and solid products exhibited a deep blue color. However, when only polyester oligomers and cobalt(II) chloride were added into the flask, violet products were obtained, which suggest that the salt coordinated with different ligands in the products with or without the phosphine oxide endcapper. UV-Vis spectroscopy was also used to characterize the color of the products. The reflective UV-Vis spectra of solid state PET complexes and macroligands are depicted in Figure 7.3, and demonstrate that the presence of phosphine oxide groups results in a novel adsorption peak around 380 nm, which leads to a blue color coordination product.

Compared to the NMR spectra of macroligands, the resonances related to the endcapper disappeared in the ^{1}H NMR spectrum and ^{31}P NMR spectra, which indicates that all the phosphine oxide groups coordinated with cobalt(II) chloride (Figure 7.2). McGrath and coworkers demonstrated that when the phosphine oxide group coordinated with metal salts (up to 20 mol%), a marked downfield shift and broadening of the NMR signal were observed since the phosphine oxide group coordinated with the

paramagnectic high spin Co (II) ion (d^9 with three unpaired electrons).[8] In this research, 100 mol% phosphine oxide end groups coordinated with paramagnectic cobalt(II) ions. As a result, NMR resonances associated with the phosphine oxide ligands were too broad to be detected. However, the resonance of the coordinated phosphine oxide end groups was detected using solid state ^{31}P NMR spectroscopy (Figure 7.4), which was performed in a much stronger magnetic filed. The position of the peak of complexes in the solid state ^{31}P NMR spectrum slightly moved downfield compared to the resonance of macroligand, which is consistent with previous reports.[8] Moreover, the results of elemental analysis also demonstrated that the phosphine oxide endcapper was quantitatively incorporated into the polymers (Table 7.2).

The other tool utilized to investigate the coordination of metal salts and phosphine oxide groups was FT-IR spectroscopy. McGrath and coworkers demonstrated that the characteristic peak of phosphine oxide at 1190 cm^{-1} weakened or disappeared after the incorporation of phosphine oxide groups coordinated with metal salts.[8] For our products, the characteristic peak of phosphine oxide at 1190 cm^{-1} was only a small shoulder of the peak of carbonyl due to low concentration (Figure 7.5). This shoulder disappeared after cobalt(II) ions were introduced. To verify this result, model polymers were prepared via blending PET with triphenyl phosphine oxide with or without cobalt(II) chloride. The characteristic peak of phosphine oxide at 1190 cm^{-1} disappeared in the spectrum of the complex (Figure 7.6), which indicated that the cobalt(II) ions preferentially coordinated with the phosphine oxide groups, even though an excess amount of carbonyl groups was present. It is interesting to note that the complexes exhibited similar inherent solution

viscosities as the corresponding macroligands (Table 7.1). This indicates that the complexes dissociated in the solutions used to measure inherent viscosity.

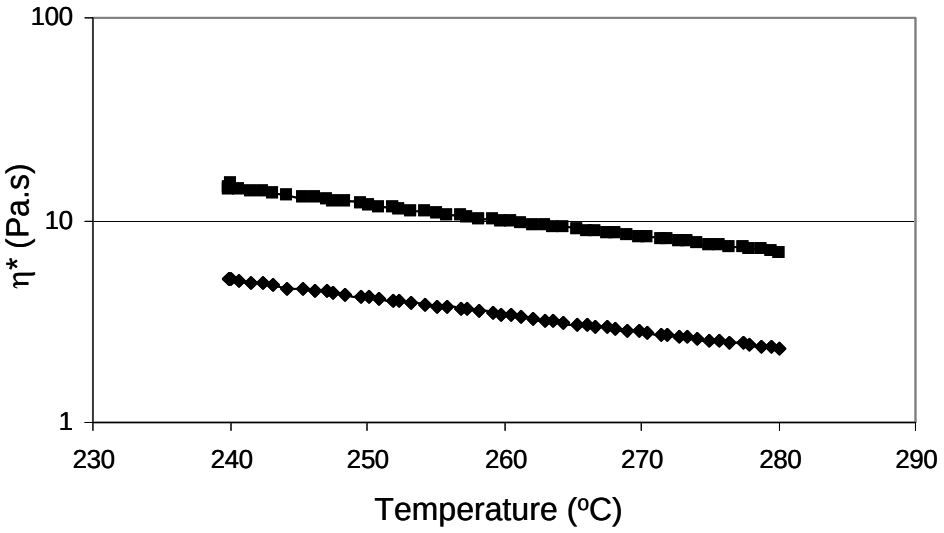

Figure 7.8 Rheological analysis (temperature ramp) of macroligands and complex: (top): complex, PET-3-5; (bottom): PET-2-5.

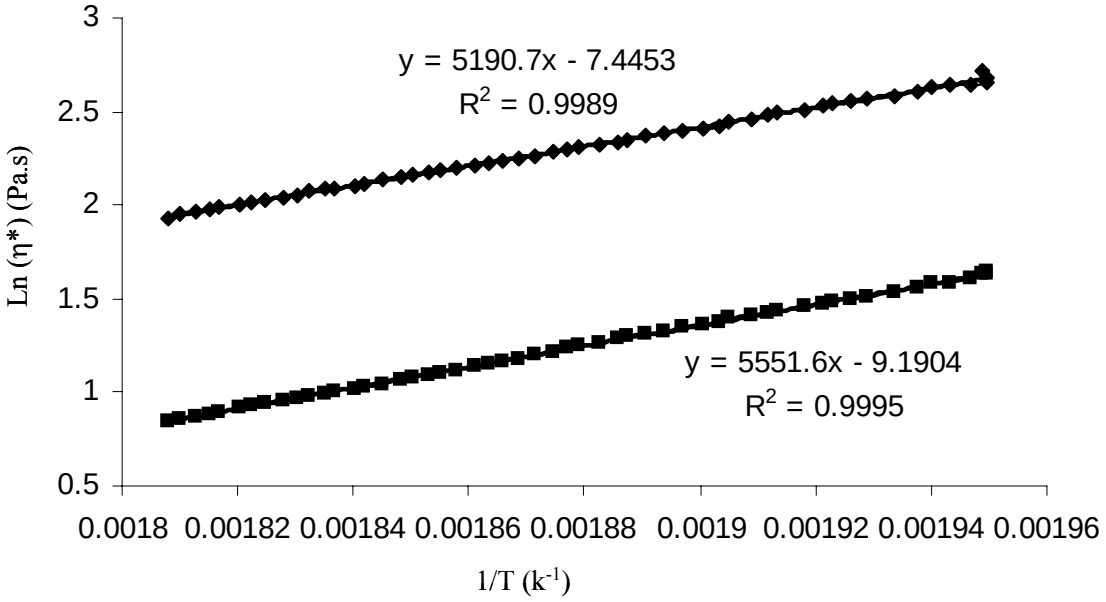

Figure 7.9 Calculation of flow activation energy of macroligand and complex: (top): complex, PET-3-5; (bottom): macroligand, PET-2-5.

7.4.2 Thermal transition and rheological analysis

Thermogravimetric analysis (TGA) demonstrated that complexes of polyester macroligands and cobalt(II) chloride exhibited not only greater thermal stability, but also a similar loss profile vs. temperature as the homo-PET. Under a nitrogen atmosphere, the onset of degradation was around 360 ºC.

DSC was used to investigate the thermal transitions of macroligands and complexes (Figure 7.7). DSC analysis was performed as follows: samples were heated to 290 ºC, and held at this temperature to eliminate the thermal history for 10 minutes. The samples were quenched to room temperature using nitrogen gas to achieve an identical thermal history, and heated to 290 ºC again at a speed of 10 ºC/min. For moderate molecular weight macroligand, PET-2-5 ($\eta_{inherent}$ = 0.25 dL/g), only a melt transition of PET was observed at around 240 ºC in the second cycle because the crystallization completed during the quenching. However, the complex (PET-3-5) with an equivalent inherent viscosity as the PET-2-5 performed similar to a high molecular weight PET. Specifically, an obvious glass transition (72 ^{o}C), crystallization transition (149 ^{o}C, ΔH = 35.0 J/g), and melt transition (240 ^{o}C, ΔH = 42.7 ^{o}C) were all observed in the DSC trace (Figure 7.7). These results indicate that cobalt(II) ions coordinated with the functional groups to improve molecular weight. However, the complex PET-3-5 exhibited a similar glass transition temperature as the homo-PET, suggesting that the salt coordinated with the phosphine oxide endgroups to form linear polymers. If metal salts are coordinated with carbonyl groups to result in crosslinking, an improvement in glass transition temperature will be observed.[5b] Moreover, the crystallization transition, melt transition and degree of crystallinity of the PET-3-5 were all similar to those of the high molecular

weight PET. This is also indicative of the formation of high molecular weight linear polymers via coordination of end groups with cobalt(II) ion.

The temperature ramp curves of macroligand (PET-2-5, $\eta_{inherent}$ = 0.25 dL/g) and complex (PET-3-5, $\eta_{inherent}$ = 0.25 dL/g) are depicted in Figure 7.8, which shows that the complex exhibits higher viscosity due to the formation of a higher molecular weight product via coordination. Moreover, one should note that the presence of a large amount of cobalt(II) ions did not result in a degradation of the polymer backbone (~ 0.5 h, > 240 ^{o}C) since they coordinated with the phosphine oxide groups. The flow activation energies of complex and macroligand were estimated using the following equation (Figure 7.9):

$$Ln(\eta^*) = A + (E_a/R)^* (1/T) \qquad \text{(Equation 2)}$$

The results of the temperature ramp corresponds to this equation quite well ($R^2 > 0.998$), and the flow activation energy (complex: 43.1 KJ/mol; macroligand: 46.1 KJ/mol) of the two samples were similar, indicating that no strong intermolecular interaction is present in this complex. This result also suggests that the one cobalt(II) ion coordinated with the two phosphine oxide end groups to form linear coordinated polymers. Moreover, no coordination with the carbonyl or with more than two phosphine oxide ligands occurred, resulting in physical crosslinks. Had that occurred, the complex would have exhibited extremely high melt viscosity (the crosslinking did not dissociate at high temperature) and/or higher flow activation energy (the crosslinking dissociated at high temperature).[18] Moreover, the coordination of one cobalt(II) ion with the two phosphine oxide ligands is consistent with previous reports.[8]

7.4.3 Morphology

When a high level of cobalt(II) chloride (2.5 mol%, 1.6 wt%) was directly blended with PET, the cobalt salt tended to aggregate to form visible particles in the organic matrix, whose sizes (~0.1 mm) were measured using optical microscopy (Figure 7.10 and Figure 7.11). The presence of the phosphine oxide endgroups helped to evenly disperse the metal salt into the PET matrixes, and no visible aggregates were observed in the complex, PET-3-5. TEM revealed that in PET-3-5 matrix, the coordinated metal salts formed approximately 100 nm size aggregates (Figure 7.12), and this is consistent with McGrath and Wang.[8]

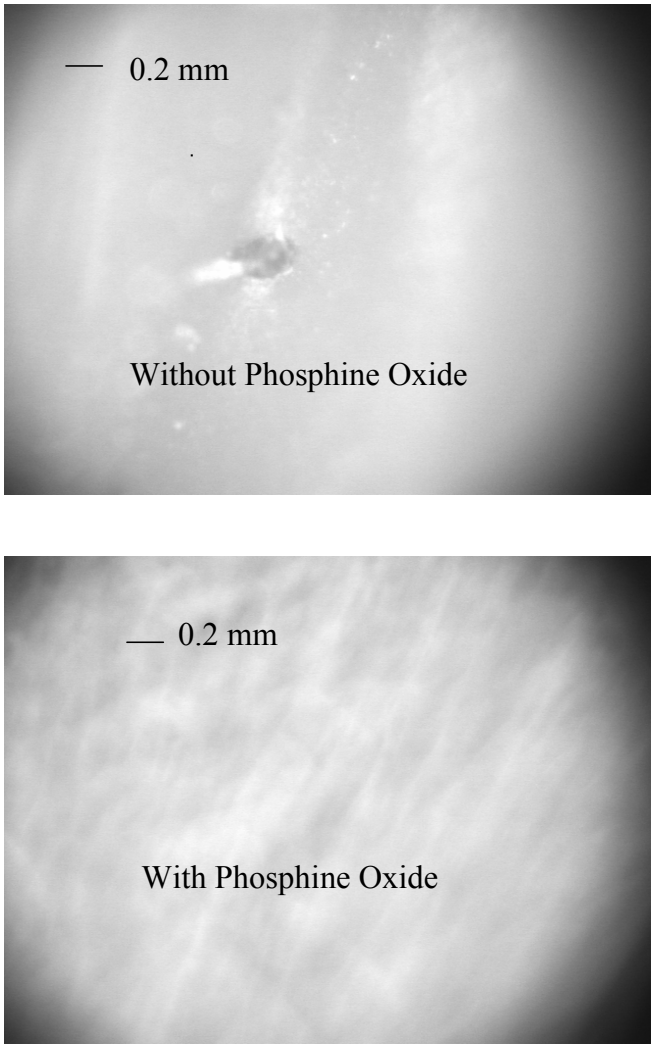

Figure 7.10 Optical micrographs of blends of PET and cobalt chloride (2.5 mol%, 1.6 wt%).

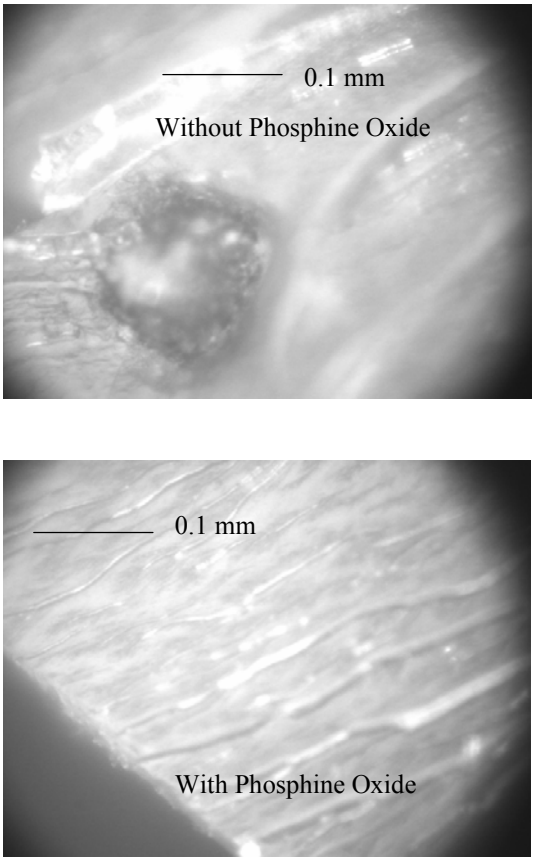

Figure 7.11 Optical micrographs of blends of PET and cobalt chloride (2.5 mol%, 1.6 wt%).

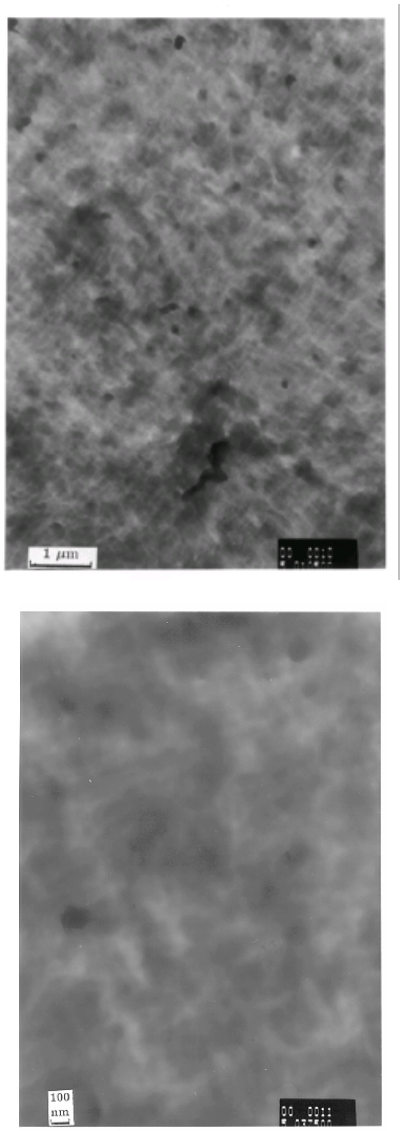

Figure 7.12 TEM analysis of complex of phosphine oxide endcapped PET and chloride, PET-3-5.

7.5 Conclusions

A phosphine oxide containing endcapper, 4-carboxyphenyl biphenyl phosphine oxide, was synthesized to prepare polyester macroligands. The purity of the endcapper was verified using NMR spectroscopy, mass spectroscopy and elemental analysis. Fully endcapped macroligands were prepared via the copolymerization of moderate molecular weight PET oligomers and endcappers. The quantitative incorporation of phosphine oxide functionality was confirmed using ^{1}H NMR spectroscopy and elemental analysis. Complexes of macroligands and cobalt(II) salt were also prepared via charging the cobalt(II) chloride at the beginning of the reaction. The results of NMR spectroscopy, FT-IR and UV-Vis all indicate that the cobalt(II) ion preferentially coordinated with the phosphine oxide end groups. The complexes exhibited higher melt viscosity than the analogues without cobalt salts. The presence of phosphine oxide end groups help to disperse the cobalt chlorine evenly into the PET matrix.

CHAPTER 8

Synthesis and Characterization of Sulfonated Liquid Crystalline Polyesters

(Published as: Lin, Q.; Pasta, J.; Wang, J.; Varun, R.; Wilkes, G. L.; Long, T. E. *Polymer International* **2002**, 51, 540.)

8.1 Abstract

Liquid crystalline (LC) polyesters based on 1,6-hexanediol, dimethyl 4,4'-biphenyldicarboxylate, and various levels of dimethyl 5-sodiosulfoisophthalate (0-20 mol %) were prepared using a conventional melt polymerization process. The presence and quantification of the ionic functionality was performed using ^{1}H NMR spectroscopy. Solution viscosities and corresponding molecular weights decreased as the ionic monomer concentration exceeded a critical value (higher than 3 mol %). Differential scanning calorimeter (DSC) indicated a maximum in the isotropic transition temperature versus mole percent ionic modification at approximately 10 mol percent. Dynamic mechanical analysis (DMTA) indicated that the glass transition temperature was suppressed due to ionic association at high concentrations (greater than 3 mol %) of ionic functionality. Polarized light microscopy (PLM) and wide angle X-ray diffraction (WAXD) was used to identify the smectic liquid crystalline and crystalline phases.

Key Words: liquid crystalline polyester, ionomer, dimethyl 5-sodiosulfoisophthalate

8.2 Introduction

Ionomers are conventionally defined as ion-containing polymers with a maximum ionic group content of approximately 15 mole %.[1-3] Due to electrostatic interactions and the thermodynamic immiscibility between ionic groups and the polymer matrix (typically nonpolar hydrocarbons), ionic groups tend to aggregate.[4] The presence of ionic groups also improves compatibility in polymer blends, and ionic aggregation also dramatically influences the mechanical properties of polymeric materials.[4-6] Although it was suggested that ionic aggregates should dissociate at sufficiently high temperatures, such complete dissociation has never been observed below 300 °C.[6] In addition, Wilkes has shown that ionic aggregation is potentially altered upon deformation. Significant research has focused on the rheological performance and ionic aggregation at melt temperatures.[7]

---

[1]Eisenberg, A., King, M. *Ion-containing Polymers,* Academic Press, **1997**.
[2]MacKnight, W. J., Earnest, T. R. *J. Macromol. Rev.* 1981, 16, 41.
[3]Eisenberg, A.; Matsura, H.; Yokoyama, T. *J. Polym. Sci. Part A* **1971**, 29, 2123.
[4]Eisenberg, A.; Hird, B.; Moore, R. B. *Macromolecules* 1990, 23, 4098.
[5]Fenton, D. E.; Parker, J. M.; Wright, P. V. *Polymer* 1973, 14, 589.
[6]Tant, M. R.; Wilkes, G. L. *J. M . S. Rev. Macromol. Chem. Phys.* **1998**, C28, 11.
[7](a)Eisenberg, A.; Matsawa, T. J. *Polym. Sci. Polym. Phys. Ed.* **1980**, 18, 479. (b) Yoshikawa, K.; Desjardins, A.; Dealy, J. M.; Eisenberg, A. *Macromolecules* **1996**, 29, 1235.
[8]Colling, P. J.; Hird, M. *Introduction to Liquid Crystals*, Taylor & Franics Inc,**1997**.
[9]Alender, C.; Jariwala, C. P.; Lee, C. M.; Griffin, A. C. *Polym. Prepr.* **1998**, 34(1),168.
[10]Blumstein, A.; Cheng, P.; Subramanyam, S.; Clough, S. B. *Macrolm. Chem., Rapid. Commun.* **1992**, 13, 67.
[11]Brandys, F. A.; Bazuin, C. G. *Polym. Prepr.* **1993**, 34(1),186.
[12]Lin, C.; Cheng, P.; Blumstein, A. *Mol Cryst Liq Cryst* **1995**,173.
[13]Roche, P.; Zhao, Y. *Macromolecules* **1995**, 28, 2819.
[14]Wieseman, A.; Zentel, R.; Pakala, T. *Polymer* **1992**, 33, 5315.
[15]Wiesemann, A.; Zentel, R.; Lieser, G. *Acta Polym* **1995,** 46, 25.

Liquid crystalline (LC) materials form a unique melt phase which has more order than an isotropic liquid, but less order than a typical crystal, and share some properties normally associated with both isotropic liquids and crystals.[8] If a small amount of ionic groups are incorporated into the liquid crystalline polymer, a novel family of materials, termed liquid crystalline ionomers, will be obtained. The synergistic interaction between ionic aggregation and liquid crystalline phases in side chain liquid crystalline polymers has received significant attention.[9-17]

Initial investigations of main chain liquid crystalline ionomers occurred in the mid-1980's and focused on organic photo-electric materials, viologen, and ionenes, which contained 1,1'-dialkyl-4, 4'-bipyridinium salts.[18] Recently, research on main chain liquid crystalline ionomers has focused on structural applications and adhesives in order to improve the intermolecular forces between the mesogen containing chains.[19] Liquid crystalline polymers typically exhibit poor transverse mechanical properties and compressive properties, in sharp contrast to very high axial properties. A second shortcoming of liquid crystalline polymers is poor polymer miscibility and adhesion to other polymeric substrates. Ionic association offers a potential solution to both poor transverse mechanical properties and adhesive performance of highly oriented polymeric materials. In fact, semicrystalline polyester ionomers, such as sulfonated PET, were extensively investigated in order to address these problems in oriented polyesters fibers.[20-22] However, liquid crystalline ionomers have received significantly less attention. Weiss and Zhang utilized interfacial polymerization methods for the preparation of liquid crystalline polyester ionomers with flexible spacers. Although the interaction between the ionic aggregation and the formation of a liquid crystalline phase

was not addressed, the data indicated a maximum isotropic temperature with increased ionic content.[23, 24] Hara and coworkers recently incorporated an ionic monomer, sodium 5-sodiosulfoisophthalic acid, into an all-aromatic liquid crystalline polyester (Vectra™) and the isotropic temperature decreased due to the domination of the *meta* linkage in the liquid crystalline phase. Moreover, the effect of counterion on the physical properties was also addressed, and the calcium salt significantly improved the tensile properties compared to both the sodium salt and non-ionomeric analogs.[25] Zentel and coworkers have also recently studied several families of main chain liquid crystalline ionomers, and it was concluded that ionic association stabilized the liquid crystalline phase.[26, 27] In addition, the interplay between ionic association and liquid crystalline phase formation has resulted in identification of novel liquid crystalline textures or supramolecular assemblies.[28]

---

[16]Yuan, G. *Polymer* **1995,** 36, 2725.
[17]Zhao, Y., Lei, Y. *Macromolecules* **1994,** 27, 4525.
[18]Han, H. S.; Bhowmik, P. K. *Trends in Polymer Science* **1995**, 3, 199.
[19]Hara, M.; Xue, Y. *Macromolecules* **1997**, 30, 3803.
[20]Hsieh, Y. L.; Hu, X. P. *Polymer* **1997**, 38, 5079.
[21]Timm, D. A.; Hsieh, Y. L. *J. Appl. Polym. Sci.* **1994**, 34, 1291.
[22]Greener, J.; Gillmore, J. R.; Daly, R. C. *Macromolecules* **1993,** 26, 6417.
[23]Zhang, B.; Weiss, R. A. *J. Polym. Sci. Polym. Chem.* **1992,** 30, 91.
[24]Zhang, B.; Weiss, R. A. *J. Polym. Sci. Polym. Chem.* **1992,** 30, 989.
[25]Xue, Y.; Hara, M.; Yoon, H. N. *Macromolecules* **1998**, 31, 1808.
[26]Wilber, G.; Cochin, D.; Zentel, R. *Macrol. Chem. Phys.* **1996**, 197, 3259.
[27]Wibert, G.; Zentel, R. *Macrol. Symp.* **1997,** 117, 239.
[28]Pabmann, M.; Wilber, G., Cochin, D.; Zentel, R. *Macromol. Chem. Phys.***1998**, 179.
[29]Watanabe, J.; Hayashi, M.; Nakata, Y.; Niori, T.; Tokita, M. *Prog Polym Sci* **1997**, 22, 1053.
[30]Takahashi, T.; Nagata, F. J. *Macromol Sci-Phys* **1991**, B30 (1&2), 25.
[31]Kroenke, W. J. *J. Appl. Polym. Sci.* **1981**, 26,1167.
[32]Tseng, H.; Hsiue, L.; Ma, C. M. *Macromol. Chem. Phys.* **1996,** 197, 2158.

Our recent efforts have focused on ionic modification of traditional smectic A (S_A) liquid crystalline polyesters using traditional melt phase polymerization methodologies. A liquid crystalline polyester based on hexanediol, and dimethyl 4,4'-biphenyl-dicarboxylate (termed as BB-6), which Watanabe and coworkers have shown to exhibit a typical smectic A structure, was chosen as the base composition.[29, 30] Dimethyl-5-sodiosulfoisophthalate (SDMI) was used as an ionic comonomer in order to obtain a novel family of semi-flexible liquid crystalline polyester ionomers.

8.3 Experimental

8.3.1 Synthesis

Liquid crystalline polyesters were prepared *via* the melt condensation of dimethyl 4,4'-biphenyldicarboxylate (Eastman Chemical Co., used as received), hexanediol (99%, Aldrich, used as received) and various levels of dimethyl-5-sodiosulfoisophthalate (SDMI, Eastman Chemical Co., used as received, 0-20 mole %). Both titanium tetraisopropoxide (20 ppm) and antimony oxide (200 ppm) were added to facilitate ester exchange and subsequent polycondensation. The reactor consisted of a 500 mL round-bottomed flask equipped with an overhead mechanical stirrer, nitrogen inlet, and condenser. The reactor containing the monomers and catalysts was degassed using vacuum and nitrogen three times, and subsequently heated to 180 °C. The reactor was maintained at 180 °C for one hour, and the temperature was increased to 270 °C over 2 h. The reaction was allowed to proceed for 30 min at 270 °C. Reduced pressure was gradually applied to 0.5 mmHg and polycondensation was allowed to continue for 2 h at

270 °C. The resulting liquid crystalline polymers were termed BB-6-x (Scheme 8.1), where x denotes the mol percent of ionic modification of the total dicarboxylate units.

8.3.2 Characterization

The inherent viscosities of the samples were measured at 30 ^{o}C in a capillary viscometer using 0.5 g/dL solution in a 60/40 w/w mixture of phenol and tetrachloroethane. ^{1}H NMR spectra were recorded on a JOEL-500 MHz spectrometer using trifluoroactetic acid-d as a solvent and methanol as an internal standard. In order to fully dissolve the copolymers in trifluoroacetic acid-d, amorphous products were obtained using liquid nitrogen to rapidly quench the copolymers from 250 °C. Thermal transitions were determined on a Perkin-Elmer DSC Pyris 1 at a heating rate of 10 °C/min under a N_2 purge. The samples were held at 300 ^{o}C for 5 minutes, and all reported data were obtained on the second heating cycle. Thermogravimetric analysis (TGA) was performed on a Perkin-Elmer TGA 7 under a nitrogen atmosphere at the rate of 10 ^{o}C/min. Dynamic mechanical properties were determined using a Perkin-Elmer DMA 7e at 1 Hz using a heating rate of 2 ^{o}C/min. The polymer films for DMA testing were prepared as follows: polymer powder samples were sandwiched between two plates, high pressure was applied and the samples were maintained in the liquid crystalline state for 15 minutes. Finally, they were quenched using ice-water to freeze the liquid crystalline texture in the solid state. Polarized light microscopy samples consisted of thin sections of film that were pressed (280 ^{o}C) in the isotropic state and subsequently quenched with ice water. The film was placed between two glass slides, heated on the hot stage, and observed during both the heating and cooling cycles. The slides were also

sheared in order to induce various oriented optically anisotropic textures. WAXD data were obtained using a vacuum Warhus camera on a Philips tabletop X-ray generator (model PW17200) with Cu K_α radiation (λ = 0.1542 nm). The instrument was operated at 40 KV and 50 mA.

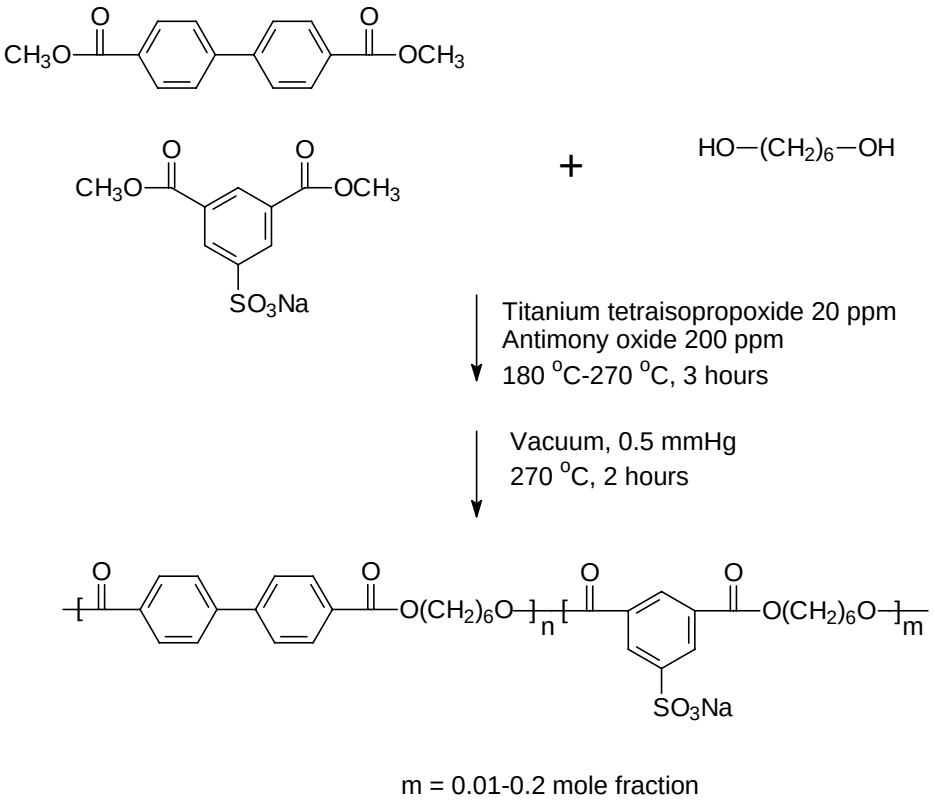

Scheme 8.1 Synthesis of sulfonated liquid crystalline polyesters, BB-6-x.

8.4 Results and discussion

8.4.1 Synthesis and characterization of copolymers

During the polymerization process for copolymers containing 0, 1 and 3 mol % of sulfonated comonomer, the melt phase was clear and homogeneous at temperatures ranging from 180 °C to 270 °C. Consequently, it was presumed that the ionic monomers were homogeneously dispersed in the melt state and were randomly incorporated into the copolymer. The similarities of their solution viscosities (Table 8.1) also indicated that small amounts (< 3 mol %) of sulfonated comonomer did not influence the capability to attain high molecular weight products. However, at higher sulfonated comonomer concentrations (>3 mol %), the melt phase was initially opaque and gradually cleared as the temperature was increased to the final polycondensation temperature 270 °C. The temperatures at which the polymer melt visually became a homogeneous liquid (T_h) are listed in Table 1. The 20 mol % ionic-modified copolymer did not become homogeneous until vacuum was applied at 270 °C. The effect of this heterogeneity during the initial stage of polymerization on the sequence distribution in the resulting copolymers is not well understood, but it is presumed that the copolymer is randomized during the latter stages of polycondensation. The optically clear melt phase during final polycondensation supports the hypothesis that the melt is homogeneous for all copolymer compositions that are listed in Table 8.1. The higher melt viscosity of copolymers containing greater than 3 mol % sulfonated monomer resulted in lower molecular weight final products for similar reaction times (120 min) and temperatures (270 °C) at reduced pressures (0.5 mm). Table 1 illustrates that the inherent viscosities of copolymer ionomers decreased as the concentration of ionic monomer exceeded 3 mol % modification. ^{1}H NMR was used to

determine the composition of the copolymers. The peak assignments are depicted in Figure 8.1 and the mole percent of ionic comonomer is listed in Table 8.1. Table 8.1 indicates that the level of ionic comonomer that was determined using ^{1}H NMR spectroscopy agreed well with the charged concentration at various levels (1, 5 and 20 mol %).

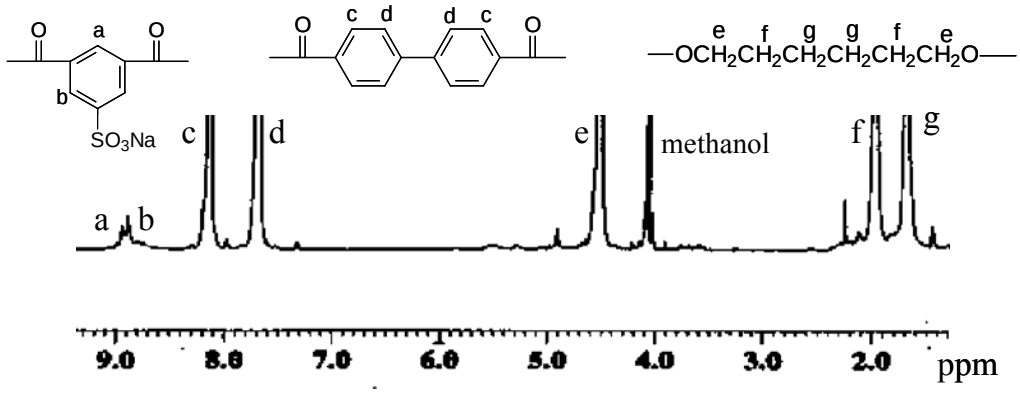

Figure 8.1 ^{1}H NMR spectrum of BB-6-1. (400 MHz, trifluoroacetic acid-d as a solvent and methanol as an internal standard)

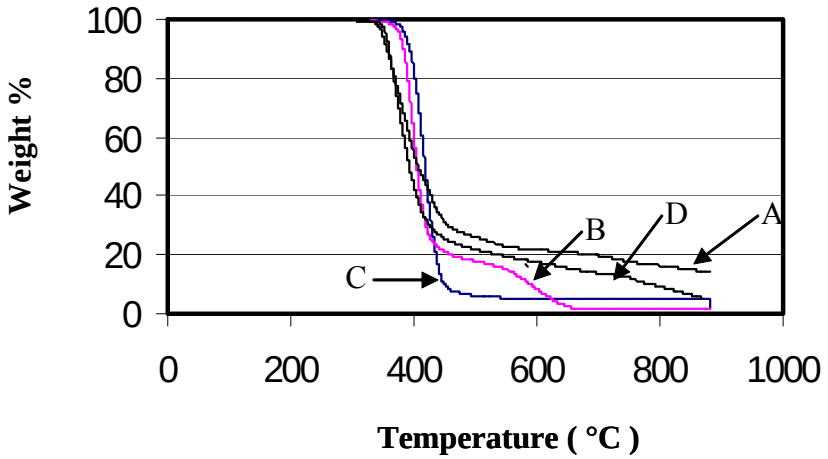

Figure 8.2 TGA of copolymers at a heating rate of 10 °C/min under a nitrogen atmosphere: (A) BB-6-20, (B) BB-6-3, (C) BB-6, and (D) BB-6-10

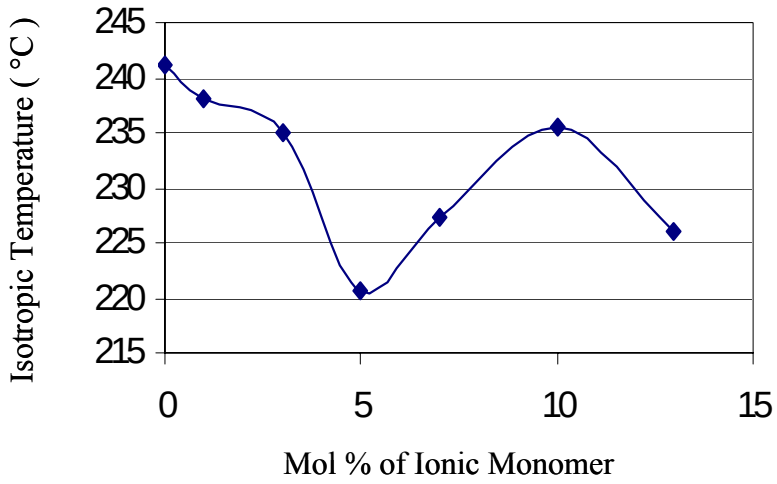

Figure 8.3 Copolymer isotropic temperature *vs* mol % ionic monomer. All data were collected using the DSC second heat at 10 °C/min.

Table 8.1 Copolymer composition, T_h^*, and copolymer solution viscosities

Sample	Mole % of Ionic Monomer at Charged[a]	Mole % of Ionic Monomer in Copolymer[b]	T_h (°C)	η (dL/g)[e]
BB-6	0	0	c	0.52
BB-6-1	1	1.1	c	0.49
BB-6-3	3	----------	c	0.54
BB-6-5	5	5.3	200	0.31
BB-6-8	8	----------	230	0.34
BB-6-10	10	----------	260	0.35
BB-6-13	13	----------	270	0.30
BB-6-20	20	20.2	270[d]	0.21

*: The temperature of the polymer melt at which a homogenous phase is observed; *a*: The mole fraction of ionic comonomer in total dicarboxylate monomer; *b*: Calculated from ^{1}H NMR spectra using trifluoroacetic acid-d as a solvent, and methanol as an internal standard; *c*: Always homogeneous; *d*: After vacuum was applied; *e*: at 30 ^{o}C in a capillary viscometry using 0.5 g/dL solution in a 60/40 w/w mixture of phenol and tetrachloroethane.

Table 8.2 Copolymer thermal transitions[a] and 5% weight loss [b]

Sample	$T_{5\%}$ (°C)	T_m (°C)	ΔH (J/g)	T_i (°C)	ΔH (J/g)
BB-6	385	210	17.7	241	36.0
BB-6-1`	379	203	15.6	238	26.1
BB-6-3	377	203	10.1	235	24.0
BB-6-5	367	202	13.8	221	24.1
BB-6-8	364	200	14.2	228	25.0
BB-6-10	378	212	17.6	235	25.4
BB-6-13	353	203	15.2	227	24.0
BB-6-20	348	206	28.8		

a: DSC data determined from the second heat at 10 °C / min; *b*: TGA data at a heating rate of 10 °C / min under a nitrogen atmosphere.

Table 8.3 d-Spacings (nm) in wide angle X-ray diffraction

BB-6	BB-6-5	BB-6-10	BB-6-20
18.9	19.1	19.1	19.0
4.41	4.43	4.22	6.69
	9.55		6.10
	6.63		5.31
	5.27		4.51
	3.04		3.78
			3.34

8.4.2 Thermal and mechanical properties

Figure 8.2 depicts the thermogravimetric analysis (TGA) of a BB-6 homopolymer and copolymers containing various levels of ionic monomer, and the temperatures for 5 % weight loss are listed in Table 2. All copolymers had high thermal stability and char yields increased with ionic monomer content. Enhanced char yield has been demonstrated earlier to be a good indication of potential flame resistance in structural applications.[31]

The isotropic and melting transition temperatures are also listed in Table 8.2. Interestingly, a maximum isotropic temperature at approximately 10 mol % ionic content was observed. The isotropic temperature versus mole percent ionic monomer (0 to 13%) is depicted in Figure 8.3 and clearly shows a reproducible maximum. Weiss' previous data depicted a similar maximum isotropic temperature with an ionic content increase for similar molecular weight samples.[23, 24] It is proposed that the ionic monomer exhibits two opposing influences on the stability of the liquid crystalline phase. The *meta* linkage is known to disrupt the symmetry of the mesogenic sequence which decreases the

isotropic transition temperature. Thus, if the ionic interaction was removed, the isotropic transition temperature would continue to decrease with an increase in the concentration of the kinked linkage. The isotropic transition temperatures for copolymers containing low concentrations of the sodiosulfonate moieties decreased presumably due to the *meta*-linkage in the isophthalate based monomer. However, the liquid crystalline phase exhibited enhanced thermal stability at higher ion concentrations (approx. 10 mol %) as indicated by an increase in the isotropic transition temperature. Since the copolymers containing 5-12 mol % ionic modification have similar solution viscosities, it was proposed that increased stability of the liquid crystalline phase was attributed to the presence of ionic aggregation in the melt phase. The isotropic temperature maximum for BB-6 sulfonated ionomers suggested that ionic aggregation stabilized the mesophase at approximately 10 mol % ionic concentration.

Zentel and coworkers compared ionomers and non-ionomers with similar chemical structures to study the effect of ionic clustering on the stability of the liquid crystalline phase.[26-28] In a similar fashion, a direct comparison was performed using a nonionic comonomer analog, dimethyl isophthalate, versus ionic comonomer modification at equivalent molar concentrations (Figure 8.4). The ionic comonomer has a larger molecular size, and is presumed to be more disruptive than the nonionic isophthalate units. If ionic association did not exist, then the copolymer liquid crystalline phase containing equivalent mole percent nonionic units was expected to be more stable. However, DSC analysis of copolymers containing 10 mol % isophthalate units indicated that only a monotropic liquid crystalline phase was present upon cooling.[32] In contrast, copolymers containing 10 mol % ionic units formed a liquid crystalline phase upon both

cooling and heating and had similar isotropic clearing temperatures as the homopolymers. This suggested that the liquid crystalline phase was more stable due to the presence of ionic aggregation. Higher levels of ionic modification (approximately 20 mol %) lead to the complete loss of liquid crystallinity due to the incorporation of a critical concentration of *meta*-linkages that completely disrupted the symmetry of the mesogenic sequence.

---

[33]Watanabe, J.; Hayashi, M. *Macromolecules 1998,* 22, 4083.
[34]Li, X.; Brisse, F. *Macromolecules* **1994**, 27, 7725.
[35]Huang, H. W.; Horie, K.; Tokita, J.; Watanabe, J. *Macromol. Chem. Phys.* **1998**, 199, 1851.
[36]Li, X.; Brisse, F. *Macromolecules* **1994**, 27, 7725.

The introduction of ionic groups into liquid crystalline polyesters and their effect on the glass transition temperature was also studied earlier.[18-21] Glass transition temperatures (using DSC) were not detected in quenched films of crystalline or liquid crystalline copolymers. Dynamic mechanical analysis (DMA) was used to study the effect of ion incorporation on the glass transition temperature. DMA exhibited a thermal transition in close proximity to typical glass transition temperatures for non-ionic semicrystalline polyesters, however, the modulus of the ionic copolymers only decreased from 10^9 to 10^8 Pa. This slight modulus decrease is typical for many semicrystalline polymers, and was also observed for non-ionic BB-6. Figure 8.5 shows the tan δ vs. temperature for various copolymers. Relative to the homopolymer, the transition temperature for BB-6-1 decreased and the magnitude of tan δ increased due to the domination of the kinked comonomer. At higher concentrations (greater than 3 mol %) of ionic functionality, the transition shifted to higher temperatures and the peak broadened, which is consistent with ionic aggregation.[19, 25] The DMA study indicated that the introduction of ionic-crosslinks into BB-6 liquid crystalline polyesters was achieved with only a small amount of ionic comonomer (3 mol %). Lower concentrations may facilitate future applications of liquid crystalline ionomers since higher ionic comonomer contents limited attainable molecular weights due to high melt viscosities.

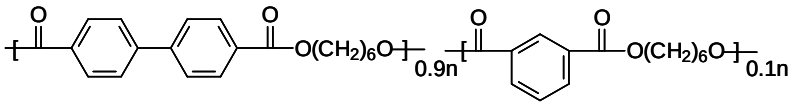

First Cooling		Second Heating	
T_i (^oC)	T_m (^oC)	T_m (^oC)	T_i (^oC)
198	167	213	Not Liquid Crystal

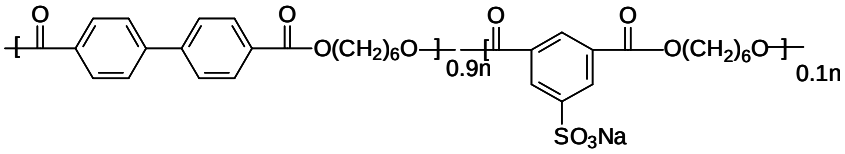

First Cooling		Second Heating	
T_i (^oC)	T_m (^oC)	T_m (^oC)	T_i (^oC)
211	169	209	239

Figure 8.4 Thermal properties of ionomer *vs* nonionomer. All data were collected using DSC at a heating or cooling rate of 10 °C/min.

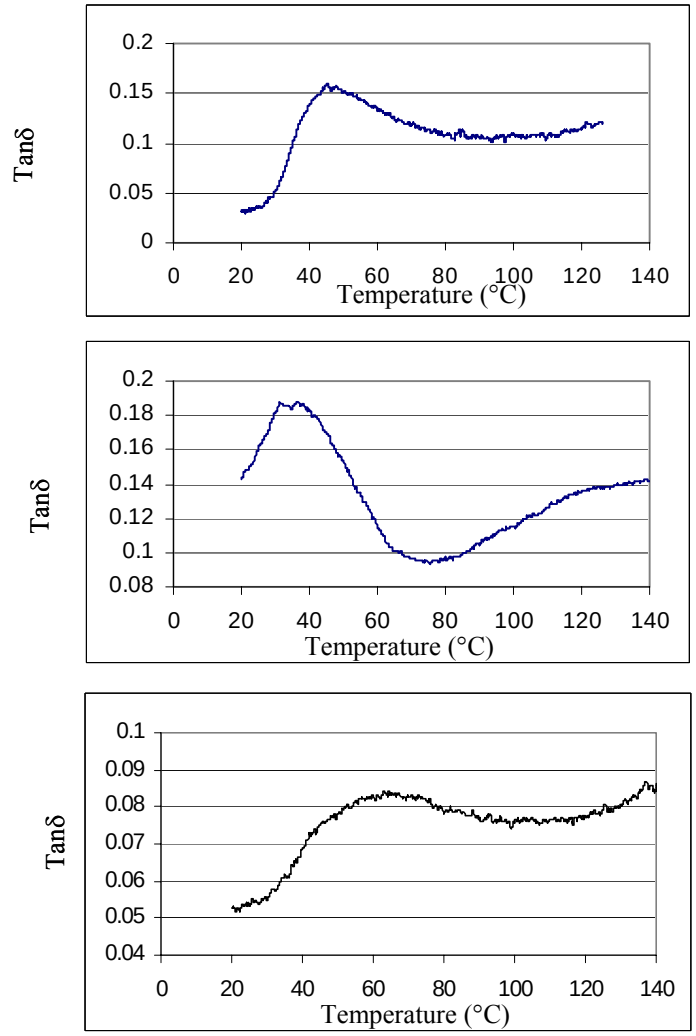

Figure 8.5 DMA of copolymers at a heating rate of 2 °C/min and 1 Hz: (from top to bottom): BB-6, BB-6-1, and BB-6-3.

8.4.3 Liquid crystalline phase structure

Previous efforts have demonstrated that BB-6 polyesters form a typical smectic A liquid crystalline phase, and some copolymers also form smectic structures.[29, 30] Typical smectic textures were not observed using polarized light microscopy due to inadequate flow of the liquid crystalline BB-6 ionomers. Thus, WAXD was used to study the solid state structure. The diffraction patterns of BB-6 and BB-6-10 partially oriented quenched films (Figure 8.6) were similar to typical smectic A textures of BB-6 fibers that were reported earlier.[32-36] There was a sharp inner reflection on the meridian and a outer broad reflection on the equator. The inner reflection was due to the layered smectic structure and the broad outer reflections were attributed to the average distance between the neighboring molecules or the neighboring mesogens within a layer. The calculated d spacings are listed in Table 3 and are similar to the theoretical values for the smectic A texture of BB-6.[32-36] These results indicated that the smectic A liquid crystalline phase was maintained in the BB-6 and BB-6-10 films. DSC analysis indicated that BB-6-20 did not form a liquid crystalline phase, and quenched films from the isotropic state were not completely amorphous presumably due to the thermal lag resulting in a low level of crystallinity. The diffraction pattern of BB-6-20 (Figure 8.6) consisted of one weak and several more intense azimuthally independent rings, typical of most unoriented semicrystalline polymers. The azimuthally independent diffraction rings indicated the crystals were unoriented in the film and the calculated d-spacings were similar to the γ type crystal.[34-36] BB-6-5 exhibited both a sharp azimuthally dependent inner ring and as well as some azimuthally independent sharp outer diffraction rings. This pattern suggests that an oriented liquid crystalline texture and an unoriented crystalline phase coexisted in

the quenched film. In a previous report, quenched films of BB-6 copolymers containing terephthalate units resulted in a similar diffraction pattern change, i.e. the intensity of the inner ring weakened and the number of outer rings increased with a decrease of liquid crystalline phase stability.[32] The diffraction of BB-6-10 was similar to the BB-6 homopolymer and indicated that the liquid crystalline phase was more stable than BB-6-5. This is attributed to ionic interactions and is consistent with the observed increase in the isotropic transition temperature.

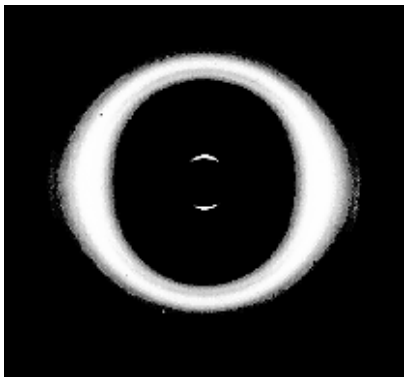

A: Smectic A BB-6

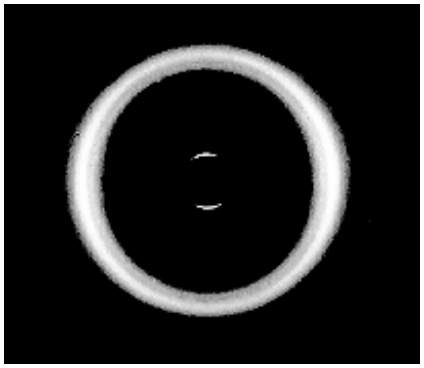

B: Smectic A BB-6-10

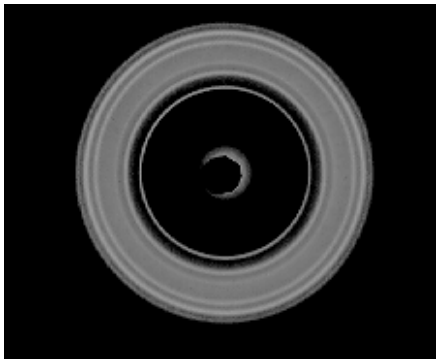

C: Semicrystal BB-6-20

Figure 8.6 WAXD patterns of quenched polymer films: (A) partially oriented smectic A liquid crystalline BB-6, (B) partially oriented smectic A liquid crystalline BB-6-10, and (C) unoriented semicrystalline BB-6-20

8.5 Conclusions

Novel liquid crystalline polyesters based on hexanediol, dimethyl 4,4'-biphenyldicarboxylate, and various levels of dimethyl 5-sodiosulfoisophthalate (0-20 mol %) were successfully prepared using conventional melt polymerization processes. Moreover, smectic liquid crystalline polymers were obtained over a broad range of ionic concentration (2-15 mol %). Although high concentrations of sulfonate groups were successfully introduced into the polyester copolymers, molecular weight was limited at ionic concentrations exceeding 3 mol %. Differential scanning calorimetry (DSC) indicated a maximum in the isotropic transition temperature (smectic LC phase to isotropic phase) versus mole percent ionic modification at approximately 10 mol percent. This maximum was attributed to the presence of ionic aggregation in the melt state. Dynamic mechanical analysis (DMA) indicated that 1.0 mol % ionic modification decreased the glass transition temperature. At higher concentrations (greater than 3 mol %) of ionic functionality, the transition temperature increased and the magnitude was decreased presumably due to ionic association. Polarized light microscopy and WAXD indicated that the BB-6 homopolymer and ionomers formed smectic A liquid crystalline phases.

CHAPTER 9

Synthesis and Characterization of Chiral Liquid Crystalline Polyesters Containing Sugar-based Diols via Melt Polymerization

(Published as: Lin, Q.; Pasta, J.; Long, T. E. *Journal of Polymer Science: Part A, Polymer Chemistry* **2003**, 41, 2512.)

9.1 Abstract

Liquid crystalline (LC) polyesters based on hexanediol or butanediol, dimethyl 4,4'-biphenyldicarboxylate, and a sugar-based diol, isosorbide or isomanide, were prepared using conventional melt polymerization. ^{1}H NMR spectroscopy confirmed that 50 mol% of the charged sugar diol was successfully incorporated into various copolyesters. Modest molecular weights were obtained, although they were typically lower than polyester analogs that did not contain sugar based diols. Thermogravimetric analysis (TGA) demonstrated that the incorporation of isosorbide or isomanide units did not decrease thermal stability in a nitrogen atmosphere. Melting points that ranged from 190 to 270 °C were achieved as a function of copolyester composition. The lined focal conic fan textures, which are a typical indication of a chiral smectic C (S_c*) LC phase, were observed upon shearing the LC melt under polarized light microscopy. Atomic force microscopy (AFM) revealed that the twisted of molecular orientation in the chiral LC phase induced periodically soft lamellar structures.

Key Words: BB-n liquid crystalline polyesters; chiral smectic C, sugar diol, isosorbide

9.2 Introduction

De Gennes initially proposed that semi-rigid main chain liquid crystalline (LC) polymers were attainable through the incorporation of both rigid and flexible segments, and main chain LC polyesters have subsequently received significant research attention. [1-3] In particular, a unique family of LC polyesters, termed BB-n polyesters, composed of both flexible methylene spacers and rigid 4,4'-biphenyldicarboxylate, has received significant attention.[2-9] The desirable performance of BB-n polyesters was attributed to an accessible smectic LC melt at relatively low temperatures, when the number of methylenes ranged between three and nine.[3] During the past two decades, Watanabe and coworkers have devoted significant attention to this family of LC polyesters.[3-9]

The incorporation of chiral units into a LC compound often induces a twisted chiral LC phase, which results in LC materials with unique mechanical, electrical and optical properties.[5, 8-15] For example, low molar mass chiral smectic C (S_c*) LC compounds and side chain S_c* LC polymers were extensively studied due to their potential application in color displays.[11] However, significantly less attention has been devoted to main chain S_c* LC polymers because optically pure comonomers are difficult to be obtained or relatively expensive. Recently, Watanabe and coworkers have investigated BB-n copolymers containing various chiral acyclic diols, such as (S)-2 methylbutylene diol, and disclosed many interesting properties associated with the S_c* LC phase, such as selective reflection of visible light and ferroelectric properties.[5-9] Thus, the identification of additional inexpensive chiral diols will likely result in significant research interest and commercial impact. Isosorbide and isomanide are inexpensive chiral sugar diols, and were successfully utilized as commoners in various polymerization processes.[12] For

example, polyesters based on isosorbide and aromatic dicarboxylic acids were synthesized via melt polymerization.[12-14] Recently, Kricheldorf and coworkers successfully utilized isosorbide to induce a cholesteric LC phase, and cholesteric nematic LC polycarbonates and polyesters were prepared in solution.[12, 15-17] Moreover, S_c* LC polymeric materials are also obtainable through doping of smectic LC polymers with low levels of isosorbide.[18] Our recent efforts have focused on the combination of smectic BB-n LC polyesters and sugar diols in order to obtain inexpensive main chain S_c* LC polymers. In this manuscript, the synthesis of LC polyesters based on hexanediol or butanediol, dimethyl-4,4'-biphenyldicarboxylate, and isosorbide or isomanide using conventional melt polymerization is reported. In addition, a preliminary analysis of the morphological structure of the LC phase is described.

---

[1](a) De Gennes, P. G.; *C R Acad Sci (Paris)* **1975,** B281, 101. (b) Goodman, I. *Encyclopedia of Polymer and Engineering;* John Wiley & Sons, **1988**; v12, p56.
[2]Krigbaum, W. R.; Asrar, J.; Ciferri, A.; Preston, J. *J. Polym. Sci.: Polym. Lett. Edi.* **1982**, 20, 109.
[3]Watanabe, J.; Hayashi, M.; Kinoshita, S.; Nakataj, Y.; Niori, T.; Tokita, M. *Prog. Polym. Sci.* **1997**, 22, 1053.
[4]Maeda, Y.; Osada, K.; Watanabe, J. *Macromolecules* **2000**, 33, 2456.
[5]Furukawa, T.; Uchinokura, O.; Takahashi, Y.; Tokita, M.; Osada, K.; Watanabe, J *Polym. J.* **2000**, 32, 122.
[6](a) Takahashi, T.; Nagata, F. *J. M. S.-Phys.* **1991**, B30 (1&2), 25. (b) Lin, Q.; Pasatta, J.; Wang, Z.; Ratta, V.; Wilkes, G. L.; Long, T. E. *Polym. Int.* **2002**, 51, 540.
[7]Tseng, H.; Hsiue, L.; Ma C. M. *Macromol. Chem. Phys.* **1996**, 197, 2158.
[8]Watanabe, J.; Hayashi, M.; Kinoshita, S.; Niori, T. *Polym. J.* **1992**, 24, 597.
[9]Krigbaum, W. R.; Watanabe, J. *Polymer* **1983**, 24, 1299.
[10]Watanabe, J.; Hayashi, M.; Atsushi, A.; Tokita, M. *Macromolecules* **1995**, 28, 8073.
[11]Collings, P. J.; Hird, M. *Introduction to Liquid Crystals, Chemistry and Physics*; Taylor & Francis Ltd, **1997**.
[12](a) Kricheldorf, H. R. *J. M. S.-Rev. Macromol. Chem. Phys.* **1997,** C37(4), 599. (b) Espinosa, M. A.; Cadiz, V.; Galia, M. J. Polym. Sci. Part A: Polym Chem 2001, 39, 2847.
[13]Luders; H.; Thiem, J. *Polym. Bull.* **1984**, 11, 365.
[14]Storbeck, R.; Rehahn, M.; Ballauff, M. *Makromol. Chem.* **1993**, 194, 53.

9.3 Experimental

9.3.1 Polymer Synthesis

LC polyesters were prepared via melt condensation of dimethyl 4,4'-biphenyldicarboxylate (Eastman, used as received) and 1,6-hexanediol or 1,4-butanediol (99%, Aldrich, used as received). Both titanium tetra(isopropoxide) (20 ppm) and antimony oxide (200 ppm) were added to facilitate ester exchange and subsequent polycondensation, respectively. The reactor consisted of a 500 mL round-bottomed flask equipped with an overhead mechanical stirrer, nitrogen inlet, and condenser. The reactor containing the diester (0.20 mol), diol (0.20 mol) and catalysts was degassed using alternate vacuum and nitrogen three times, and subsequently heated to 180 °C. The reactor was maintained at 180 °C for approximately 3 h, and subsequently increased to 220 °C and maintained for 2 h. Finally, the temperature was raised to 275 °C and maintained for 1 h. Vacuum was applied gradually up to 0.5 mm Hg, and polycondensation was allowed to proceed for 2 h at 275 °C. However, the final temperature for BB-4 copolymers was raised to 290 °C to maintain adequate stirring. The resulting LC polyesters are termed BB-6(4)-xS(M), where x denotes the mol% of residual sugar diol units in the final copolymer, S denotes isosorbide, M denotes isomanide, and (4) and (6) represent butanediol and hexanediol, respectively.

---

[15]Kricheldorf, H. R.; Schwarz, G. *J. Polym. Sci. Part A: Polym. Chem.* **1996**, 34, 603.
[16]Kricheldorf, H. R. *Polym. Prep.* **1999**, 40(2), 568.
[17]Sun, S.; Schwarz, G.; Kricheldorf, H. R, Chang, T. *J. Polym. Sci. Part A: Polym. Chem.* **1999**, 37, 1125.
[18]Vill, V.; Fisher, F.; Thiem, J. Z *Naturforsch* **1984**, 44a, 675.
[19]Sun, S.; Gerken, A.; Chang, T. *Macromolecules* **1996**, 29, 8077.
[20]Majdoub, M.; Loupy, A.; Fleche, G. *Eur. Polym. J.* **1994**, 12, 1431.

9.3.2 Polymer Characterization

Inherent viscosities were measured at 25 ^{o}C in a capillary viscometer using a 0.5 g/dL solution in a 50/50 w/w mixture of phenol and tetrachloroethane. ^{1}H NMR spectra were recorded on a Varian 400 MHz spectrometer using CF_3CO_2D as a solvent and $CHCl_3$ as an internal standard. Thermal transitions were determined on a Perkin-Elmer DSC Pyris 1 at a heating rate of 10 °C/min under a nitrogen atmosphere, and all reported transitions were obtained using the second heating cycle. Thermogravimetric analysis (TGA) was performed on a Perkin-Elmer TGA 7 under a nitrogen atmosphere at a heating rate of 10 ^{o}C/min. Optical micrographs were obtained on a Zeiss Axioplan polarizing optical microscope with a THMS 600 hot stage. Reflective UV-Vis spectra were obtained on a Perkin-Elmer-300 spectrometer. Samples for atomic force microscopy (AFM) were trimmed and ultramicrotomed with a Reichert-Jung Ultracut E equipped with a diamond knife. Tapping mode AFM was performed with a Digital Instruments Dimension 3000, using micro-fabricated cantilevers with force constants of approximately 40 N/m.

9. 4 Results and discussion

9.4.1 Composition and molecular weights

The synthetic process for semi-rigid polyesters via conventional melt polymerization consists of two steps, i.e. transesterification and subsequent polycondensation under reduced pressure. The transesterification time was increased to ensure that the less reactive secondary diol was efficiently incorporated into the copolyesters. However, ^{1}H NMR spectroscopy (Table 9.1) indicated that only 50 mol%

of the charged sugar diol was incorporated into the copolymers presumably due to the lower reactivity of the secondary alcohol in the sugar diols. Figure 9.1 depicts a typical ^{1}H NMR spectrum for a copolyester containing isosorbide, and resonances were assigned based on earlier literature.[19-21]

The presence of a less reactive secondary diol also had a significant effect on the attainable molecular weight. During melt polymerization, BB-6 copolymers exhibited much lower melt viscosities than the BB-6 homopolymer. Solution viscometry (Table 9.1) also confirmed that the obtained BB-6 copolymers had lower molecular weights than the BB-6 homopolymer that was prepared using an identical synthetic methodology. As expected, BB-4 copolymers exhibited higher melt viscosities than BB-6 analogs since butanediol was a shorter flexible spacer. However, solution viscosity measurements indicated that only low molecular weight BB-4 copolymers were obtained (Table 9.1).

9.4.2 Thermal Properties

The incorporation of sugar diols did not have a significantly detrimental effect on thermal stability under an inert atmosphere, which was consistent with the earlier literature.[17] The temperature for 5% weight loss under a nitrogen atmosphere ranged from 360 to 390 °C (Table 9.2) and exhibited a similar weight loss profile versus temperature to the corresponding homopolymer. The thermal transitions obtained using DSC are also summarized in Table 9.2. The nonsymmetrical sugar diols decreased the stability of the LC phase, and the isotropic temperature decreased with an increase in isosorbide content. Interestingly, the BB-6-5S exhibited two transitions above the melt transition temperature (Figure 9.2). This observation suggested that BB-6-5S exhibited different LC phases at different temperatures. In a similar fashion, BB-6 copolymers

containing (S)-2 methylbutylene diol, exhibited multiple LC phases;[3] however, only BB-6-5S exhibited this behavior for all BB-6 copolyesters that were investigated in this study.

Table 9.1 Characterization of isosorbide (S) and isomanide (M) containing LC polyesters

Sample*	Mol % of Charged Sugar Diol [a]	Mol % of Residual Sugar Diol[b]	$\eta_{inherent}$ (dL/g)[c]	Color[d] (nm)
BB-6	0	0	0.65	White
BB-6-5M	10.0	5.4	0.45	Red (750)
BB-6-5S	10.0	5.2	0.40	Blue (500)
BB-6-10S	20.0	10.2	0.37	Yellow (680)
BB-4-5S	10.0	5.1	0.28	Blue (500)
BB-4-10S	20.0	10.3	0.25	Yellow (660)

*: S denotes isosorbide and M denotes isomanide; *a*: Mol fraction of sugar diol in the total diol monomer; *b*: measured using ^{1}H NMR spectroscopy; *c*: Determined at 25 ^{o}C in a capillary viscometer (0.5 g/dL solution in a 50/50 w/w mixture of phenol and tetrachloroethane); *d*: Film was quenched from liquid crystalline state using ice-water, and the wavelength represents the onset of decreasing reflection in the reflection spectrum.

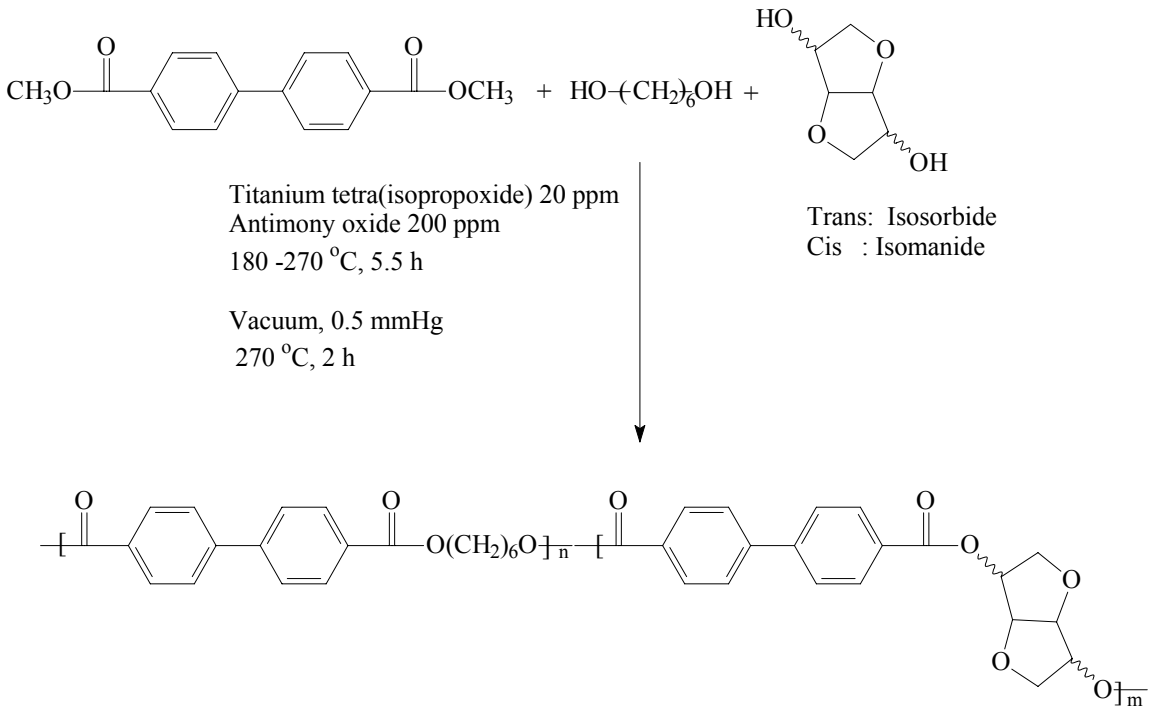

Scheme 9.1 Synthesis of BB-6 LC copolyesters containing isosorbide or isomanide units

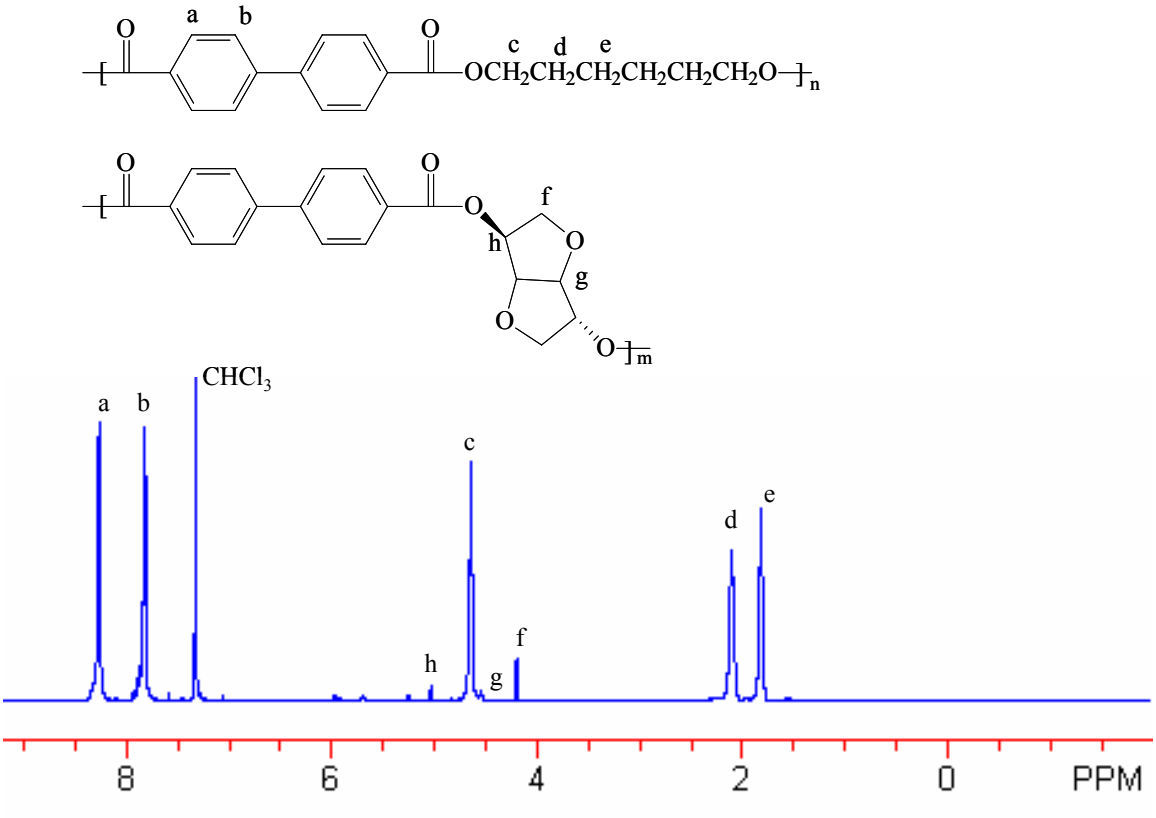

Figure 9.1 ^{1}H NMR spectrum of BB-6-5S

9.4.3 Liquid Crystalline Structure

Polarized light microscopy of BB-6 homopolymer revealed only batonnet textures due to the high melt viscosity and high molecular weight.[9] However, copolymers containing either sugar diol had suitable melt viscosities for the observation of smectic LC textures. Focal conic fan textures, a typical indication of S_c or S_a LC phase, were observed using polarized light microscopy for BB-6 copolymers above the melt transition temperature (220 $^{\circ}$C) (Figure 9.3).[9] Upon shearing the copolyester melt, the lined focal conic fan textures, which are unique for the S_c* LC phase, were observed.[62] BB-6-5S exhibited various textures that were related to different LC phase structures at different temperatures, and this observation was consistent with DSC results that indicated two LC transitions. Between the melt transition and first LC transition temperature, both lined focal conic fan-shaped textures and Schlieren textures, which are typical indications of S_c or nematic LC phase, were observed (Figure 9.4).[62] After the temperature was increased to the second liquid crystalline range (220°C), only batonnet textures were observed (Figure 9.4). This suggested that the second LC phase was a smectic LC phase.[9] Based on these results and previous reports dealing with BB-6 copolymers containing low levels of substituted chiral linear diols, the two phases were assigned to S_c^* and S_a.[8-62]

9.4.4 Optical Properties

Polymers with S_c* textures often exhibit unique optical properties.[3,8] During polymerization, a colored LC polymer melt was observed at various temperatures (Table 9.1). This colored LC melt phase was quenched using nitrogen gas or ice-water.

However, if the films were quenched from the non-colored isotropic state, they were white in color due to a low level of crystallinity. Figure 9.5 depicts the reflective UV-Vis spectra of various quenched films prepared. The BB-6 film and BB-6-5S that were quenched from the isotropic state had similar UV-Vis spectra. However, the BB-6-5S film quenched from the LC state exhibited a different spectrum, and the reflection initially decreased at approximately 500 nm. The color of the quenched LC film was associated with the onset of a reflection decrease in the reflective UV-Vis spectra (Figure 9.6). These observations suggested that different quenched Sc* textures led to different optical properties. It was presumed that the broad wavelength range of reflected light was due to the quenching process.

Table 9.2 Thermal performance of LC polyesters

Sample	$T_{5\%}$ (°C)[a]	T_m (°C)[b]	ΔH (J/g)	T_i (°C)	ΔH (J/g)
BB-6	385	206	17.7	240	36.0
BB-6-5S	383	201	16.5	225	27.8
BB-6-5M	379	200	14.4	228	24.4
BB-6-10S	364	194	14.9	218	23.6
BB-4-5S	363	268	21.7	291	35.1
BB-4-10S	371	239	23.6	270	33.2

a: Temperature at 5% weight loss using TGA at a heating rate of 10 °C/min in a nitrogen atmosphere; *b*: Obtained using DSC from the second heating cycle at a heating rate of 10 °C/min.

[21]*Aldrich Liberal of ^{1}H and ^{13}C FT-NMR* **1993**, 1, 406B.
[22]Hara, H.; Satoch, T.; Toya, T.; Iida, S.; Orii, S.; Watanabe, J. *Macromolecules* **1988**, 21, 14.
[23]Huang Y., Yang, Y. Q.; Petermann, J. Polymer 1998, 39, 5301.
[24]Haung Y.; Loos, J.; Yang, Y. Q.; Petermann, J. *J. Polym. Sci. Part B: Polm. Phy.* **1998**, 36, 439.
[25]Nishio, N.; Yammana, T.; Takahashi, J *J. Polym. Sci., Polym. Phy. Ed.* **1985**, 23, 1043.

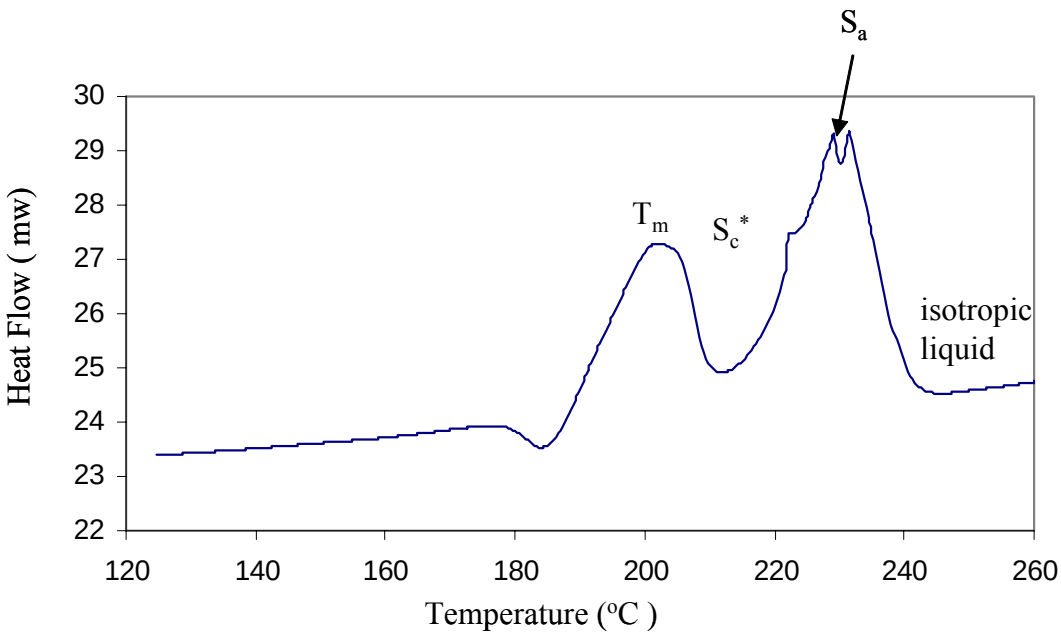

Figure 9.2 Typical DSC of BB-6-5S (determined on second heating at a heating rate of 10 °C/min)

A 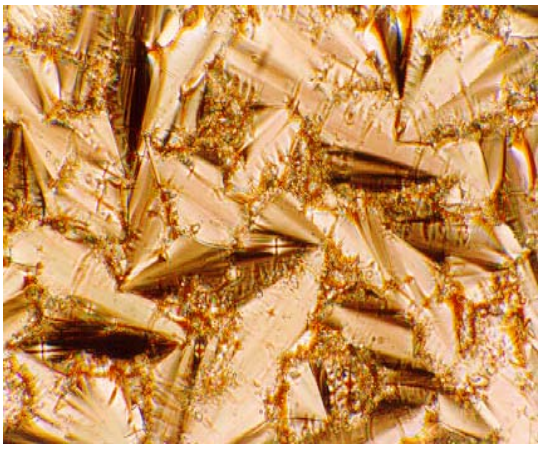

B 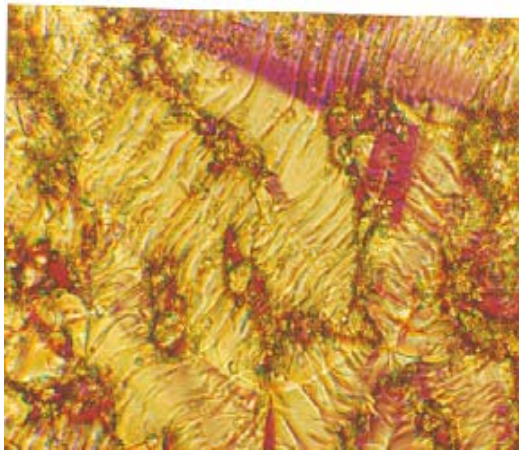

Figure 9.3 Photographs of focal conic fan texture (A: BB-6-5M, 212 °C) and lined focal conic fan texture (B: BB-6-5M, 212 °C) from polarized light microscopy

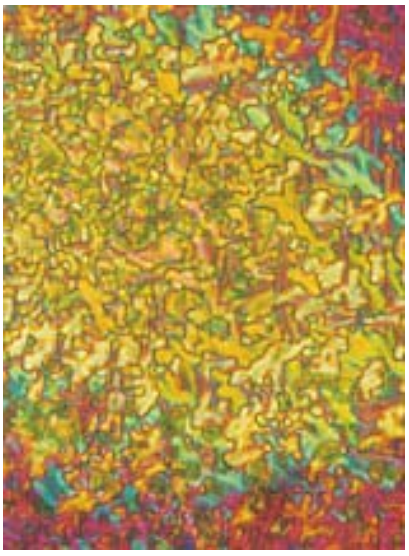

A

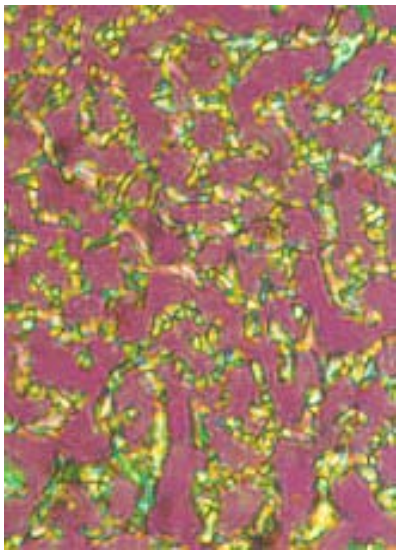

B

Figure 9.4 LC textures of BB-6-5S at different temperatures under polarized light microscopy: A: Schlieren texture at 212 °C; B: Batonnet texture at 220 °C.

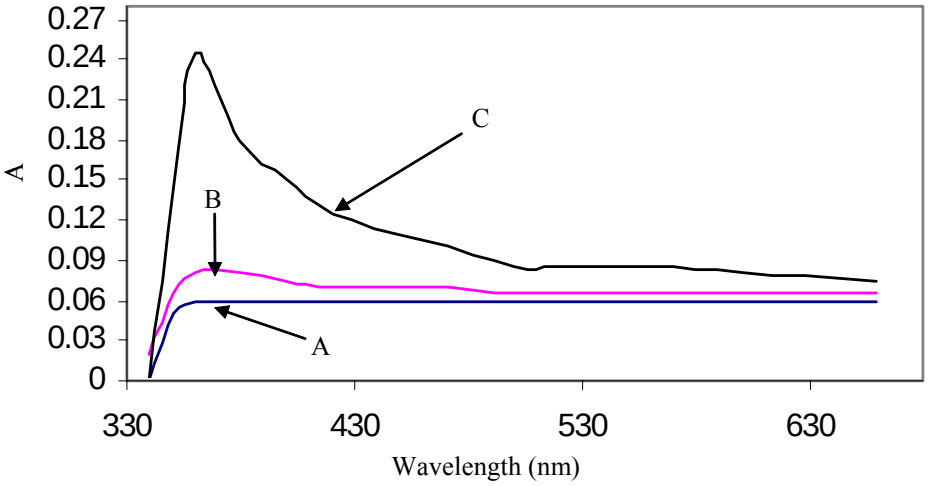

Figure 9.5 Reflective UV-Visible spectra: A: BB-6 quenched at 0 ^{o}C from LC state; B: BB-6-5S quenched at 0 ^{o}C from LC state; C: BB-6-5S quenched at 0 ^{o}C from isotropic state.

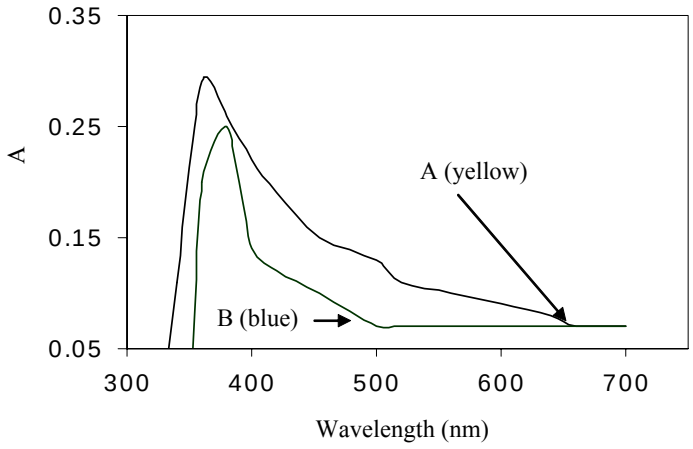

Figure 9.6 Reflective UV-Visible spectra: A: BB-6-10S quenched from LC state at 0 ^{o}C; B: BB-6-5S quenched from LC state at 0 ^{o}C.

9.4.5 Morphology

Micro-scale lamellar or fingerprint structures that originate from a twisted LC phase were observed earlier using electron microscopy and atomic force microscopy (AFM).[22-25] In this report, AFM in the tapping mode was used to study the morphology of the LC polyesters. Only BB-6 homopolymer and BB-6-5M copolymer had sufficient mechanical properties for sample preparation, and the resulting micrographs are shown in Figure 9.7 and Figure 9.8. The phase data for BB-6 homopolymer suggested that the modulus of the scanned surface was homogeneous. However, soft lamellar structures periodically appeared as deep color bands at the cut surface of BB-6-5M with a distance of approximately 1200 nm (Figure 9.8). The width of this lamellar structure was approximately 20 nm, which was consistent with the thickness of a LC lamellar layer.[3] Since these structures were not observed on the homopolymer surface, the possibility of amorphous layers between the LC lamellar layers was excluded. Moreover, height data did not reveal these lamellar structures, which excluded the possibility of surface artifacts that resulted from sample cutting. Thus, periodical soft lamellar structures were induced due to twisted LC structures.

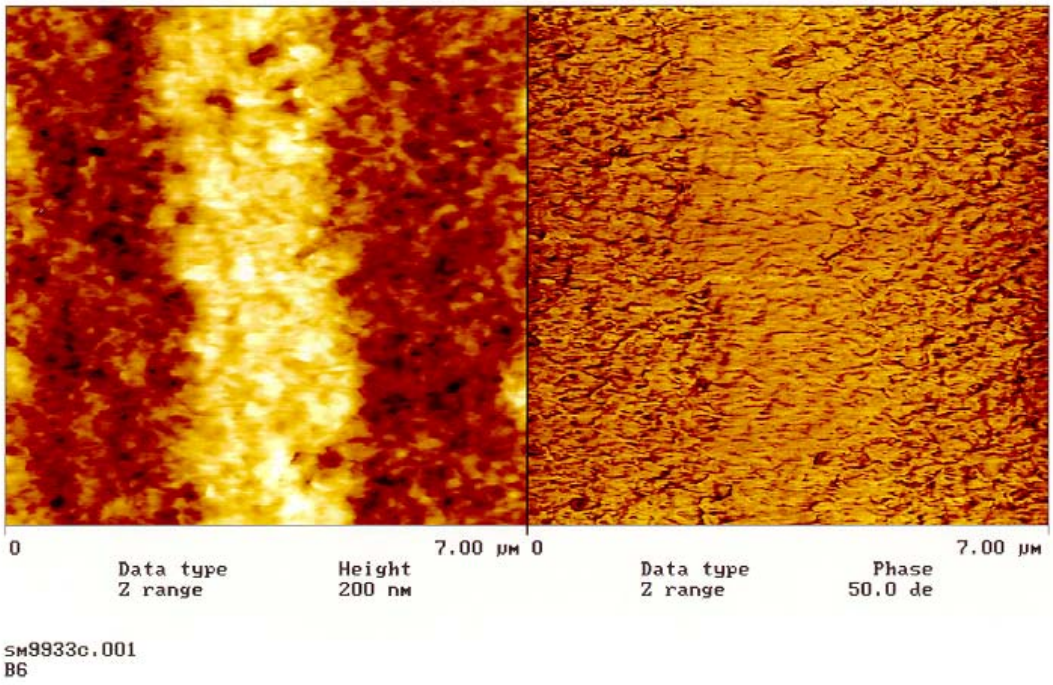

Figure 9.7 AFM of BB-6 indicating homogenous morphology

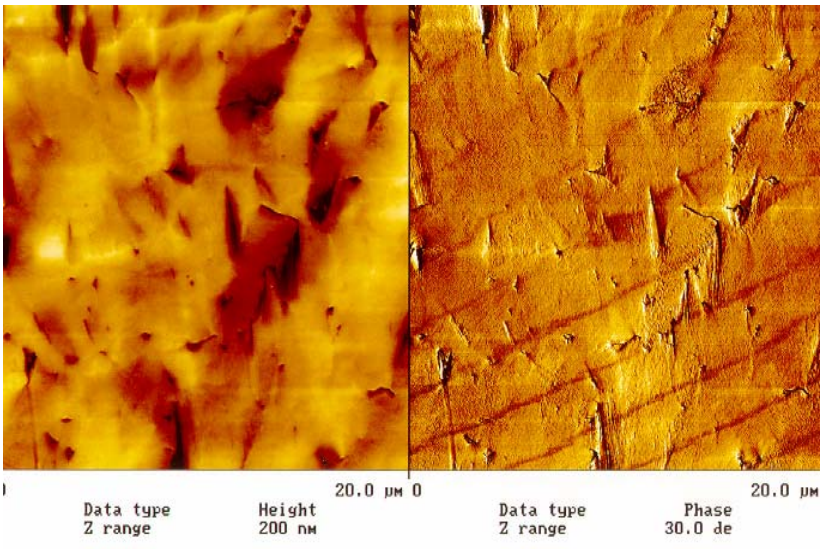

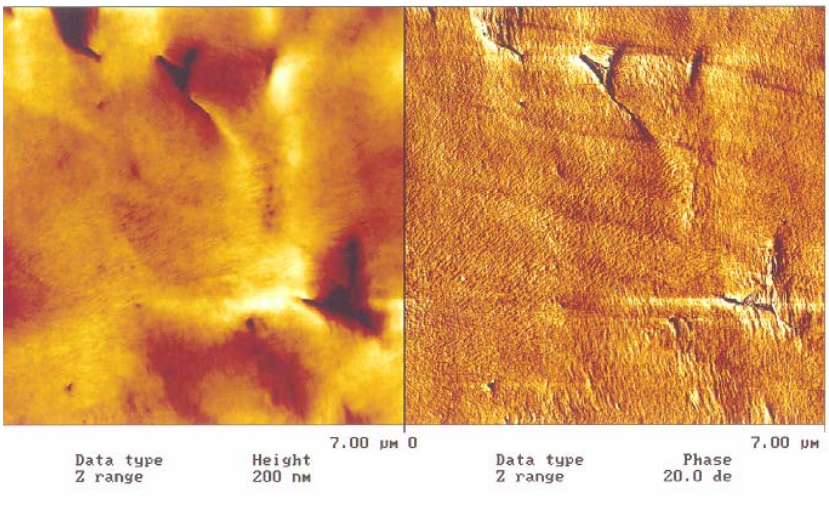

Figure 9.8 AFM of BB-6-5M indicating periodically soft lamellar structures

9.5 Conclusions

Liquid crystalline polyesters based on hexanediol or butanediol, dimethyl 4,4'-biphenyldicarboxylate, and various levels of isosorbide or isomanide, were prepared using conventional melt polymerization. ^{1}H NMR spectroscopy confirmed that 50 mol% of the charged sugar diol was successfully incorporated into various copolyesters. Modest molecular weights were obtained, although they were typically lower than polyester analogs that did not contain sugar based diols. Thermogravimetric analysis (TGA) demonstrated that the incorporation of isosorbide or isomanide units did not decrease thermal stability in a nitrogen atmosphere. Melting points that ranged from 190 to 270 °C were achieved as a function of copolyester composition. Polarized light microscopy suggested that a small amount of incorporated sugar diol induced S_c* LC phase, which was revealed via the observation of lined focal conic fan textures. AFM demonstrated that approximately 1.2 μm soft lamellar structures due to the twisted LC textures appeared periodically.

CHAPTER 10

Synthesis and Characterization of a Novel AB_2 Monomer and Corresponding Hyperbranched Poly(arylene ether phosphine oxide)s

(Publsihed as: Lin, Q.; Long, T. E. *Journal of Polymer Science: Part A, Polymer Chemistry* **2000**, 38, 3736.)

10.1 Abstract

A novel AB_2 monomer, 4-(fluorophenyl)-4',4"-(bishydroxyphenyl) phosphine oxide, was synthesized. The monomer was successfully polymerized to a modest molecular weight with various catalysts, including K_2CO_3 and $Cs_2CO_3/Mg(OH)_2$. Hyperbranched polymers exhibited exceptionally high thermal stability and solubility in conventional polar organic solvents and basic water solutions.

10.2 Introduction

Hyperbranched polymers contain a well-defined plurality of peripheral functionalities.[1] These functionalities subsequently serve as sites for further chemical modification or as templates for noncovalent intermolecular association.[2,3] In most cases, hyperbranched polymers are obtained with a one-step polymerization process involving AB*n*-type monomers. Hyperbranched architectures are typically easier to prepare than more well-defined dendritic architectures and offer many similar performance advantages.

---

[1]Frechet, J. M. J. *Science* **1994**, 263, 1710.
[2]Chu, F.; Hawker, C. J. *Macromolecules* **1996**, 29, 4370.

Poly(arylene ether)s are conventionally aromatic polymers containing thermally stable and fully oxidized linkages, such as sulfone, ketone, phosphine oxide, and ether groups. McGrath et al.[4] demonstrated various polymerization methodologies for the synthesis of high molecular weight poly(arylene ether)s with dipolar aprotic solvents in the presence of weak bases such as potassium carbonate. Significant research attention continues to be devoted to the improvement of the physical properties of linear poly(arylene ether)s.[4–6] Hyperbranched poly(arylene ether ketone) analogues have been studied in significant detail.[2,7–13] In addition, Martinez and Hay[14,15] recently proposed the efficient synthesis and characterization of hyperbranched poly(arylene ether sulfone)s with a $K_2CO_3/Mg(OH)_2$ catalyst system for nucleophilic aromatic substitution. The utility of the aryl phosphine oxide moiety as the activating group also contributes to improving performance characteristics, such as high thermal stability, inherent flame resistance, and potential for association via hydrogen bonding, in comparison with poly(arylene ether sulfone)s. The phosphine oxide group is an exceptionally good electron-donating group and facilitates the subsequent coordination with various metal ions or the formation of relatively strong hydrogen bonds. Particular attention was devoted to the introduction of peripheral phenol functionality to provide facile reactive centers for subsequent derivatization. Derivatization was utilized to control the solubility and intermolecular association of the hyperbranched poly(arylene ether phosphine oxide)s. The research efforts described herein focus on the synthesis and characterization of a novel AB_2 monomer containing phosphine oxide and corresponding hyperbranched poly(arylene ether phosphine oxide)s containing peripheral phenol functionality.

10.3 Experimental

10.3.1 Synthesis

Scheme 10.1 summarizes the monomer synthetic methodology.

Bis–(4-methoxyphenyl) Phosphinic Chloride (3). Bis-(4-methoxyphenyl) phosphinic acid (**1**; 55.6 g, 0.2 mol; 99%; Aldrich) was dissolved in 200 mL of thionyl chloride (99%; Aldrich) at 55 °C for 1 h. The temperature was raised to 80 °C to remove excess thionyl chloride (bp: 79 °C). Vacuum (0.50 mm Hg) was subsequently used to remove any trace quantities of thionyl chloride. The product was red and was immediately utilized without further purification or isolation.

4-Fluorophenylmagnesium Bromide (2). In a three-necked, round-bottom flask equipped with a magnetic stir bar, reflux condenser, and addition funnel, magnesium powder (6.0 g, 0.25 mol; 99%; Aldrich) was added and subsequently flushed with ultrapure argon. Approximately 200 mL of tetrahydrofuran (THF) and iodine (20 mg; 99%; Aldrich) was added.[16] The heterogeneous mixture was stirred at 25 °C until the iodine color was lost, and a solution of 1-bromo-4-fluorobenzene (35 g, 0.2 mol; 99%; Aldrich) in THF (50 mL) immediately was added dropwise over a 1 h period. The temperature was then raised to 65 °C and maintained at reflux for 6 h. The product was used without isolation or characterization.

---

[3](a) Frechet, J. M. J.; Hawker, C. J. *React. Funct. Polym.* **1995**, 26, 127. (b) Wooley, K. L.; Hawker, C. J.; Lee, R. *Polym. J.* **1994**, 26, 187. (c) Hawker, C. J.; Lee, R.; Frechet, J. M. J. *J. Am. Chem. Soc.* **1991**, 113, 4583; (d) Kim, Y. H.; Webster, O. W. *Macromolecules* **1992**, 25, 5561.

[4]Riley, D.; Gungor, A.; Srinivasan, S. A.; McGrath, J. E. *Polym. Eng. Sci.* **1997**, 37, 1501.

[5]Smith, C. D.; Grubbs, H.; Gungor, A.; Webster, H. F.; Wightman, J. P.; McGrath, J. E. *High Perform. Polym.* **1991**, 3, 211.

[6]Yang, J.; Gibson, H. W. *Macromolecules* **1999**, 32, 8740.

[7]Regan, K.; Engel, R. *J. Chem. Soc. Chem. Commun.* **1990**, 1084.

[8]Regan, K.; Engel, R. *J. Chem. Soc. Perkin. Trans. 1* **1991**, 987.

4-(Fluorophenyl)-4',4"(-(bismethoxyphenyl) Phosphine Oxide (4). The solution of compound **3** in THF was added to the compound **2** solution via an addition funnel at room temperature over 30 min. The temperature was raised to 65 °C and maintained at reflux for 6 h until the homogeneous solution changed to a transparent yellow color. THF was removed with distillation under a nitrogen purge, and vacuum was finally applied to ensure complete removal. Isolation of the final product was accomplished by the addition of 300 mL of toluene and 300 mL of a 10% H_2SO_4 solution, and the mixture was allowed to stir at 60 °C for 30 min. The organic layer was separated and washed repeatedly with 200 mL of a 1 N NaOH solution and then with 300 mL of deionized water. The toluene was removed in a distillation apparatus, and a colorless oil product was produced that was subsequently dried *in vacuo* at 80 °C for 24 h. The product was analyzed and used without further purification. ^{1}H NMR analysis indicated that the product (purity: 98%) contained only trace amounts of residual toluene. Typical isolated yields ranged from 80 to 85%. ^{1}H NMR (DMSO-d_6, ppm): δ 7.01–7.11 (m, 4H, ArH_1), 7.37–7.41 (m, 2H, ArH_4), 7.45–7.52 (m, 4H, ArH_2), 7.59–7.71 (m, 2H, ArH_3), 3.93 (s, 3H, OCH_3). ^{13}C NMR (DMSO-d_6, ppm): δ 55.1; 116.5; 117.1; 122.6, 123.5; 131.0, 131.9; 135.3; 135.4; 162.6; 162.7, 160.1. ^{31}P NMR (DMSO-d_6, ppm): δ 25.6. MS (CI): [MH^+]: 357 Da.

4-(Fluorophenyl)-4*,4(-(bishydroxyphenyl) Phosphine Oxide (5). In a 500-mL, three-necked flask, compound **4** (56.96 g, 0.16 mol), 200 mL of glacial acetic acid, and 200 mL of hydrobromic acid (HBr; 37%; Aldrich) were added, and the reaction was maintained at 125 °C under a nitrogen purge for 48 h until the solution changed to a dark color. The solution was subsequently added to approximately 1 L of deionized water,

and the precipitated product was easily collected with a filter funnel. Typical isolated yields were 90–95 %. The crude product was purified by column chromatography, eluting initially with CH_2Cl_2 and subsequently with CH_2Cl_2/CH_3CH_2OH (9/1) to give the final purified product. The chromatographic yield was calculated to be 92 % (mp: 118.2 °C). ^{1}H NMR [DMSO-d_6, correlation spectroscopy (COSY), ppm]: δ 6.75–6.88 (m, 4H, ArH_1), 7.29–7.45 (m, 4H, ArH_2), 7.31–7.45 (m, 2H, ArH_4), 7.59– 7.69 (m, 2H, ArH_3), 10.19 (s, 2H, OH). ^{13}C NMR (DMSO-*d*6, ppm): δ 116.3; 116.8; 122.4, 123.5; 130.8, 131.6; 134.2; 135.1; 161.2; 162.5, 166.0. ^{31}P NMR (DMSO-*d*6, ppm): δ 26.1. MS (CI): [MH^+]: 329 Da. ELEM. ANAL. Calcd. for $C_{18}H_{14}O_3PF$: C, 65.86%; H, 4.30%. Found: C, 65.58 %; H, 4.49 %.

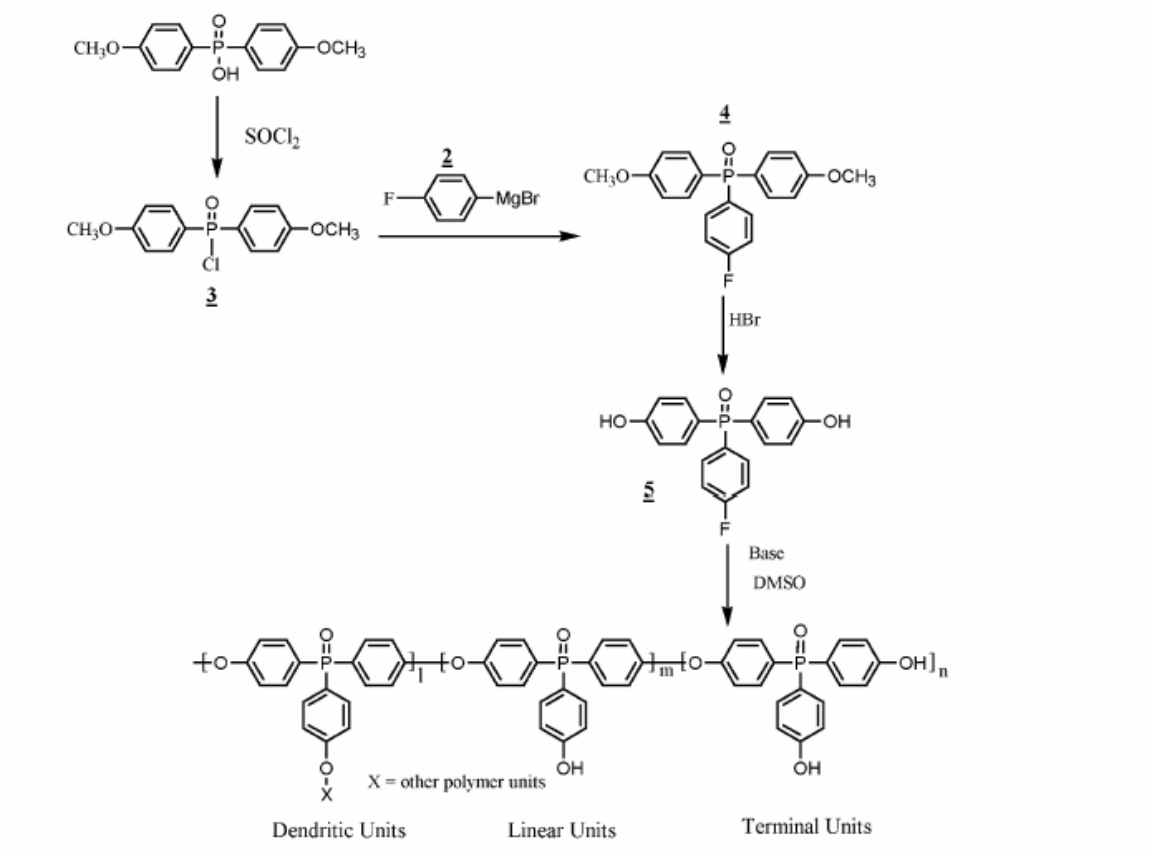

Scheme 10.1 Synthetic strategy for the AB_2 monomer and corresponding hyperbranched poly(arylene ether phosphine oxide)s.

Synthesis of Hyperbranched Polymers. The polymers (**P-1**–**P-5**) were synthesized with dimethyl sulfoxide (DMSO; vacuum-distilled from calcium hydride) as a solvent. Monomer, catalyst, dry DMSO, and toluene (distilled from calcium hydride under nitrogen) were added to a threenecked, round-bottom flask. To ensure anhydrous reaction conditions, the reaction temperature was raised to 135–140 °C to remove the toluene/water azeotrope with a Dean–Stark trap. The temperature was then raised to 189 °C and maintained at reflux. The reactions are summarized as follows and were allowed to proceed for various times:

P-1. 0.33 M, catalyst: K_2CO_3, 21 h.

P-2. 0.50 M, catalyst: $Cs_2CO_3/Mg(OH)_2$, 4 h.

P-3. 0.33 M, catalyst: $Cs_2CO_3/Mg(OH)_2$, 21 h.

P-4. 1.00 M, catalyst: $Cs_2CO_3/Mg(OH)_2$, 21 h.

P-5. 0.50 M, catalyst: $Cs_2CO_3/Mg(OH)_2$, 4 h; 5 mol % 4,4'-dichloro-diphenylsulfone (BP Amoco; used as received), 2 h.

After the solution cooled, the reaction was diluted with 30 mL of DMSO, and the precipitated salts were removed by filtration. The polymer solution was poured into a water/acetic acid solution (90/10) to precipitate the polymer and form the terminal phenol. The polymer was collected with a filter funnel and then extracted with ethanol for 48 h to remove any unreacted monomer and residual solvent (DMSO). The final polymer was dried in a vacuum oven at 180 °C for 24 h. ^{1}H NMR (DMSO-*d*6, ppm): δ 7.18–7.22 (4H, ArH1), 7.50–7.65, (4H, ArH2), 7.28–7.46 (2H, ArH3), 6.81–6.90 (2H, ArH4). ^{31}P NMR (DMSO-*d*6, d): 26.2.

P-6. Monomer (3.29 g, 0.01 mol), K_2CO_3 (0.8 g, 0.0051 mol), and phenyl sulfone (10.0 g; 97%; Aldrich) were added to a three-necked, round-bottom flask under a nitrogen atmosphere. The reactor temperature was maintained at 130 °C for 1 h and 160 °C for 4 h to remove moisture. The temperature was subsequently raised to 270 °C for 5 h, and the temperature was increased to 350 °C for 30 min. After the solution cooled, dimethyl formamide was added to solubilize the diphenyl sulfone, and the insoluble polymer product containing inorganic salt was isolated. Aqueous rinses efficiently removed the inorganic salts from the polymer product. The final polymer product was dried *in vacuo* at 180 °C for 24 h.

10.3.2 Characterization

^{1}H, ^{13}C, and ^{31}P NMR analyses were performed on a Varian 400-MHz spectrometer in DMSO-d_6. Molecular weights were determined with a Waters 150C gel permeation chromatograph equipped with a refractive index detector (DRI) in *N*-methyl pyrolidone (NMP; 1% P_2O_5) at 60 °C with polystyrene standards. Thermal-transition temperatures were determined with a PerkinElmer DSC-7 at 10 °C/min.

10.4 Results and discussion

^{1}H NMR analysis of compound **5** confirmed the quantitative disappearance of the resonance at 3.93 ppm that was assigned to the protons of the OCH_3 group in precursor compound **4**. This observation confirmed quantitative hydrolysis in the presence of HBr. In addition, ^{13}C NMR (Figure 10.1) analysis of compound **5** confirmed the absence of an aliphatic carbon resonance, with the exception of the NMR solvent (DMSO-d_6) peak in

the aliphatic region. Because of coupling with ^{19}F or ^{31}P, which also have 1/2 spin, the ^{13}C NMR resonances associated with carbon atoms C_g, C_h, and C_c were split into two resonances of equal intensity. Overlapping ^{1}H NMR resonances for H_2 and H_4 were observed in compound 5; however, two dimensional 1H NMR (COSY) confirmed the structure of the monomer (Figure 10.2). The assignment of the COSY spectrum is depicted in Figure 10.2, and resonances at 7.29–7.45 ppm were assigned to protons H_2 and H_4 in compound **5**.

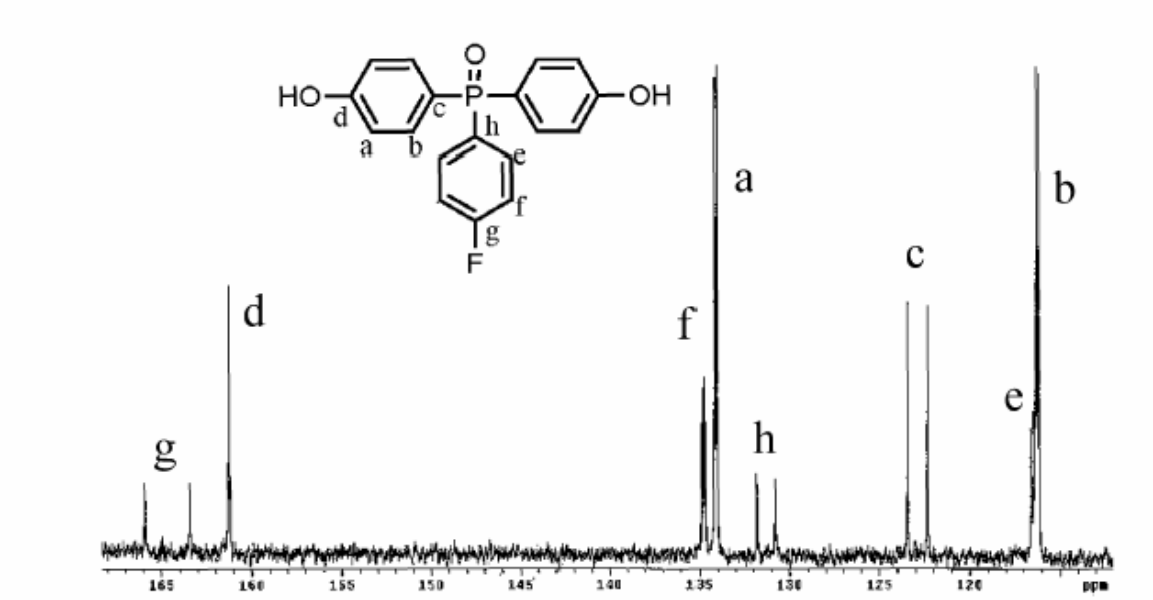

Figure 10.1 ^{13}C NMR spectrum of monomer **5** (DMSO-d_6, 100 MHz).

---

[9]Shalai, K.; Hart, H. *J. Org. Chem.* **1991**, 56, 6059.
[10] Kadei, K.; Moors, R.; Vogtle, F. *Chem. Ber.* **1991**, 56, 6905.
[11]Regan, K.; Engel, R. *J. Chem. Soc. Chem. Commun.* **1992**, 757.
[12]Miller, T. M.; Neeman, T. X.; Kwock, E. W.; Stein, S. M. *J. Am. Chem. Soc.* **1993**, 115, 356.
[13]Uhrich, K. E.; Hawker, C. J.; Frechet, J. M. J.; Turner, S. R. *Macromolecules* **1992**, 25, 4583.
[14]Martinez, C. A.; Hay, A. S. *J. Polym. Sci. Part A: Polym. Chem.* **1997**, 35, 2015.
[15]Martinez, C. A.; Hay, A. S. *J. Macromol. Sci. Pure Appl. Chem.* **1998**, 35, 57.
[16]Mashima, K.; Kuasano, K.; Sato, N.; Matsumura, Y.; Nozaki, K.; Kumobayashi, H.; Sayo, N.; Hori, Y.; Ishizaki, T.; Akutaagawa, S.; Takaya, H. J Org Chem 1994, 59, 3064.

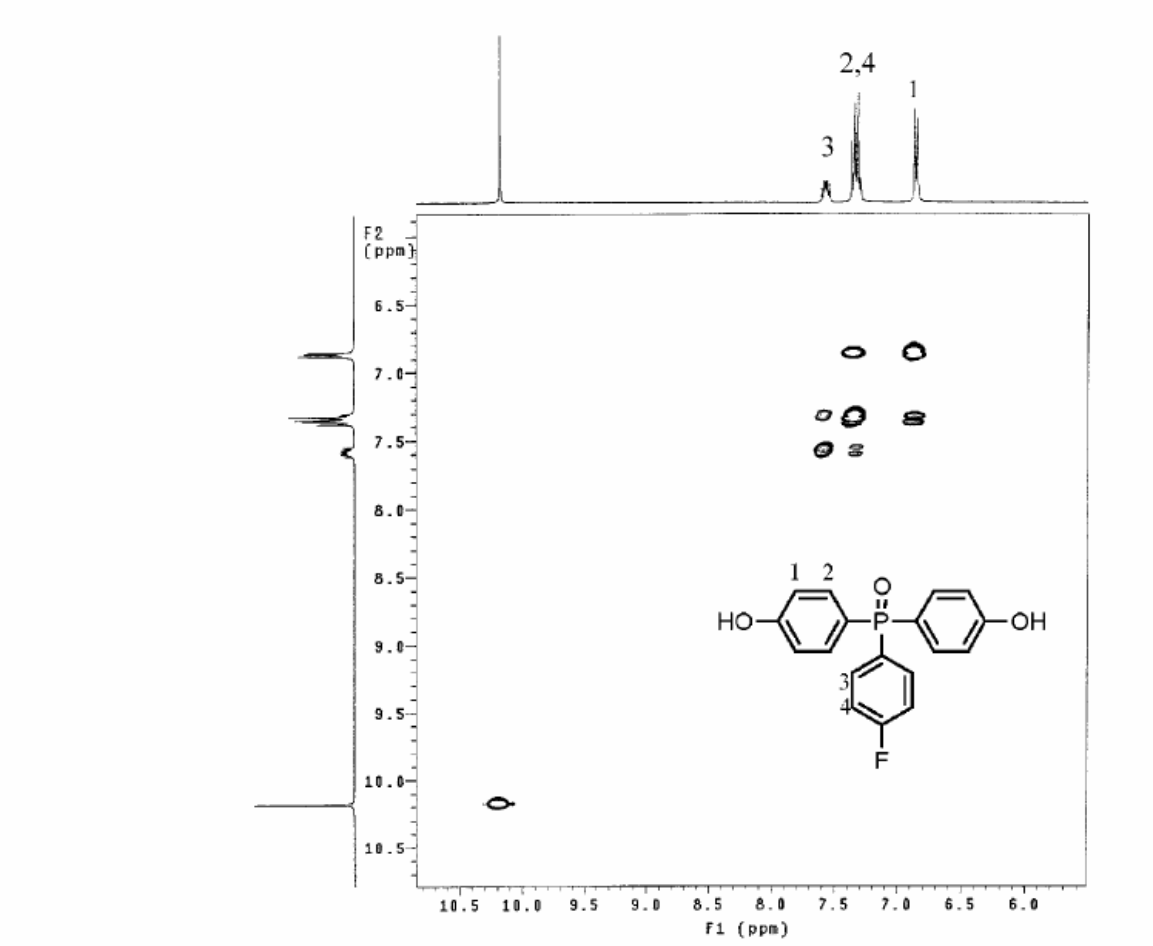

Figure 10.2 COSY spectrum of monomer **5** (DMSO-d_6, 400 MHz).

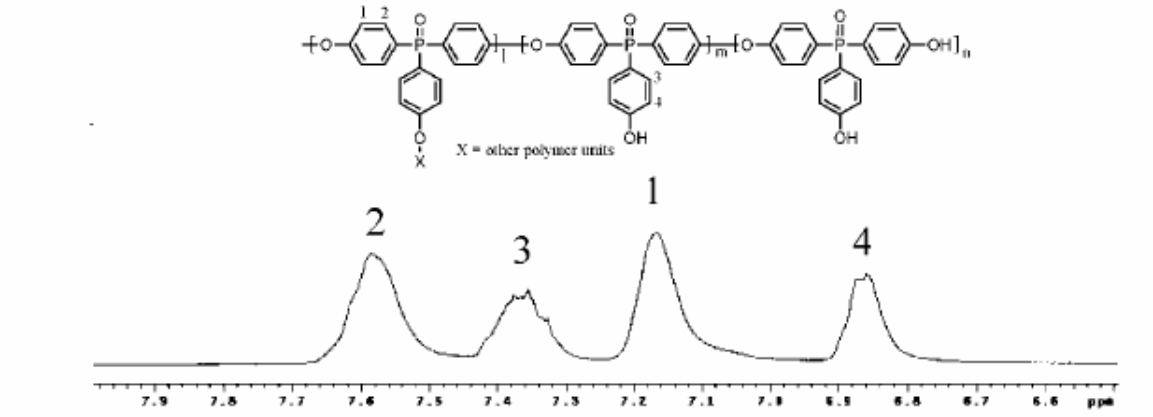

Figure 10.3 ^{1}H NMR spectrum of hyperbranched polymer P-4 (DMSO-d_6, 400 MHz).

Table 10.1 Isolated yields and GPC data of hyperbranched polymers

Samples	Yield (%)	M_n^a	M_w	M_w/M_n
P-1	75	1,550	7,750	5.0
P-2	92	3,560	14,600	4.1
P-3	94	3,080	26,400	8.6
P-4	45	5,670	57,260	10.1
P-5	90	8,720	29,600	3.4

Previous polymerization research efforts have demonstrated that electron-withdrawing phosphine oxide significantly decreases the nucleophilicity of the phenolate intermediate.[4] To achieve a high molecular weight polymer product, specific solvents such as phenyl sulfone and an extremely high temperature (350 °C) were used. Our initial efforts with phenyl sulfone and high temperatures were unsuccessful at obtaining a soluble product. Consequently, DMSO was utilized at lower temperatures in an attempt to preserve the solubility of the hyperbranched polymer product. The broad resonances in the ^{1}H NMR spectrum suggest the formation of a soluble high molecular weight

polymeric product (Figure 10.3). Moreover, the ^{1}H NMR chemical shifts and integration were consistent with the formation of a hyperbranched polymer structure. Weight-average molecular weights (*Mw*; Table 10.1) for the hyperbranched poly(arylene ether phosphine oxide)s were consistent with values reported earlier for hyperbranched poly(arylene ether sulfone)s[14] and poly(arylene ether ketone)s.[2] Because of the highly irregular, branched, three-dimensional structures, gel permeation chromatography (GPC) does not provide an accurate measurement of molecular weights, and calibrated GPC typically results in a lower molecular weight, especially a number-average molecular weight (M_n).[2,3] The cesium carbonate catalyst in the presence of magnesium hydroxide, as proposed by Martinez and Hay,[14] resulted in higher molecular weights than similar reaction conditions employing potassium carbonate Table 10.1 indicates that higher monomer concentrations in DMSO resulted in higher molecular weight products (Table 10.1, **P-4** vs **P-3**) but lower yields (45%). This is presumably due to the formation of insoluble, high molecular weight products. The programmed addition of monomer or copolymerization will be pursued to obtain higher M_n's with narrow molecular weight distribution products. Our preliminary results indicated that the addition of 4,4'-dichloro-diphenylsulfone (A_2) comonomer during the polymerization resulted in higher M_n products (**P-5** vs **P-2**) and high yields (90 %) in a relatively short time (6 h). All polymer products were readily soluble at room temperature in various organic solvents, including DMSO, dimethyl formamide, dimethyl acetamide, NMP, and basic water. Differential scanning calorimetry indicated the absence of any thermal transitions below 350 °C, with the exception of a transition at 100 °C that was attributed to the presence of residual water. It is proposed that the abundance of phenolic end groups is capable of efficient

hydrogen bonding with other polar compounds. Glass-transition temperatures for hyperbranched poly(arylene ether ketone)s and poly(arylene ether sulfone)s were earlier reported to be 127 and 277 °C, respectively.[2,14] McGrath et al.[4] earlier demonstrated that poly(arylene ether phosphine oxides) have higher glass-transition temperatures than corresponding ketone and sulfone analogues.

10.5 Conclusions

A novel AB_2 monomer, 4-(fluorophenyl)-4',4"-(bishydroxyphenyl) phosphine oxide, was synthesized. The monomer was successfully polymerized to a modest molecular weight with various catalysts, including K_2CO_3 and $Cs_2CO_3/Mg(OH)_2$. Hyperbranched polymers exhibited exceptionally high thermal stability and solubility in conventional polar organic solvents and basic water solutions.

CHAPTER 11

Polymerization of A_2 with B_3 Monomers: A Facile Approach to Hyperbranched Polyarylates

(Publshed as: Lin, Q.; Long, T. E. *Macromolecuels*, submitted)

11.1 Abstract

Hyperbranched polymers have received significant attention due to their unique combination of low viscosity, excellent solubility, and facile synthesis. This manuscript describes an efficient approach to hyperbranched polyarylates via the polymerization of A_2 and B_3 monomers. A dilute bisphenol A (A_2) solution was added slowly to a dilute 1,3,5-benzenetricarbonyl trichloride (B_3) solution at 25 °C to prepare hyperbranched polyarylates in the absence of gelation. The molar ratio of A_2:B_3 was maintained at 1:1, and the maximum final monomer concentration was ~ 0.08 M. Two model compounds were synthesized in order to identify ^{1}H NMR resonances for linear, dendritic and terminal units, and the final degree of branching was determined to be ~ 50%. ^{1}H NMR spectroscopy and derivitization of terminal groups indicated that the phenol functionalities were quantitatively consumed during the polymerization. All results indicated that these hyperbranched polyarylates had structures similar to traditional hyperbranched polymers derived from AB_n monomers. Moreover, the hyperbranched polymers exhibited lower glass transition temperatures relative to their linear analogues.

11.2 Introduction

Flory initially described an approach for the preparation of hyperbranched polymers from AB_2 monomers in 1952.[1] Extensive research resumed approximately ten years ago in an effort to develop an economical replacement for perfect dendritic polymers.[2] In most cases, hyperbranched polymers are prepared using a one-step polymerization of AB_n monomers,[3-9] and typically exhibit highly irregular structures and large molecular weight distributions. This is a direct consequence of the one-step methodology, and it was suggested that hyperbranched polymers resembled conventional networks immediately prior to the gel point.[10-11] The similarity of intermediates in a A_2 with B_3 process to intermediates in the formation of polymeric networks led chemists to consider the polymerization of A_2 with B_3 monomers as an alternative synthetic route. This complementary method is attractive since many A_2 and B_3 monomers are readily available, and have received significant attention in the synthesis of conventionally branched polymers. [11-19]

---

[1]Flory, P.J. *J. Am. Chem. Soc.* **1952**, 74, 2178.
[2](a) Kim, Y.H.; Webster, O. W. *J. Am. Chem. Soc.* **1990**, 112, 4592. (b) Harth, E. M.; Hecht, S.; Helm, B.; Malmstrom, E. E.; Frechet, J. M. J.; Hawker, C. J. *J. Am. Chem. Soc.* **2002**, 124, 3926.
[3]Hawker, C. J.; Lee, R.; Frechet, J. M. J. *J. Am. Chem. Soc.* **1991**, 113, 4583.
[4]Wooley, K. L.; Hawker, C. J.; Lee, R.; Frechet, J. M. J. *Polym. J.* **1994**, 26, 187.
[5]Frechet, J. M. J. *Science* **1999**, 263, 1710.
[6]Chu, F. K.; Hawker, C. J. *J. Chem. Soc. Perkin Trans.* **1993**, 2717.
[7]Parker, D.; Feast, W. J. *Macromolecules* **2001**, 34, 2048.
[8]Lin, Q, Long, T. E. *J. Polym. Sci. Part A: Polym. Chem.* **2000**, 38, 3736.
[9](a) Wu, F. I.; Shu, C. F. *J. Polym. Sci. Part A: Polym. Chem.* **2001**, 39, 2536. (b) Wu, F. I.; Shu, C. F. *J. Polym. Sci. Part A: Polym. Chem.* **2001**, 39, 3851. (c) Bolton, D. H.; Wooley, K. J. *Polym. Sci. Part A: Polym. Chem.* **2002**, 40, 823.
[10](a) Antonietti, A.; Rosenauer, C. *Macromolecules* **1991**, 24, 3434. (b) Frechet, J. M. J.; Hawker, C. J.; Gitsov, I.; Leon, J. W. *J. Macro. Sci. Pur. and Appl. Chem.* **1996**, 1399.

Watanebe and coworkers reported the synthesis of hyperbranched aromatic polyamides, which were derived from aromatic diamines (A_2) and trimesic acid (B_3).[11] Kinetic calculations predicted that the first condensation reaction of A_2 with B_3 was faster than subsequent propagation, thus leading to an accumulation of A-ab-$(B)_2$ intermediates. Thus, it was proposed that the remainder of the process resembled more common AB_2 polymerizations. Frechet and coworkers reported the synthesis of hyperbranched polyether epoxies *via* proton transfer polymerization from 1,2,7,8-diepoxyoctane (A_2) and 1,1,1-tri(hydroxymethyl)ethane (B_3) using a 1:1 molar ratio of monomers (2 equivalents of A groups and 3 equivalents of B groups).[12,13] These reactions were stopped immediately prior to the gel points to form highly branched molecules. After these two pioneering reports, a flurry of research led to the development of several new experimental procedures.[15-19] For example, Okamoto and coworkers synthesized hyperbranched polyimides via a slow addition of a dilute solution of A_2 to a dilute solution of B_3.[19]

---

[11](a) Burchard, W. *Macromolecules* **1972**, 5, 604. (b) Burchard, W. *Macromolecules* **1977**, 10, 919. (c) Burchard, W. *Adv. Polym. Sci.* **1983**, 48, 1. (d) Burchard, W. *Adv. Polym. Sci.* **1999**, 143, 113.

[12]Jikei, M.; Chon, S. H.; Kakimoto, M.; Kawauchi, S.; Imase, T.; Watanabe, J. *Macromolecules* **1999**, 32, 2061.

[13]Emrick, T.; Chang, H. T.; Frechet, J. M. J. *Macromolecules* **1999**, 32, 6380.

[14]Emrick, T.; Chang, H. T.; Frechet, J. M. J. *J. Polym. Sci. Part A: Polym. Chem.* **2000**, 38, 4850

[15]Monticelli, O.; Mariani, A.; Voit, B. I.; Komber, H.; Mendichi, R.; Pitto, V.; Tabuani, D.; Russo, S. *High Perform. Polym.* **2001**, 13, 45.

[16]Russo, S.; Boulares, A.; da Rin, A.; Mariani, A.; Cosulich, M. E. *Macromol. Symp.* **1999**, 143, 309.

[17]Jikei, M.; Kakimoto, M. A. *High Perform. Polym.* **2001**, 13, 33.

[18](a) Komber, H.; Voit, B. I.; Monticelli, O.; Russo, S. *Macromolecules* **2001**, 34, 5487. (b) Kricheldorf, H. R.; Vakhtangishvili, D.; Fritsch, D. *J. Polym. Sci.: Part A, Polym Chem.* **2002**, 40, 2967. (c) Fritsch, D.; Vakhtangishvili, L.; Kricheldorf, H. R. *J. M. S. Pure Appl. Chem.* **2002**, 139, 1335.

Our recent efforts have focused on the synthesis of hyperbranched analogues of engineering polymers to obtain the combined properties of hyperbranched polymers (low melt viscosity, multi-functionality, and the possibility of acting as molecular encapsulants) and good thermal stability.[8] These novel hyperbranched polymers are useful as modifiers in blends with linear polymers, thin coatings, gas separation membranes, and micro-electronic materials. Polyarylates are a class of engineering thermoplastics that exhibit high glass transition temperatures, good thermal stability, and selective gas permeation.[20,21] Turner and coworkers reported the synthesis of hyperbranched polyarylates using commercially available AB_2 monomers, such as 5-acetoxyisophthalic acid and 5-(2-hydroxyethoxy)isophthalic acid.[22,23] In addition, several bisphenols containing different linking groups, such as biphenol, 4,4'-(hexafluoroisopropylidene)diphenol, 4,4'-sulfonyldiphenol or 4,4'-bis(hydroxyphenyl)phenylphosphine oxide, were investigated to improve the performance of linear polyarylates.[20,24] These monomers lead to hyperbranched polymers with unique properties such as liquid crystalline morphologies, high thermal stabilities, and low dielectric constants.

Very few reports of hyperbranched polyarylates exist because the required AB_n monomers are not easily synthesized.[25] The preparation of hyperbranched polyarylates that are derived from A_2 and B_3 monomers represents a facile route to novel hyperbranched polyarylates. The synthesis of hyperbranched polyarylates that are derived from bisphenol-A and 1,3,5-benzenetricarbonyl trichloride are reported herein, and spectroscopic and thermal analyses indicate similar chemical structures and thermal properties to hyperbranched polymers that are derived from traditional AB_n monomers.

11.3 Experimental

11.3.1 Materials

Bisphenol A (Bis A) (monomer grade) was graciously donated by the Dow Chemical Company, and was dried in a vacuum oven (0.50 mm Hg) at 80 ºC for 18 h. 1,3,5-Benzenetricarbonyl trichloride (BTC) (99%), anhydrous triethylamine (TEA) (99%), phenol (99%), and acetyl chloride (99%) were purchased from Aldrich and used as received. Chloroform (Burdick &Jackson, high purity) was stirred over calcium hydride, and distilled under nitrogen. Methanol was purchased from EM Science and used as received.

11.3.2 Synthesis

Synthesis of a hyperbranched polyarylate with ammonium carboxylate terminal groups (P-1). BTC (1.99 g, 0.0075 mol) was dissolved in 50 mL of freshly distilled chloroform in a 250-mL, thoroughly dried, three-necked flask equipped with a magnetic stir bar, reflux condenser, and addition funnel. Bis A (1.71 g, 0.0075 mol) and 1.52 g (0.015 mol) TEA were added to 100 mL of freshly distilled chloroform in an addition funnel, and slight heating was required to completely dissolve the Bis A. After a homogeneous solution was obtained, the solution was slowly added to the reaction flask over 1 h. The homogenous reaction was maintained at 23 ^{o}C for 24 h. Water (10 mL) was subsequently added in order to quench the residual acid chloride, and the heterogeneous solution was stirred for 30 min. The solution was washed twice with basic water, acidic water, and deionized water, then precipitated into methanol. The white product was filtered, and dried at 40 $^{\circ}$C in a vacuum oven for 24 h. ^{1}H NMR

(chloroform-d, ppm): δ 1.42 (br, -$NCH_2C\underline{H}_3$ terminal group), 1.75 (br, 6H, -Ar-$C(CH_3)_2$-Ar-), 4.44 (br, -$NC\underline{H}_2CH_3$ terminal group), 7.34 (br, 4H, aromatic protons from Bis A), 7.50 (br, 4H, aromatic protons from Bis A), 8.93- 9.22 (br, 3H, aromatic protons from BTC).

Synthesis of a hyperbranched polyarylate with methyl ester terminal groups (P-2). The synthetic method was similar to P-1 preparation except that the reaction solution was directly poured into methanol without the addition of water. The white product was filtered, re-dissolved in chloroform, then washed with basic water, acidic water and deionized water twice. The purified product was precipitated into methanol, and collected in a filter funnel. The product was dried at 40 °C in a vacuum oven for 24 h. ^{1}H NMR (chloroform-d, ppm): 1.42 (br, -$NCH_2C\underline{H}_3$ terminal group), 4.00 (br, 2.9 H, -OCH_3), 4.44 (br, -$NC\underline{H}_2CH_3$ terminal group), 7.18 (br, 4H, aromatic protons from Bis A), 7.34 (br, 4H, aromatic protons from Bis A), 8.99-9.93 (br, aromatic protons from BTC). ^{13}C NMR: (chloroform-d, ppm): 14.8 (-$N\underline{C}H_2CH_3$ terminal group), 31.6 (-Ar-$C(\underline{C}H_3)_2$-Ar-), 42.3 (-Ar-$\underline{C}(CH_3)_2$-Ar-), 53.4 (-OCH_3), 62.4 (-$NCH_2\underline{C}H_3$ terminal group), 121.6 (Bis A), 128.7 (Bis A), 148.6 (Bis A), 154.2 (Bis A), 132.1-136.3(BTC), 164.9-165.6 (C=O).

Synthesis of hyperbranched polyarylates with methyl ester terminal groups (P-3, P-4, P-5). The synthetic method was similar to P-2 preparation except that different monomer concentrations and polymerization times were used as summarized in Table 1.

Synthesis of 1,3-methyl-5-phenyl-benzenetricarboxylate (1). Phenol **(**4.71 g, 0.05 mol), 13.27 g (0.05 mol) BTC, and 5.06 g (0.05 mol) TEA were dissolved in 100

mL chloroform in a thoroughly dried, three-necked flask with a magnetic stir bar and reflux condenser, and allowed to react at room temperature for 24 h. The solution was poured into methanol to precipitate the product. The crude product was a viscous oil, and TLC indicated three compounds. The compounds were separated using column chromatography with a 2:1 v/v mixture of dichloromethane and hexane. ^{1}H NMR spectroscopy and mass spectroscopy indicated that the second fraction was the targeted model compound. The product was a crystalline white solid with a melting point of 82.3 ºC. ^{1}H NMR (chloroform-d, ppm): δ 3.98 (s, 6H, -OCH_3), 7.23-7.32 (m, 3H, aromatic protons from phenol), 7.51-7.43 (m, 2H, aromatic protons from phenol), 8.93 (s, 1H, aromatic proton from BTC), 9.02 (s, 2H, aromatic protons from BTC). ^{13}C NMR (chloroform-d, ppm): δ 53.0 (-OCH_3), 121.7 (Phenol), 126.5 (Phenol), 129.5 (Phenol), 130.8(BTC), 131.7 (BTC), 135.6 (BTC), 150.8 (BTC), 163.8 (C=O), 165.6 (C=O). MS(CI): 377 m/z (MH^+, calcd 377 m/z). Anal. Calcd for $C_{22}O_6H_{16}$: C, 64.96; H, 4.49. Found: C, 64.66; H, 4.63.

Synthesis of 1-methyl-3,5-phenyl-benzenetricarboxylate (2). The synthetic method was similar to the preparation of compound (1) except that the molar ratio of BTC to phenol was 1:2. The crude product was a viscous oil, and TLC indicated four compounds. The compounds were separated using column chromatography with a 2:1 v/v mixture of dichloromethane and hexane. ^{1}H NMR spectroscopy and mass spectroscopy indicated that the third fraction was the targeted compound. The product was a crystalline white solid with a melting point of 93.5 ºC. ^{1}H NMR (chloroform-d, ppm): δ 4.02 (s, 3H, -OCH_3), 7.23-7.34 (m, 6H, aromatic protons from phenol), 7.43-7.48 (m, 4H, aromatic protons from phenol), 9.10 (s, 2H, aromatic protons from BTC), 9.21 (s,

1H, aromatic proton from BTC). ^{13}C NMR (chloroform-d, ppm): δ 53.0 (-OCH_3), 121.7 (phenol), 126.5 (phenol), 129.9 (phenol), 131.2 (phenol), 132.1 (phenol), 136.0 (BTC), 150.8 (BTC), 163.8 (C=O), 165.6 (C=O). MS(CI): 315 m/z (MH^+, calcd 315 m/z). Anal. Calcd for $C_{27}O_6H_{29}$: C, 70.21; H, 4.28. Found: C, 69.95; H, 4.39.

Confirmation of the absence of phenol terminal groups on methyl ester terminated hyperbranched polyarylates. P-4 (0.50 g, 1.30 mmol) and TEA (0.10 g, 1.00 mmol) were dissolved in 20 mL freshly distilled chloroform in a 100-mL, thoroughly dried, three-necked flask. Acetyl chloride (0.08 g, 1.10 mmol) was added slowly using a syringe, and the reaction was maintained at 23 ^{o}C for 24 h. The solution was poured slowly into methanol to precipitate the product. The white powder was filtered and dried in a vacuum oven at 40 $^{\circ}$C for 24 h. The product was redissolved in chloroform. The solution was washed with water and reprecipitated. The ^{1}H NMR spectrum of the product was identical to the starting materials, and confirmed the absence of phenyl acetates due to the presence of residual phenol end groups.

[19]Fang, J.; Kita, H.; Okamoto, K. *Macromolecules* **2000**, 33, 4639.
[20]Han, H., Bhowmik, P. K. *Prog. Polym. Sci.* **1997**, 22, 1431.
[21]Kharul, U. K.; Kulkarni, S. S.; Kulkarni, M. G.; Houde, A. Y.; Charati, S. G.; Joshi, S. G. *Polym.* **1998**, 39, 2011.
[22]Turner, S. R., Walter, F.; Voit, B. I.; Mourey, T. H. *Macromolecules* **1994**, 24, 1611.
[23]Turner, S. R.; Voit, B. I.; Mourey, T. H. *Macromolecules* **1993**, 26, 4617.
[24]Knauss, D. M.; McGrath, J. E., Kashiwagi, T. *ACS Symposium Series (Fire and Polymers)* **1995**, 599, 41.
[25]Choi, S. H.; Lee, N. H.; Cha, S. W.; Jin, J. I. *Macromolecules* **2001**, 34, 2138.
[26]Maruyama, Y.; Kakimoto, M.; Imai, Y. *J. Polym. Sci. Part A: Polym. Chem.* **1986**, 24, 3555.
[27]Voit, B. I. *J. Polym. Sci. Part A: Polym. Chem.* **2000**, 38, 2505.
[28](a) Gooden, J. K.; Gross, M. L.; Mueller, A.; Stefanescu, A. D.; Wooley, K. L. *J. Am. Chem. Soc.* **1998**, 120, 10180. (b) Chu, F. K.; Hawker, C. J.; Pomery, P. J.; Hill, D. *J. T. J. Polym. Sci. Part A: Polym. Chem.* **1997**, 35, 1627,
[29]Hawker, C. J.; Frechet, J. M. J. *J. Am. Chem. Soc.* **1990**, 112, 7638.
[30]Unrich, K. E.; Hawker, C. J.; Frechet, J. M. J.; Turner, S. R. *Macromolecules* **1992**, 25, 3843.

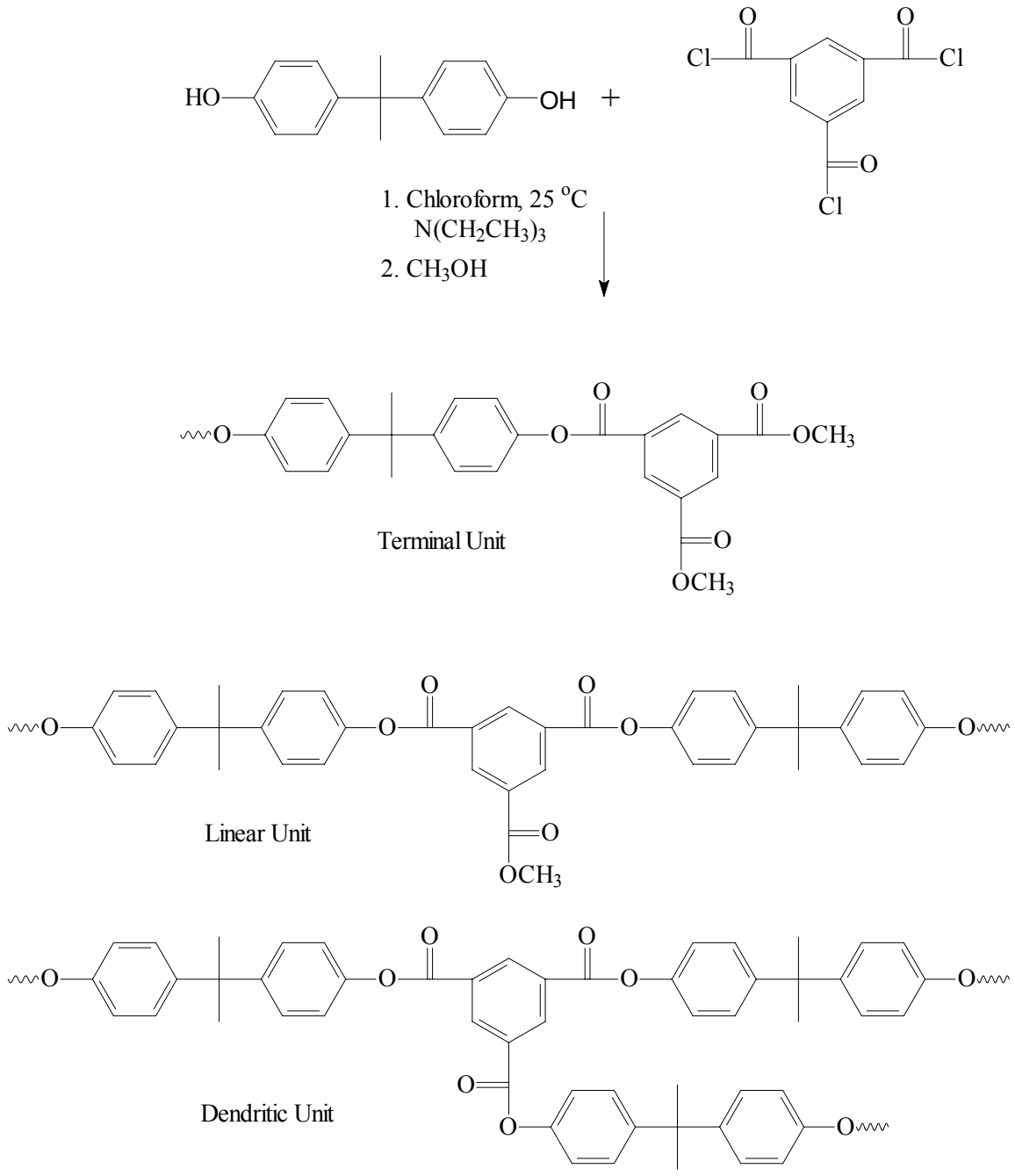

Scheme 11.1 Synthesis of methyl ester terminated hyperbranched polyarylates via polymerization of A_2 and B_3 monomers

11.3.3 Characterization

^{1}H and ^{13}C NMR analyses were performed on a Varian Unity 400 MHz spectrometer at ambient temperature. Two gel permeation chromatography (GPC) instruments equipped with different detectors were used to measure the molecular weights. GPC measurements were conducted on a Waters 2690 chromatograph equipped with a differential refractive index detector (Viscotek Laser Refractometer) and an on-line differential viscometric detector (Viscotek 100) coupled in parallel, using polystyrene standards. A Waters styragel HR0.5, HR2, HR3, HR4 column bank was used. The flow rate was 1.0 mL/min, injection volume was 100 μL, and the column temperature was 40 ºC. Additional GPC measurements were performed on a Waters SEC (515 pump, 717 autosampler) with an external 410 refractive index detector. Multiangle laser light scattering (MALLS) was also performed using an in-line Wyatt Minidawn. A Polymer Laboratories PLgel, 5 micron MIXED-C column with a length of 300 mm and inner diameter of 7.5 mm was used. The flow rate was 1.00 mL/min and the temperature was 40 °C. Thermal transition temperatures were determined using a Perkin-Elmer DSC-7 at 10 °C/min, and all reported data were obtained from the second heating. Thermogravimetric analysis (TGA) was performed on a Perkin-Elmer TGA 7 under a nitrogen atmosphere at a heating rate of 10 $^{\circ}$C/min.

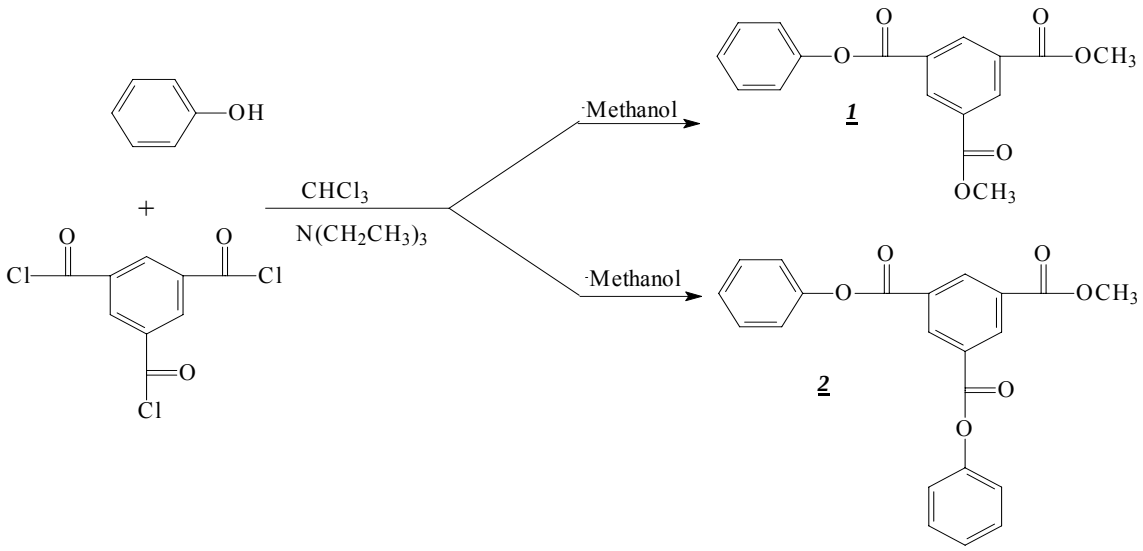

Scheme 11.2 Synthesis of model compounds (1 and 2)

11.4 Results and discussion

Hyperbranched polymers are generally synthesized using a one-step polymerization of AB_n monomers, and the synthetic methodologies are similar to those of their linear analogues.[1-9] The common products that result from polymerization of A_2 and B_3 monomers are networks, and hyperbranched products are only obtained under highly restricted reaction conditions.[12-19] Thus, it is essential to select suitable reaction conditions that avoid gelation, and the specific conditions for polymerization of bisphenol A and 1,3,5-benzenetricarbonyl trichloride for the preparation of hyperbranched polyarylates without gelation are discussed in this report. Furthermore, it is also important to compare the chemical structure, such as the degree of branching (DB) and the composition of the terminal groups, which are obtained from different synthetic methods.

11.4.1 Polymerization

Polyarylates with tailored architectures are typically prepared using a variety of interfacial or melt methodologies.[24,26] Linear, high molecular weight polyarylates are commonly synthesized using interfacial methods that employ weakly basic aqueous bisphenolate solutions and organic diacid chloride solutions.[24,26] However, this method leads to cross-linked products if A_2 and B_3 monomers are used. One approach for preparing hyperbranched polyarylates from A_2 and B_3 monomers that avoids gelation is to conduct solution polymerizations wherein a dilute solution of one monomer is slowly added to a dilute solution of the other monomer (Scheme 11.1). The order of addition of the monomer solution will significantly influence the structures of the final polyarylates. When the A_2 dilute solution was slowly added to the B_3 dilute solution, gelation was avoided and hyperbranched polymers were obtained in a high yield (> 90 %). In contrast, when the dilute B_3 solution was added to the dilute A_2 solution (irrespective of the rate of B_3 addition), only crosslinked products were obtained. It was presumed that a high local concentration of B functional groups during the addition promoted cross-linking.

Specific reaction conditions for the polymerization of A_2 and B_3 monomers in the absence of gelation were determined. Chloroform was able to dissolve low levels of the monomers and hyperbranched products, and was used as the polymerization solvent. The polymerizations were conducted at ambient temperature due to the high reactivity of acid chlorides. Bisphenol A (Bis A) and 1,3,5-benzenetricarbonyl trichloride (BTC) were used as the A_2 and B_3 monomers, but structural variations are achievable using other bisphenols. The final molar ratio of A_2 to B_3 monomers was maintained at 1:1, in an effort to generate similar hyperbranched architectures to those derived from traditional

AB_2 monomers. It was determined that the final concentration of monomers should not exceed 0.08 M in order to avoid gelation. The reaction completion was expected in several hours; however in order to ensure quantitative reaction, the reactions were allowed to proceed for 24 h. Although the polymerization times were typically 24 h, significantly longer times were investigated (> 72 h) and gelation was not observed. The stoichiometric ratio of A groups (phenols) to B groups (acid chlorides) was 2:3, and various reagents were used to react with remaining acid chlorides for the introduction of peripheral functionality. One process involved simply quenching the terminal acid chlorides with water in the presence of triethylamine as an acid scavenger to produce peripheral carboxylic acid functionalities (P-1). ^{1}H NMR spectroscopy confirmed the expected triethylammonium salts of the carboxylic acid terminal groups. Water soluble hyperbranched polymers that were derived from 5-acetoxyisophthalic acid with carboxylic salts as terminal groups were reported earlier.[22-23] However, the P-1 salt was not water soluble, and only swelling occurred. Methanol was alternatively used to consume terminal acid chloride groups in the hyperbranched polyarylates. ^{1}H NMR spectroscopy (Figure 11.1) confirmed the presence of methyl ester terminal groups in addition to minor levels (5-8 mol%) of TEA salts (presumably due to the premature hydrolysis of the acid chlorides during transfer or storage). An interesting area for further study involves the use of alcohols containing chiral or fluoro alkyls for the preparation of hyperbranched polyarylates with an extended range of tailored functional terminal groups.

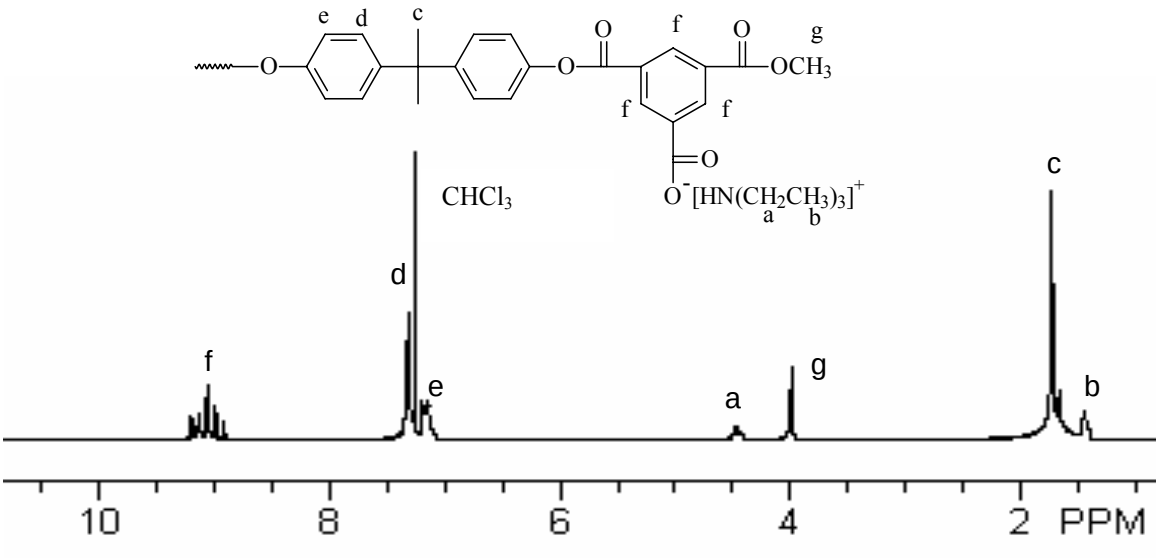

Figure 11.1 ^{1}H NMR spectrum of a methyl ester terminated hyperbranched polyarylate (P-2, 400 MHz, $CDCl_3$)

11.4.2 Determination of the degree of branching (DB).

Structures of the polymeric products that are derived from A_2 and B_3 monomers compared to AB_n monomers are not well-understood.[27] In theory, hyperbranched polymers prepared from AB_n monomers will have a focal unit (Figure 11.2), whereas those from A_2 and B_3 monomers will not. In practice, however, most hyperbranched polymers derived from AB_n monomers do not have focal units due to intramolecular cyclization side reactions (Figure 11.2).[7,28] The effect of focal units on the properties of hyperbranched polymers is difficult to determine because of the less than well-defined nature of the structures.

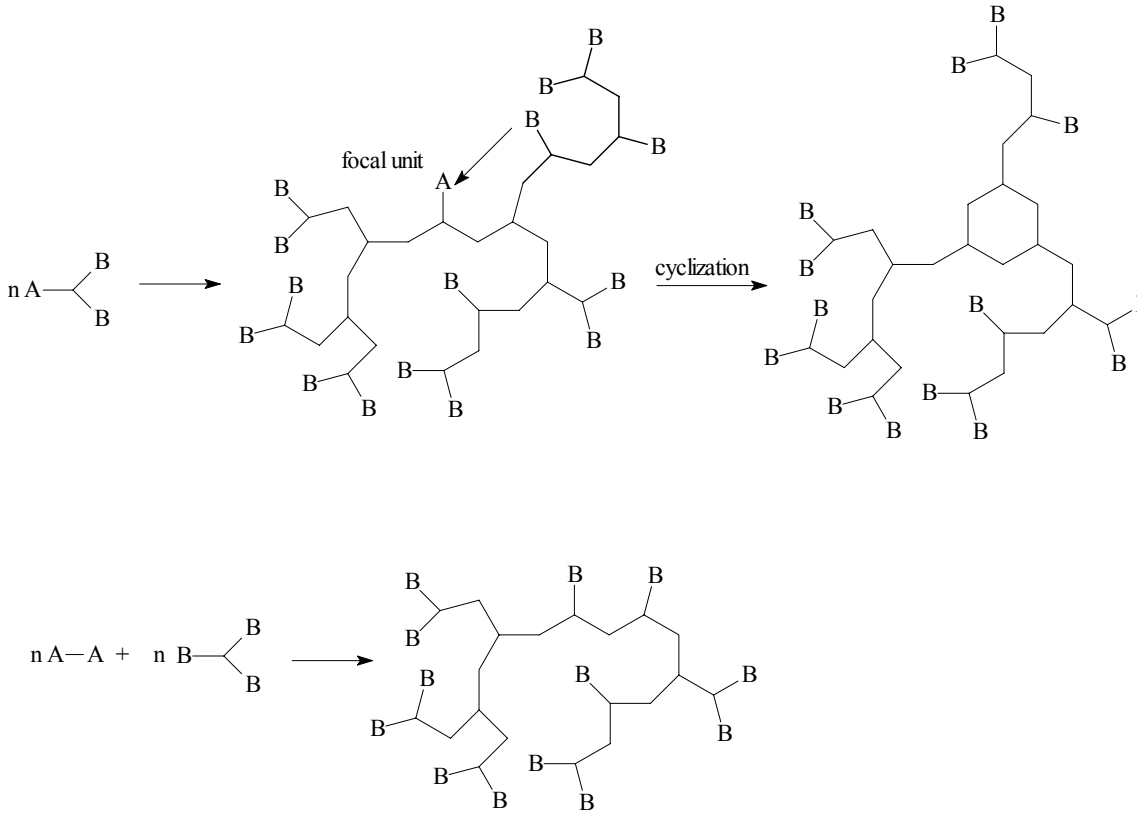

Figure 11.2 Schematic representation of hyperbranched polymers obtained from one-step polymerization of AB_n monomers and polymerization of A_2 and B_3 monomers

Unlike dendrimers with a perfect structure, hyperbranched polymers have highly irregular structures due to the one-step process. Hyperbranched polymers contain three types of units including terminal units with two end groups, linear units with one end group, and internal dendritic units. In order to better define the chemical structures of hyperbranched polymers, Frechet and coworkers quantified the degree of branching (DB) using Equation 1:[3,29]

$$DB = (D + T)/(D + T + L) \qquad \text{(Equation 1)}$$

where D, T and L refer to the numbers of dendritic, terminal, and linear units in the hyperbranched polymers, respectively. Experimentally, DB is usually determined using ^{1}H NMR spectroscopy and a comparison of the integrals of the resonances of the respective units in the hyperbranched polymers. The ^{1}H NMR spectra of hyperbranched polyarylates showed that the resonances from the hydrogens in the three possible BTC units (D, L and T) had different shifts due to the difference in their chemical environments (Figure 11.3). Model compounds, 1 and 2, were synthesized (Scheme 11.2) to establish ^{1}H NMR assignments for quantifying the relative percentages of the different types of units. The assignment of ^{1}H NMR resonances of hydrogens in linear, dendritic and terminal units is depicted in Figure 11.3. The calculated DBs based on the relative percentages of those units ranged between 45% and 55%, and agreed well with the theoretical DB (50 %) for hyperbranched polymers. Hyperbranched polyarylates that were derived from AB_n monomers (5-acetoxyisophthalic acid and 5-(2-hydroxyethoxy)isophthalic acid) and hyperbranched polyamides from diamines (A_2) and trimesic acid (B_3) also had DBs near 50%.[18,22-23] Thus, it was concluded that both

synthetic methodologies (AB_n and A_2/B_3) resulted in hyperbranched polymers with similar DBs.

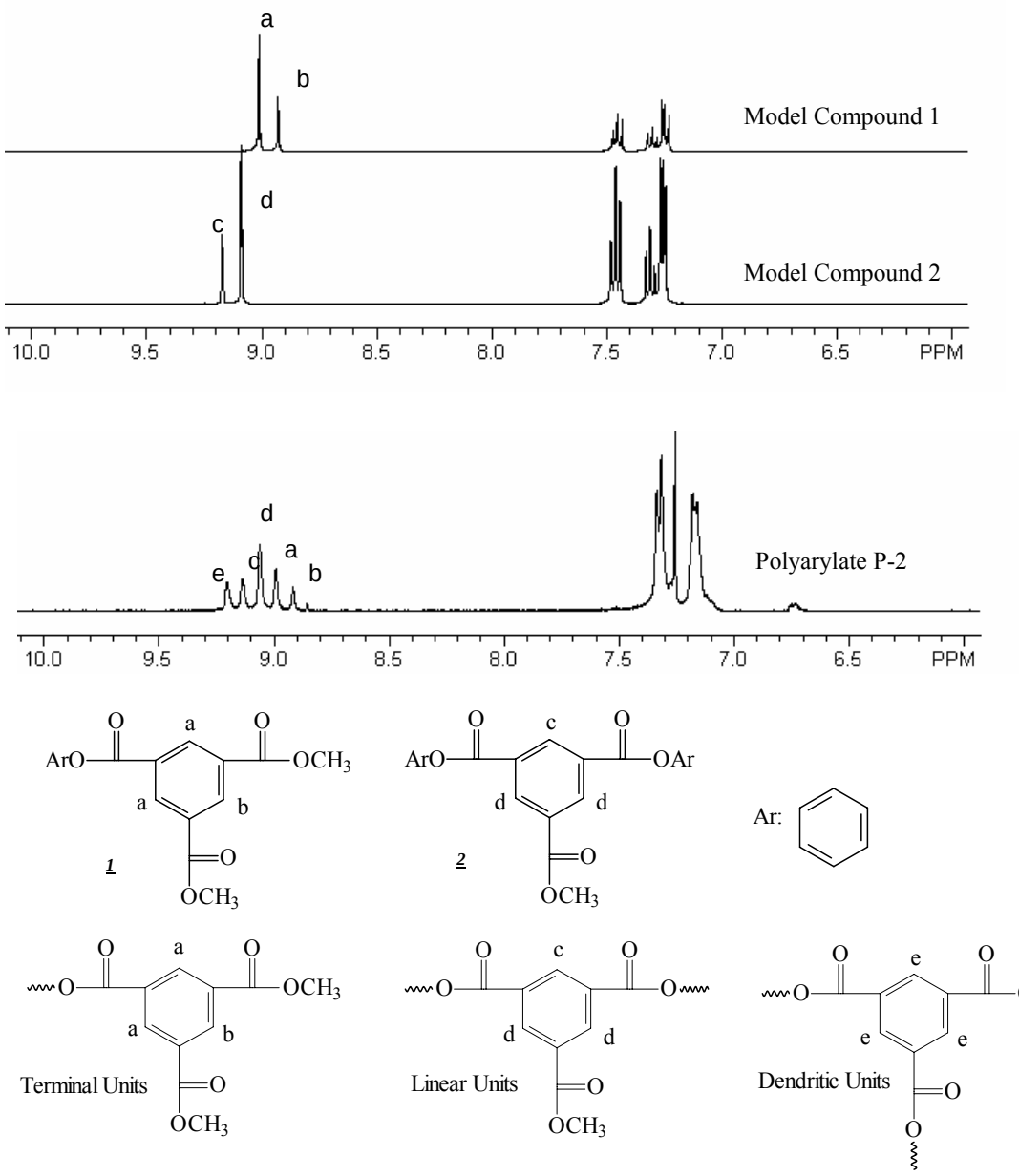

Figure 11.3 Comparison of ^{1}H NMR spectra (400 MHz, $CDCl_3$) of model compounds (1 and 2) and a methyl ester terminated hyperbranched polyarylate (P-2)

Conventional hyperbranched polymers that are derived from a one-step polymerization of AB_n monomers only possess B functional groups as terminal units (Figure 11.2). However, Voit and coworkers have shown that the composition of the terminal groups of hyperbranched polyamides derived form A_2 and B_3 monomers depended on the molar ratio of the two monomers.[18] In most cases, a hyperbranched polyamide had both A (amine) and B (carboxylic acid) terminal groups. In the present work, the final molar ratio of A_2:B_3 was 1:1, and the terminal groups were expected to be identical to hyperbranched polymers derived form AB_n monomers. Two methodologies, ^{1}H NMR spectroscopy and derivatization of terminal groups, were used to confirm the structure of the terminal groups. A detectable resonance related with the phenol group (A functionality) was not observed in the ^{1}H NMR spectra of hyperbranched polyarylates. In addition, the attempted derivatization of any phenol end groups with acetyl chloride did not result in the appearance of new ^{1}H NMR resonances that are associated with a phenyl acetate. These results indicated that when the ratio of two monomers was 1:1, the hyperbranched polyarylates did not contain residual phenol groups and resembled products derived from AB_2 monomers.

11.4.3 Molar mass characterization.

Two GPC instruments equipped with different detectors (RI, MALLS and viscometer) were used to measure the molecular weights of hyperbranched polyarylates. As expected based on the prior literature, the GPC traces exhibited character due to the existence of different molecular weight products with highly irregular structures (Figure 11.4).[8, 22-23] The use of a light scattering detector required the determination of a specific

refractive index increment, dn/dc, which was measured using a differential refractometer. The dn/dc value for the hyperbranched polyarylates in chloroform was approximately 0.14 mL/g. The measured molecular weights of a P-4 sample using three different detectors and calibration approaches were in a good agreement (Table 11.1). This was attributed to the moderate weight average molecular weights that resulted in small differences in measured values using different detectors.

Table 11.1 Molecular weights and glass transition temperatures of hyperbranched polyarylates

Sample	[M][a] (mol/L)	M_n (g/mol)	M_w (g/mol)	M_w/M_n	T_g (°C)
P-1[b]	0.05	3300	10000	3.03	128
P-2[b]	0.05	3540	12300	3.48	136
P-3[b]	0.06	5600	15700	2.81	150
P-4[b]	0.08	7950	22200	2.79	154
P-4[c]	0.08	9300	26000	2.79	154
P-4[d]	0.08	6903	20200	2.93	154
P-5[e]	0.08	8667	21300	2.45	153

a: Concentration of monomer; b: GPC data were obtained using the RI detector; c: GPC data were obtained using the viscometric detector and RI detector; d: GPC data were obtained using the MALLS and RI detector; e: Reaction time was 48 hours and GPC data were obtained using a RI detector.

It is also interesting to compare the GPC results of the hyperbranched polyarylates to earlier hyperbranched products derived from AB_n monomers. In a similar fashion to the polymerization of AB_n monomers, molecular weights of hyperbranched polyarylates that were obtained from the polymerization of A_2 and B_3 monomers increased with the monomer concentration prior to the critical point.[7-8,22-23] However, in contrast to previous reports dealing with the synthesis of hyperbranched polymers from AB_n monomers or A_2 and B_3 monomers, the molecular weight distribution of the polyarylates did not increase with an increase in molecular weight, and remained relatively constant (Table 11.1).[7,12] Several families of hyperbranched polymers derived from AB_n monomers exhibited a maximum number average molecular weight (approximately 10,000 g/mol) due to intramolecular cyclization.[7-8,22-23] The number average molecular weights of P-4 and P-5 (~9000 g/mol) were close to this maximum value (Table 11.1). In fact, weight average molecular weights are preferred for the characterization of hyperbranched polymers,[30] and the weight average molecular weights of the hyperbranched polyarylates were moderate and ranged between 10,000 and 22,000. During the polymerization of AB_n monomers, the weight average molecular weights continually increased with the reaction time.[7] However, in the present work, the longer reaction times did not have a significant effect on the weight average molecular weights. P-4 (maintained reaction for 24 h) and P-5 (maintained reaction for 48 h) had similar weight average molecular weights (Table 11.1).

The relationship between intrinsic viscosity and molecular weight was measured across the molecular weight distribution in the GPC viscometric experiment, and was analyzed using the Mark-Houwink equation $[\eta] = kM^{\alpha}$. The value of α approaches 0.5 at

a θ condition and is generally between 0.65 and 0.75 for linear random coils in a good solvent. However, α values for P-4 and P-5 were approximately 0.25, which is a typical value for many families of hyperbranched polymers.[8,22-23] These small values are consistent with highly branched, compact, and globular structures. The α values for P-1, P-2 and P-3 were close to zero due to relatively low molecular weights.[22-23]

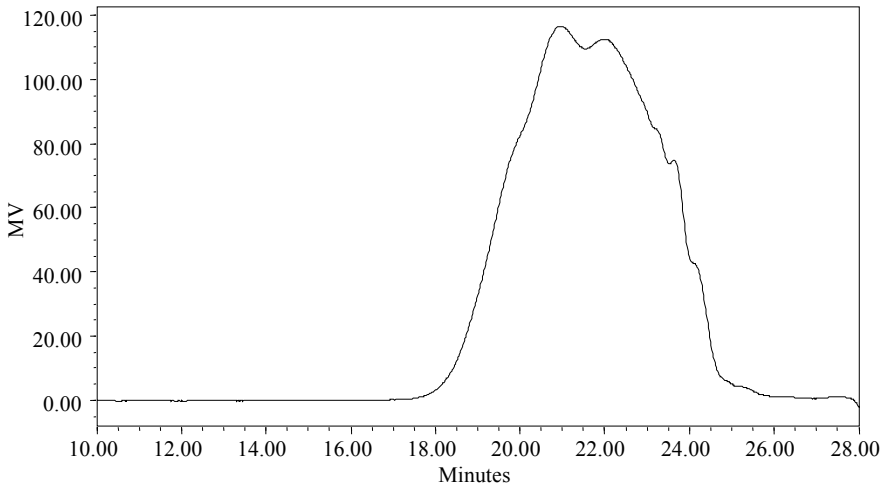

Figure 11.4 Characteristic polymodal GPC trace of a methyl ester terminated hyperbranched polyarylate (P-4)

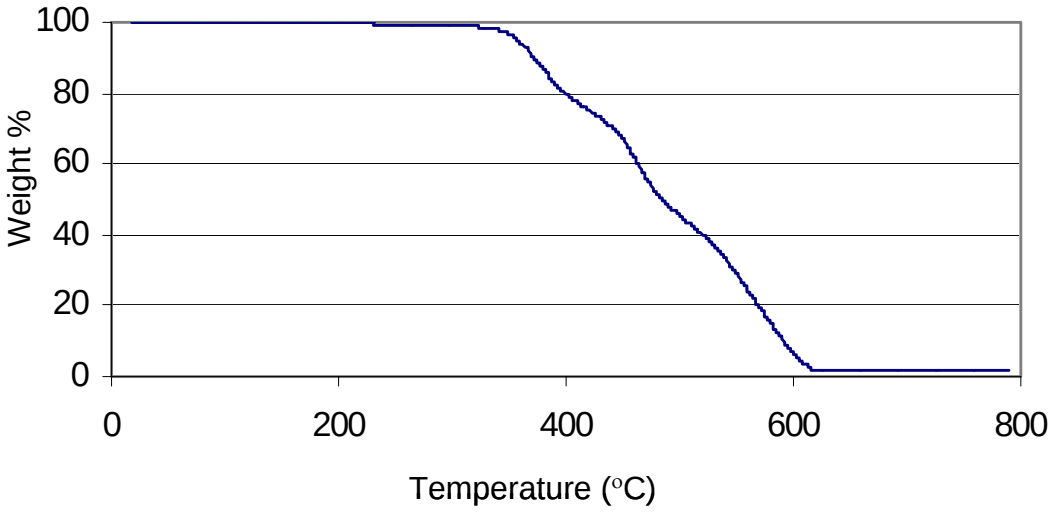

Figure 11.5 Thermogravimetric analysis of a methyl terminated hyperbranched polyarylate (P-2) under nitrogen

11.4.4 Thermal properties

The glass transition temperatures of the hyperbranched polyarylates increased with increasing molecular weight, and typically ranged between 130 and 150 ^{o}C. No obvious crystallization and melt transitions were observed in DSC analysis, which suggested that the products were amorphous. The hyperbranched polyarylates had lower glass transition temperatures relative to their linear analogs derived from bisphenol A and isophthaloyl chloride via interfacial polymerization (~ 200 ^{o}C), and this was presumed to be due to irregular branching and a high concentration of end groups.[26] The hyperbranched polyarylates exhibited excellent thermal stability due to their highly aromatic structure (Figure 4), and the onset of polymer degradation was 390 ºC in a nitrogen environment.

11.5 Conclusions

Hyperbranched polyarylates were prepared via adding a dilute bisphenol A (A_2) solution to a dilute 1,3,5-benzenetricarbonyl trichloride (B_3) solution. The order of addition and solution concentrations were important reaction parameters to avoid gelation, and concentration changes within the dilute regime did not affect molecular weight distributions (~ 3.00). These hyperbranched polyarylates had structures similar to those prepared from more common AB_n monomers in terms of the degree of branching (47-55%) and exclusive B terminal functionality. The hyperbranched polymers exhibited lower solution viscosities, which were characteristic of hyperbranched polymers (Mark-Houwink constants (α) were 0.25), and glass transition temperatures ranged from 130 to 150 ºC depending on molecular weight.

CHAPTER 12

Final Conclusions

Architecture exerted pronounced effects on the properties of ionomers. The stability of ionic aggregates of telechelic ionomers decreased dramatically with an increase in temperature. The effect of branching structures on the properties of ionomers depended on the branching degree. Flexible backbone and a low degree of branching tended the formation of intramolecular ionic aggregates. The clustering point of PET random ionomers was around 5 mol% based on the results from DSC and rheological analysis. The meta structure of ionic units destabilized the LC phase; however, the presence of ionic aggregates stretched the chains to stabilize the LC phase. A small fraction of incorporated PEG end groups increased the crystallization rate dramatically. Moreover, the PEG endgroups tended to aggregate on the surface of PET to result in a PEG rich layer, which improved biocompatibility and decreased the adsorption of protein. The PEG end groups also plasticed the ionic clusters of PET ionomers, and resulted in a water soluble polyester. A phosphine oxide endcapper was synthesized, and fully endcapped macroligands were also prepared using PET oligomer and endcapper. Phosphine oxide end groups coordinated with metal salt preferencely to form linear high molecular weight. Two inexpensive chiral monomers, isosorbide and isomanide, were successfully incorporated into BB-6 LC polyesters. A small amount of incorporated isosorbide or isomanide induced the chiral LC structures.

A novel AB2 monomer, 4-(fluorophenyl)-4',4"-(bishydroxyphenyl) phosphine oxide, was synthesized. The monomer was successfully polymerized to a modest molecular weight with various catalysts, including K_2CO_3 and $Cs_2CO_3/Mg(OH)_2$.

Moreover, an efficient approach to hyperbranched polyarylates via the polymerization of A_2 and B_3 monomers. A dilute bisphenol A (A_2) solution was added slowly to a dilute 1,3,5-benzenetricarbonyl trichloride (B_3) solution at 25 °C to prepare hyperbranched polyarylates in the absence of gelation.

Vita

Qin Lin, son of Qidong Lin and Ruangxian Wang, was born in October 14th, 1970 in Fuzhou, China. He graduated from Middle School of Fujian Teacher University in June, 1990. In September of the same year, he began his undergraduate study in Department of Material Science and Engineering, Tianjin University. He got his B. E in July 1994. In September of the same year, he entered the graduate school in Department of Polymer at Nanjing university, and got Master Degree in July 1997. He began his empolyment in Analytical Center, Fujian Teacher Unviversity. At there, he met Yuping Wei, and get married in July 1998. In August 1998, he left China to Blacksburg, a small townin Virginia, and joined the Department of Chemistry in Virginia Tech. Upon his finish of Ph.D program in Virginia Tech, he will work as post doctoral research associate in Chemistry Department, Virginia Tech.